UNIVERSITY
OF TASMANIA

The Mutagenic Activity of Oxazolopyridine Compounds

Hsien Hooi (Victor) Lee

BSc (Medical Bioscience) (Hons), GradCertRes

School of Natural Sciences (Chemistry)

College of Sciences and Engineering

A thesis submitted in fulfilment of the requirements for the degree of Doctor of Philosophy

University of Tasmania, Hobart, Australia

June 2018

Table of contents

Declaration of originality

This thesis contains no material which has been accepted for a degree or diploma by the University or any other institution, except by way of background information and duly acknowledged in the thesis, and to the best of my knowledge and belief no material previously published or written by another person except where due acknowledgement is made in the text of the thesis, nor does the thesis contain any material that infringes copyright.

Authority of access

This thesis is not to be made available for loan or copying for two years following the date this statement was signed. Following that time the thesis may be made available for loan and limited copying and communication in accordance with the *Copyright Act 1968.*

Hsien Hooi (Victor) Lee

School of Natural Sciences (Chemistry)

College of Sciences and Engineering

University of Tasmania

June 2018

Abstract

Planar heterocycles such as benzoxazoles are biologically active and often used as a scaffold for drug discovery. However, due to some toxicities associated with this group of compounds, analogues of benzoxazoles such as benzothiazoles, benzimidazoles and more recently, the oxazolopyridines have been developed in medicinal chemistry programs. The oxazolopyridine is an easy and versatile scaffold to synthesise as it is stable and has many sites for the addition of functional groups. The oxazolopyridine scaffold is also highly polar, contributing to improved target interaction in biological systems. This results in the anti-bacterial, anti-fungal, anti-parasitic and anti-inflammatory activities, and in sirtuin modulation of the oxazolopyridines. In fact, oxazolopyridines are shown to be non-toxic *in vitro* and *in vivo* in some studies, making it a very suitable scaffold for drug candidates. However, the full toxicity profile of the oxazolopyridine compounds, which include mutagenicity, is unknown and needs to be investigated to determine any unwanted effects. The oxazolopyridines and imidazopyridines are structurally similar and have some similar biological activities, but more concerningly, the carcinogen, 2-amino-1-methyl-6-phenylimidazo[4,5-b]pyridine (PhIP) **46** also belongs to the imidazopyridine family. In the current study, 2-(3-aminophenyl)oxazolopyridine, **60** was chosen as the lead compound given its structural similarities to PhIP **46**. It was therefore hypothesised that compound **60** may be genotoxic (DNA damaging) and mutagenic, where its mode of action is similar to PhIP **46** via the amino group attached. Toxicology screens were conducted on compound **60** *in vitro.* Consistent with previous studies, compound **60** was found to be non-cytotoxic in the colony forming assay. However, compound **60** was genotoxic in cells in the γH2AX assay. The non-cytotoxic but genotoxic nature of compound **60** was found to be attributed by the ability of the cells to repair the DNA damage to maintain survival after 24 hours. Compound **60** was later found to be mutagenic in the Ames test indicating that the cellular repair of the DNA damage is error-

prone. In fact, compound **60** is a pro-mutagen which is dependent on oxidation and enzymatic bio-activation by liver enzymes for activity. More importantly, compound **60** was also found to transform cells in the soft agar invasion assay.

Further studies were carried out to determine the genotoxic and mutagenic mode of action of compound **60**. Through quantitative structural-activity relationship (QSAR) determination, the amino group of compound **60** was not the factor for activity. This was supported by the generated Hammett plot using analogues of 2-aryloxazolopyridine where it was understood that the activity of compound **60** was driven by molecular electron density and not solely by the presence of the amino group as hypothesised. This was an important turning point for this study where the focus was shifted towards studying the electron density on the oxazolopyridine core. Given that activation is oxidation dependent, selected 2-aryloxazolopyridine analogues were found to produce *N*-oxides at the pyridine ring of the oxazolopyridine core. The 2-phenyloxazolopyridine-*N*-oxides were also found to be genotoxic in cells and was thought to be the active species. However, it was found that the 2-aryloxazolopyridine-*N*-oxides still required further bio-activation by liver enzymes to be mutagenic in cells. This has led to further QSAR determination of the roles of the nitrogen atoms in the oxazolopyridine core. It was therefore proposed that upon the *N*-oxidation of the pyridine nitrogen, a second oxidation event on the oxazole nitrogen may occur to generate the active mutagen. Identification of the mutagenic species by enzymatic bio-activation of a 2-aryloxazolopyridine analogue was attempted using ultra pressure liquid chromatography and mass spectrometry (UPLC-MS). There was evidence that the 2-aryloxazolopyridine-*N*-oxide was formed under these conditions but more work was required to identify the mutagenic species. Therefore, the evidence presented in this thesis is the first detailing the mutagenic mode of action and liability of the oxazolopyridine compounds which has been widespread in drug development. In fact, this may have significant ramifications for the use of the oxazolopyridine scaffold in the future.

Acknowledgements

First and foremost, I would like to thank the University of Tasmania for granting me the TGRS scholarship which allowed me to pursue my dreams in doing my PhD in Australia. Without this opportunity, I would not have embarked on such a wonderful and unforgettable journey!

To my research supervisors (Jason Smith, Nuri Güven and Mark Ambrose). Jason, from the moment I approached you years ago, I knew I had chosen the right supervisor as you have been very supportive ever since. Despite coming from a biological background, you have always guided me on the Chemistry aspects of my project with so much patience and passion. I will never forget the opportunities you have given me to learn at my own pace, explore new frontiers and share my research findings in conferences and symposiums. As a result, I have grown to be a versatile researcher who always wants to try new things. I am very grateful for all you have done and I aspire to be a supervisor like you someday. Nuri, I admire your attention to detail and efficiency in providing me useful feedback. Despite being strict in your supervision, I know it comes from a good place and is for your students' own good. Thanks for motivating me during those 'down' times and constantly providing me with useful career tips and advice. I have definitely learnt a lot from you. Mark, you are like a 'big brother' to me. You are such a down-to-earth supervisor whom I had so much fun learning from and working with. Thanks for understanding my situation of shuttling between the Sandy Bay campus and MSP and offering to help with some of my experiments when I was very busy and could not be at two locations. However, I have yet to try your self-proclaimed delicious Singaporean fried noodles!

Thanks to Nathan Kilah (Inorganic Chemistry group), Alireza Ariafard and Rasool Babaahmadi (Computational Chemistry group) and David Nichols (Central Science Laboratory) for the X-ray crystallography, computational chemistry and UPLC-MS work performed for my project. To James Horne and Richard Wilson (Central Science Laboratory),

thanks for the technical support and guidance with the analytical instruments. I am very grateful for the friendliness, help, time and effort you all have provided me.

To the lab managers, Peter Traill and Murray Frith for the continuous support, patience and care you have showered us with. To the laboratory technicians, Melissa Aubrey, Brendon Schollum and Graham Meredith thanks for your help in ordering and providing reagents needed for my experiments in a timely manner. To everyone in Pharmacy, especially Monika Corban, Monila Nadikudi, Jamuna Chhetri, Mia XinYin, Monica Lu, Nicole Bye, Vanni Caruso, Qi Lean, Jack Voutnis and Victoria Hadley, thanks for adding so much colours into my PhD life with the laughter, friendships, comraderies and encouragements. I will never forget the great experiences we had together! To everyone in Chemistry, especially Bianca Deans, Isabel Hyland, Ali Gouran, James Howard, Sui Ching, Krystel Wolley, Jeremy Just, John Robertson, Steve Abel, Thomas Nicholls and Trish McKay, thanks for the help and being such great lab mates and friends. To everyone in the Medical Science Precinct, especially Joanne Pagnon, David Steele and Sarah Kane, thanks for the provided help and technical support at MSP.

Last but not least, my mum and partner who have always been my pillars of strength and avid supporters. To my beloved partner, thanks for always being there for me, rain or shine, wherever and whenever. To my beloved mum, it's not easy being a single mother and having to brave through the world while raising me up. Your love, determination and perseverance have always motivated me to never give up, which have resulted in the successful completion of my PhD thesis. To my buddies in Malaysia, Australia and around the globe who always find time to call me just to make sure everything is fine, thanks! I love you all very much!

I therefore would like to dedicate my thesis to all of you, who have made this possible for me.

Victor Lee

Abbreviations

^{13}CNMR	Carbon-13 nuclear magnetic resonance
^{1}HNMR	Hydrogen-1 nuclear magnetic resonance
4-NQO	4-Nitroquinoline-1-oxide
53BP1	Tumour suppressor p-53 binding I
A	Adenine
Acetyl-coA	Acetyl coenzyme A
AMP	Adenosine monophosphate
ANOVA	Analysis of variance
AP	Apurinic/apyrimidic
APC	Adenomatous polyposis coli
APE1	Apurinic/apyrimidic endonuclease I
aprt	Adenine phosphoribosyltransferase
ATM	Ataxia telangiectasia mutated
ATP	Adenosine triphosphate
ATR	Ataxia telangiectasia mutated Rad3 related
BCL2	Overexpression of B-cell lymphoma II
BER	Base excision repair
BRAF	Rapidly accelerated fibrosarcoma homolog B
BRCA1	Breast cancer I
BRCA2	Breast cancer II
BrdU	Bromodeoxyuridine
BS1	6-31G(d) basis set
BS2	Larger basis set

C	Cytosine
CD_3OD	Deuterated methanol
$CDCl_3$	Deuterated chloroform
CHO	Chinese hamster ovary
COM	Committee of Mutagenicity
CRL8155	Human lymphoblast cells
CYP	Cytochrome P450
cyt c	Cytochrome c
DAPI	2-(4-Amidinophenyl)-1*H* -indole-6-carboxamidine
DFT	Density functional theory
dG	Deoxyguanosine
dhfr	Dihydrofolate reductase
DiMeIQx	2-Amino-3,4,8-trimethylimidazo[4,5-*f*]quinoxaline
DMEM	Dulbecco's Modified Eagle's medium
DMSO	Dimethyl sulphoxide
DMSO-D_6	Deuterated dimethylsulphoxide
DNA	Deoxyribonucleic acid
DPQ	3,4-Dihydro-5-[4-(1-piperidinyl)butoxyl]-1-(2*H*)-isoquinolinone
DSBs	DNA double strand breaks
EACC	European Collection of Cell Culture
EDTA	Ethylenediaminetetraacetic acid
EU	European Union
FAD^+	Flavin adenine dinucleotide
FBS	Fetal bovine serum
FEN1	Flap endonuclease I

FISH	Fluorescence *in situ* hybridisation
G	Guanine
G2/M	Growth II to mitosis checkpoint
H2A	H2A subunit of histone
HAT	Human African trypanosomiasis
HCAs	Heterocyclic amines
HCT116	Colorectal carcinoma cells
HeLa	Henrietta Lacks' immortalised cells
HepG2	Human hepatocellular carcinoma cells
hisD	Histidine
His^+	Histidine prototrophy
His^-	Histidine-requiring
HMGB1	High-mobility group protein B1
hNTH1	Human endonuclease III
hOGG1	Human 8-oxoguanine DNA N-glycosylase I
hprt	Hypoxanthine phosphoribosyltransferase
HR	Hazard ratio
HRC	Homologous recombination DNA repair
HTS	High throughput screening
Hz	Hertz
IC_{50}	Half maximal inhibitory concentration
ICH	International Conference on Harmonisation of Technical Requirement for Registration of Pharmaceuticals for Human Use
IQ	2-Amino-3-methylimidazo[4,5-*f*]quinoline
IQx	2-Amino-3-methylimidazo[4,5-*f*]quinoxaline

IRC	Intrinsic reaction coordinate
KU55933	2-(4-Morpholinyl)-6-(1-thianthrenyl)-4H-pyran-4-one
L6	Rat skeletal myoblast cells
lacI	*Lac* repressor
lacZ	β-Galactosidase
LB	Luria-Bertani
LDH	Lactate dehydrogenase
LigIII	DNA ligase III
LRMS	Low resolution mass spectrometry
m/z	Mass over charge ratio
MCL-5	Human B-lymphoblastoid cells
mCPBA	Meta-chloroperbenzoic
MDC1	Mediator of DNA damage checkpoint I
MeIQ	2-Amino-3,4-dimethylimidazo[4,5-*f*]quinoline
MeIQx	2-Amino-3,8-dimethylimidazo[4,5-*f*]quinoxaline
MIC	Minimum inhibitory concentration
MRM	Multiple reaction monitoring
MRSA	Methicillin-resistant *Staphylococcus aureus*
MS	Mass spectrometry
MTT	3-(4,5-Dimethylthiazol-2-yl)-2,5-diphenyltetrazolium bromide
MxHCl	Methoxyamine hydrochloride
NAD^+	Nicotinamide adenine dinucleotide
NADPH	Reduced nicotinamide adenine dinucleotide
NAT	*N*-Acetyltransferase
NBS1	Nijmegen breakage syndrome I

NEIL1	Endonuclease VIII-like I
NEIL2	Endonuclease VIII-like II
NER	Nucleotide excision repair
NF1	Neurofibromin I
NF2	Neurofibromin II
NHEJ	Non-homologous end joining DNA repair
NMR	Nuclear magnetic resonance
NSAIDs	Non-steroidal anti-inflammatory drugs
OHP	OH terminal
OR	Odds ratio
p53	Tumour protein p53
PARP1	Poly-(ADP-ribose) polymerase I
PBS	Phosphate buffered saline
PCNA	Proliferating cell nuclear antigen
PFA	Paraformaldehyde
PhIP	2-Amino-1-methyl-6-phenylimidazo[4,5-*b*]pyridine
PNKP	Polynucleotide kinase phosphatase
POLD1	DNA polymerase delta I
POLE	DNA polymerase epsilon
POLK	DNA polymerase kappa
polyλ	DNA polymerase λ
Polβ	DNA polymerase β
QSAR	Quantitative structure-activity relationship
R^2	Correlation coefficient
Rad51	Rad51 protein

Rad3	Rad 3 protein
RAS	Retrovirus associated
Rec_{50}	Ratio of 50% lethal dose
RET	Rearranged during transfection
RFC	Replication factor C
ROS	Reactive oxygen species
RR	Relative ratio
RT	Room temperature
S139	Serine-139
SAI	Soft agar invasion
SD	Standard deviation
SEA	Staphylococcal enterotoxin type A
SIRT1	Sirtuin I
SQ motif	Amino acid sequence motif
SRC	Sarcoma
SSBs	DNA single strand breaks
supF	Tyrosine amber suppressor tRNA gene
SYBR	*N*',*N*'-Dimethyl-N-[4-[(E)-(3-methyl-1,3-benzothiazol-2-ylidene)methyl]-1-phenylquinolin-1-ium-2-yl]-*N*-propylpropane-1,3-diamine
T	Thymine
TFT	Trifluorothymidine
THF	Tetrahydrofuran
TIC	Total ion count
TK	Thymidine kinase

TLC	Thin layer chromatography
TLS	Trans-lesion synthesis
Trolox	6-Hydroxy-2,5,7,8-tetramethylchromane-2-carboxylic acid
TS	Template switching
UK	United Kingdom
UPLC	Ultra pressure liquid chromatography
UPLC-MS	Ultra pressure liquid chromatography and mass spectrometry
US	United States of America
USFDA	United States Food and Drug Administration
VEGF	Vascular endothelium growth factor
VHL	Von Hippel-Lindau
WST-1	Water soluble tetrazolium I
XRCC1	X-ray repair cross-complementing I
Y142	Tyrosine-142
ΔG	Gibbs energy
γH2AX	Phosphorylated H2A subunit of histone

Chapter 1 Introduction

1.1 Oxazolopyridines in medicinal chemistry

1.1.1 Introduction to planar heterocycles

Heterocycles are cyclic organic compounds which contain at least one non-carbon atom as part of the ring. These cyclic systems can be divided into aromatic and aliphatic heterocycles (Figure 1). For the aromatic heterocycles, the carbons and heteroatom are sp^2 hybridised and results in a planar structure [1]. Heterocycles can occur as single ring systems or fused ring systems consisting of two or more rings (Figure 1). Naturally occurring aromatic fused heterocycles (with some examples) include DNA bases (adenosine and guanine), amino acids (tryptophan), coenzymes (acetyl coenzyme A [Acetyl-CoA], nicotinamide adenine dinucleotide [NAD^+] and flavin adenine dinucleotide [FAD^+]) and vitamins (B2, B9 and E) [2]. In synthetic chemistry, aromatic heterocycles have been exploited as molecular scaffolds for use as building blocks of biological active compounds such as drugs and pesticides [3]. Due to their ability to mimic natural occurring compounds they can be tuned to have improved selectivity and/or affinity to key biological targets which highlights the importance of this group of molecules in medicinal chemistry and agriculture [2,3].

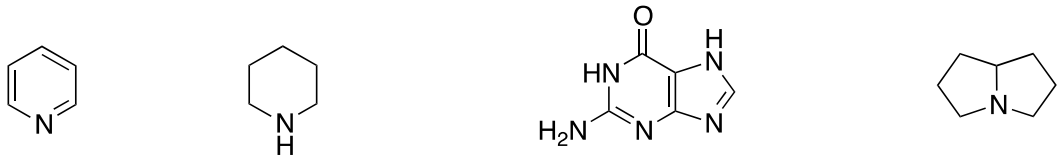

1 **2** **3** **4**

Figure 1: Examples of heterocycles. Heterocycles can be divided into different groups: unsaturated (pyridine **1**), saturated (piperidine **2**), fused unsaturated (guanine **3**) and fused saturated (pyrrolizidine **4**).

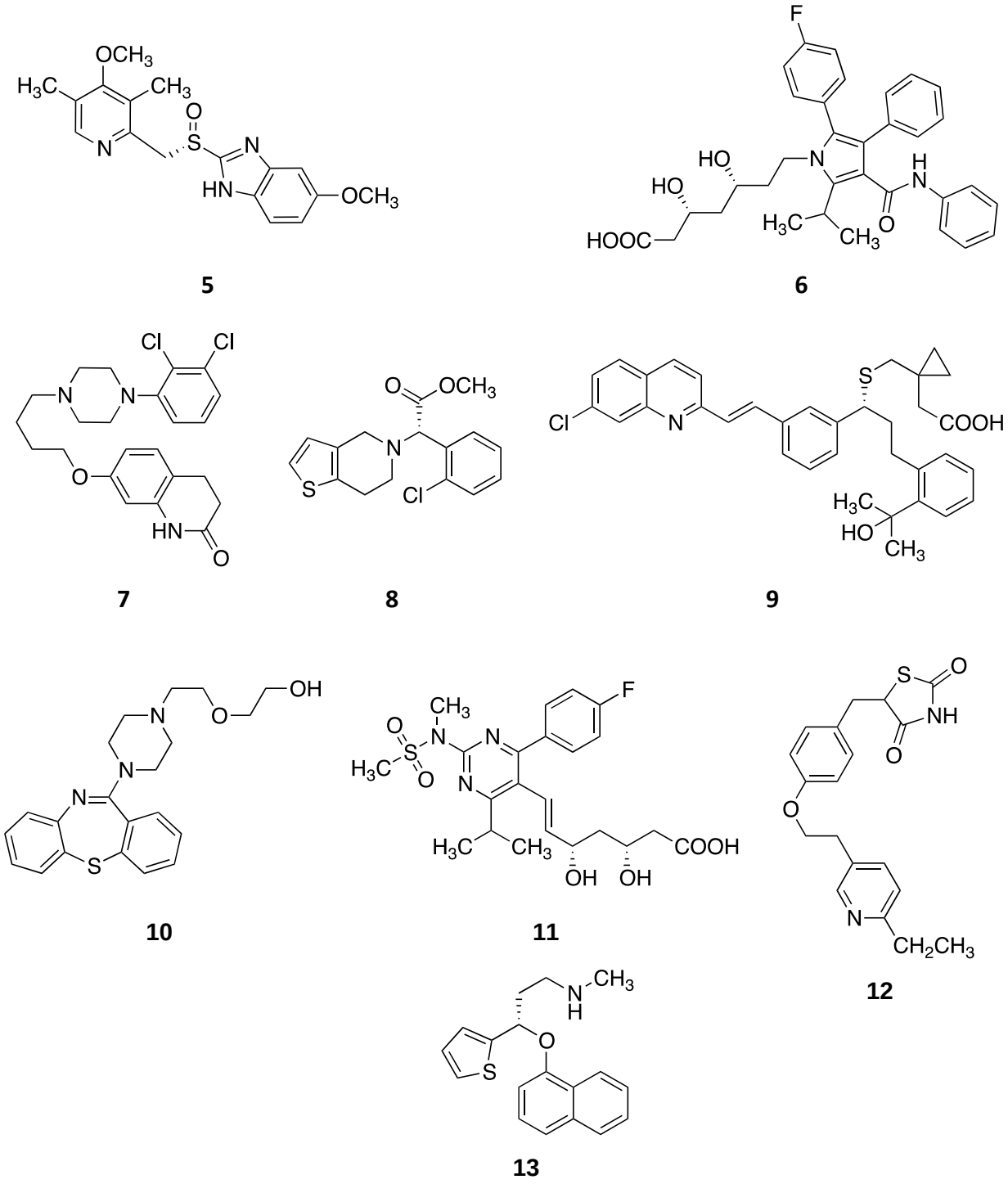

Figure 2: Heterocycle drugs. Nine heterocycle drugs which made the top 10 drugs by retail sales in the US in 2010 [4]. The brand, generic name and indication of these drugs are as follows: Nexium (Esomaprazole) **5**, anti-ulcer; Lipitor (Atorvastatin) **6**, cholesterol regulator; Abilify (Aripiprazole) **7**, anti-psychotic; Plavix (Clopidogrel) **8**, platelet aggregation inhibitor; Singulair (Montelukast) **9**, anti-histamine; Seroquel (Quetiapine) **10**, anti-psychotic; Crestor (Rosuvastatin) **11**, cholesterol regulator; Actos (Piolitazone) **12**, anti-diabetic; Cymbalta (Duloxetine) **13**, anti-depressant.

In the United States, more than 80% of top small molecule drugs prescribed in 2010 contain a heterocycle as part of the structure [4]. In fact, most of the top small molecule drugs in the US contain heterocycles (Figure 2). Other common and widely prescribed commercial drugs containing heterocycles include diazepam, isoniazid, metronidazole, azidothymidine, chlorpromazine, antipyrine, methorrexate and captopril [5].

In drug discovery, the main advantage of working with heterocycles lie within their structural versatility enabling structural variation to effect biological activity in terms of potency and selectivity via bio-isostearic replacements, lipophilicity, polarity and aqueous solubility [4]. For these reasons, heterocyclic compounds make up the largest group of compounds researched in medicinal chemistry [6]. Of the approximately 20 million compounds identified until the early 2000s, more than 60% are fully or partially aromatic and half from this population are heterocyclic. Among them, sulphur and nitrogen-containing heterocycles are most commonly synthesised [6]. Other heterocycles containing oxygen, phosphorus and selenium have also been synthesised [5]. Benzoxazoles are heterocycles containing oxygen and nitrogen in a five membered ring fused to a benzene and are commonly featured in medicinal chemistry. The benzoxazole scaffold can be manipulated by substituting the heteroatoms with sulphur and nitrogen to give benzothiazoles, benzimidazoles and oxazolopyridines, all of which have been reported to possess biological activity. A SciFinder® search of these molecules indicate that numerous compounds with reported biological activity as of January, 2018 (Figure 3).

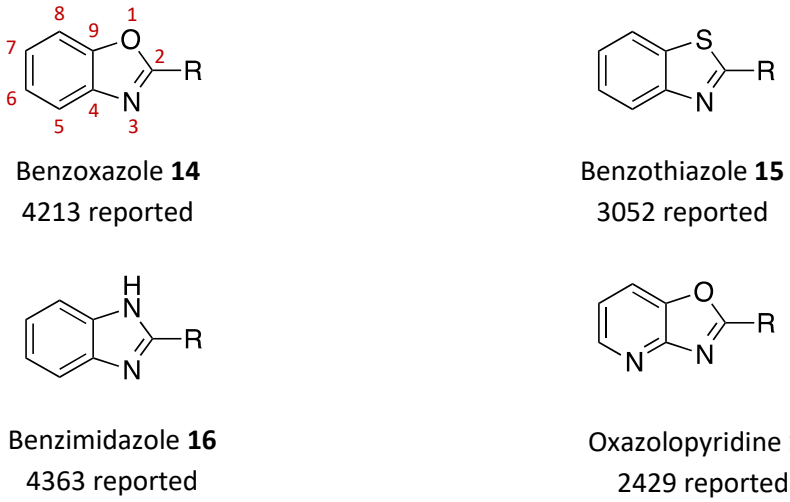

Figure 3: The frequency of biologically active benzoxazole and its substituted analogues. Report frequencies were based on a search on SciFinder®. R= hydrogen or any group.

1.1.2 Bio-activities of benzoxazoles

Benzoxazoles play an important role in drug discovery due to multiple bio-activities such as anti-microbial [7-9], anti-viral [10], anti-parasitic [11,12], anti-inflammatory [13,14], anti-cancer [15,16] activity and compounds of this type play a role in regulating blood glucose levels in diabetic patients [17] (Table 1). The synthesis of benzoxazole analogues can be achieved by a single step via the condensation of 2-aminophenol and various aldehydes [18,19]. The convenience and efficiency of synthesising this scaffold makes benzoxazole analogues ideal drug candidates for the pharmaceutical industry [4]. Among the various benzoxazoles reported, it was found that in the benzoxazole fused ring system, substitution at position C2 has the largest effect on the biological activity of the molecule while the substitution at position C6 modulates the biological activity [20-22].

Table 1: The structures of benzoxazole analogues which are biologically active.

Activity/target	Biologically active structure(s)
Anti-microbial	
Staphylococcus aureus [7]	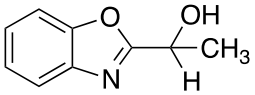 **18** 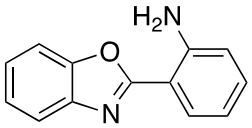 **19**
Bacillus subtilis [8]	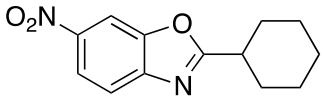 **20**
Pseudomonas aeruginosa [8]	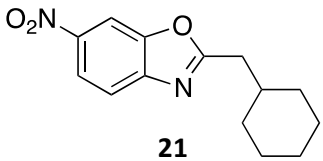 **21**
Candida albicans [8]	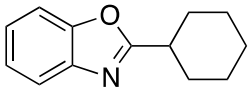 **22** 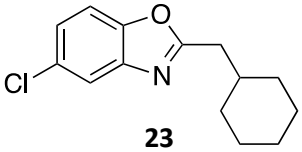 **23**
Mycobacterium tuberculosis [9]	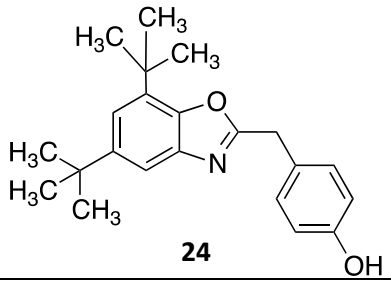 **24**
Anti-viral	
HIV-reverse transcriptase inhibitor [10]	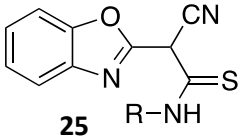 **25** **R=** $(CH_2)_2CH_3$ **(25a)**, $CH_2C_6H_5$ **(25b)**
Anti-parasitic	
Leishmania donovani [11]	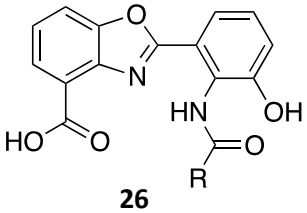 **26** **R=**  **(26a) ,** 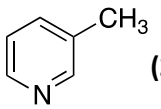 **(26b)**
Hymenolepis Nana (tapeworm) [12]	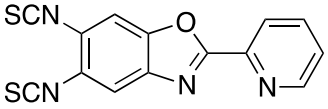 **27**

Nematospiroides dubius (nematode) [12]	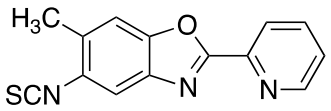 **28**
Analgesic and anti-inflammatory [13 14]	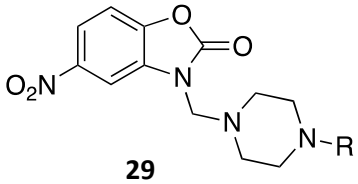 **29** **R=** 4-fluorophenyl **(29a)**, 2-flurophenyl **(29b)**, 4-chlorophenyl **(29c)**, 2-chlorophenyl **(29d)** 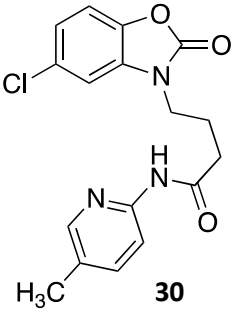 **30**
Anti-cancer [15 16]	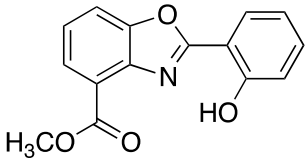 **31** 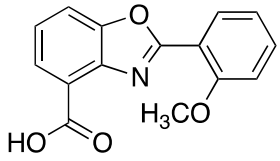 **32**
Anti-diabetic Hypoglycaemic agent [17]	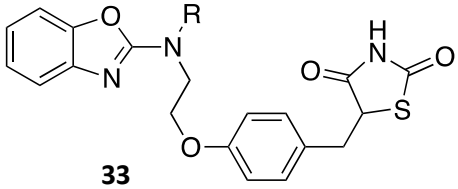 **33**

Due to the high bio-activities and easy synthesis of benzoxazoles, some benzoxazoles have been developed as non-steroidal anti-inflammatory drugs (NSAIDs) such as Benoxaprofen® and Flunoxaprofen® and muscle relaxants such as Zoxazolamine®. Despite their effectiveness, these drugs have been recalled due to adverse side effects that included kidney failure [23], hepatoxicity [24-26] and gastrointestinal abnormalities [27]. Despite the toxicity reported on some benzoxazoles, the benzoxazole scaffold is generally not considered toxic nor is it a structural motif to avoid which may cause unwanted adverse effects [28,29]. In fact, benzoxazoles are not classified under the pan assay interference compounds (PAINS), which is a group of structural motifs to be avoided in medicinal chemistry [28]. These toxicity reports however prompted the need to discover alternatives to benzoxazoles. Therefore, this has led to the recent discovery of a closely related class of compounds, the oxazolopyridines.

1.1.3 Discovery and synthesis of oxazolopyridines

Oxazolopyridines are characterised by the fusion of an oxazole ring and a pyridine ring and are derivatives of benzoxazoles. Replacement of one carbon atom in the benzene ring of the benzoxazole with nitrogen results in an oxazolopyridine. This is an attractive strategy in the drug discovery field. This structural change increases the polarity of the molecule and influences the adsorption of the compound, which can be manipulated during the molecular design phase [30]. The presence of nitrogen in the molecule increases the likelihood of hydrogen bond formation with water molecules or polar receptors in biological systems. This in turn enhances the target selectivity of the molecule [31]. The stable and rigid properties of oxazolopyridines as well as the many sites for the addition of functional groups also make this group of compounds a versatile scaffold for synthetic chemistry [32]. The synthesis of oxazolopyridine analogues **17** can be achieved readily, with the most common method of synthesis involving the condensation of 2-amino-3-hydroxypyridine **34** and carboxylic acids **35** under strong acidic conditions such as polyphosphoric acid and boric acid at high temperatures (Figure 4) [33].

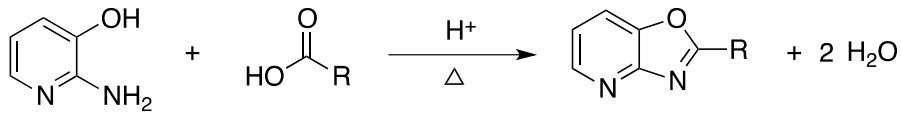

34 **35** **17**

Figure 4: The condensation reaction of 2-amino-3-hydroxypyridine and carboxylic acids.

However, due to the harsh conditions and long reaction times, various strategies have been employed to overcome these issues. The efficient synthesis of oxazolopyridine can be achieved in two steps by reaction of 2-amino-3-bromo-5-methyl-pyridine **36** with an acid chloride, **37** followed by the cyclisation of the intermediate, **38** into the oxazolopyridine, **39** catalysed by

Cu(I) and in the presence of the ligand, 1,10-phenanthroline [34]. This method is conducted at lower temperatures and provides high yields but requires the use of Cu(I) catalyst (Figure 5).

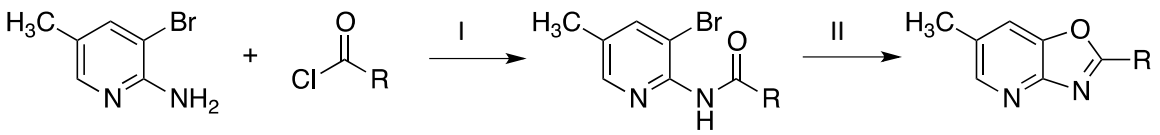

36 **37** **38** **39**

Figure 5: The CuI catalysed two steps reactions of 2-amino-3-bromo-5-methylpyridine and acid chlorides. Reaction conditions: I. 4-dimethylaminopyridine, CH_2Cl_2, 0 °C to room temperature (RT) and II. CuI catalyst, 1,10-phenanthroline, Cs_2CO_3, tetrahydrofuran (THF), 24 hours.

A one step microwave reaction method to synthesise oxazolopyridines that does not require solvents or additional catalysts and acts through the condensation reaction of 2-amino-3-hydroxypyridine and carboxylic acid was described previously [32]. Given the different strategies to conveniently obtain oxazolopyridines, upscaling of synthesis in a pharmaceutical setting becomes economically feasible [30]. Similar to benzoxazoles, analogues of oxazolopyridines are biologically active ranging from anti-bacterial [35,36], anti-fungal [37], anti-parasitic [38,39], anti-inflammatory [40] effects and a sirtuin modulator [41]. Most importantly, pre-clinical screens using human cell lines and animal models indicated that oxazolopyridines are generally non-toxic [38,39]. For these reasons and especially their low toxicity, oxazolopyridines have become a major focus for drug discovery as an alternative scaffold to benzoxazoles.

1.1.4 Bio-activities of oxazolopyridines

1.1.4.1 Anti-bacterial effects

A quantitative structure-activity relationship (QSAR) study manipulating the R group on the phenyl ring of the 2-aryloxazolopyridines **40** fused ring system was reported, with some analogues were highly potent against Gram negative bacteria. Analogues of **40a-b** were most active when tested in *Escherichia coli*, *Klebsiella pneumoniae* and *Pseudomonas aeruginosa* where the minimum inhibitory concentration (MIC) values in these microorganisms (6.20 – 12.5 µg/mL) were better than known antibiotics, chloramphenicol and erythromycin [35]. The replacement with electron donating groups such as 4-OCH_3 and 4-NH_2 at this position was shown to increase the anti-microbial effect.

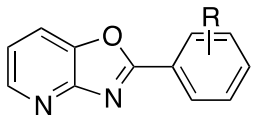

40

R = 4-OCH_3 **(40a)**, 4-NH_2 **(40b)**, 2-OCH_3 **(40c)**, 2-NO_2 **(40d)**, 3-OCH_3 **(40e)**

Compounds **40c-e** with different R groups of the phenyl ring of the 2-aryloxazolopyridine fused ring system were tested in Gram negative bacteria [36]. It was concluded that the anti-bacterial activity of oxazolopyridines were not specific. These analogues were effective against both Gram positive bacteria, namely methicillin-resistant *Staphylococcus aureus* (MRSA) and *Bacillus subtilis*, and Gram negative bacteria namely *E.coli* and *Pseudomonas diminuta*. The MIC values in these microorganisms (1.56 – 25 µg/mL), were more active than known antibiotics such as ampicillin and streptomycin. Furthermore, *in silico* analysis of these molecules indicated that the inhibition of MRSA was attributed to the docking of the oxazolopyridine derivatives on the *Staphylococcal* enterotoxin type A (SEA) protein [36].

1.1.4.2 Anti-fungal effects

Both benzoxazoles and oxazolopyridines have demonstrated potent anti-fungal activity. Generally, oxazolopyridines were better anti-fungal agents as compared to benzoxazoles when tested in *Candida albicans* [37]. Substitution at C5 of the oxazolopyridine fused ring system was found to be essential for its anti-fungal activity. Substituting this position with a strong electron withdrawing nitro group significantly increased reactivity [37]. Consequently, compounds with the nitro group in position C6 of the fused ring system and different R groups at the phenyl ring such as compounds **41a-e** potently inhibited against *C. albicans* with very low MIC values [37].

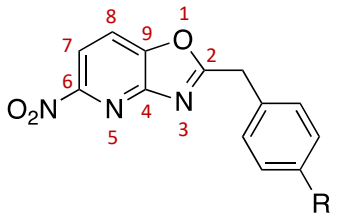

41

R= H **(41a)**, OCH_3 **(41b)**, Br **(41c)**, Cl **(41d)**, NO_2 **(41e)**

1.1.4.3 Anti-parasitic effects

High throughput screening (HTS) on 87,000 compounds against *Trypanosoma brucei*, which is responsible for causing the human African trypanosomiasis (HAT) disease, found the 2-aryloxazolopyridine compound **42** to be very potent against the kinetoplastid of *T. brucei* with a half maximal inhibitory concentration (IC_{50}) of 90 nM [38]. It also had a high selectivity index for the parasite as compared to other related parasites of the same family [38].

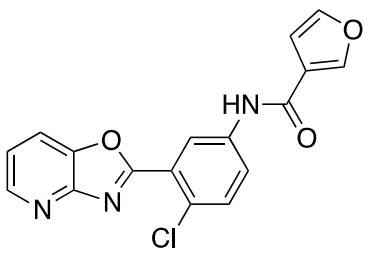

42

Further to this, replacing the chlorine at position C2 of the phenyl of the 2-aryloxazolopyridine with fluorine to give compound **43a**, significantly increased the anti-parasitic activity in *T. brucei* by approximately two-fold [39]. Maintaining the fluorine group at this position but substitution at position C6 of the oxazolopyridine fused ring system with a phenyl, 4-fluorophenyl and 3-chlorophenyl groups represented by compounds **43b-d** further improved the potency represented by lower IC_{50} values [39].

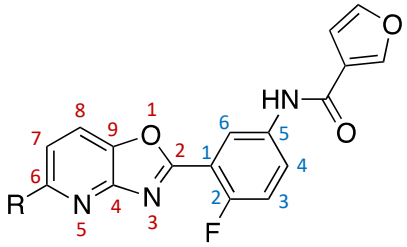

43

R= H **(43a)**, phenyl **(43b),** 4-fluorophenyl **(43c)**, 3-chlorophenyl **(43d)**,

1.1.4.4 Anti-inflammatory effects

Oxazolopyridine derivatives were also found to be have anti-inflammatory effects in rats. Analogues of 2-aryloxazolopyridine **40** with different R groups on the phenyl ring effectively reduced oedema in rats by 62-66%. The substitution at C2 or C6 of the phenyl ring of the 2-aryloxazolopyridine with fluorine and cyano (electron donating groups) represented by compounds **40f-h**, enhanced the anti-inflammatory effect. The three analogues were also tested in other standard anti-inflammatory assays to test for analgesic, anti-pyretic and anti-arthritic effects and were more effective than known anti-inflammatory drugs namely phenylbutazone, aspirin and ibuprofen [40].

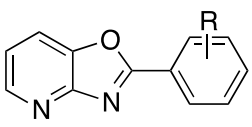

40

R= 2-F **(17f)**, 2-CN **(17g)**, 2,6-F_2 **(17h)**

1.1.4.5 Sirtuin Modulation

Some oxazolopyridine derivatives have been indicated to activate the sirtuin I (SIRT1) gene. SIRT1 is a protein deacetylase which is dependent on the levels of NAD^+ essential in glucose and insulin homeostasis [41].

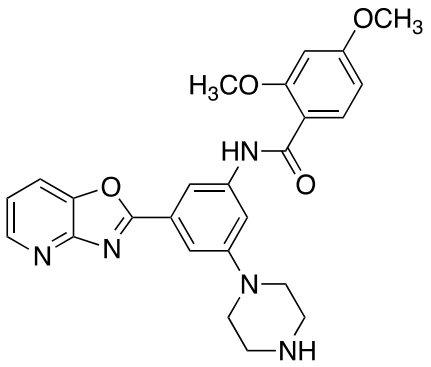

44

From a library of 2-aryloxazolopyridine compounds screened, compound **44** increased activation of SIRT1 at only 0.5 µM. An increase in mitochondrial content and survival in diabetic mice fed with a high fat diet was reported upon treatment with compound **44** at levels comparable to resveratrol, a supplement taken by diabetic patients [41].

1.1.5 The development of oxazolopyridines in drug discovery

The discovery of multiple bio-activities of oxazolopyridines have prompted the development of these compounds into drug candidates. Moreover, oxazolopyridines satisfy the criteria of a drug candidate owing to its lack of stereogenic carbon atoms preventing the complication of stereoisomers, its convenience in synthesis and having drug-like features like low molecular weight which complies with the Lipinski rule-of-five [39]. The versatility of this molecular scaffold in terms of functionalisation by chemical substitution and its stability also makes the synthesis of these structural analogues to be practical and economically feasible. Most reports on the anti-bacterial, anti-fungal and anti-parasitic effects of oxazolopyridines were only

conducted on test pathogens and there was still a lack of reports on the cytotoxicity in human cells. Some studies have attempted to establish the toxicity profiles in mammalian cells such as rat skeletal myoblast L6 [38,39], human lymphoblast CRL8155 [39] and human hepatocellular carcinoma HepG2 [39] cells, where oxazolopyridines were found to be non-cytotoxic. Moreover, only one study has been conducted in mice, which interestingly demonstrated the permeability of the oxazolopyridine analogues into the central nervous system [39]. Furthermore, a series of 2-arylimidazopyridine analogues have been identified to have potent anti-parasitic activity against *Trypanosoma spp*. with compound **45** showing highest potency [39]. This discovery was initiated by the discovery of anti-parasitic activity reported in 2-aryloxazolopyridines [38,39]. Similar to the oxazolopyridines, the anti-parasitic 2-arylimidazopyridine **45** was also found to be non-cytotoxic *in vitro* and *in vivo* [38,39]. Despite the potential medicinal properties of imidazopyridines, they are structurally related to the known carcinogen 2-amino-1-methyl-6-phenylimidazo[4,5-b]pyridine (PhIP) **46** (Figure 6). Given the potential of oxazolopyridines and imidazopyridines to be developed into drugs, more biological screenings are required to fully determine the potential toxicity of this group of compounds. Screening using mammalian cells may give a more reliable indication on toxicity and the effect upon acute exposure to the test compounds. However, chronic exposure to oxazolopyridine in more complex organisms such as in animal models and humans are required to fully understand its pharmacokinetic and adverse toxicities.

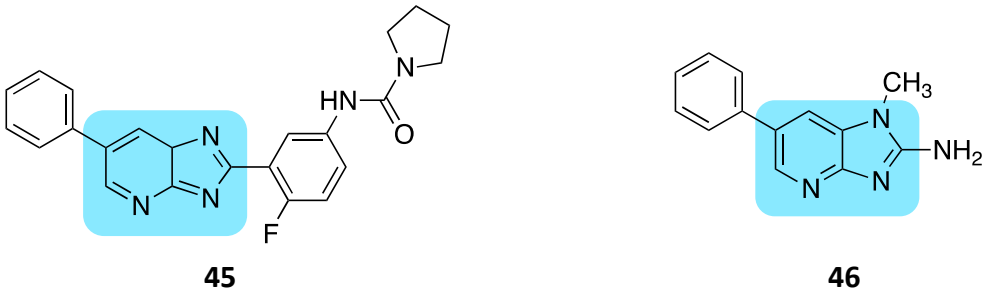

45 **46**

Figure 6: Structural similarities (blue box) of the anti-parasitic 2-arylimidazopyridine **45** as reported previously [39] and the carcinogen, PhIP **46**.

1.2 PhIP, a carcinogenic heterocyclic amine

1.2.1 Introduction to carcinogenic heterocyclic amines

Numerous amides and amines are found in the smoke emitted from industrial areas, cigarette and the burning of meat products such as beef, chicken or fish [42]. These compounds are converted into heterocyclic amines (HCAs) via incomplete combustion and nitroreduction [43] and 2-amino-1-methyl-6-phenylimidazo[4,5-b]pyridine (PhIP) belongs to this group of compounds. HCAs have been found to be mutagenic when tested on *Salmonella thyphimurium* TA98 in the Ames test. HCAs are classified into six main classes (Figure 7).

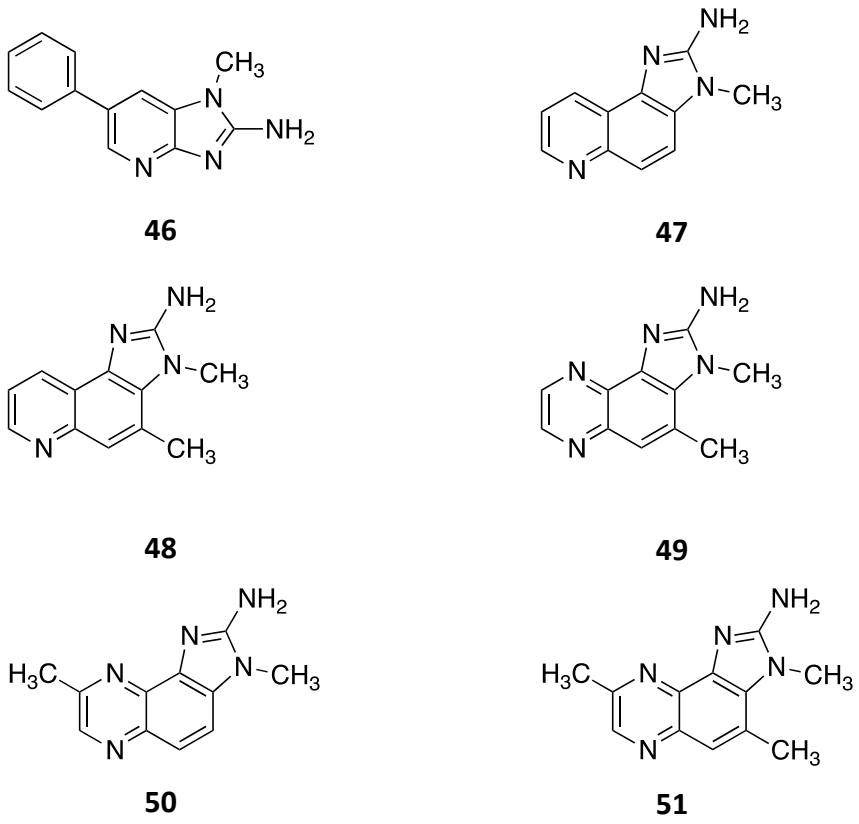

Figure 7: The six classes of heterocyclic amines. Heterocyclic amines can be divided into: 2-amino-1-methyl-6-phenylimidazo[4,5-b]pyridine (PhIP) **46**, 2-amino-3-methylimidazo[4,5-*f*]quinoline (IQ) **47**, 2-amino-3,4-dimethylimidazo[4,5-*f*]quinoline (MeIQ) **48**, 2-amino-3-methylimidazo[4,5-*f*]quinoxaline (IQx) **49**, 2-amino-3,8-dimethylimidazo[4,5-*f*]quinoxaline (MeIQx) **50** and 2-amino-3,4,8-trimethylimidazo[4,5-*f*]quinoxaline (DiMeIQx) **51**.

1.2.2 Carcinogen derived from food, PhIP 46

The most abundant and common HCAs derived from the cooking of meat are PhIP, **46** and MeIQX, **50** [44]. Creatine or creatinine in meat are converted to HCAs when heated at high temperatures during grilling or roasting through the Maillard reaction [45]. The *N*-methyl-amino-imidazo moiety of PhIP, **46** is derived from creatine or creatinine while the source of the other rings are derived from amino acids and monosaccharides often found in flavourings and other marinades added to the meat [46,47]. The amount of PhIP **46** detected in meat usually ranges from nearly undetectable levels to levels as high as a few hundred nano grams per gram of meat depending on the cooking method [48]. For example, the composition of food additives affect the amount of PhIP **46** formed during cooking. It was found that the amount of amino acids and sugars in marinades added during the cooking of meat correlated with the amount of PhIP **46** detected [49]. Cooking temperatures also play an important role where temperature-dependent increases in PhIP **46** were detected between 160- 250 °C [50].

The discovery that cooking of meat produced compounds which are mutagenic have led to a series of studies conducted on this group of compounds. Through the Ames test and analytical techniques, it was found that the main causative agent is PhIP **46** and this has led to the intensive research in this area using animal models and human studies [51,52] . In support of this finding, increased incidence of tumours was reported in rats exposed to PhIP **46** [53]. Specifically, the mutagen targeted the mammary glands in female rats, prostate glands and colon in male rats and lymphoid cells in both males and females [53]. Similarly, PhIP **46** also increased the incidence of lymphoma in mice regardless of gender [54]. Further studies conducted on rats have revealed that PhIP **46** potently targeted the prostate and seminal vesicles in male rats leading to the formation of tumours at those regions [55,56].

In humans, there was a correlation between the incidence of cancer and the type of food frequently consumed. The high intake of grilled meat has been associated with an increased incidence of cancer affecting the colorectal region [57] and stomach [58] and the high intake of fried food has been associated with higher risk of lung cancer [59]. The high intake of HCAs derived from food has been associated with breast cancer affecting the female population [60]. In the male population, the intake of PhIP **46** has been associated with an increased risk in prostate cancer by 1.2-fold [61]. The increased risk of various cancers with the intake of cooked meat and processed meat in humans has been widely reported (Table 2).

The association of cancer with PhIP **46** has been long established with the accepted mode of action understood to involve the formation of mutagenic PhIP-DNA adducts in non-malignant cells leading to the formation of cancer [52].

Table 2: Association of different types of cancer with the intake of cooked meat in humans

Site of cancer	Findings*	N (Age or gender group if stated)	References
Colon	OR = 1.8	2707 (Above 30)	[62]
	RR = 2.0	13894 (male)	[63]
	OR = 2.0	1658 (40-80)	[64]
	OR = 1.4	3402 (30-79, male)	[65]
Colorectal	HR = 1.4	519978 (35-70)	[66]
	OR = 4.6	893 (23-80)	[67]
	OR = 2.0	2164 (45-80)	[68]
	OR = 8.8	1454	[69]
	OR = 4.4	460 (20-88)	[70]
Lung	RR = 1.2	5368	[71]
	OR = 1.7	900	[72]
Breast	RR = 1.1	31552	[73]
	OR = 1.5	4089 (25-75, female)	[74]
	HR = 1.6	35372 (35-69, female)	[75]
	OR = 2.4	635 (female)	[76]
	OR = 1.9	3015 (25-64, female)	[77]
	OR = 3.4	683 (post-menopause)	[78]
Prostate	HR = 1.1	175343 (50-71, male)	[79]
	HR = 1.5	3892 (Above 35, male)	[80]
	RR = 1.4	29361 (55-74, male)	[61]
	OR = 8.3	923	[81]
	RR = 1.6	51529 (40-75, male)	[82]
	Positive correlation	787	[83]
Bladder	HR = 1.2	300933 (50-71)	[84]
	HR = 1.1	82002	[85]
	RR = 1.6 (bacon)	173229 (30-75)	[86]
	OR = 2.7	720 (40-89)	[87]
Stomach	HR = 1.7	61433 (Female)	[88]
	RR = 1.3 (bacon)	120852 (55-69)	[89]
	OR = 1.6	8735 (Below 75)	[90]
Pancreas	OR = 2.2	867 (20-65)	[91]

1.2.3 The formation of PhIP-DNA adduct

PhIP **46** is a pro-carcinogen whereby metabolic bio-activation in the liver is required for its carcinogenicity. The liver produces metabolic enzymes which are involved in the chemical modification of xenobiotics mainly for detoxification and excretion and can be divided into two phases (Figure 8) depending on their roles.

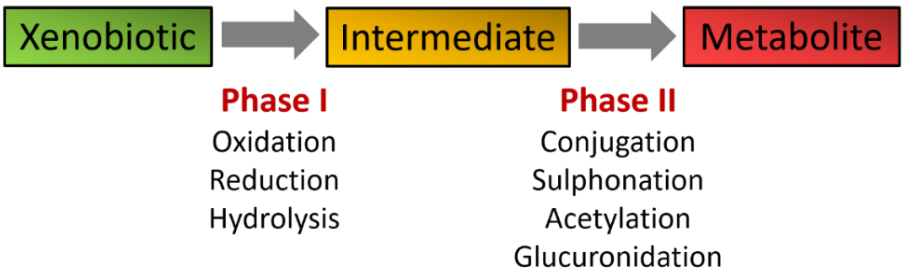

Figure 8: Flow diagram to show the metabolism of xenobiotics by liver enzymes. Metabolism catalysed by microsomes in the liver can be categorised into phase I reactions such as oxidation, hydrolysis, reduction and phase II reactions such as conjugation, sulphonation, acetylation and glucuronidation.

The current understanding on the activation of PhIP **46** is through phase I hepatic cytochrome P450-mediated *N*-hydroxylation and proceeded by phase-II esterification of the *N*-hydroxylamines into reactive hydroxamate esters which are reactive and covalently bind to DNA causing DNA damage (Figure 9). In phase I, the exocyclic primary amino group of PhIP **46** is converted into a hydroxyamino group to give PhIP *N*-hydroxylamine **52** by cytochrome P450 (CYP) 1A2 due to its high specificity and catalytic activity for *N*-hydroxylation [92,93] (Figure 9). Other cytochrome P450 species such as CYP1A1, CYP1B1, CYP2A3 and CYP3A4 are involved in the *N*-hydroxylation reaction but at a lower capacity [94-98]. The PhIP *N*-hydroxylamine **52** reacts poorly with DNA and undergoes esterification by phase II enzymes namely *N*-acetyltransferase (NAT), sulfotransferase, prolyl tRNA synthetase and phosphorylase to give rise to PhIP esters **53** such as *N*-acetoxy, *N*-sulphonyloxy, *N*-prolyloxy and *N*-phosphatyl [99-101] (Figure 9).

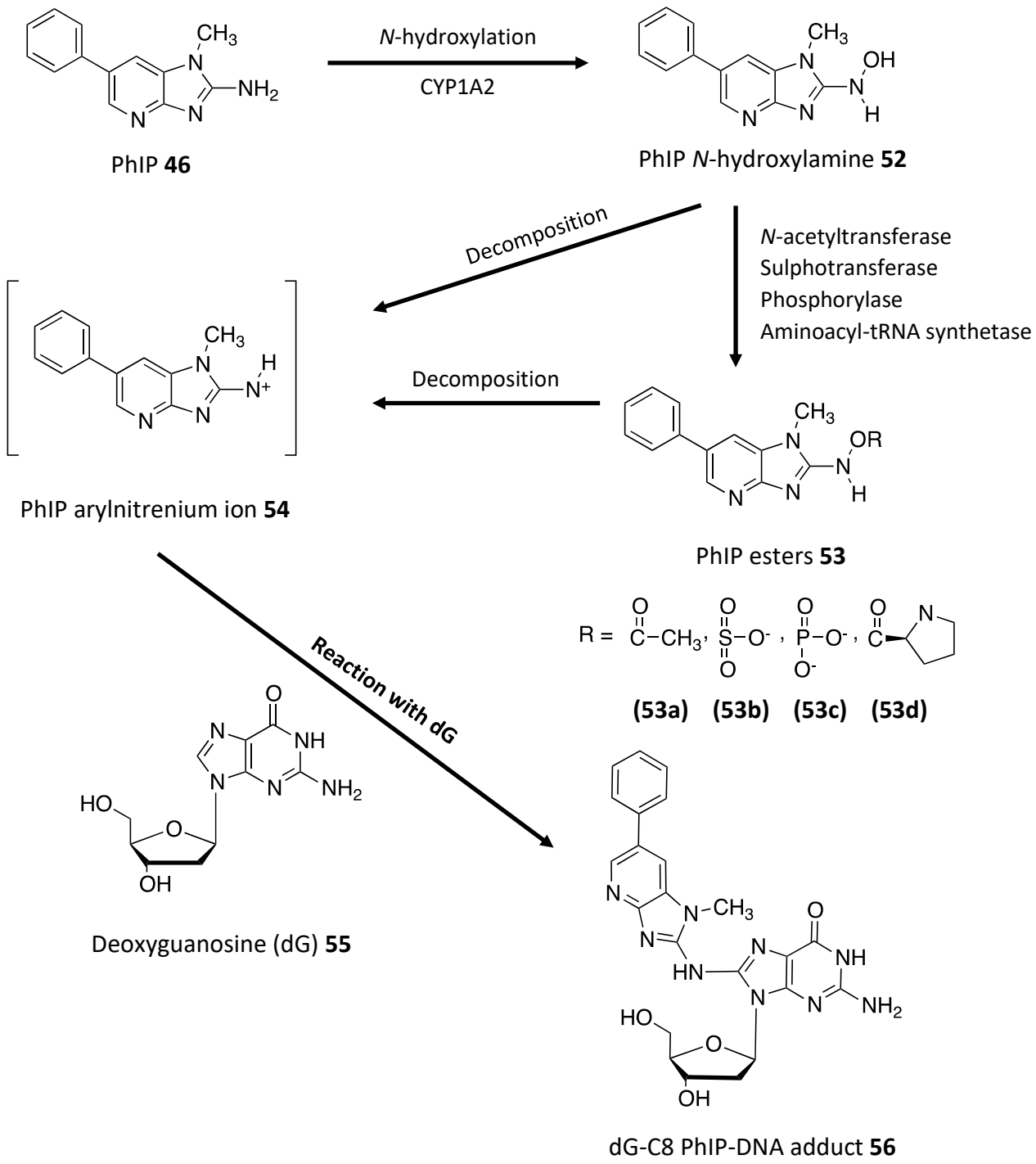

Figure 9: Schematic representation of the formation of PhIP-DNA adduct. The bio-activation of PhIP **46** is initiated via *N*-hydroxylation by CYP1A2 to form the *N*-hydroxy PhIP **52** intermediate. The *N*-hydroxy PhIP **52** undergoes esterification to form PhIP esters **53** and then decomposition to form the reactive intermediate, PhIP arylnitrenium ion **54**. The PhIP arylnitrenium ion **54** reacts with deoxyguanosine **55** to give the dG-C8 PhIP-DNA adduct **56**.

NAT is the major enzyme involved in the esterification of PhIP and HCAs mainly by NAT1 and NAT2 isoforms. Among the two isoforms, *N*-hydroxylamines more readily bind to NAT2 where the precursor undergoes *O*-acetylation to form the *N*-acetoxy metabolites [102,103]. The PhIP *N*-acetoxy esters **53** produced are transient where the ester moieties of these metabolites serve as leaving groups to giving rise to electrophilic PhIP arylnitrenium ions **54** (Figure 9). The PhIP arylnitrenium ion **54** reacts with the nucleophilic DNA base (with preference for dG **55**) [52,104] (Figure 9). It has been considered for many years that the generation of PhIP arylnitrenium ion **54** is only through the activity of phase II enzymes. However, the PhIP arylnitrenium ions **54** can also be generated from PhIP *N*-hydroxylamines **52** through the protonation of the *N*-hydroxylamino group [105,106]. The PhIP arylnitrenium ion **54** forms a covalent bond (an N-C bond) with the C8 of dG, **55** hence forming a dG-C8 PhIP-DNA adduct **56** [107-112] which is the basis for its DNA damaging ability (Figure 9). The arylnitrenium ion is the mode of action of PhIP and other HCAs that cause DNA damage.

The levels of the phase I enzyme, particularly CYP1A2, determines the activation of PhIP **46**. The liver is the main site for bio-activation and metabolism *in vivo* of PhIP **46** and other HCAs due to the high expression of CYP1A2 enzymes [93]. The level of CYP1A2 expression in the liver has been shown to affect the PhIP-DNA adduct levels in both hepatic and extrahepatic tissues. Studies conducted in rodents and monkeys have shown that in animals with overexpression of CYP1A2 and treated with PhIP **46**, the levels of PhIP-DNA adducts in hepatic and extrahepatic tissues increased [113-115]. This highlights the importance of the *N*-hydroxylation step in the activation of PhIP **46**. However, PhIP-DNA adducts were also detected in extrahepatic tissues with lower metabolic capacity such as the colon in rats fed with PhIP **46** [115]. *N*-Acetoxy-PhIP **53a** was also found in blood samples of the rat which indicates that the PhIP metabolites produced in the liver can leave the liver and circulate in the

bloodstream and affect other organs [115]. PhIP-DNA adducts were also reported in other organs such as the mammary gland [116]. In the urinary bladder, PhIP-DNA adducts were not detected in rats which also implies that the non-conjugated *N*-hydroxylamines are not excreted through the urine [117].

Extrahepatic phase II enzymes also contribute to the bio-activation of PhIP **46** leading to formation of PhIP-DNA adducts in other tissues where they are involved in the modification of *N*-hydroxylamines and *N*-acetoxy derivatives in the bloodstream or those generated *in situ* [115,116,118]. Although the expression of phase I enzymes such as cytochrome P450 are lower in extrahepatic tissues, this does not apply to phase II enzymes where the rate of esterification reactions by these enzymes in extrahepatic tissues matches that of the liver or are even higher [114-116]. In female rats, the rate of enzymatic activity of NAT in the esterification of *N*-hydroxy-PhIP **52** was found to be 16 times higher in the mammary glands than the liver [116]. The level of PhIP-DNA adducts detected in the mammary glands were 10 times higher than in the liver [116,119]. The expression of NAT1 and NAT2 were detected in human mammary epithelial cells where the catalytic activity of NAT1 enzymes for the *N*-hydroxy-PhIP **52** metabolite was reported [120,121]. Sulphotransferases were also reported to be expressed in the human mammary epithelial cells, where both NAT1 and sulphotransferases contributed to the increase in PhIP-DNA adducts in those cells upon exposure to PhIP **46** [121,122].

1.2.4 Mutagenic properties of PhIP

In the bacterial cells, the presence of DNA adducts has been used as an indicator of the severity of mutagenesis [52,123]. The presence of these adducts has been shown to be associated in the increase in mutagenicity in the *Salmonella* system. The induction of mutagenicity in *Salmonella* TA98 was found to be very efficient where around 25 adducts are required to cause a mutation event [123]. In *Salmonella* TA1538, the preference of PhIP **46** for guanine in DNA

adduct formation was verified through the deletion of GC in a run of GCs in the histidine (*hisD*) gene [124,125]. Moreover, in *Salmonella* TA100 used to evaluate base substitution specificity, GC→TA transversion was predominantly detected where the error-prone bypass of the dG-C8 adduct appeared to be related to the induction of this type of mutation [126]. The lack in affinity for other DNA bases commonly associated with mutagenesis such as adenine was also verified using other Salmonella strains which are specific for AT frameshift alterations [127].

In mammalian cells, PhIP **46** is a potent DNA damaging agent where it has been associated with the formation of DNA adduct formation, DNA strand breaks and chromosomal aberrations [128,129]. While the predominant mode of action for mutagenesis in *Salmonella* systems is frameshift mutations, base substitutions at guanine bases have been reported to be more common in mammalian cells. Mutations induced by PhIP **46** have been evaluated in Chinese hamster ovary (CHO) cells through the hypoxanthine phosphoribosyltransferase (*hprt*), dihydrofolate reductase (*dhfr*) and adenine phosphoribosyltransferase (*aprt*) genes and in lymphoblastoid cells through the *hprt* gene. In these studies, G→T transversion occurred most frequently with preference for guanine nucleotides adjacent to other guanine or adenine nucleotides. In cells with proficient DNA repairing capabilities, approximately 25% of the mutations caused by PhIP **46** occurred at guanine specifically at the 5'-GCAGA-3' sequence detected in the tyrosine amber suppressor tRNA (*supF*) vector. Similarly, in CHO cells via the *dhfr* gene, mutations at guanine nucleotides were detected mainly at the CAGG sequence while one of the mutants contained mutations at the CAGA sequence. Frameshift mutations induced by HCAs in mammalian cells have been detected and similar to the base substitution scenario, guanine nucleotides adjacent to other guanine or adenine nucleotides were affected. A guanine deletion causing a -1 frameshift mutation has been reported in CHO cells exposed to PhIP **46** which accounted for approximately 57% of the frameshift mutations detected in that study.

The role of PhIP-DNA adducts in mutation was further studied using the *supF* shuttle vector in mammalian cells. It was reported that the frequency of mutation linearly increased with the levels of PhIP-DNA adducts where 85-93% of the mutations induced consisted of base substitutions while the remainder were base deletions. Further analysis using ^{32}P-post-labelling of the *supF* plasmid revealed that PhIP **46** preferentially formed adducts with guanine nucleotides with dG-C8 PhIP-DNA adducts **56** forming the majority of it. The guanine adducts formed with PhIP were also found to be distributed in a non-random manner in the *supF* plasmid where the adduct concentrations differed between guanine sites. Mutations were detected at the adduct sites where adduct concentrations did not affect the presence of mutations at a particular site. While these studies reported mainly on GC→TA transversion-type of base substitution, a site-specific mutagenesis study using oligodeoxynucleotides with a single dG (5'-TCCTCCTXGCCTCTC-3', where X= A,T,C or G) reported that dG-C8 PhIP-DNA adducts **56** were involved in G→T transversions [130].

In animals, cytogenic assays to detect for chromosomal aberrations, exchanges of sister chromatid and micronucleated normochromatic erythrocytes have been conducted on peripheral and bone marrow samples from rodents dosed with HCAs. These studies reported that HCAs and their respective adducts are weakly clastogenic *in vivo* where alteration in the chromosomal structure was not detected [131-135]. Consistent with findings *in vitro*, HCAs have been reported to cause base modifications namely substitution and/or deletion *in vivo* in transgenic mice using the lac repressor (*lacI*) or β-galactosidase (*lacZ*) reporter genes for mutation, where the majority of these reports were on PhIP **46** and MeIQX **50** [131,136-140]. Similar findings were also reported in mouse colonic crypt cells [141-143] and in a microbial animal-mediated assay system [144].

1.3 Cellular response to DNA damage

1.3.1 DNA repair mechanism following base modifications

The formation of DNA adducts following base modification is repaired via two mechanisms namely the base excision repair (BER) and nucleotide excision repair (NER) [145,146]. Out of the two, BER is the pre-dominant repair mechanism, which is initiated by the activation of DNA glycosylases [145]. The damaged base (in the case of HCA-induced damage it is guanine) is removed from the DNA structure by cleaving of the *N*-glycosidic bond, which links the damaged base to the deoxyribose of the DNA backbone structure. Despite the fact that DNA glycosylases have diverse structures, they act in a similar fashion. This involves a base flipping mechanism where the targeted damaged base is 'flipped' to an extra helical position away from the DNA to allow the cleavage of the *N*-glycosidic bond [147]. The resulting intermediate product of BER is the formation of apurinic/apyrimidic (AP) or abasic sites which are repaired by apurinic/apyrimidic endonuclease I (APE1) [148,149]. The role of APE1 is to cleave the phosphodiester bond rapidly at the 5' direction towards the AP site which in turn creates a single-strand break with exposed 3'-OH and 5'-deoxyribose phosphate termini [150]. In addition, some glycosylases have associated AP lyase activity, which targets the AP site via β-elimination and result in the formation of a 3'-phospho-α,β-unsaturated aldehyde and 5'-phosphate [151]. The endonuclease VIII-like type I (NEIL1) and type II (NEIL2) enzymes belong to the family of these bifunctional glycosylases that are specific for oxidised bases. They therefore target the AP sites and facilitate β- and δ- eliminations, where 3'-phospho-α and β-unsaturated aldehydes are converted to 3'-phosphates [151].

Irrespective of whether the AP sites are targeted by APE1 or bifunctional glycosylases, the cleavage of the phosphodiester bond results in the formation of a BER intermediate strand, which consists of 3'- and 5' blocking lesions [152]. To finalise DNA repair via DNA synthesis

and ligation by DNA polymerase and DNA ligase, these lesions need to be removed. APE1 is also a bi-functional enzyme in the BER pathway and has the 3'-phosphodiesterase activity. This allows the restoration of 3'-OH termini from 3'-phospho-α and β-unsaturated aldehyde lesions generated by glycosylases. In contrast, 3'-phosphate lesions generated by NEIL1 and NEIL2 are converted to 3'-OH by polynucleotide kinase phosphatase (PNKP), which has 3'-phosphatase activity [150,153]. Finally, the 5'-deoxyribose phosphate termini is removed by DNA polymerase β with its associated 5'-deoxyribose phosphate lyase activity [153].

Following the removal of the DNA lesions, DNA polymerase and DNA ligase are recruited to the sites of damage to allow the replacement of the nucleotide on the single strand breaks (i.e the sites of repair) formed in the process of BER. There are two pathways that replace nucleotides at sites of DNA damage namely short-patch BER and long-patch BER [154]. Short-patch BER constitutes 80-90% of cellular BER and involves single nucleotide gap filling. The 5'-deoxyribose phosphate termini is removed by DNA polymerase β during DNA synthesis, while ligation of the incorporated nucleotide is carried out by DNA ligase I or III and the X-ray repair cross-complementing protein (XRCC1) [154,155]. In contrast, long-patch BER involves the filling of a multiple nucleotide gap and is initiated due to 5'-blocking lesions that DNA polymerase β lyase activity. Long-patch BER involves DNA polymerase δ and ε, flap endonuclease I (FEN1), replication factor C (RFC), proliferating cell nuclear antigen (PCNA) and DNA ligase I [154,155]. The 3'-OH termini are elongated by the incorporation of nucleotides into the gap, while the 5'-lesion is removed by DNA polymerase β,δ and ε in the presence of PCNA. This results in the formation of 'flap' oligonucleotide which is then removed by FEN1 before DNA ligase I sequentially repairs the DNA strand via DNA ligation [151,155,156].

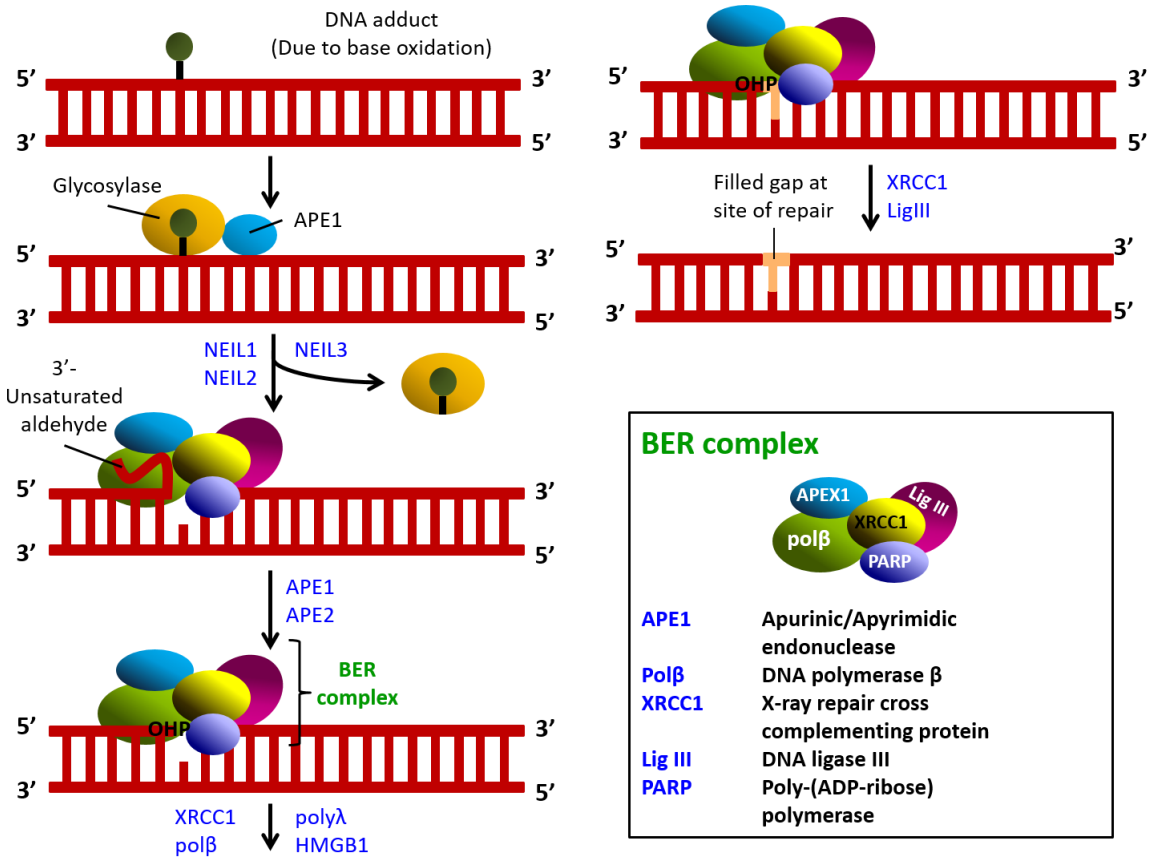

Figure 10: Schematic representation of short-patch base excision repair (BER). A DNA adduct is removed by the sequential activity of APE1, NEIL1, NEIL2, DNA polymerase, DNA ligase and XRCC1. [Abbreviations not mentioned in the figure: NEIL 1 (Endonuclease VIII-like), polyλ (DNA polymerase λ), HMGB1 (High-mobility group protein B1) and OHP (OH terminal)].

Other secondary proteins are also involved in the BER repair cascade. XRCC1 is involved as a molecular scaffold, which aids in the assembly of the enzymes involved in the BER cascade which includes DNA glycosylases, APE1, DNA polymerase β, PNKP, DNA ligase III and aprataxin [157] (Figure 10). XRCC1 binds to the nicked and gapped DNA at its *N*-terminal domain which allows the recruitment of the BER enzymes [158]. Poly-ADP ribose polymerase 1 (PARP1) binds to XRCC1 in response to DNA damage and acts in a synergistic manner. PARP1 also detects DNA strand breaks and activates itself and modifies other protein substrates by rapid ADP-ribosylation. This post-translational protein modification allows the recruitment of XRCC1 to the sites of DNA damage and activate XRCC1. Due to the negative

charge of the activated poly-(ADP-ribose) residues, PARP1 slowly detaches from the DNA structure to allow the recruitment of other BER proteins to the site of repair [159] (Figure 10).

1.3.2 Base excision repair leading to the formation of double strand breaks

DNA adducts are typically considered less detrimental to DNA structure and cell survival compared to DNA double strand breaks (DSBs). However, in most instances more than one DNA adduct will occur, some of them in close vicinity, which can lead to clustered DNA damage. If these sites are opposed to each other, near simultaneous BER on opposing strands can lead to two DNA single strand breaks (SSBs) which indirectly produce a DSB [160] (Figure 11). This is supported by numerous *in vitro* studies using DNA plasmids where DSBs were formed when the irradiated DNA plasmids have been treated with end lesion recognising enzymes [161-164]. Clustered DNA damage in bacterial cells that is repaired via the BER pathway was reported to give rise to DSBs [165]. Glycosylases involved in BER facilitate this conversion since DSBs were detected in wild type cells but not in mutant cells that lacked these enzymes [165]. Similar results were obtained from gamma-irradiated human cells [166]. Cells with down-regulated expression of the two major glycosylases, human endonuclease III (hNTH1) and human 8-oxoguanine DNA N-glycosylase I (hOGG1) showed less radiation-induced cytotoxicity and were less prone to show DSBs [166].

Cells are able to overcome the induced DNA damage to maintain survival using nucleosomes which suppress the formation of DSBs caused by BER. However, this suppression is not efficient and only work to a certain extent depending upon factors such as the type of lesion or DNA glycosylase involved, the orientation of the oxidative lesion with reference to the histone octamer, the distance between the lesion cluster and the local sequence and the stagger between opposing lesions found on the DNA strand determine the rate of suppression [167]. PARP-1 was also found to reduce the frequency of the production of DSBs from clustered DNA damage by

extending the ability of BER enzymes to process DNA single strand breaks [168]. Taking these into consideration, the formation of DSBs is not a straight-forward one and can arise from many factors.

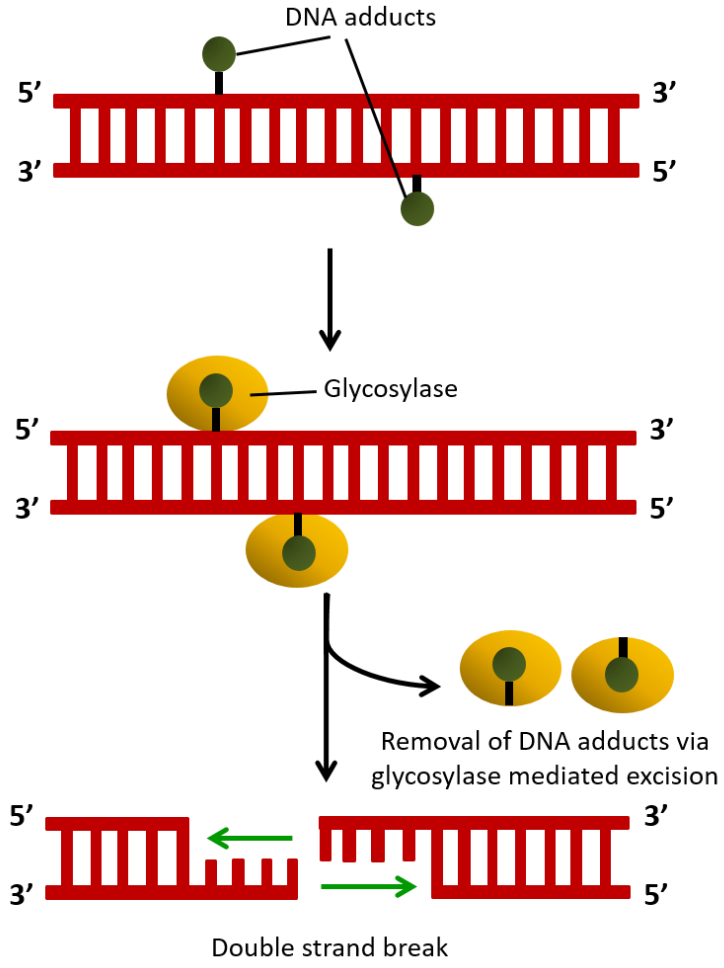

Figure 11: Schematic representation on the formation of DSBs from clustered DNA damages. The simultaneous occurrence of two opposing BER events and the activity of the glycosylases result in the formation of DSBs.

1.3.3 The formation of γH_2AX foci following DSBs and its significance

Upon the formation of DSBs, a cascade of reactions take place involving various proteins to maintain the genomic integrity but also to reduce the probability of mutagenesis which will lead to cell death or carcinogenesis [169] (Figure 10). One protein which is of interest is the H_2A in histone, which is bound to the chromosomal DNA in mammalian cells [170]. The H_2A protein is rapidly modified by phosphorylation within seconds after the formation of DSBs resulting in the formation of a γH_2AX complex [171]. Therefore, detection of the γH_2AX complex is a good indicator for DNA damage in cells. The mechanism of modification of this protein will be explained in detail in this section.

The γH_2AX complex is formed when serine 139 (S139) on the carboxy-terminal tail of the H_2AX histone variant is rapidly phosphorylated by the ataxia telangiectasia mutated (ATM) kinase or ataxia telangiectasia mutated Rad3 related (ATR) in response to DNA damage [171,172] (Figure 12). The formation of this complex ensures that a microenvironment is generated to recruit different repair proteins in the form of the breast cancer I (BRCA1), mediator of DNA damage checkpoint (MDC1), tumour suppressor p-53 binding protein I (53BP1) and Rad51 to the site of DNA damage for repair [173] (Figure 12). Despite many studies aimed at understanding the regulation of the formation of the γH_2AX complex, it is still poorly understood to date. While preliminary studies have been focused mainly on the identification of the repair proteins and histone modifications downstream of the γH_2AX complex, other studies have identified that upstream modifications play an important role in the regulatory mechanism [174]. For example, tyrosine 142 (Y142) on the carboxy-terminal tail of the H_2AX, situated only three amino acids away from S139 is phosphorylated prior to DNA damage. Once DNA damage is sensed, Y142 first has to be dephosphorylated, which is a prerequisite for the phosphorylation of S139 by ATM/ATR [174,175].

The formation of γH$_2$AX is extremely rapid and is the immediate response following DNA damage [176]. The γH$_2$AX therefore acts as an intermediate prior to the recruitment of other repair machineries to restore the damage at the site such as homologous recombination and non-homologues end joining depending on the nature of the DSB formed on the DNA [177]. The γH$_2$AX is therefore seen as a bio-marker of DNA damage and repair [176]. In DNA repair studies, cells were irradiated to induce DNA damage and was verified through the detection of γH$_2$AX proteins on the DNA [178-180]. These lesions were found to be repaired rapidly *in vitro*, typically within 24 hours shown by the reduced detection of γH$_2$AX proteins [178-180]. Therefore, this allowed colonogenic survival of the cells tested [179].

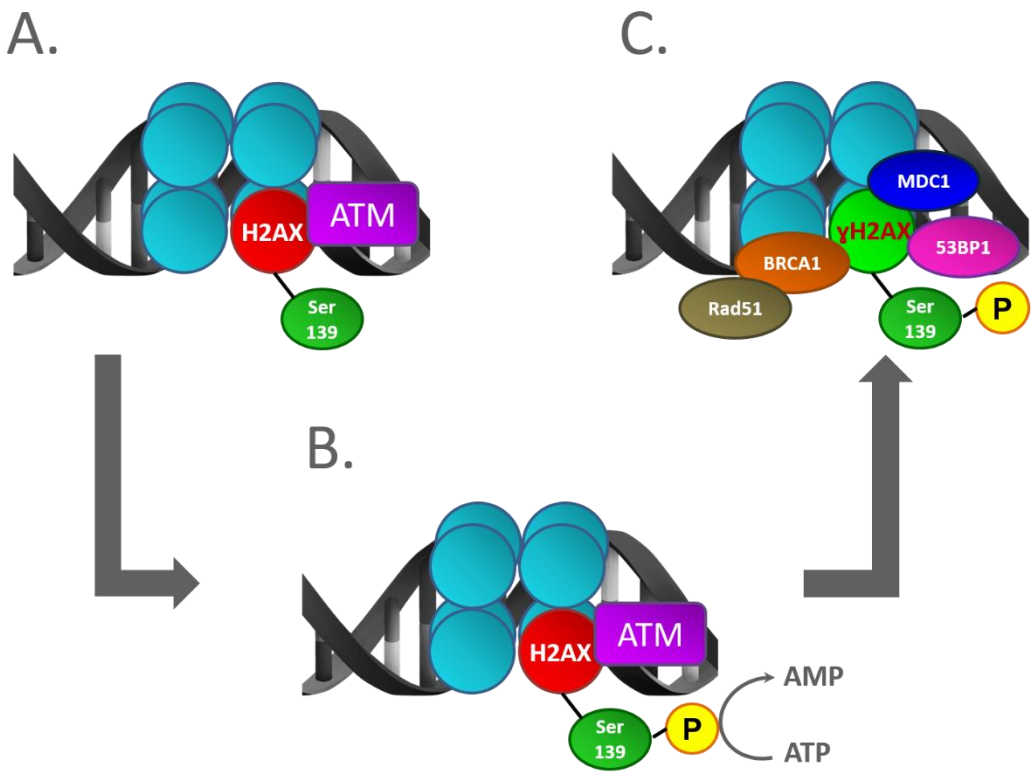

Figure 12: Schematic representation of the formation of γH2AX protein complex during repair of DNA damage. Upon the detection of a DSB; (A) Ataxia telangiectasia mutated (ATM) kinase binds to the site of DNA damage, (B) The carboxy terminal of S139 in H2AX is rapidly phosphorylated by ATM forming γH$_2$AX and (C) The γH$_2$AX complex formation recruits other repair proteins such as breast cancer I (BRCA1), mediator of DNA damage checkpoint (MDC1), tumour suppressor p-53 binding protein 1 (53BP1) and Rad51 to the site.

1.3.4 Consequences of DNA mutations leading to cancer development

Gene mutations arising from erroneous cellular DNA repair do not necessarily lead to the development of cancer. Cells can employ strategies to remove these mutations to maintain genomic integrity by utilising DNA polymerases for DNA replication proof-reading [181] or post-replication DNA repair pathways such as trans-lesion synthesis (TLS) and template switching (TS) [182,183]. However, mutations on the DNA polymerase genes will not only alter the proof-reading capabilities of the enzyme but further exacerbate the problem by wrongly incorporating nucleotides amplifying the amount of mutations. Mutations of DNA polymerase genes such as DNA polymerase delta I (*POLD1*) and DNA polymerase epsilon (*POLE*) have been associated with polymerase associated polyposis (PPAP) in colorectal adenomas and carcinomas [181,184]. An inactivating mutation of DNA polymerase kappa (*POLK*) was found to cause erroneous TLS repair leading to the development of cancer in cells exposed to carcinogens [185].

Another consequence of mutation is the overexpression of B-cell lymphoma II (BCL2) proteins which inhibit cell death. The mutation of the *BCL2* family gene has been associated with the translocation and activation of the BCL2 protein linked to the development of B-cell lymphoma [186,187], prostate [188], breast [189] and colorectal [190] cancers. BCL2 proteins have been identified to localise at the outer mitochondrial membrane [191,192]. This in turn affects mitochondrial integrity, which inhibits the release of mitochondrial cytochrome c (cyt c), a prerequisite for apoptotic cell death [193]. Mutations of proto-oncogenes in cells result in oncogenes, which transform normal cells to become cancerous [194]. Oncogenes are typically overexpressed to produce proteins, which stimulate cell division, inhibit cell differentiation and prevent cell death [194]. The mutation of proto-oncogenes has been associated with different types of cancer (Table 3).

Table 3: Mutation of proto-oncogenes in the development of human cancers.

Proto-oncogene	Protein function	Type of mutation	Associated cancers	References
Retrovirus associated (*RAS*) family [*KRAS*, *HRAS* and *NRAS*].	Signal transduction during mitosis.	Mutation in codons 12, 13 or 61.	Lung, colorectal, pancreatic, oral carcinoma and leukaemia.	195-198
Rearranged during transfection (*RET*).	Tyrosine kinase receptor.	Activating point mutation.	Thyroid.	199
Sarcoma (*SRC*).	Non-receptor tyrosine kinase.	Mutation in codon 531.	Colorectal.	200,201
Rapidly accelerated fibrosarcoma homolog B (*BRAF*).	Serine/threonine kinase.	Activating point mutation.	Melanoma, colorectal and thyroid.	202-204

Gene mutations are not only involved in activating proto-oncogenes but also the inhibition of tumour suppressor (TS) genes in cancer development. TS genes regulate cell growth by inhibiting cell proliferation and tumour development [205]. Cells respond to gene mutations by undergoing apoptopic cell death as a result of TS gene activation [206]. In cancer cells, TS genes are typically mutated, which removes negative regulators of cell proliferation resulting in abnormal cell proliferation and in the development of solid tumours [205]. The inhibition of TS genes has been associated with different types of cancers due to the absence of the regulatory proteins they encode (Table 4).

Table 4: Mutation of some TS genes in the development of human cancers [207,208].

TS gene	Protein function	Associated cancers
Tumour protein p53 (*p53*)	DNA transcription factor and cell cycle and apoptosis regulator.	Most forms of sporadic tumours.
E-cadherin	Intercellular communications and signal transduction activation of *p53*.	Most forms of sporadic tumours.
Adenomatous polyposis coli (*APC*)	Inactivation of cytoplasmic β-catenin and prevents the formation of the DNA transcription complex.	Colorectal and familial adenomatous polyposis.
BRCA1	Activates *p53* and other DNA transcription factors and involved in DNA repair by binding to Rad51.	Breast and ovary.
Breast cancer II (*BRCA2*)	Transcription factor with histone acetyl-transferase activity and involved in DNA repair by binding to Rad51.	Breast and ovary.
Von Hippel-Lindau (*VHL*)	Suppresses the expression of vascular endothelium growth factor (*VEGF*) gene.	Clear-cell carcinoma and von Hippel-Lindau syndrome.
Neurofibromin I (*NF1*)	Inactivates the *RAS* oncogene.	Neurofibromas.
Neurofibromin II (*NF2*)	Involved in membrane-cytoskeleton interactions.	Schwannomas and meningiomas.

Cancer development, although typically multi-factoral, shares one thing where gene mutations are the pre-requisite for the onset of cancer. The main strategy to minimise human exposure to mutagens is to conduct stringent toxicology screening of environmental chemicals, pharmaceuticals and food products using guidelines established by the regulatory bodies.

1.4 Screening for mutagens and carcinogens

1.4.1 *In vitro* toxicology screening of compounds in drug discovery

Toxicology screening plays an important role in the field of drug discovery to evaluate the safety of compounds isolated from natural sources, crude extracts and novel chemical entities. The United States Food and Drug Administration (USFDA) demands comprehensive toxicity screens for drug and food products before they are allowed to be marketed. Whether the tested compounds have protective or deleterious effects, *in vitro* screening is conducted prior to testing in more complex systems such as animal models and human clinical trials. Moreover, *in vitro* results can provide a rapid indication of the toxicity profile of the compound before its use in animals and humans, which conforms to ethical principles and is also a significant economic consideration. The cytotoxicity profile together with the pharmacokinetics of a compound are important to estimate dose ranges to be tested in pre-clinical models and subsequently in patients. The IC_{50} is used as a measure of cytotoxicity if the test compound follows a dose-dependent response within the tested range. A wide array of assays are used to determine cell viability by measuring different end-points. These assays are commonly divided into the measurements of cell proliferation, metabolic activity and plasma membrane integrity (Table 5).

Table 5: Assays commonly used in the determination of cell viability, principle and limitations.

Assay	Principle of measurement	Limitations
Cell proliferation assays		
Colony formation assay	Considered the "gold standard" in the determination of cell viability [209]. Measures the reproductive integrity of the cells, testing the ability of cells to undergo unlimited divisions to form colonies of at least 50 cells which is later enumerated [210,211].	Cannot discriminate from other natural causes of loss in cellular clonogenic potential such as apoptosis and necrosis [212]. Affected by sub-optimal growth medium, error in colony counting and loss of cell during trypsinisation [211,213]. Time consuming and does not work in all cell types.
DNA synthesis measurement	The integration of bromodeoxyuridine (BrdU) and radiolabelled (^{3}H-thymidine) nucleosides in the DNA synthesised *de novo* during cell replication indicative of cellular proliferation [214].	False positives caused by DNA repair, gene duplication and abortive cell cycle re-entry [214]. Quantification is labour intensive and radioisotopes are health hazards [215].
Metabolic activity assays		
Tetrazolium-based assays (MTT, WST-1 or similar)	Most widely used cell viability assay. Tetrazolium salts such as 3-(4,5-dimethylthiazol-2-yl)-2,5-diphenyltetrazolium bromide (MTT) and water soluble tetrazolium I (WST-1) are used as redox sensors and reduced into formazan by NADPH produced by metabolically active cells [216,217]. Formazan can be quantified spectrophotometrically and its amount	Tetrazolium can be reduced by anti-oxidants such as ascorbic acid and polyphenols and superoxides [218-220]. Pro-oxidants increases the expression of glucose-6-phosphate dehydrogenase which artificially increases NADPH levels in the cell causing survival overestimation [221]. Tetrazolium can be reduced

	is proportional to the number of metabolically active cells [216].	by high amounts of mitochondria in growth II to mitosis (G2/M) cycle arrest cells which are non-viable [222].
ATP content assay	The amount of ATP present in metabolically active cells is quantified by measuring the bioluminescence emitted by the conversion of luciferin by luciferase where ATP is the co-factor for the enzyme. The amount of light emitted is proportional to the amount of ATP in the cell [223,224].	Fatty acids, luciferin-like products and resveratrol which may be present in the growth medium inhibit luciferase activity [225]. Quenching of luminescence by test compounds may occur [212]. Direct inhibitors of enzymes of the electron transport chain in the mitochondria reduces the amount of ATP produced but not necessarily viability such as capsaicin [226] and quercetin [227].
Plasma membrane integrity		
Lactate dehydrogenase (LDH) release measurement	This method measures the release of the cytoplasmic enzyme, LDH into the supernatant of the cell culture due to cell membrane damages in non-viable cells [228]. In the assay, LDH converts lactate into pyruvate and where the co-factor, NAD^+ is reduced to NADH. The amount of NADH can be quantified using tetrazolium-based dyes [229].	LDH inhibitors that may be present in the test vessel may lead to underestimation of LDH levels such as chloroquine [230]. Detergent-like molecules like sapnonins increase the permeability of viable cell membrane leading to the leak of LDH into the supernatant which leading to overestimation [231].
Trypan blue exclusion test	Non-viable cells and cells undergoing necrosis have compromised membrane integrity which allows the penetration of the trypan blue dye into the cell staining it blue. The proportion of non-	Only detects intact non-viable cells. Compromised cell membrane integrity by detergent-like molecules may cause false positive results [230].

viable (blue) and viable (clear) cells is determined microscopically [232].	Trypan blue is a weak acid and has affinity for basic proteins where stained extracellular proteins may cause false determination of non-viable cells [233].

1.4.2 *In vitro* screening of carcinogens required by regulatory bodies

In addition to direct toxicity that leads to cell death, another type of toxicity relates to DNA integrity. Some compounds can either directly or indirectly cause DNA damage. The general perception is that all genotoxic compounds are potently cytotoxic resulting in cell death. However, this is only true to a certain degree depending on the type of DNA damage induced by the genotoxic agent. Genotoxic agents that cause detrimental types of DNA damage such as DNA double strand breaks are easily picked up during cytotoxicity screening [234]. However, genotoxic agents that cause slight modifications to the DNA by affecting DNA base and nucleotide structure can be missed during cytotoxicity screening [235]. However, it is especially these small lesions in the DNA that pose the biggest danger to the organism since base and nucleotide modifications are the major source of gene mutations [236]. Therefore, sensitive genotoxicity assays should be conducted in addition to pure cytotoxicity screening to identify mutagens and carcinogens early in the drug development process. The USFDA, International Conference on Harmonisation of Technical Requirement for Registration of Pharmaceuticals for Human Use (ICH) and Committee of Mutagenicity (COM) have provided guidelines for the genotoxicity screening of drugs and consumables [237-240] (Table 6). The general approach for genotoxicity screening should assess mutagenicity using the bacterial reverse gene mutation test, also known as the Ames test [241]. This method has the demonstrated ability to detect agents that cause genetic changes and will identify most of the known carcinogenic compounds to

humans and rodents. The second approach involves the determination of *in vitro* genotoxicity using mammalian cells and/or *in vivo* animal models [238].

Table 6: The summary of two recommended workflow options in the screening of carcinogens by the ICH and USFDA.

Recommended workflows	
Option 1	**Option 2**
i. Evaluating gene mutation in bacteria (such as Ames test via the *Salmonella* system). ii. Evaluating chromosomal damage via cytogenetic tests *in vitro* (such as chromosome aberration, micronucleus or mouse lymphoma L5178Y thymidine kinase (TK) gene mutation assays) iii. Evaluating chromosomal damage *in vivo* using rodent hematopoietic cells (for the detection of chromosomal aberrations or micronuclei in metaphase cells).	i. Evaluating gene mutation in bacteria (such as Ames test via the *Salmonella* system). ii. Evaluating genotoxicity *in vivo* using rodent hematopoietic cells (for the detection of micronuclei) and liver tissues (for the detection of DNA strand breakage).

The suggested *in vitro* screening such as the Ames test coupled with chromosome aberration, micronucleus and mouse lymphoma L5178Y TK gene mutation assays in mammalian cells are considered sufficiently validated and are commonly used. Option 1 is typically utilised during drug screening although option 2 is equally suitable since both options assess both *in vitro* and *in vivo* conditions (Table 6). Option 1 is preferred due to the high throughput capability of *in vitro* systems as compared to *in vivo* especially in the screening of large compound libraries [238]. Although a positive mutagenicity result is obtained from one *in vitro* assay, it is sufficient to reject this when negative results are obtained from at least two subsequent *in vivo* assays [238]. In the European Union (EU), animal testing of cosmetic products is prohibited by the EU 7th

Amendment Directive due to animal ethics concerns [237]. Therefore, *in vivo* screenings are not conducted and *in vitro* screens play a more important role in determining the safety of these products.

The recommended bacterial mutation assay is the Ames test which is considered the "gold standard" in genotoxicity testing and is usually conducted prior to tests on mammalian cells and rodents. The Ames test is a widely accepted short-term assay due to its simplicity and high throughput capability for screening compound libraries. This assay uses *Salmonella* strains, which have mutations in the gene for histidine synthesis, an essential amino acid needed for cell growth. Therefore, these mutated bacteria cannot grow in substrates that lack histidine. New mutations induced at the site of these pre-existing mutations or in nearby regions of the gene have the potential to restore gene function, which would allow the bacteria to synthesise histidine and to subsequently grow to form colonies. Therefore, the Ames test is referred to as a mutation reversion assay. The *Salmonella* strains used carry mutations in different genes in the histidine operon. It is important to note that these mutations were designed to respond to mutagens, which act via different mechanisms, mainly frameshift, base substitution mutations and transitions/transversions (Table 7). However, this also highlights one of the potential limitations of this assay where other mutations caused by a mutagen other than those listed cannot be picked up by this assay.

The recommended *Salmonella* strains for genotoxicity screening by USFDA are TA100, TA98, TA1535, TA1537 and TA102 [238]. USFDA guidelines stipulate that a single bacterial mutation Ames test which clearly shows the presence of a mutation is sufficient and repeats using other *Salmonella* strains are not required [238]. The TA98 and TA100 strains are commonly used in screens as they can accurately determine up to 90% of population mutagens [242,243]. Subsequently, *in vitro* screens using mammalian cells are conducted to complement or confirm the findings of the Ames test. This involves the detection of chromosomal changes by detecting

chromosomal aberrations, micronuclei but also by mutation detection in the mouse lymphoma L5178Y TK reporter gene [238,240].

Table 7: The different type of genes which are manipulated in *Salmonella* strains used in the Ames test and type of mutations these strains are used to detect [244].

Allele	*Salmonella* strain	DNA target sequence	Type of mutation
hisG46	TA100 , TA1535	GGG	Base pair substitution
hisD3052	TA98 , TA1538	CGCGCGCG	Frameshift
hisC3076	TA1537	+1 frameshift near CCC run	Frameshift
hisD6610	TA97	+1 cytosine at a run of Cs	Frameshift
hisG428	TA102 , TA104	TAA (ochre)	Transitions/transversions

Micronuclei are whole chromosomes or chromosome fragments that are left behind during mitotic cell division. These whole chromosomes or chromosome fragments develop a nuclear membrane in the cytoplasm and are usually detected during interphase as an additional small nucleus [245]. The formation of micronuclei is caused by genotoxic agents that induce chromosomal breaks, in the case of clastogens and/or the gain/loss of chromosomes in the case of aneugens [245,246]. The presence of chromosomal breakage or loss is determined through microscopic analysis using fluorescent dyes that stain DNA such as 2-(4-amidinophenyl)-1*H* -indole-6-carboxamidine (DAPI) and Hoechst. Using the fluorescence *in situ* hybridisation (FISH) method, the origin of whole chromosomes and chromosome fragments can be identified [247,248]. Overall, the micronucleus test is sensitive and can be used to determine genotoxicity at very low concentrations and the determination of the end-point is easy and straight forward [247]. Therefore, the ICH highly recommends the micronucleus test assay among all *in vitro* assays due to its reliability [249].

The *in vitro* chromosomal aberration test is used to detect for structural abnormalities of the chromosome in mammalian cells and is therefore only used for the detection of clastogens [250]. Structural aberrations can occur on the chromosome or chromatid where the latter is the common type of aberration caused by mutagens [251]. In this test, cells are exposed to the test compound (with or without metabolic pre-activation) for approximately 1.5 normal cell cycle lengths [251,252]. At different pre-determined intervals after exposure to the test compound, a metaphase-arresting substance is added, DNA is stained using Hoechst or Giemsa stains and viewed under the microscope for chromosomal structure analysis [251]. Similar to the micronucleus test, very low concentrations of the test compound can be used in this assay as it is highly sensitive and reliable [253].

The TK gene mutation assay uses mouse lymphoma cells L5178Y$^{TK+/-}$. The assay detects the genetic changes in the TK gene caused by base pair substitutions and frameshift mutations [254,255]. TK is responsible for the phosphorylation of thymidine deoxyriboside to form a deoxythymidylate, which is salvaged for DNA replication. Mutated cells deficient in thymidine kinase activity cannot phosphorylate the cytotoxic thymidine analogue, trifluorothymidine (TFT) and incorporate it into the DNA during replication [254]. Therefore, the mutants survive in the presence of TFT [254]. The level of mutagenicity induced by the compound is measured by the number of growing mutant colonies after treatment. Alternatively, BrdU can used as the selective agent for this assay although TFT is preferred as it is 50 times more potent and more sensitive than BrdU [256].

1.4.3 Limitations of the "gold standard" Ames test

The onset of effects caused by mutagens such as the formation of a tumour requires a significant amount of DNA damage to develop. Therefore, not every mutagen can be identified by short term *in vitro* assays. Despite the reliability of these assays as claimed by many studies, *in vitro*

systems are artificial systems and cannot be used to represent the more complex systems of an organism. In addition, there is considerable interspecies variations between bacterial or animal models and humans, which can lead to the identification of false negative results. For these reasons, many false negative results have been reported for compounds that could potentially be mutagenic [257].

First developed in the 1970s, the Ames test is still extensively used today to screen for potential mutagens and is considered the "gold standard" due to its reliability, reproducibility and accuracy [241]. In the classic method, bacteria are exposed to the test compound to test for mutagenicity. However, bacteria are prokaryotes, which cannot replicate eukaryotic conditions due to differences in structure, physiology and metabolic processes. One key difference is the inability of bacteria cells to produce metabolic enzymes such as microsomes. For this reason, this method is unable to detect the mutagenicity of some azo dyes, polychlorinated pesticides and heterocylic amines, which require enzymatic bio-activation by microsomes.

In the 1980s, microsomes were incorporated into the Ames test [258,259] for this limitation and a revised method is used in toxicology screens to this day. In this improved Ames assay, test compounds are pre-incubated with rat S9 liver microsome extract, which can be purchased commercially [258]. The rats for the production of the S9 extract were specifically pre-treated with phenobarbital or Aroclor 1254 to increase the production and enhance the bio-activation capacity of their hepatic microsomes [258,260,261]. Due to the introduction of this pre-incubation step with S9 extract, pro-mutagens previously reported to be non-mutagenic were identified to be indeed mutagenic [258,262,263]. The metabolic bio-activation of pro-mutagens by microsomes increases the likelihood of short-lived mutagenic metabolites reacting with bacterial test strains [244,264]. It is important to note that the addition of liver extract into the system may contribute to artefacts since it was reported that liver extract can induce spontaneous mutations in *Salmonella* test strains [258]. The effect of S9 liver extract on the number of revertant colonies caused by

spontaneous mutations has been determined previously (Table 8). Some *Salmonella* strains (TA97, TA102 and TA104) were in fact sensitive to the presence of S9 liver extract in a dose dependent manner [258,265].

Table 8: Number of spontaneous revertant colonies according to the type of *Salmonella* strains with or without S9 liver extract in the Ames test [258,265].

***Salmonella* strain**	**Number of spontaneous revertant colonies**	
	-S9 extract	**+S9 extract**
TA97	75-100*	100-200*
TA98	20-50	20-50
TA100	75-200	75-200
TA102	100-300*	200-400*
TA104	200-300*	300-400*
TA1535	5-20	5-20
TA1537	5-20	5-20
TA1538	5-20	5-20

**key differences in the number of spontaneous revertant colonies*

In addition, the use of pooled human S9 liver extract is thought to provide a more representative toxicological result [263,266]. Rat S9 liver extract has been shown to behave differently to those isolated from human liver when reacted with carcinogens isolated from smoke condensate [267]. This could be attributed by the differences in microsome isoforms found in extracts of rat and human origin [260]. A comparative study of rat and human S9 liver extracts suggested that human liver extracts are more sensitive than rat due to the increase in mutagenicity seen when exposed to known carcinogens [263]. The use of human S9 liver extract is limited due to the obvious difficulty in acquiring human liver samples in sufficient quantity with the significant human

associated ethical concerns. The use of human S9 liver extract in toxicology studies has attracted more attention recently due to advances in the commercial production of human S9 liver extract and the realisation of its value in providing more representative data to evaluate genotoxicity in humans [263]. However, rat S9 liver extract is still widely used today as it is significantly cheaper and more readily available.

Despite the advantages of adding a pre-incubation step, many recent studies in the field of drug discovery that utilise the Ames test, still do not incorporate this pre-incubation step. Often, this work focuses on bioactive compounds isolated from natural products or newly synthesised compounds, which have the potential to be developed into drug candidates. Consequently, there may be a significant element of bias against the detection of any mutagenic activity in the way these analyses were conducted. Moreover, the genotoxicity screening of these studies do no follow the recommended ICH and USFDA guidelines and their conclusion are often based on only one toxicity assay. Conclusions on genotoxicity should be based on the parallel use of different bio-assays, since some assays are more sensitive than others and can detect different types of DNA damage as discussed **(refer to section 1.4.2)**. As no single *in vitro* assay is perfect (including the ones recommended by ICH and USFDA), other *in vitro* assays should be used to complement them to obtain robust and reliable results.

1.4.4 Alternative *in vitro* screening methods for genotoxicity

The onset of mutagenesis leading to cancer is a complex process and many factors come into play in the genotoxicity response by bacterial and mammalian test systems *in vitro*. To improve the genotoxicity screening of test compounds and to acknowledge the limitations of the "gold standard" Ames test, additional testing paradigms such as the γH_2AX, comet and soft agar invasion assays have been developed. These assays have been demonstrated to be more accurate, robust and sensitive to detect genotoxicity [268-274]. Moreover using the γH_2AX assay

in liver cells to complement the Ames test significantly improved the accuracy in detection of genotoxicity by 15 % compared to performing the Ames test alone [268]. The γH$_2$AX and comet assays are regarded to be as or even more sensitive than other mammalian cell based assays such as micronucleus and chromosomal aberration assays [268,273]. While the Ames test measures the indirect end-point of genotoxicity (as in the onset of mutations leading to the formation of revertant colonies), the γH$_2$AX and comet assays measure the direct damage on the structure of DNA itself such as the detection of cellular response to DNA breaks and the presence of DNA breaks respectively [275].

The γH$_2$AX protein is the phosphorylated form of H2A histone subunit in response to DNA damage caused by single or double strand breaks [176] and therefore acts as a biomarker for potential genotoxicity activity. The immunofluorescence assays employs the use of monoclonal antibodies that will specifically detect nuclear γH$_2$AX sites. The primary antibody binds specifically to the γH$_2$AX protein and to allow visual detection of these sites, a secondary antibody tagged with a fluorophore is added to bind specifically to the primary antibody. Under the microscope, the illuminated spots represent the sites of DNA damage called foci and the severity of genotoxicity is measured by determining the number of foci in the nucleus. The γH$_2$AX assay is a very sensitive method that is capable of detecting a single foci in the nucleus [276] and is able to detect DNA damage levels 100-times lower than the detection limit of the comet assay [277]. The induction of γH$_2$AX is one of the earliest cellular responses to DNA damage, occurs within a few seconds following the exposure to DNA damaging agents and reaches maximum levels after 30 minutes [278]. This assay also allows the analysis of individual intact cells attached to the test vessel omitting the additional step of preparing cell suspensions or lysates, which is required for other bio-assays [237]. Since the sample is not heavily disrupted post-treatment, cellular morphology and distribution can be determined to reveal more information about the mode of action of the test compound.

Aside from γH_2AX, other repair proteins such as 53BP1, MRE11, RAD50, BRCA1 and Nijmegen breakage syndrome I (NBS1) co-localise at the same DNA damage site [279-282]. To verify the reliability of the γH_2AX assay, detection of these co-localised proteins can be conducted [283,284]. However, the detection of γH_2AX foci alone is sufficient for the determination of genotoxicity. MRE11, 53BP1 and NBS1 proteins dissociate from the protein complex at different stages of mitosis, while γH_2AX is formed throughout the cell cycle [285-287]. Moreover, the SQ motif found in the carboxy terminal tail of the H2AX histone subunit is highly conserved in plants and animals making it a universal DNA damage marker [172]. As with many bio-assays, the γH_2AX also has its limitations such as the presence of background γH_2AX staining due to spontaneous DNA damage occurring in the cell and false positive results have been reported for some phenolic compounds, which are known to be non-carcinogenic [288,289]. Indirect mechanisms associated with cytotoxic concentrations of the test compound such as DNA fragmentation in cells undergoing apoptosis and necrosis may induce the production of γH_2AX foci leading to false positive results [212]. As the γH_2AX foci appear as fluorescent spots under microscopic observation, overlapping of γH_2AX foci may cause an under reporting of genotoxicity [178].

The comet assay or also known as the single-cell gel electrophoresis assay is another test that can be utilised to evaluate genotoxicity. The method is used for the detection and quantification of DNA damage caused by single or double strand breaks, oxidative base damage, alkali-labile sites and cross-linking events between DNA and protein [290]. There are two variants of the assay, which are widely used: the neutral comet assay is more sensitive for the detection of single and double strand DNA breaks while the alkaline comet assay is more sensitive for the detection of single strand DNA breaks, base damage and alkali-labile sites [291-294]. Under very alkaline conditions (pH 13), denaturation and unwinding of the DNA can occur allowing the detection of more subtle forms of DNA damage such as single stranded breaks [291,294,295]. In the comet

assay, individual cells are exposed to the test compound to induce DNA damage, then embeded in an agarose matrix, lysed and electrophoresed in an electric field based on charge differences (Figure 13). Genotoxic agents that induce DNA strand breaks forming DNA fragments, will migrate away from the nucleus towards the anode. DNA can be stained using propidium iodide or *N*',*N*'-dimethyl-N-[4-[(E)-(3-methyl-1,3-benzothiazol-2-ylidene)methyl]-1-phenylquinolin-1-ium-2-yl]-*N*-propylpropane-1,3-diamine (SYBR) Green and viewed using fluorescence microscopy. The stained migrating DNA fragments form a tail from the nucleus that appears like a comet, which gives the assay its name [290,291]. The "head" of the comet represents the nucleus with intact DNA, which is too large to migrate in the electric field and the "tail" of the comet represents the DNA fragments (Figure 13). The extent of genotoxicity is measured by determining the proportion of DNA in the "tail" in comparison to the "head" via visual examination or by using image analysis and integration of intensity profiles using imaging software [291,296,297] (Figure 13).

The advantages of the comet assay are its simplicity, high sensitivity, speed, versatility in the detection of different types of DNA damage and is a well-established method [291,296,298]. Similar to the γH2AX assay, the comet assay is also affected by DNA fragmentation during apoptosis and necrosis at cytotoxic concentrations of the test compound [299]. Due to the high sensitivity of the comet assay, spontaneous oxidative DNA damage due to reactive oxygen species (ROS) also affects the readout [212]. The length of the comet "tail" is proportional to the amount of DNA damage up to where the amount of DNA damage reaches saturation point. The increased amount of DNA fragments produced at the saturation point affects their migration on the agarose gel [298].

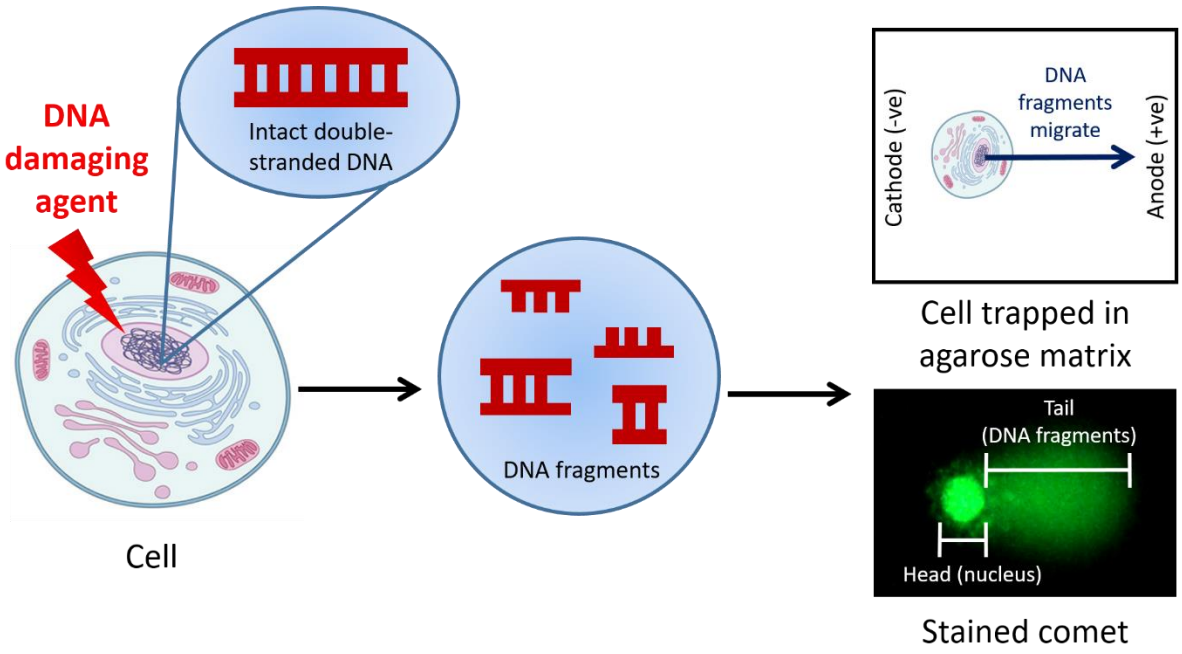

Figure 13: Schematic representation of the comet assay. Exposure of the cell to a DNA damaging agent results in the formation of DNA fragments. Small negatively charged DNA fragments travel away from the nucleus, which is the comet head in the electric field towards the positively charged anode forming the comet tail.

Unlike the γH2AX and comet assays, which measures the response to and presence of DNA damage, the soft agar invasion (SAI) assay measures the end-point of the mutation process: cell transformation. The SAI assay is performed *in vitro* and used as an indicator of mutagenicity prior to *in vivo* testing. This method is widely used and represents the preferred mutagenic transformation assay as it is quicker than *in vivo* testing and relatively simple to perform.

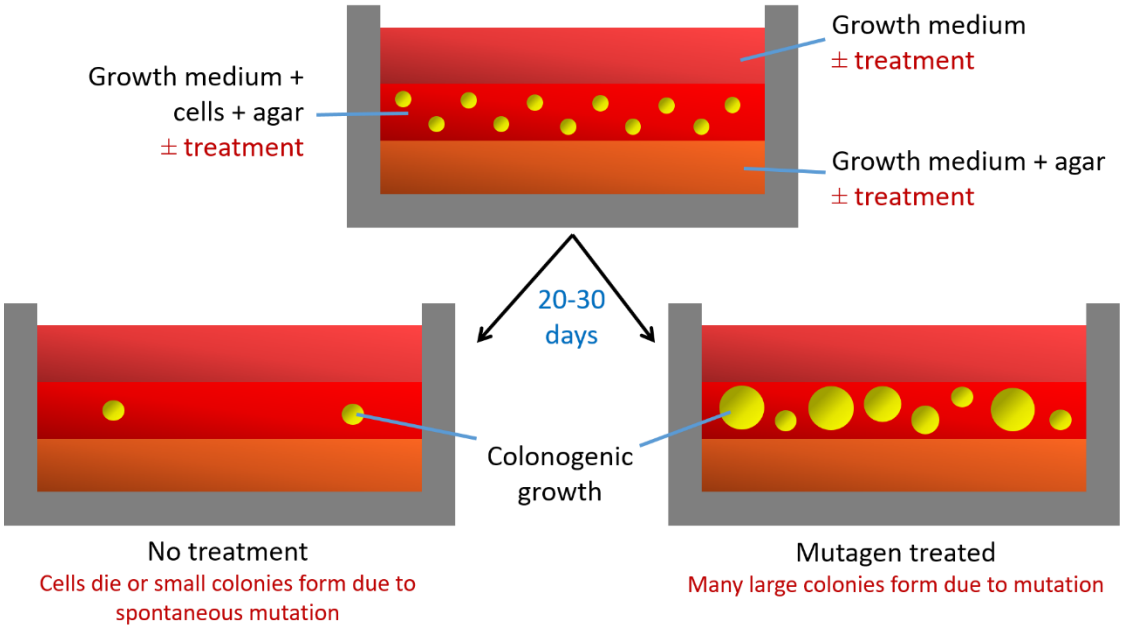

Figure 14: Schematic representation of the soft agar invasion assay. Cells embedded in an agar matrix upon exposure to a mutagen, undergoes mutation and able to grow uncontrollably in an anchorage-independent manner forming large colonies. Some cells however experience spontaneous mutation resulting in the formation of small colonies in the agar matrix in untreated cells.

The SAI assay embeds mammalian cells in a soft agar layer supplemented with growth medium, which sits on a base agar layer with a higher concentration of agar supplemented with growth medium as well (Figure 14). The addition of the base agar layer prevents the cells from adhering to the culture plate creating a "floating" environment for the cells. Normal adherent cells are not able to grow in the agar matrix due to anchorage-dependent growth where cells depend on extracellular matrix contacts to grow and divide (Figure 14). This is because the detachment of cells from the correct extracellular matrix disrupts integrin ligation and forces the cells to undergo apoptotic cell death, called anoikis [300]. Mutated and transformed cells are able to grow and divide regardless of the extracellular environment where they are able to form colonies in an anchorage-independent manner (Figure 14). For toxicology screens, test compounds are supplemented in the agar layers and cells are continuously treated with the test

compound for 20-30 days. Mutagenic compounds that are able to transform cells result in increased colony numbers and size [301] (Figure 14). Although the SAI assay is quicker than *in vivo* assays, the assay still requires almost a month to complete [274]. Cell retrieval upon completion for DNA or protein analysis cannot be done as the cells are trapped in the agar matrix [274].

Alternative methods for the detection of genotoxicity measure different end-points of DNA damage and each is associated with specific advantages and disadvantages. However, these methods give a better indication of the nature of DNA damage in a more sensitive and representative manner as they are directly conducted on mammalian cells. The main advantage of *in vitro* screens is the speed at which results can be obtained. However, these methods can only be used as complementary and confirmatory assays to the Ames test at the early stages of drug development and further *in vivo* screening is required prior to clinical trials in humans to minimise long term health hazards in patients.

1.5 The mutagenic potential of oxazolopyridines

1.5.1 Reported genotoxicity in benzoxazoles and related analogues

Benzoxazoles as discussed previously are a popular molecular scaffold for drug discovery as they are both synthetically versatile and biologically active. Therefore, benzoxazoles have been developed into commercial drugs such Benoxaprofen, Flunoxaprofen and Zoxazolamine but were soon recalled due to toxicity issues [23-27]. These are good examples to illustrate that stringent drug screening and understanding of the association between chemical structure and adverse side effects are essential to ensure drug safety. Genotoxicity and mutagenicity are adverse side effects, which are not easily detected given their complexity and sometimes non-obvious nature. Especially mutagenicity, which typically requires a long time to manifest and is not rapidly detected by standard *in vitro* screening methods. The genotoxicity of benzoxazoles has only been reported recently and our understanding of how they interact with DNA is very limited. This however justifies the need to investigate the genotoxic and mutagenic liabilities of benzoxazole related analogues (such as benzimidazoles, benzothiazoles and oxazolopyridines). Particularly when they have structural similarities to known carcinogens such as PhIP **46**.

Derivatives of 2,5-disubstituted benzoxazole and benzimidazole derivatives have been shown to be genotoxic in the *Bacillus subtilis rec* assay [302]. Compounds **57a-c** were most genotoxic with the ratio of 50% lethal dose (Rec_{50}) values of 2.22, 1.74 and 1.61 respectively. Compound **57a** was closely related to the known DNA damaging agent, 4-nitroquinoline-1-oxide (4-NQO) with a Rec_{50} value of 2.22 [302]. Between the two benzoxazoles, the presence of the amine group at position C4 of the phenyl ring in **57a** as compared to position C6 of the benzoxazole fused ring system in **57b** enhanced the mutagenicity of the compound. The Rec_{50} values of benzimidazoles were generally lower than the benzoxazoles.

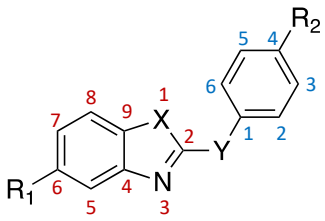

57

ID	X	Y	R_1	R_2
57a	O	CH_2	CH_3	NH_2
57b	O	CH_2	NH_2	CH_3
57c	NH	CH_2O	H	H

Similarly, benzoxazole and benzimidazole derivatives with anti-microbial and anti-viral activities were also found to be genotoxic and the genotoxicity of benzimidazoles was inferior compared to benzoxazoles [303]. Benzoxazole compounds **58a-d** were most genotoxic with Rec_{50} values of 1.85, 1.74, 1.60 and 1.50 respectively, although not as genotoxic as 4-NQO (Rec_{50}=2.21) [303].

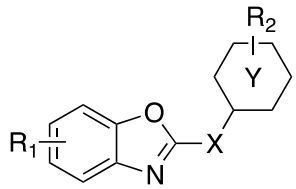

58

ID	X	Y	R_1	R_2
58a	-	C_6H_4	6-CH_3	2-Cl
58b	CH_2	C_6H_4	5-NH_2	4-CH_3
58c	-	C_6H_5	5-(*p*-fluorobenzamido)	H
58d	-	C_6H_4	H	4-$NHCH_3$

The genotoxicity of benzoxazole derivatives was further investigated in HeLa cells using the comet assay and in the *Salmonella* system using the Ames test [304]. Compounds **59a** and **59b** were mildly mutagenic compared to the mutagen, 2-aminofluorene when tested in the Ames test using *Salmonella* TA98 and TA 100 strains. These compounds also required enzymatic bio-activation (in the presence of S9 liver extract) to be mutagenic. Compound **59a** was mildly genotoxic in HeLa cells via the comet assay at 25 µM but the study was limited by the lack of

understanding of the mode of action in genotoxicity and mutagenicity of these compounds from a molecular perspective [304].

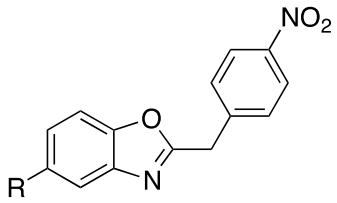

59

R= H **(59a)**, NO_2 **(59b)**

These studies have demonstrated that increasing the electron density at position C2 of the benzoxazole or benzimidazole fused ring systems led to an increase in genotoxicty. Substituting amino or nitro groups at position C6 of the fused ring systems or at any position on the phenyl ring attached to C2, significantly enhanced the genotoxicity and mutagenicity of these compounds.

1.5.2 Oxazolopyridine as a potential mutagen

A collaborative multi-disciplinary study between Baell's group at Monash Institute of Pharmaceutical Sciences (Monash University, Melbourne, Australia), Eskitis Institute for Cell and Molecular Therapies (Griffith University, Brisbane, Australia) and our group (University of Tasmania, Hobart, Australia) synthesised a small library of oxazolopyridines from a lead compound, which was identified by HTS of 87,000 compounds. This screen was designed to identify compounds active against *Trypansoma brucei rhodesiense*, which is responsible for Human African trypanosomiasis (HAT) also known as sleeping sickness. This approach identified the 2-aryloxazolopyridine compound **42**, which potently inhibited the growth of *T.b. rhodesiense in vitro* [38]. Importantly, unlike other pharmacological approaches against HAT, compound **42** showed no overt cytotoxicity in mammalian cells up to high micromolar concentrations. At the same time compound **42** was also described as non-mutagenic in the

Ames test (without S9 extract) [38], which made the compound an ideal development candidate against HAT. This study is one of many in the field of medicinal chemistry that supports the potent bio-activity of oxazolopyridine compounds and their potential as safe and effective drug candidates.

However, a full toxicological characterisation of oxazolopyridines had not been conducted yet since this molecular scaffold is only slowly gaining popularity in medicinal chemistry over the past decade. Toxicity tests are commonly conducted *in vitro* and only some *in vivo* screens have been reported to date [38-41]. Therefore, more in-depth investigations were needed to identify oxazolopyridine-related toxicities that may have been missed in the primary screens or may manifest only with time. Importantly, the modes of action of these biologically active oxazolopyridines are not fully understood and their detailed interactions with biological molecules are unknown. This lack of knowledge therefore impairs the ability to predict any putative adverse effects of these compounds. Benzoxazoles have been studied extensively over many years but reports of genotoxicity have only surfaced recently [302-304]. Therefore, there is the risk that the closely related oxazolopyridines could also be genotoxic.

The 2-(3-aminophenyl)oxazolopyridine **60** for the current study showed some structural resemblance to the known carcinogen, PhIP **46** (Figure 15A). Both 2-(3-aminophenyl)oxazolopyridine **60** and PhIP **46** share similar heterocyclic cores and an attached amino group (Figure 15A). Moreover, the imidazopyridine molecular core **61** is isoelectronic with that of the oxazolopyridine **17** (Figure15B). In fact, the imidazopyridine compounds showed similar anti-parasitic activity as the oxazolopyridines and also low toxicity as shown by the development of imidazopyridines from the initial compound library screen **(Refer to Figure 6, section 1.1.5)**. The amino group is responsible for the mutagenicity in PhIP **46** through the formation of PhIP arylnitrenium ion **54**, which reacts with the guanine base of the DNA to form mutagenic DNA adducts as previously reviewed **(refer to section 1.2.3)**. For

these reasons, the safety of oxazolopyridines developed as anti-parasitic agents was questioned as hydrolysis of the amide would generate a free amino group (Figure 16), which has led to the research questions that was addressed in the current study.

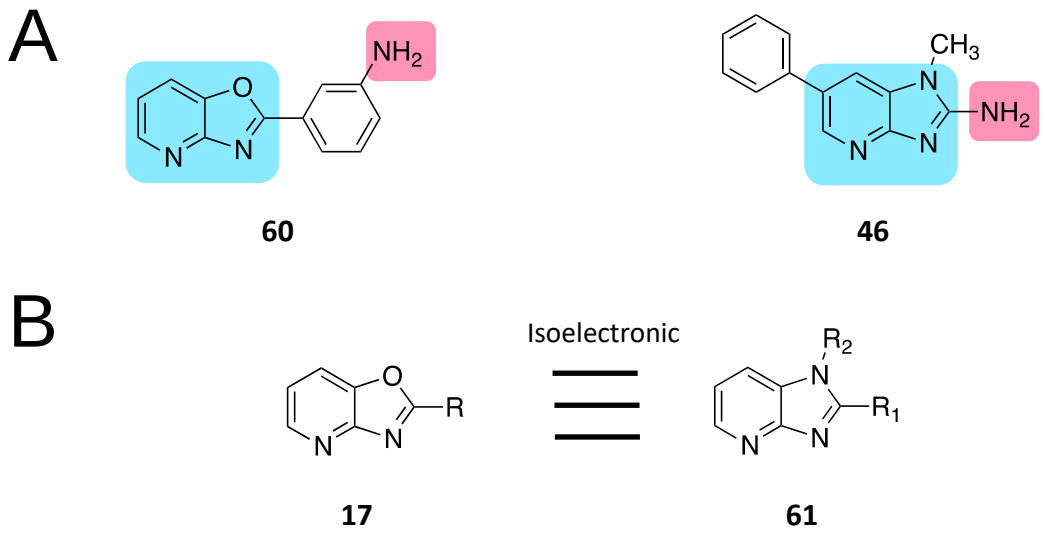

Figure 15: Structural relatedness of imidazopyridine (such as PhIP) and oxazolopyridine compounds. (A) The 2-(3-aminophenyl)oxazolopyridine **60** is structurally similar to the carcinogen, PhIP **46** due to the presence of the aromatic heterocyclic core (blue box) and the attached amino group (red box). (B) The heterocyclic core of oxazolopyridine, **17** is isoelectronic to that of imidazopyridine, **61**.

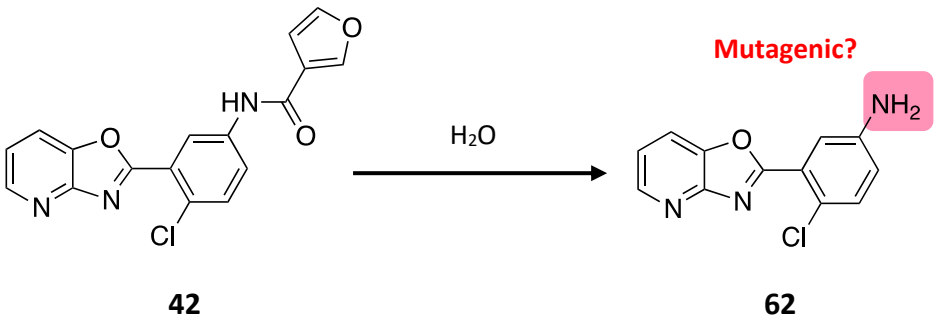

Figure 16: Hydrolysis of amide containing oxazolopyridine compounds. For example, the anti-parasitic compound, 2-aryloxazolopyridine **42** can undergo hydrolysis to generate a free amino group (red box) such as in compound **62**.

1.5.3 Significance of study and research questions.

The mutagenicity of oxazolopyridines has not been tested and reported to date although this group of compounds are structurally similar to the carcinogen, PhIP **46**. Moreover, reports of genotoxicity and mutagenicity of the very closely-related group of molecules, the benzoxazoles have started to surface only recently [302-304]. The investigation and understanding of the mutagenic potential of the oxazolopyridines are very important especially in the field of drug discovery to prevent any unforeseen adverse effects if drugs belonging to this family were to be developed clinically. The lack of cytotoxicity, high biological activity and versatile nature of oxazolopyridines for chemical synthesis make this scaffold attractive for developing drug candidates.

Prior to the current study, some 2-aryloxazolopyridine analogues were observed to be genotoxic during a preliminary study conducted at the University of Tasmania (unpublished data). The current study is the first to determine the mutagenicity of oxazolopyridines and will provide the basis for a better understanding of their mutagenicity. This could also inform about the potential risks of other closely related medicinally important molecular scaffolds namely benzoxazoles, benzimidazoles and benzothiazoles used in drug discovery and ultimately could lead to the development of safer drugs. In addition, this study will highlight the importance of developing efficient and sensitive methods to determine compound mutagenicity. Due to the structural similarities between the 2-(3-aminophenyl)oxazolopyridine **60** and PhIP **46**, it was hypothesised that: **The 2-(3-aminophenyl)oxazolopyridine 60 may be genotoxic and mutagenic to cells due to the presence of the amino group using PhIP 46, as a model.** Chronic exposure of organisms to these compounds may lead to the development of cancer. Therefore, the aims of the current study are to investigate the following research questions.

Research question 1:

Is the lead oxazolopyridine compound 60 toxic and mutagenic to cells?

It was hypothesised that 2-(3-aminophenyl)oxazolopyridine **60** maybe genotoxic and mutagenic to cells. To evaluate the cytotoxicity, genotoxicity and mutagenicity of oxazolopyridine compounds, *in vitro* assays were carried out using mammalian cell lines such as HepG2 and human colorectal carcinoma (HCT116) cells as these two tissues are involved in the metabolism and absorption of xenobiotic agents in the body. PhIP **46** was used as the carcinogenic reference compound in the *in vitro* assays for the current study.

Research question 2:

Is there a structural correlation for oxazolopyridines in genotoxicity and mutagenicity?

If oxazolopyridines are found to be genotoxic and mutagenic, what structural aspects of the molecular scaffold is responsible for their genotoxicity? Therefore, the determination of QSAR of different oxazolopyridine analogues was carried out *in vitro*. Results obtained from previous experiments led to the synthesis of other oxazolopyridine analogues and related compounds to determine structural moieties in the oxazolopyridine scaffold responsible for its genotoxicity and mutagenicity.

Research question 3:

What is the mode of action of oxazolopyridines in mutagenicity?

The QSAR experiments may provide a correlation on the mutagenic mode of action of the oxazolopyridine compounds. However, to obtain solid evidence, the mutagenic active species of the oxazolopyridine needs to be identified. Therefore, the mode of action of the bio-activation of oxazolopyridines was determined by combining chemical and biological approaches such as synthesis, analytical chemistry, enzymatic reactions and *in vitro* assays.

Chapter 2 Methodology

2.1 Chemical synthesis of molecular probes

2.1.1 General experimental

2.1.1.1 Solvents and reagents

All reagents and standards used for chemical synthesis were purified by standard laboratory methods. For drying, anhydrous magnesium sulphate was used as the drying agent for organic extracts unless stated otherwise and solvents removed using rotary evaporation under reduced pressure.

2.1.1.2 Thin layer chromatography (TLC)

Thin layer chromatography (TLC) was performed using Merck silica gel 60 F254 aluminium backed sheets. Separated spots on the TLC plate were visualised using a 254 nm ultra-violet lamp and/or by treatment with phosphomolybdic acid (37.5 g), ceric acid (7.5 g), sulphuric acid (37.5 mL and water (750 mL) dip.

2.1.1.3 Column chromatography

Column and flash chromatography was performed using Merck flash grade silica (32-63 μm) according to the general methods as previously described [305].

2.1.1.4 Nuclear magnetic resonance (NMR)

Synthesised compounds were dissolved in deuterated chloroform ($CDCl_3$), methanol (CD_3OD) or dimethylsulphoxide (DMSO-D_6). NMR spectra were recorded using a Bruker Avance III (Billerica, Massachusetts, US) operating at 400 MHz for proton (^1H) and 100 MHz for carbon

(^{13}C). Chemical shifts were recorded as δ values in parts per million (ppm) and referenced to the solvent used. For instance, $CDCl_3$ solvent references were at 7.26 ppm (^{1}H) and 77.16 ppm (^{13}C), CD_3OD solvent references were at 3.31 ppm (^{1}H) and 49.3 ppm (^{13}C), DMSO-D_6 solvent references were at 2.50 ppm (^{1}H) and 39.52 ppm (^{13}C). Proton resonances were annotated using these abbreviations on the ^{1}H spectra, s = singlet; d = doublet; t= triplet; m = multiplet; bs = broad singlet; dd = doublet of doublet; tt= triplet of triplets; ddd = doublet of doublets of doublets; ttt= triplet of triplets of triplets, *J* = coupling constant (Hz) and number of protons. The interpretation of NMR spectra with respect to chemical shifts and solvents peaks were based on previously published values [306].

2.1.1.5 Mass Spectrometry (MS)

MS was performed using the Kratos Concept ISQ (Wharfside, Manchester, UK) using electron ionisation with 70eV electrons with an accelerating voltage of 5.3 kV or a Waters Xero Triple Quadrupole (Rydalmere, NSW, Australia) using 2.5 kV needle voltage with direct infusion electrospray ionisation measuring positive ions. Accurate mass was also measured by 'peak matching' at 10,000 resolution against perfluorokerosene. The mass was determined via the low resolution MS (LRMS) mode. The mass spectrometry analyses were performed by the Central Science Laboratory at the University of Tasmania. The molecular ions and fragments are quoted with the relative intensities of the peaks referenced to the most intense (100 %).

2.1.1.6 X-ray crystallography

X-ray diffraction data for the compound were collected with monochromated Cu Kα radiation (λ = 1.54178 Å) from an Incoatec IμS Cu microsource on a Bruker D8 Quest (Billerica, Massachusetts, US), equipped with a PHOTON 100 CMOS detector (Bruker, Billerica, Massachusetts, US). Single crystals were mounted on nylon loops with viscous immersion oil,

and placed into a chilled nitrogen stream (Oxford Cryosystems Cobra), and the data were collected at 100(2) K with the APEX3 software. Series of ϕ and ω scans were performed to a maximum resolution of 0.81 Å. The structure was solved using charge flipping methods in SUPERFLIP [307] and refined using full-matrix least-squares on F^2 with SHELXL [308] within the OLEX2 suite [309] as previously described. Non-hydrogen atoms were refined with anisotropic displacement parameters. Hydrogen atoms on carbon were visible in the diffraction map, but were included at calculated positions and ride on the atoms to which they are attached. Molecular graphics were produced with OLEX2 as previously described [309]. The x-ray crystallography analyses were performed by the Inorganic Chemistry group at the University of Tasmania.

2.1.1.7 Microwave assisted reactions

Reactions which involved the use of a microwave reactor were conducted in a sealed glass tube heated in a CEM Discover Microwave reactor (Matthews, North Carolina, US).

2.1.1.8 Syntheses of compounds

Test compounds used in this study were synthesised based on methods previously described [32,38,310,311]. Compounds were arranged based on sequence of appearance in chapters 3 to 5.

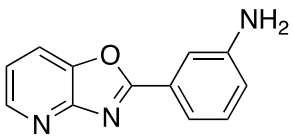

Synthesis of 3-(oxazolo[4,5-*b*]pyridine-2-yl)aniline (60). A mixture of 2-amino-3-hydroxypyridine (1.00 g, 9.08 mmol) and *m*-aminobenzoic acid (1.25 g, 9.08 mmol) in polyphosphoric acid (30 g, 14.5 mL) was heated at 180 °C for 5 hours, poured into an ice bath while hot and neutralised with solid $NaHCO_3$. The resulting precipitate was filtered, washed with water and dried under vacuum. The crude precipitate was purified via flash chromatography on silica gel (Eluent: dichloromethane: hexane, 50:50) to give compound **60** as a beige solid. Whole spectral

data matches that of previously reported [38]. ^{1}H NMR ($CDCl_3$/DMSO-d_6) δ: 5.02 (bs, 2H), 6.63 (ddd, *J* = 1.2, 2.4, 8.1 Hz, 1H), 7.03 (m, 2H), 7.31 (m, 2H), 7.61 (dd, *J* = 1.2, 8.1, 1H), 8.24 (dd, *J* = 1.2, 4.8 Hz, 1H). ^{13}C NMR ($CDCl_3$/ DMSO-d_6) δ: 113.1, 116.7, 117.6, 118.4, 119.4, 126.3, 129.2, 142.3, 145.7, 147.0, 155.5, 165.3. LRMS $[M=H]^+$: 212 m/z.

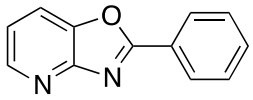

Synthesis of 2-phenyloxazolo[4,5-*b*]pyridine (61). A mixture of 2-amino-3-hydroxypyridine (1.11 g, 10 mmol) and benzoic acid (1.22 g, 10 mmol) in polyphosphoric acid (30 g, 14.5 mL) was heated at 180 °C for 5 hours, poured into an ice bath while hot and neutralised with solid $NaHCO_3$. The resulting precipitate was filtered, washed with distilled water and dried under vacuum. The crude precipitate was purified via flash chromatography on silica gel (Eluent: ethyl acetate: hexane 50:50) to give compound **61** as a yellow solid. Whole spectral data matches that of previously reported [32]. ^{1}H NMR ($CDCl_3$) δ: 7.30 (dd, *J* = 5.0, 8.2 Hz, 1H), 7.54-7.56 (m, 2H), 7.58-7.60 (m, 1H), 7.87 (dd, *J* = 1.4, 8.1 Hz, 1H), 8.33 (dd, *J* = 0.9, 7.8 Hz, 2H), 8.59 (dd, *J* = 1.4, 4.9 Hz, 1H). ^{13}C NMR ($CDCl_3$) δ: 118.2, 120.1, 126.6, 128.3, 129.1, 132.5, 143.2, 146.8, 156.5, 165.8.

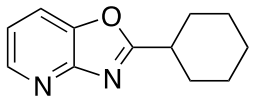

Synthesis of 2-cyclohexyloxazolo[4,5-*b*]pyridine (62). A mixture of 2-amino-3-hydroxypyridine (0.22 g, 2 mmol) and cyclohexane carboxylic acid (0.26 g, 2 mmol) was heated in the microwave reactor at 250 °C for 12 minutes. Saturated $NaHCO_3$ was added and the mixture was extracted with dichloromethane, dried with anhydrous $MgSO_4$ and evaporated to dryness. The crude product was purified using flash chromatography on silica gel (Eluent: ethyl acetate: hexane, 30:70) to give compound **62** as a white solid. Whole spectral data matches that of previously reported [32]. ^{1}H NMR ($CDCl_3$) δ: 1.27-1.46 (m, 3H), 1.67-1.77 (m, 3H), 1.84-1.88 (m, 2H), 2.16 (dd, *J* = 2.7, 13.3 Hz, 2H), 2.99 (ttt, *J* = 3.6, 7.3, 11.3, 15.0 Hz, 1H), 7.21 (dd, *J*

= 5.0, 8.1 Hz, 1H), 7.72 (dd, *J* = 1.1, 8.1 Hz, 1H), 8.49 (d, *J* = 4.8 Hz, 1H). ^{13}C NMR ($CDCl_3$) δ: 25.3, 25.5, 25.7, 30.3, 38.3, 45.5, 117.8, 119.5, 142.8, 146.0, 156.0, 173.5.

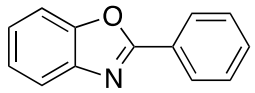

Synthesis of 2-phenylbenzo[*d*]oxazole (63). A mixture of 2-aminophenol (1.09 g, 10 mmol) and benzoic acid (1.22 g, 10 mmol) in polyphosphoric acid (30 g, 14.5 mL) was heated at 180 °C for five hours, poured into an ice bath while hot and neutralised with solid $NaHCO_3$. The resulting precipitate was filtered, washed with water and dried under vacuum. The crude precipitate was purified via flash chromatography on silica gel (Eluent: ethyl acetate: hexane, 25:75) to give compound **63** as a yellow solid. Whole spectral data matches that of previously reported [312]. ^{1}H NMR ($CDCl_3$) δ: 7.34-7.38 (m, 2H), 7.53 (d, *J* = 1.8 Hz, 1H), 7.54 (d, *J* = 2.0 Hz, 2H), 7.59 (dd, *J* = 3.5, 6.5 Hz, 1H), 7.78 (dd, *J* = 3.3, 6.3 Hz, 1H), 8.27 (dd, *J* = 2.0, 6.5 Hz, 2H).

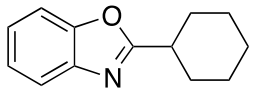

Synthesis of 2-cyclohexylbenzo[*d*]oxazole (64). A mixture of 2-aminophenol (0.22 g, 2 mmol) and cyclohexane carboxylic acid (0.26 g, 2 mmol) was heated in the microwave reactor at 250 °C for 12 minutes. Saturated $NaHCO_3$ was added and the mixture was extracted with dichloromethane, dried with anhydrous $MgSO_4$ and evaporated to dryness. The crude product was purified using flash chromatography on silica gel (Eluent: ethyl acetate: hexane, 10:90) to give compound **64** as a white solid. Whole spectral data matches that of previously reported [312]. ^{1}H NMR ($CDCl_3$) δ: 1.26-1.37 (m, 3H), 1.65-1.74 (m, 3H), 1.84 (tt, *J* = 3.7, 7.5, 13.1 Hz, 2H), 2.16 (dd, *J* = 2.9, 13.1, 16.0 Hz, 2H), 2.93 (ttt, *J* = 3.6, 7.1, 11.3, 14.9 Hz, 1H), 7.24-7.25 (m, 1H), 7.26-7.27 (m, 1H), 7.42-7.47 (m, 1H), 7.65-7.69 (m, 1H). ^{13}C NMR ($CDCl_3$) δ: 25.6, 25.8, 30.4, 27.9, 110.2, 119.6, 123.9, 124.3, 141.2, 150.6, 170.3.

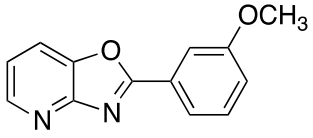

Synthesis of 2-(3-methoxyphenyl)oxazolo[4,5-*b*]pyridine (40e). A mixture of 2-amino-3-hydroxypyridine (0.36 g, 3.29 mmol) and *m*-methoxybenzoic acid (0.50 g, 3.29 mmol) was heated in the microwave reactor at 170 °C for 8 minutes. Saturated $NaHCO_3$ was added and the mixture was extracted with dichloromethane, dried with anhydrous $MgSO_4$ and evaporated to dryness. The crude product was purified using flash chromatography on silica gel (Eluent: ethyl acetate: hexane, 50:50) to give compound **40e** as a white solid. Whole spectral data matches that of previously reported [36]. ^{1}H NMR ($CDCl_3$) δ: 3.87 (s, 3H), 7.08 (d, *J* = 7.6 Hz, 1H), 7.25 (t, *J* = 6.0 Hz, 1H), 7.40 (t, *J* = 7.6 Hz, 1H), 7.81-7.86 (m, 3H), 8.54 (d, *J* = 4.6 Hz, 1H). ^{13}C NMR ($CDCl_3$) δ: 55.5, 112.4, 118.2, 119.2, 120.1, 120.5, 127.6, 130.1, 143.1, 146.7, 156.3, 160.0, 165.6.

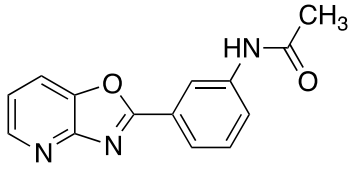

Synthesis of *N*-(3-(oxazolo[4,5-*b*]pyridine-2-yl)phenyl)acetamide (65). Compound **60** (0.10 g, 0.47 mmol) was dissolved in dichloromethane and pyridine (0.5 mL) and then acetyl chloride (51 µL, 0.71 mmol) to the mixture and the reaction stirred at room temperature, overnight. The reaction mixture was diluted with ethyl acetate (5 mL) and washed with water, concentrated HCl (2 M) and saturated $NaHCO_3$, dried with anhydrous $MgSO_4$ and evaporated to dryness. The crude product was purified via flash chromatography on silica gel (Eluent: ethyl acetate: hexane, 60:40) to give compound **65** as a white solid. ^{1}H NMR ($CDCl_3$) δ: 2.25 (s, 3H), 5.28 (s, 1H), 7.30 (dd, *J* = 4.9, 8.0 Hz, 1H), 7.40 (t, *J* = 7.9 Hz, 1H), 7.83 (d, *J* = 7.9 Hz, 1H), 7.92 (t, *J* = 7.5 Hz, 2H), 8.39 (s, 1H), 8.54 (bs, 1H), 8.71 (bs, 1H). ^{13}C NMR ($CDCl_3$) δ: 24.6, 118.8, 119.3, 120.4, 123.6, 124.2, 126.7, 129.8, 139.2, 143.3, 146.2, 155.9, 165.7, 169.4. LRMS $[M=H]^+$: 254 m/z.

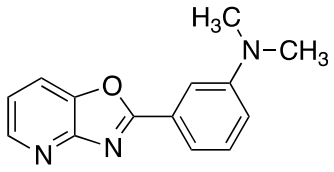

Synthesis of *N,N*-dimethyl-3-(oxazolo[4,5-*b*]pyridin-2-yl)aniline (66). A mixture of compound **60** (0.10 g, 0.47 mmol), formaldehyde (0.04 g, 1.18 mmol) and formic acid (0.5 mL) was heated under reflux at 90 °C for 4 hours. Saturated $NaHCO_3$ was added and the mixture was extracted with dichloromethane, dried with anhydrous $MgSO_4$ and evaporated to dryness. The crude product was purified via flash chromatography on silica gel (Eluent: ethyl acetate) to give compound **66** as a white solid. ^{1}H NMR ($CDCl_3$) δ: 3.07 (s, 6H), 7.00 (d, *J*= 8.8 Hz, 1H), 7.28 (dd, *J* = 5.0, 8.0 Hz, 1H), 7.40 (t, *J* = 8.0 Hz, 1H), 7.68 (d, *J* = 7.6 Hz, 1H), 7.73 (s, 1H), 7.85 (d, *J* = 7.6 Hz, 1H), 8.56 (d, *J* = 4.6 Hz, 1H). ^{13}C NMR ($CDCl_3$) δ: 41.0, 112.1, 117.0, 118.1, 120.0, 127.2, 129.8, 143.2, 146.7, 150.4, 156.6, 166.4. LRMS $[M=H]^+$: 240 m/z.

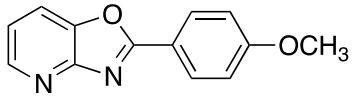

Synthesis of 2-(4-methoxyphenyl)oxazolo[4,5-*b*]pyridine (40a). A mixture of 2-amino-3-hydroxypyridine (0.36 g, 3.29 mmol), *p*-methoxybenzoic acid (0.50 g, 3.29 mmol) and boric acid (0.20 g, 3.29 mmol) was heated in the microwave reactor at 170 °C for 8 minutes. Saturated $NaHCO_3$ was added and the mixture was extracted with dichloromethane, dried with anhydrous $MgSO_4$ and evaporated to dryness. The crude product was purified using flash chromatography on silica gel (Eluent: ethyl acetate: hexane, 30:70) to give compound **40a** as a white solid. Whole spectral data matches that of previously reported [32]. ^{1}H NMR ($CDCl_3$) δ: 3.86 (s, 3H), 7.00 (d, *J* = 8.4 Hz, 2H), 7.22 (dd, *J* = 4.9, 8.0 Hz, 1H), 7.79 (d, *J* = 8.0 Hz, 1H), 8.22 (d, *J* = 8.9 Hz, 2H), 8.50 (s, *J* = 4.0 Hz, 1H). ^{13}C NMR ($CDCl_3$) δ: 55.5, 114.5, 118.0, 118.8, 119.6, 130.1, 143.1, 146.1, 156.6, 163.2, 166.0.

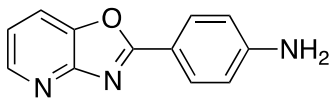

Synthesis of 4-(oxazolo[4,5-*b*]pyridine-2-yl)aniline (40b). A mixture of 2-amino-3-hydroxypyridine (2.20 g, 20 mmol) and *p*-aminobenzoic acid (2.70 g, 20 mmol) in polyphosphoric acid

(30 g, 14.5 mL) was heated at 185 °C for five hours, poured into an ice bath while hot and neutralised with solid $NaHCO_3$. The resulting precipitate was filtered, washed with water and dried under vacuum. The crude precipitate was dissolved in ethyl acetate and methanol, then recrystallized with hexane to give compound **40b** as a yellow solid. Whole spectral data matches that of previously reported [310]. ^{1}H NMR (CD_3OD) δ: 4.87 (bs, 2H), 6.77 (d, *J* = 8.4 Hz, 2H), 7.33 (dd, *J* = 4.9, 7.8 Hz, 1H), 7.98-8.01 (m, 3H), 8.39 (d, *J* = 4.9 Hz, 1H). ^{13}C NMR (CD_3OD) δ: 114.1, 115.0, 119.4, 120.6, 131.0, 144.4, 146.3, 154.9, 157.6, 168.9.

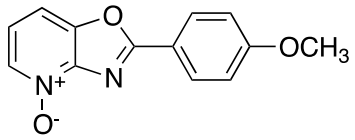

Synthesis of 2-(4-methoxyphenyl)oxazolo[4,5-*b*]pyridine 4-oxide (67). A mixture of compound **40a** (0.10 g, 0.44 mmol) and *m*-chloroperbenzoic acid (0.085 g, 0.49 mmol) in dichloromethane was stirred at room temperature for 3 hours. Saturated $NaHCO_3$ was added and the mixture was extracted with dichloromethane, dried with anhydrous $MgSO_4$ and evaporated to dryness. The crude product was purified using flash chromatography on silica gel (Eluent: methanol: dichloromethane, 12:88) to give compound **67** as a white solid. ^{1}H NMR (CD_3OD) δ: 3.92 (s, 3H), 7.16 (d, *J* = 8.3 Hz, 2H), 7.46 (t, *J* = 7.6 Hz, 1H), 7.90 (d, *J* = 8.3 Hz, 1H), 8.29 (d, *J* = 8.3 Hz, 2H), 8.35 (d, *J* = 6.4 Hz, 1H). ^{13}C NMR (CD_3OD) δ: 56.2, 113.7, 116.0, 118.4, 122.0, 131.7, 137.1, 148.5, 148.6, 165.8, 167.9. LRMS $[M=H]^+$: 243 m/z.

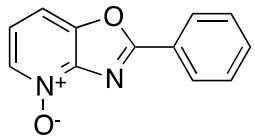

Synthesis of 2-phenyloxazolo[4,5-*b*]pyridine 4-oxide (68). A mixture of compound **61** (0.10 g, 0.51 mmol) with *m*-chloroperbenzoic acid (0.097 g, 0.56 mmol) in dichloromethane was stirred at room temperature for 24 hours. Saturated $NaHCO_3$ was added and the mixture was extracted with dichloromethane, dried with anhydrous $MgSO_4$ and evaporated to dryness. The crude product was purified using flash chromatography on silica gel (Eluent: methanol: dichloromethane, 10:90) to give compound **68** as an off-white solid. Crystals suitable for single

crystal x-ray analysis were grown by dissolving the solid in ethyl acetate and recrystallized with hexane. The compound crystallises in the triclinic space group *P*-1, with two molecules in the asymmetric unit. ^{1}H NMR (CD_3OD) δ: 7.51 (dd, *J* = 6.6, 8.3 Hz, 1H), 7.62 (t, *J* = 7.80 Hz, 2H), 7.69 (ttt, *J* = 1.2, 2.5, 6.9, 8.7 Hz, 1H), 7.94 (dd, *J* = 0.5, 8.3 Hz, 1H), 8.33 (dd, *J* = 1.4, 8.8 Hz, 2H), 8.39 (dd, *J* = 0.5, 6.4 Hz, 1H). ^{13}C NMR (CD_3OD) δ: 113.9, 122.7, 126.4, 129.5, 130.4, 134.7, 137.3, 148.4, 148.6, 167.5. LRMS $[M=H]^+$: 212 m/z.

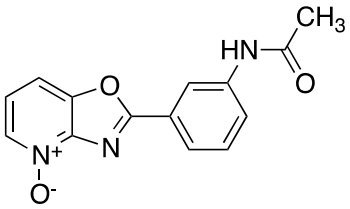

Synthesis of *N*-(3-(oxazolo[4,5-*b*]pyridine-2-yl)phenyl)acetamide 4-oxide (69). A mixture of compound **65** (0.10 g, 0.40 mmol) with *m*-chloroperbenzoic acid (0.152 g, 0.88 mmol) in dichloromethane was stirred at room temperature for 48 hours. Saturated $NaHCO_3$ was added and the mixture was extracted with dichloromethane, dried with anhydrous $MgSO_4$ and evaporated to dryness. The crude product was purified using flash chromatography on silica gel (Eluent: methanol: dichloromethane, 15:85) to give compound **69** as a yellow solid. ^{1}H NMR (CD_3OD) δ: 2.18 (bs, 3H), 7.52 (t, *J* = 7.5 Hz, 1H), 7.57 (t, *J* = 8.6 Hz, 1H), 7.85 (d, *J* = 8.6 Hz, 1H), 7.96 (d, *J* = 8.6 Hz, 1H), 8.07 (d, *J* = 7.9 Hz, 1H), 8.40 (d, *J* = 6.2 Hz, 1H), 8.62 (s, 1H). ^{13}C NMR (CD_3OD) δ: 24.1, 114.3, 120.7, 123.0, 125.2, 126.1, 127.2, 131.3, 137.7, 141.5, 148.7, 148.9, 167.6, 172.2. LRMS $[M=H]^+$: 270 m/z.

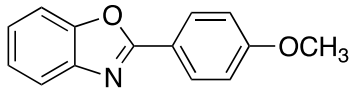

Synthesis of 2-(4-methoxyphenyl)benzo[*d*]oxazole (70). A mixture of 2-aminophenol (0.36 g, 3.29 mmol) and *m*-methoxybenzoic acid (0.50 g, 3.29 mmol) was heated in the microwave reactor at 250 °C for 2 minutes. Saturated $NaHCO_3$ was added and the mixture was extracted with dichloromethane, dried with anhydrous $MgSO_4$ and evaporated to dryness. The crude product was purified using flash chromatography on silica gel (Eluent: ethyl acetate: hexane, 20:80) to give compound **70** as a white solid. Whole spectral data matches that of

previously reported [312]. ^{1}H NMR ($CDCl_3$) δ: 3.89 (d, *J*= 1.4 Hz, 3H), 7.03 (d, *J*= 7.5 Hz, 2H), 7.30-7.35 (m, 2H), 7.55 (d, *J*= 7.6 Hz, 1H), 7.74 (d, *J*= 7.2 Hz, 1H), 8.20 (d, *J*= 7.2 Hz, 2H). ^{13}C NMR ($CDCl_3$) δ: 55.5, 110.5, 114.5, 119.7, 119.8, 124.5, 124.7, 129.5, 142.3, 150.8, 162.5, 163.3.

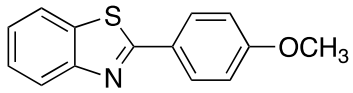

Synthesis of 2-(4-methoxyphenyl)benzo[*d*]thiazole (71). A mixture of 2-aminothiophenol (0.41 g, 3.29 mmol) and *p*-methoxybenzoic acid (0.60 g, 3.95 mmol) was heated in the microwave reactor at 220 °C for 4 minutes. Concentrated HCl (2 M) was added followed by saturated $NaHCO_3$ and the mixture was extracted with dichloromethane, dried with anhydrous $MgSO_4$ and evaporated to dryness. The crude product was purified using flash chromatography on silica gel (Eluent: ethyl acetate: hexane, 25:75) to give compound **71** as a white solid. Whole spectral data matches that of previously reported [313]. ^{1}H NMR (CD_3OD) δ: 3.88 (s, 3H), 7.07 (dd, *J* = 8.8 Hz, 2H), 7.39 (t, *J* = 8.1 Hz, 1H), 7.50 (t, *J* = 8.1 Hz, 1H), 7.96 (d, *J* = 9.0 Hz, 2H), 8.02 (d, *J* = 9.0 Hz, 2H). ^{13}C NMR (CD_3OD) δ: 56.0, 115.9, 122.8, 123.1, 123.6, 126.5, 127.4, 127.8, 128.6, 130.4, 136.1, 155.3, 164.1, 170.2.

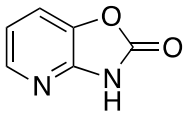

Synthesis of oxazolo[5,4-*b*]pyridine-2(1*H*)-one (72). A mixture of 2-amino-3-hydroxypyridine (1.00 g, 9.08 mmol) and 1,1-carboyldiimidazole (2.20 g, 13.6 mmol) in THF (20 mL) was refluxed at room temperature for 7 hours. THF was removed through evaporation and residue was dissolved in dichloromethane (20 mL). Concentrated NaOH (2 M) was added and the aqueous layer was collected and neutralised using concentrated HCl (2 M) for the formation of precipitate. The precipitate was filtered, washed with water and dried under vacuum to give compound **72** as a white solid. Whole spectral data matches that of previously reported [311]. ^{1}H

NMR (CD_3OD) δ: 7.11 (dd, *J* = 5.3, 8.1 Hz, 1H), 7.53 (d, *J* = 8.1 Hz, 1H), 8.02 (d, *J* = 5.3 Hz, 1H).

2.2 Reagents and test compounds in biological assays

All reagents used in this study were obtained from Sigma-Aldrich (Castle Hill, NSW, Australia) unless otherwise specified. PhIP **46** was purchased from Toronto Research Chemicals Inc. (Ontario, Toronto, Canada) and dissolved in dimethyl sulphoxide (DMSO) to produce a 50 mM stock solution. Stock solution of DNA repair inhibitors, 3,4-dihydro-5-[4-(1-piperidinyl)butoxyl]-1-(2*H*)-isoquinolinone (DPQ) (5 mM), methoxyamine hydrochloride (MxHCl) (5 M) and 2-(4-morpholinyl)-6-(1-thianthrenyl)-4H-pyran-4-one (KU55933) (10 mM) were prepared in DMSO. A stock solution of 6-hydroxy-2,5,7,8-tetramethylchromane-2-carboxylic acid (Trolox) (0.5 M) was prepared in DMSO. All compounds synthesized in this study **(refer to section 2.1.1.7)** were prepared in DMSO to produce stock solutions of 10 mM or 50 mM depending on compound solubility. Stock solutions were aliquoted into single-use Eppendorf tubes and stored at -20 °C until use. All plastic materials used for cell culture were obtained from Corning-*In Vitro* Technologies (Mulgrave, Victoria, Australia) and for bacterial culture were obtained from LabServ-Thermo Fisher Scientific (Scoresby, Victoria, Australia) unless otherwise specified.

2.3 Cell culture

HepG2 and HCT116 cells were obtained from the European Collection of Cell Culture (EACC). HepG2 cells were maintained in Dulbecco's Modified Eagle's medium (DMEM) and HCT116 cells were maintained in McCoy's 5A medium supplemented with glucose (1 g/L), fetal bovine serum (FBS) (10 %), penicillin (100 U/mL) and streptomycin (100 mg/mL) under standard culture conditions (37 °C, 5% CO_2, 95% air). Both cell lines were routinely cultured

in T-25 flasks and were passaged every three to four days or when the culture reached approximately 80% confluency. During each passage, cells were washed with phosphate buffered saline (PBS) without Ca^{2+} or Mg^{2+} (5 mL, 0.8% NaCl), followed by a brief wash with ethylenediaminetetraacetic acid (EDTA) (1 mL, 1mg/mL) and then incubated with a trypsinising mixture (1 mL, 0.5 g/L trypsin and 0.2 g/L EDTA) (Gibco, Life Technologies, Victoria, Australia) for 3 minutes under normal conditions to allow cell detachment from the surface of the flask. A cell suspension was then prepared by the addition of growth medium (9 mL) to obtain a trypsin to growth medium dilution ratio of 1:9 to deactivate the further proteolytic activity of trypsin. The cell density was determined via manual counting using the Neubauer chamber. Cells were diluted using growth medium to obtain the desired density per T-25 flask for HepG2 (2.0×10^6 cells) and HCT116 (1.0×10^6 cells). To exclude toxic effects, the concentration of DMSO was maintained at or below 0.1% (v/v) for all cell culture experiments.

2.4 Cryopreservation of cells

HepG2 (6.0×10^6 cells) or HCT116 (3.0×10^6 cells) were seeded in T-75 flasks, grown to 80% confluency, trypisinised and resuspended in growth medium to achieve a final volume of 10 mL. The cell suspension was centrifuged using an Elmi CM-6MT swinging bucket centrifuge (Skyline Ltd, Riga, Latvia) (500× g, RT, 5 minutes). The supernatant layer was removed and the pellet was resuspended in growth medium (1mL, 20% FBS and 10% DMSO), then placed into a cryotube. The temperature of the cryotube was lowered to -80 °C over a period of 24 hours in an isopropanol-containing tube box prior to long-term storage in liquid nitrogen.

2.5 Thawing of cells

Cryopreserved cells were thawed in a water bath (37 °C, 2 minutes) and carefully added into a T-75 flask containing pre-warmed growth medium (15 mL). The cells were grown under standard conditions for 24 hours to allow cell attachment to the surface before the growth medium was replaced to remove residual DMSO. Standard protocols of cell culture were carried out when the cells reached approximately 80% confluency.

2.6 Cell culture assays

2.6.1 Preparation of controls used in assays

The hydrogen peroxide stock (200 mM) was prepared in PBS and was used as the positive control for genotoxicity assays. The hydrogen peroxide stock was always prepared fresh and discarded after each experiment. The stock solution was diluted in growth medium (1:1000) to obtain a working concentration of 200 µM. The blank control consisted of growth medium and DMSO (0.001%). In all cell culture experiments, the DMSO content was standardised to 0.001% for all wells to allow comparisons.

2.6.2 Colony forming assay

The cytotoxicity of compounds was tested using the colony formation assay, which measures the reproductive ability of a single cell to form a colony of at least 50 cells in the continued presence of a potential toxin [210]. The colony formation assay was chosen for this study due to its high sensitivity and the inclusion of all cells in determining their reproductive ability when exposed to the test compounds. A fraction of cells will retain the capacity to produce colonies depending on the cytotoxic properties of the compound they are exposed to [210]. The colony forming assays were performed as previously described [314] with modifications outlined below.

2.6.2.1 Methods for the colony forming assay

HepG2 cells were grown in six-well plates and HCT116 cells in 100 mm petri dishes. Depending on cell type, HepG2 cells (1000 cells/well) and HCT116 cells (400 cells/dish) were seeded in the growth vessels. To ensure even distribution of cells, the growth vessels were moved gently at the north-south and east-west directions several times. Cells were then grown under standard conditions for 24 hours. After 24 hours, the growth medium was removed and replaced with pre-warmed growth medium containing test compounds and grown for a further 12 days under standard conditions. Hydrogen peroxide (200 µM) was used as the positive control).

After 12 days, cells were washed with PBS (HepG2, 1 mL or HCT116, 10mL) twice. Cells were then fixed (RT, 15 minutes) with PFA (2% in PBS; HepG2, 1mL or HCT-116, 5 mL). Then, Coomassie blue dye (HepG2, 1 mL or HCT116, 5 mL), which consisted of Brilliant Blue R-250 (0.25 %), methanol (40%), acetic acid (10%) and deionised water was added to each well or petri dish respectively and cells were stained (RT, 10 minutes). The dye was then removed by gentle washing with PBS once followed by distilled water twice. The stained cells were left to air dry for at least 24 hours prior to colony counting.

Viable colonies consisting of 50 cells or more were manually counted under an INV-100 light microscope BEL INV-100 light microscope (Aktivlab, Mount Barker, SA, Australia). Colony formation was expressed as percentage viability of the untreated control cells using the formula below:

$$\text{Percentage viability} = \frac{\text{Number of colonies per treatment group}}{\text{Number of colonies in the untreated control}} \times 100\ \%$$

Three replicates were prepared and used to calculate the mean for each independent experiment. Three independent experiments were conducted and the average of mean for three experiments (± standard deviation) was reported.

2.6.2.2 Cytotoxic dose-response relationship

Cells were treated with increasing concentrations of compound **60** (0.001, 0.01, 0.1, 1, 10 and 100 μM). Growth media containing the desired concentrations of test compounds were added respectively. The same steps were repeated for PhIP in growth medium to achieve the concentrations of 0.001, 0.01, 0.1, 1, 10 and 100 μM. The assay was then conducted as per **section 2.6.2.1**.

2.6.2.3 DNA repair inhibitors and compound 60 treatment in HepG2 cells

HepG2 cells were pre-treated with growth media (2 mL) containing the DNA repair inhibitors, DPQ (1.5 μM), KU55933 (2.1 μM) or MxHCl (1.4 μM) for one hour under normal conditions. Growth media containing the inhibitors was removed and replaced with fresh growth media (2 mL) supplemented with or without compound **60** (10 μM) as indicated. The assay was then conducted as per **section 2.6.2.1**.

2.6.3 Immunofluorescence assay in HepG2 cells

Immunofluorescence assays are highly sensitive and can be used to detect the expression of cellular proteins. This technique was used for the detection of γH2AX and 53BP1 proteins, where positive staining indicates the presence of DNA damage. Due to the close relationship of γH2AX and 53BP1 proteins in the repair complex [179], co-localisation staining can be conducted to confirm the presence of DNA damage to assess the reliability of the results

obtained. Immunofluorescence staining was performed as previously described [283,315] with modifications outlined below.

2.6.3.1 Methods for the immunofluorescence assay

Round glass coverslips (18 mm diameter and 0.17 mm thickness) were sterilised through immersion in ethanol (70 %) and placed into individual wells of a 12-well plate. Each coverslip was washed with PBS (1 mL) twice and residual PBS was removed. HepG2 cell suspension (1 mL, 2.0×10^5 cells) was added to the centre of the coverslip in the well. To ensure even distribution of cells, the vessel was moved gently at the north-south and east-west directions several times. The cells were grown under normal conditions for 24 hours to allow cell attachment onto the coverslip.

After 24 hours, the growth medium was removed and cells on the coverslip were treated accordingly and grown under standard conditions for 30 minutes. Hydrogen peroxide (200 µM) was used as the positive control. At the end of the treatment period, the coverslip was washed with pre-warmed PBS (1 mL) twice, drained and fixed with PFA (4 % in PBS and NaOH added to improve solubility) at RT for 10 minutes. The PFA solution was removed and the cells were permeabilised with buffer A (1 mL) made of Triton-X100 (0.15 %), horse serum (10%) and PBS. The coverslip was incubated at RT on an orbital shaker (100 rpm, 1 hour). The cells were then washed with buffer A (1 mL) twice and the coverslip was removed from the wells, dabbed dry on a clean tissue without disrupting the coverslip surface where the cells are attached to and placed in a humidified chamber. On the centre of the coverslip, Merck mouse anti-phospho-histone H2A.X (Ser139) antibodies [JBW301] (50 µL, 1:1000 in buffer A) was added and the humidified chamber was gently swirled in circular motion to ensure the antibodies covered the entire surface of the coverslips. The samples were incubated with the primary antibodies in the humidified chamber (4 °C, 24 hours).

After 24 hours, the coverslips were placed back into empty wells of a 12-well plate and were washed thrice with buffer B (1 mL) made of Triton-X100 (0.15 %), FBS (5%) and PBS (0.5×) at RT with 10 minutes incubation per washing step. Under darkened conditions, Abcam Alexa Fluor 488 conjugated goat anti-mouse antibodies [ab150117] (50 µL, 1:10000) in buffer C made of Triton-X100 (0.15 %), FBS (10%) and PBS, was added to the centre of the coverslip ensuring full surface coverage. Samples were exposed to the secondary antibody in the dark (RT, 1 hour). The coverslips were washed thrice with buffer C (1 mL) and once with PBS (1 mL) at RT with 10 minutes incubation per washing step. Then, DAPI solution (50 µL, 1:10000 in PBS) was added to the coverslips and incubated (RT, 2 minutes). Finally, the coverslips in the wells were washed twice with PBS (1 mL, 0.5×) at RT, removed from the wells with a pair of forceps, dabbed dry on a clean tissue and mounted on a glass microscope slides with Thermo Fisher Slow Fade® Gold anti-fade mounting reagent (50 µL). The mounted coverslip was left to air-dry for at least 12 hours in the dark at RT before conducting fluorescence microscopy. Fluorescent images were captured using a Nikon DS-Qi digital camera (Melville, New York, US) attached to a Nikon Eclipse 50i fluorescent microscope set at 60× magnification (Melville, New York, US)

The captured images were edited using a the Photoscape® photo-editing software (Version 3.7, App Team, London, UK) by altering three parameters namely sharpness, brightness and contrast using the same parameters for all images. Using the batch editor function of the program, all images were in parallel standardised with regards to sharpness, brightness and contrast levels of +8, +9 and +10 respectively. The images were then opened using the Microsoft Paint program (Washington, US) where green foci within the DAPI stained nucleus were manually scored. Each foci forming unit regardless of its size was considered as one foci. Genotoxicity was expressed as the average number of foci/cell in a cell population. For each independent experiment, 80 nuclei were haphazardly sampled in the captured images and

scored per treatment condition. The average number of foci per nucleus (± standard deviation) obtained from 80 cells was reported.

2.6.3.2 Co-localisation of γH2AX and 53BP1 proteins

HepG2 cells were treated with compound **60** (10 µM) and PhIP **46** (10 µM) for 30 minutes under standard conditions as per **section 2.6.3.1**. To the standard protocol, an additional immunostaining step using a 53BP1 antibody was included. For co-staining experiments, Abcam rabbit anti-53BP1 antibodies [ab36823] (50 µL 1:500 in buffer A) was performed together with Merck mouse anti-phospho-histone H2A.X (Ser139) antibodies as per **section 2.6.3.1**. Similarly, the secondary antibody used for the detection of the anti-53BP1 antibodies was Abcam Alexa Fluor 594 conjugated goat anti-rabbit antibodies [ab150084] (50 µL, 1:10000 in buffer C) was together with Abcam Alexa Fluor 488 conjugated goat anti-mouse antibodies as per **section 2.6.3.1**.

2.6.3.3 Genotoxic dose-response relationship

HepG2 cells were treated with increasing concentrations of compound **60** or PhIP **46** (0.001, 0.01, 0.1, 1, 10 and 100 µM) before cells were processed for immunostaining as per **section 2.6.3.1**.

2.6.3.4 Kinetics of DNA damage repair

HepG2 cells were treated with compound **60** (10 µM) or hydrogen peroxide (200 µM) for 30 minutes under standard conditions. At the beginning, four identical experimental sets corresponding to different time points (0.5, 8, 24 and 48 hours) with three replicates each were prepared. At the end of 30 minutes treatment, the first set of cells was fixed and stored in PBS at 4 °C. For the remaining batches, growth media was replaced with fresh medium (without

test compound) and cells left to recover under standard growth conditions. Subsequently, cells were fixed at different time points (8, 24 and 48 hours) and stored in PBS at 4 °C. Immunostaining was then conducted as per **section 2.6.3.1**.

2.6.3.5 QSAR studies and compound *N*-oxidation in genotoxicity

HepG2 cells were treated with compounds **40a, 40b, 40e, 60, 61, 62, 63, 64, 65, 66, 68, 70, 71** and **72** (10 µM) for 30 minutes. The assay was then conducted as per **section 2.6.3.1**.

2.6.3.6 Effect of compound oxidation on genotoxicity

HepG2 cells were pre-treated with Trolox (10 µM) under standard growth conditions (2 hours). After that, the Trolox-containing growth media was removed and replaced with growth media containing compound **60** (10 µM) and/or Trolox (10 µM) as indicated and the cells were incubated under standard growth conditions for another 30 minutes. Immunostaining was then conducted as per **section 2.6.3.1**.

2.6.4 Comet assay in HepG2 cells

The comet assay is a sensitive method to determine the presence of DNA strand breaks by DNA damaging agents. In the presence of a genotoxic agent, DNA damage occurs forming fragments, which can travel away from the nucleus on the electric field during electrophoresis. As a result, a fluorescent comet motive appears after DNA staining, where the comet head represents the cellular nucleus and the tail represents released DNA fragments due to induced DNA strand breaks [291,292]. In this study, the percentage tail length was used to determine the severity of DNA damage caused by the test compounds. The comet assays were performed as previously described [316] with modifications as outlined below.

2.6.4.1 Methods for the comet assay

In a 6-well plate, HepG2 cells (5.0×10^5 cells/ well) were seeded and grown under standard conditions for 3 to 4 days. The cells were treated with compound **60** or PhIP **46** (10 µM) under normal conditions for 30 minutes. After treatment, the growth medium was removed and PBS (500 µL) were added to each well to scrape the cells off the surface of the well with a cell scraper. The resulting cell suspension was mixed gently and the cell density was determined using a Neubauer chamber. Cell viability was determined using the trypan blue exclusion method. This was done by mixing the cell suspension (10 µL, 10^6 cells/mL) with trypan blue dye (5 µL, 0.4% in deionised water) in an Eppendorf tube. Cells were incubated with the dye at room temperature for two minutes and the numbers of viable cells (colourless) and dead cells (blue) were determined by manual scoring using standard light microscopy.

Microscope slides coated with agarose were prepared a day prior to the experiment. This was done by dipping the microscope slides with ethanol (100 %) to remove impurities on the surface of the slide and subsequent flaming to remove the residual ethanol. The slides were then dipped in normal melt agar (1 % in milli-Q water, autoclaved) up to one third of the slide. The underside of the slides were immediately wiped with a clean paper towel and the slides were air-dried overnight. To the agarose-coated slides, low melt agar (80 µL, 0.5% in milli-Q water, microwaved) was added and then covered with a coverslip. The thin layer of agar underneath the coverslip was left to solidify at room temperature for 30 minutes. The coverslip was then removed gently with a pair of forceps. The cell suspension (10 µL, 5.0×10^5 cells) was added to low melt agar (70 µL) in an Eppendorf tube and mixed by gentle flicking. Then, the low melt agar mixture containing cells (80 µL) was added onto the solidified layer of agar and covered with a coverslip. The second layer of agar underneath the coverslip was left to solidify

(RT, 30 minutes). The coverslip was removed gently with a pair of forceps. The third and fourth layers of low melt agar without cells were prepared following previous steps.

Prepared slides containing the four layers were submerged in cold lysis buffer consisted of NaCl (2.5 M), EDTA (100 mM), Tris-base at pH 10 (10 mM), Triton X-100 (1%) and water. The slides were incubated (4 ºC, 1 hour) to allow cell lysis. The slides were then removed from the lysis buffer and placed side by side in the Fisher Biotech electrophoresis gel tank [OL120705143] (Wembley, WA, Australia). The buffer reservoirs of the gel tank were filled with electrophoresis buffer consisted of NaOH (300 mM), EDTA (1 mM) and water adjusted to pH 13 until slides were fully covered and incubated in the buffer at 4 ºC for 20 minutes to allow DNA unwinding. Electrophoresis was performed on the slides using the Bio-rad Model 200/2.0 power supply (Hercules, California, US) (25 V, 300 mA, 4 ºC, 30 minutes). The slides were washed thrice with the neutralisation buffer (2 mL) consisted of Tris-base (0.4 M) and water adjusted pH 7.5 for 5 minutes during each washing step.

DNA was stained by adding Invitrogen SYBR safe (80 µL) onto the top agar layer and incubated (RT, 5 minutes). Excess stain was removed by dipping the slides in chilled distilled water. Clean coverslips were placed on the agar layer side of the slides and viewed under the microscope immediately. Comet images were captured using a Nikon DS-Qi IMC digital camera (Melville, New York, US) attached to a Nikon Eclipse 50i fluorescent microscope (Melville, New York, US). The length of the comet head and tail were manually determined. Genotoxicity was expressed as the percentage of tail length of the entire comet calculated using the formula below:

$$\text{Percentage tail length} = \frac{\text{Length of comet tail}}{\text{Length of comet head} + \text{tail}} \times 100\ \%$$

50 Nuclei were measured and used to calculate the mean for each independent experiment. Two independent experiments were conducted and the average of the mean for both experiments (± standard deviation) was reported.

2.6.5 Soft agar invasion assay in HepG2 cells

The soft agar assay was used to evaluate the cellular transformation potential of test compounds. This assay relies on the genetic transformation capacity of the cells by a mutagenic compound [274]. Adherent cells such as HepG2, are normally not able to grow when embedded in soft agar due to their requirement of anchorage-dependent growth. This characteristic, can however be reversed as a result of gene mutations [300]. Therefore, cells that are able to grow and form colonies in soft agar indicate the presence of mutation events leading to cellular transformation. The colony forming assays were performed as previously described [274] with modifications outlined below.

2.6.5.1 Methods for the soft agar invasion assay

Bacteriological grade agar broth (1% in Milli-Q water) was prepared by autoclaving (121 °C, 5 minutes). The double strength medium made of DMEM (2×), FBS (20 %), glucose (2 g/L), penicillin (200 U/mL) and streptomycin (200 mg/mL) was maintained at 40 °C using a water bath along with the autoclaved agar broth. The agar broth (20 mL) was added to the double strength medium (20 mL) in a 50 mL tube to obtain an agar-growth media mixture of DMEM (1×), FBS (10 %), glucose (1 g/L), penicillin (100 U/mL), streptomycin (100 mg/mL) and agar (0.5%). Test compounds were added into the agar-growth media mixture to achieve final concentrations as indicated. The agar-growth mixture was transferred into 6-well plate (2mL/ well) and allowed to solidify (RT, 5 minutes), which formed the first agar layer of the assay. If

not used on the same day, agar-containing 6-well plates were stored at 4 °C and used within one week from the date of preparation.

Next, agarose broth (0.7 % in Milli-Q water) was prepared by heating in a microwave and maintained, together with the double strength growth medium at 40 °C using a water bath. The agar broth (20 mL) was added to the double strength growth medium (20 mL) in a 50 mL tube to obtain the agarose-growth media mixture of DMEM (1×), FBS (10 %), glucose (1 g/L), penicillin (100 U/mL), streptomycin (100 mg/mL) and agarose (0.35%). Test compounds were added into the agarose-growth media mixture to achieve final concentrations as indicated. With the agarose-growth media mixture still in its liquid form, HepG2 cells (2500 cells/mL) were seeded and mixed gently to achieve an even distribution. The resulting mixture containing cells (2 mL) was added on the first agar layer prepared earlier and allowed to solidify (RT, 5 minutes). This formed the second layer for the assay. Finally, the third layer, which consisted of standard DMEM growth media with/without test compounds as indicated, was added.

Cells were grown under standard growth conditions for 20 to 30 days. The top medium layer was replaced every 3 to 4 days for cell maintenance. After 20 to 30 days, the top layer was removed, crystal violet solution (1 mL, 0.005% in PBS) containing ethanol (2 %) was added into each well and the colonies were stained (37 °C, 24 hours). Stained colonies were viewed under a BEL INV-100 light microscope (Aktivlab, Mount Barker, SA, Australia) and images were captured for analysis. Colonies with diameters above the pre-determined baseline value of 50 µm were included in the analysis. Colony formation was expressed as colony volume, V calculated using the formula $V = \frac{4}{3}\pi r^3$. Three independent experiments were conducted and the results from these experiments were represented as a scatter-plot. The mean colony volume (± standard deviation) from these experiments was also reported.

2.7 Growth of bacterial culture

Salmonella typhimurium strain TA100 was grown in Luria-Bertani (LB) broth (2mL) supplemented with ampicillin (100 µg/mL) overnight (37 ºC, 18-24 hours) with shaking.

2.8 Preparation of controls used in assays

PhIP **46** (10 µM) was used as reference compound for mutagenicity in the Ames test while the blank control consisted of growth medium and DMSO (0.001%). In all bacterial culture experiments, the DMSO content was standardised to 0.001% for all wells to allow comparisons.

2.9 Ames test

The Ames test is regarded as the "gold standard" to assess mutagenicity and is required by the ICH and USFDA. *Salmonella* TA100 was used as the test organism in the Ames test because it is commonly used in toxicological screens [242,243] In addition, *Salmonella* TA100 can detect point mutations that can arise through chemical-induced DNA base modifications [244], which is the mutagenic mode of action of the reference compound, PhIP **46**. The *Salmonella* TA100 strain used in this study carries a defect in its *hisD* gene and hence is histidine-requiring (His^-) and cannot grow in the absence of exogenous histidine [243]. Thus, this strain can revert to histidine prototrophy (His^+) under conditions of selection either spontaneously or else by chemical induction via a point mutation in the *hisD* gene [241]. In this experiment, the number of revertant colonies recovered at the end of incubation was enumerated to evaluate the extent of mutagenicity (reflected by bacterial cells mutability) caused by the test compounds. The Ames assays with and without S9 liver extract were performed as previously described [241,258] with modifications outlined below. The minimal agar for the Ames test was prepared based on the composition previously described [317] with the omission of $Na_3C_6H_5O_7$.

2.9.1 Methods for the Ames test

Overnight His$^-$ *Salmonella* TA100 culture was diluted in LB broth to 1:100 and grown at 37 ºC for three hours in a shaking incubator to mid-exponential to early stationary growth phase (10^6 to 10^8 cfu/mL). The Ames test was performed by mixing His$^-$ *Salmonella* TA100 culture (100 µL); Ames activation buffer (500 µL) consisted KCl (33 mM), $MgCl_2$ (8 mM), glucose-6-phosphate (5 mM), NADPH (4 mM) and Na_3PO_4 (102 mM); rat S9 liver extract [SLBR5811V] (100 µL); and test compounds as indicated. For treatments without S9 liver extract, the equivalent volume of PBS was used to replace the extract. The reaction mixture was incubated on a shaking incubator (37 ºC, 30 minutes). After incubation, the reaction mixture (100 µL) was spread plated on bacteriological agar supplemented with glycerol (0.2 %), histidine (0.5 µg/mL), K_2HPO_4 (40 mM), KH_2PO_4 (15 mM), $(NH_4)_2SO_4$ (7.5 mM), $MgSO_4$ (0.41 mM) and Milli-Q water. The bacterial cells were grown (37 ºC, 4 days) and the number of revertant colonies were manually scored. The number of His$^+$ revertant colonies in treatment plates (with or without S9 liver extract) were corrected by subtracting the number of revertant colonies formed in the non-treatment plates (with or without S9 liver extract) due to spontaneous mutation events. Mutagenicity reflected by bacterial cell mutability, was expressed as number of His$^+$ revertant colonies per plate. Three replicates were prepared and used to calculate the mean for each independent experiment. Three independent experiments were conducted and the results reported represent the average of the mean (± standard deviation).

2.9.2 Detection of pro-mutagens and effect of *N*-oxidation on mutagenicity

His$^-$ *Salmonella* TA100 cells were treated with compound **60** (10 µM) or PhIP **46** (10 µM) (37 ºC, 30 minutes). In another experiment, bacterial cells were treated with compounds **40a, 61** and **65** (10 µM) and their corresponding *N*-oxides, **67**, **68** and **69** (10 µM) (37 ºC, 30 minutes). The assay was then conducted as per **section 2.9.1**.

2.10 Enzymatic bio-activation with S9 liver extract

Upon the enzymatic bio-activation of the oxazolopyridine compound using S9 liver extract, UPLC-MS was used to monitor the reaction and identify the active species. UPLC-MS is the main method used for the detection of drug metabolites in complex biological matrices. This is due to the high sensitivity and specificity of the method, which can provide structural information for biochemical assays such as the one in this experiment using S9 liver extract in a buffered solution. Enzymatic bio-activation of the oxazolopyridine compounds were conducted as previously described for PhIP **46** [318] with modifications outlined below. The UPLC-MS analyses were performed by the Central Science Laboratory at the University of Tasmania.

2.10.1 Methods for enzymatic bio-activation with S9 liver extract

In a stoppered tube placed on ice, the reaction buffer (1 mL), which consisted of rat S9 liver extract [SLBR5811V] (1 mg/mL), $MgCl_2$ (15 mM), NADP (10 mM), glucose-6-phosphate (150 mM), glucose-6-phosphate dehydrogenase (125 U/mL) and Na_3PO_4 (0.1 M) adjusted to pH 7.4 was prepared. To the buffer, the test compound (1 µM) was added and the reaction mixture was incubated on a shaking water bath (37 °C, 100 rpm, 3 hours). After incubation, equivalent volume of ice-cold methanol (500 µL) was added to the reaction mixture (500 µL) in a clean Eppendorf tube and incubated on ice (5 minutes) for protein precipitation. The precipitate was removed via centrifugation using the Eppendorf 5417R centrifuge machine (North Ryde, NSW, Australia) (1500× g, 4 °C, 5 minutes). The methanolic extract in the supernatant layer was stored at -80 °C until further analysis using ultra pressure liquid chromatography and mass spectrometry (UPLC-MS).

2.10.2 Analysis of enzymatic bio-activated metabolites via UPLC-MS

The UPLC-MS analysis was conducted using the Waters Acquity H-class UPLC system (Milford, Massachusetts, US) instrument and chromatography was performed using a Waters Aquity BEH C18 column (2.1 × 100 mm × 1.7 μm) (Milford, Massachusetts, US). The UPLC was operated with mobile phases consisting of formic acid (0.1 % in water) (solvent A) and acetonitrile (solvent B). A gradient elution was carried out where initially, solvent A (100%) followed by a gradient to solvent B (52.5%) over 5 minutes. This was held for 1 minute before returning to initial conditions and re-equilibration for 3 minutes. The UPLC was operated at a flow rate of 0.35 mL/min, temperature of 45 ºC and the sample injection volume of 2 μL. The UPLC was coupled to a Waters Xevo® triple quadrupole mass spectrometer (Milford, Massachusetts, US). Analyses were undertaken using multiple reaction monitoring (MRM) in positive electrospray ionisation mode. Electrospray ionisation was performed with a capillary voltage of 2.7 kV, and individual cone voltages and collision energies for each MRM transition, as described (Table 9). Other parameters set include the desolvation temperature (450 °C), flow rate of the nebulising gas, N_2 (950 L/h) and flow rate of the cone gas, N_2 (50 L/h). MRM transition dwell times were 0.047 second. For the total ion count (TIC) mode, the operation conditions were the same except that it was operated in full scan mode, over the mass over charge ratio (m/z) of 100-300.

Table 9: Quantitation and confirmation MRM and electrospray ionisation parameters of each analyte.

Analytes	Mass to charge ratio (m/z)		Cone (V)	Collision (V)
	Pre-cursor	Products		
40a	227.2	184.1 / 212.2	61	39 / 31
67	243.2	211.1 / 226.2	61	38 / 29

2.11 Computational methods

Gaussian 16 [319]was used to fully optimize all the structures reported in this study at the B3LYP level [320-322] of density functional theory (DFT) using the CPCM [323] solvation model. The 6-31G(d) basis set (BS1) was used for all atoms. Frequency calculations were carried out at the same level of theory as those for the structural optimization. Transition structures were located using the Berny algorithm. Intrinsic reaction coordinate (IRC) calculations [324] were used to confirm the connectivity between transition structures and minima. To further refine the energies obtained from the B3LYP/BS1 calculations, we carried out single-point energy calculations for all of the structures with a larger basis set (BS2) using the CPCM solvation model [320-322] at the M062X [325] level. BS2 utilizes def2- TZVP basis set on all atoms. All thermodynamic data were calculated at the standard state (298.15 K and 1 atm). To estimate the corresponding Gibbs free energies, entropy corrections were calculated at the B3LYP/BS1 level and added to the single point potential energies. The computational analyses were performed by the Computational Chemistry group at the University of Tasmania.

2.12 Statistical analyses

Data was expressed as mean ± SD as indicated in the figure legends unless stated otherwise. Statistical significance was performed using Student t-test or one-way analysis of variance (ANOVA) where appropriate, followed by Bonferroni's multiple comparison tests to determine the differences between control and treatment group or between treatment groups. The correlation coefficient (R^2) analysis was also performed to determine the linearity of the relationship between two variables when necessary. In all the assays conducted, $p< 0.005$ was considered statistically significant. Statistical analyses were conducted using the GraphPad Prism version 7.01 program (GraphPad Software Inc, California, US).

Chapter 3 Cytotoxicity and genotoxicity of compound 60

3.1 Overview and rationale

To obtain more representative data on possible cytotoxicity in humans, the cytotoxicity screening of 2-(3-aminophenyl)oxazolopyridine, **60** was conducted in HepG2 and HCT116 cells. The two cell lines were chosen on the basis that their tissue origins (liver and intestine) are involved in the pharmacokinetics of orally ingested drugs, mainly absorption and metabolism [326]. The liver is the site for drug metabolism where hepatocytes produce microsomes required for phases I and II of drug metabolism [327]. The colon is the main site for absorption of orally ingested drugs where colon epithelial cells produce metabolic enzymes involved in drug metabolism. Moreover, testing the lead compound in two cell lines also allowed the determination of cell line-dependent cytotoxicity. Cell line-dependent cytotoxicity is important to understand the mode of action of a compound due to the intrinsic differences between cell types such as the expression of functional proteins such as enzymes and receptors.

Genotoxicity is also commonly linked to cytotoxicity where genotoxic agents damage the DNA of the cell and compromises the genomic stability of the cell preventing cell replication leading to apoptotic death. Genotoxicity screening was conducted on compound **60** due to the structural similarity to the known carcinogen, PhIP **46** and the positive genotoxicity of other oxazolopyridine analogues as observed previously at the University of Tasmania (unpublished data). An initial determination of genotoxicity of compound **60** was conducted in HepG2 and HCT116 cells. Among the two cell lines, the genotoxicity in HepG2 cells was more important since the liver is the main site for drug metabolism. Therefore, the genotoxicity of genotoxic or pro-genotoxic drugs can be detected in these cells.

3.2 Aims

Only two cytotoxicity screens in mammalian cells [38,39] and one in a rodent model [39] have been conducted to date for oxazolopyridine compounds. These reports were not able to demonstrate cytotoxicity but are not sufficient to completely rule out the safety of oxazolopyridine compounds. There is still a lack of knowledge about the cytotoxicity of oxazolopyridines in mammalian cells which should be thoroughly examined before these compounds are further developed into drugs. Due to the preliminary data that highlight genotoxicity of some oxazolopyridine analogues conducted at the University of Tasmania (unpublished data), the following evaluations were conducted to reproduce and extend these findings. The overall aim of this section was to evaluate the cytotoxicity and genotoxicity of 2-(3-aminophenyl)oxazolopyridine **60**. In the experiments outlined in this section, the carcinogen, PhIP **46** was used as the reference compound for genotoxicity based on the hypothesis that compound **60** may be genotoxic and mutagenic due to structural similarities to PhIP **46**. The following experiments were performed to address the objectives:

- Dose-response cytotoxicity determination of compound **60** and PhIP **46** in HepG2 and HCT116 cells.
- Dose-response genotoxicity determination of compound **60** and PhIP, **46** in HepG2 cells.
- Understanding the repair of DNA damage induced by compound **60**, if present, in HepG2 cells.

3.3 Methodology

The methods for chemical syntheses and analyses are described in **section 2.1**. The methods for the biological assays conducted in this chapter are described in sections **2.6.2**, **2.6.3** and **2.6.4**.

3.4 Results and discussion

3.4.1 Cytotoxic determination of compound 60

Most mutagens are also classed as cytotoxic but PhIP **46** is one of the few exceptions, being widely described as non-cytotoxic [328,329]. The dose-response cytotoxicities of 2-(3-aminophenyl)oxazolopyridine **60** and PhIP **46** in HepG2 and HCT116 cells were determined using different concentrations (0.001 to 100 µM) of the test compounds. Compound **60** only showed any cytotoxicity at 100 µM in HepG2 cells (Figure 18), while no cytotoxicity was detected up to 100 µM in HCT116 cells (Figure 18). In contrast, it was found that PhIP **46** showed cytotoxicity from 0.001 µM in HepG2 cells but not cytotoxic in HCT116 cells at any concentration (Figure 18). The positive control, hydrogen peroxide was potently cytotoxic in both HepG2 and HCT116 cells with no residual viability detected after treatment (Figure 18).

Based on the results shown, PhIP **46** was mildly cytotoxic in HepG2 cells at low nano-molar concentrations although not cytotoxic in HCT116 cells. This indicated that HepG2 cells were more sensitive to PhIP **46** compared to HCT116 cells, which suggests that the effect could be cell line selective. The liver is the centre for chemical metabolism and produces metabolic cytochrome P450 enzymes required for the bio-activation of PhIP **46** into arylnitrenium ions, which subsequently react with genomic DNA [105,106]. Although intestinal cells also produce cytochrome P450 enzymes, the number of expressed isoforms that are actively involved in drug metabolism and their amounts are significantly lower in the intestine compared to the liver

[330,331]. The reaction of PhIP **46** and DNA may compromise cellular genomic integrity, which subsequently disrupt DNA replication leading to the initiation of apoptotic cell death [332]. Therefore, it was not surprising that mild cytotoxicity was observed for PhIP **46** especially in HepG2 cells.

In either HepG2 or HCT116 cells, compound **60** was not cytotoxic due to the lack of a dose-response up to 10 µM. However at 100 µM, a decrease in cell viability was observed in HepG2 cells and it is the threshold concentration where compound **60** becomes toxic. It is important to note that 100 µM is a relatively high concentration for cells to be exposed to and can likely cause non-specific toxicity. Compound screens for hit discovery are commonly performed at concentrations of up to 10 µM as concentrations beyond that will cause non-specific toxicity and exceed acceptable therapeutic doses in patients [333]. High concentrations of test compound may lead to promiscuous inhibition of metabolic enzymes or surface proteins leading to unintended cell death [334]. Chemical overloading can also disrupt the redox balance in cells that can lead to the production of ROS, which can damage DNA, proteins and lipids and can initiate cell death [335].

At a high concentration (100 µM), HepG2 cells were more sensitive to compound **60** compared to HCT116 cells, which could support a role of chemical metabolism by liver enzymes for compound toxicity. The positive control used in these experiments, hydrogen peroxide was potently cytotoxic in HepG2 and HCT116 cells as no residual viability was detected in these cell lines. In a cellular context, hydrogen peroxide induces oxidative stress through the production of ROS and is rapidly converted to harmful free radicals resulting in cell death [336]. The consistent cellular response to hydrogen peroxide indicated that the decrease in cell viability detected for the test compounds in this experiment were reliable results.

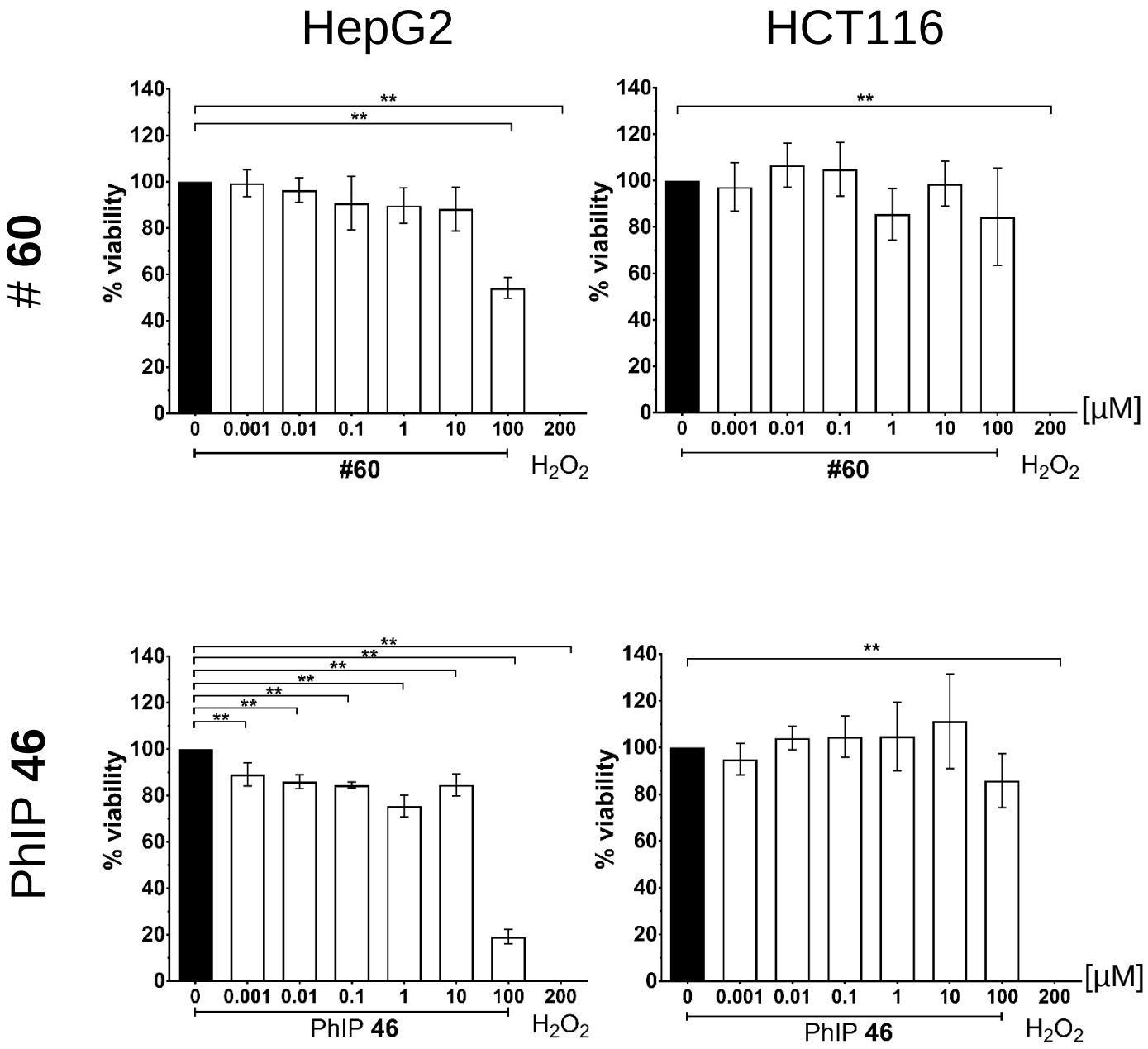

Figure 18: Cytotoxicity of compound 60 and PhIP 46. Viability of cells was assessed by colony formation assay. HepG2 and HCT116 cells were exposed to increasing concentrations (0 to 100 µM) of: Compound **60** in HepG2 and HCT116 cells; and PhIP **46** over 12 days. Hydrogen peroxide (200 µM) was used as positive control. Viability data represent the mean of three independent experiments with three replicates per experiment and is expressed as % of untreated control. Error bars represent SD and ** denotes P<0.01. # denotes compound number.

Similar to reports on the lack of cytotoxicity of oxazolopyridine compounds, compound 60 was also not cytotoxic. Despite the lack of cytotoxicity for compound **60**, its genotoxicity is not known. Therefore, this can be investigated through the quantification of DNA damage induced by compound **60**.

3.4.2 Genotoxic determination of compound 60

3.4.2.1 Immunostaining of genotoxicity indicator proteins, γH2AX and 53BP1

Immunostaining was conducted to detect γH2AX and 53BP1 foci, which are DNA damage markers indicative of genotoxic activity. For this reason, genotoxicity assessment was only performed in HepG2 cells since these cells are widely used in biochemical and nutritional studies, and are regarded to closely resemble primary cultured hepatocytes [337]. Moreover, liver cells are actively involved in drug metabolism, which allow the sensitive detection of pro-genotoxins which may not be detected in other cell lines [337]. Due to the lack of cytotoxicity of 2-(3-aminophenyl)oxazolopyridine **60** and mild cytotoxicity of PhIP **46**, the following experiments were conducted at 10 μM, which is the commonly accepted concentration in HTS by the pharmaceutical industry [338] unless stated otherwise.

The presence of nuclear γH2AX and 53BP1 protein foci was determined through the detection of the characteristic nuclear immunopositive after staining (Figure 19). Cells treated with compound **60** (10 μM), PhIP **46** (10 μM) and the positive control, hydrogen peroxide (200 μM) showed the presence of γH2AX and 53BP1 foci (Figure 19). Little to no γH2AX and 53BP1 foci were detectable in untreated cells (Figure 19). Only cells with intact nuclei were analysed in this experiment shown by DAPI-stained nuclear DNA (blue) (Figure 19). Panels corresponding to γH2AX, 53BP1 and DAPI signals were merged to confirm the location of the foci within the nucleus of the cell. This can be seen by the presence of γH2AX (green) and

53BP1 (red) foci within a DAPI-stained nucleus (blue) (Figure 19). The merged panels shows the co-localisation of γH2AX and 53BP1 foci illustrating the close relationship of the two proteins (Figure 19).

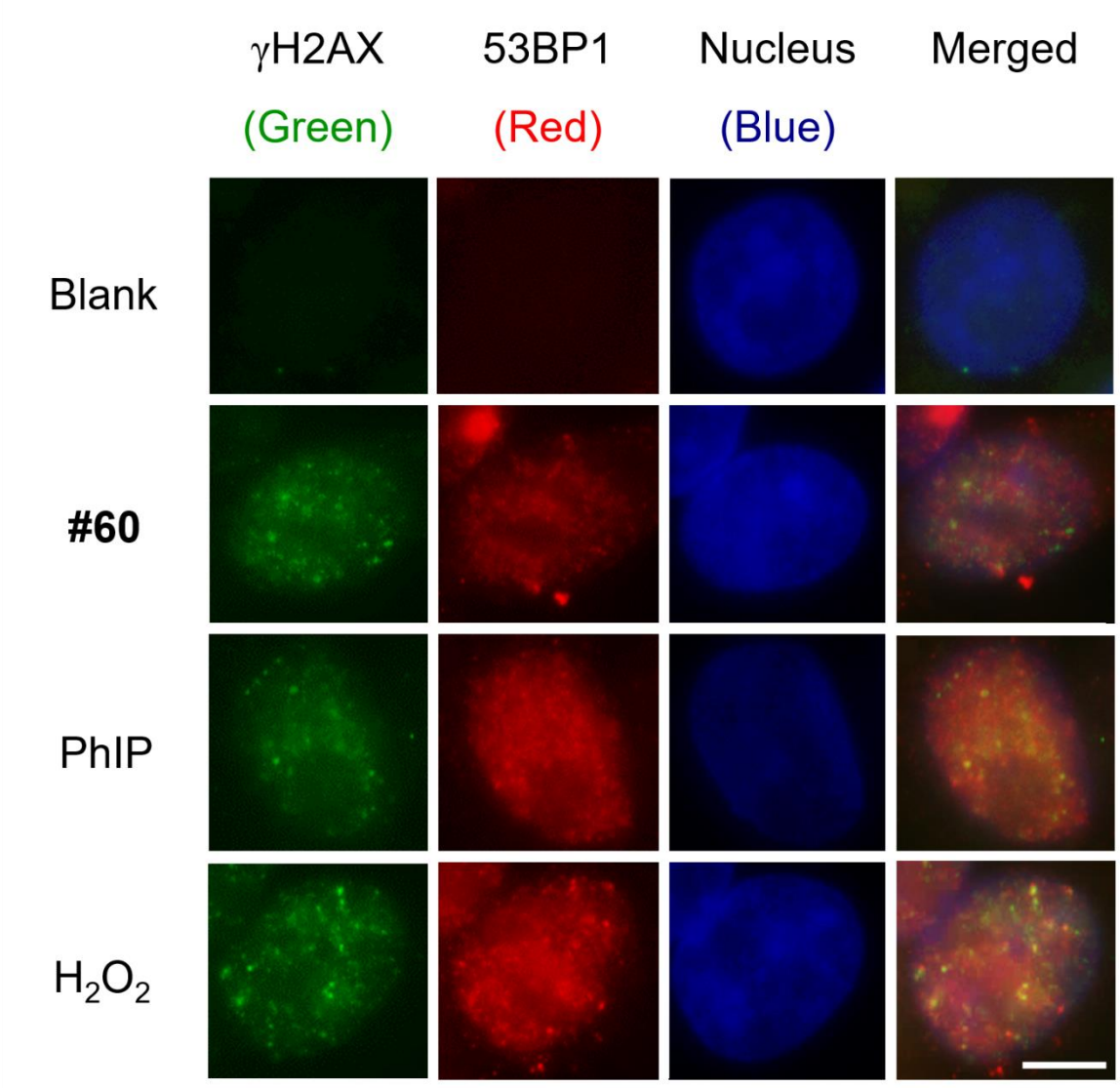

Figure 19: DNA damage detection in HepG2 cells. Cells were incubated with compound **60** (10 µM) or PhIP **46** (10 µM) for 30 minutes prior to immunofluorescence detection of γH2AX and 53BP1 foci indicative of DNA damage. **Green:** γH2AX protein staining (γH2AX foci); **Red:** 53BP1 protein staining (53BP1 foci), **Blue:** DAPI staining of nuclear DNA and **Merged:** Co-localisation of 53BP1 and γH2AX foci. Hydrogen peroxide (200 µM) was used as positive control. Panels show exemplary images of the 80 nuclei analysed in one independent experiment. Scale bar represents 10 µm. # denotes compound number.

In the presence of DNA damage such as strand breaks, a homologous recombination repair cascade is initiated leading to the formation of the γH2AX protein [339,340]. The H2AX subunit of the histone protein located in the nucleus of the cell is phosphorylated to form γH2AX by the ataxia telangiectasia mutated (ATM) protein [341]. This process recruits additional proteins such as 53BP1 to the site of damage [283,339]. The co-localisation of γH2AX and 53BP1 foci allowed the evaluation of the fidelity and accuracy of the immunostaining method used in the proceeding experiments. When the cells were exposed to hydrogen peroxide (200 μM), γH2AX foci were detected. This was expected as hydrogen peroxide damages the DNA to form strand breaks [342,343]. The presence of γH2AX foci in cells treated with PhIP **46** is consistent with previous reports that have reported similar findings [344] although PhIP **46** is a base modifier and does not form strand breaks [345]. This however is supported by reports that γH2AX can be produced by other sources of DNA damage aside from DNA strand breaks and the γH2AX assay should only be used as an indirect means of monitoring of double strand breaks [346]. For these reasons, the presence of the γH2AX foci was used as an indicator of DNA damage, even though the nature of that damage is not known. Surprisingly, compound **60 (**10 μM) caused γH2AX and 53BP1 foci indicative of DNA damage and genotoxicity.

3.4.2.2 Genotoxic dose-response determination of compound 60

To accurately determine the extent of genotoxicity of 2-(3-aminophenyl)oxazolopyridine **60** and PhIP **46**, a dose-response relationship was established using different concentrations (0 to 100 μM) in HepG2 cells. The magnitude of genotoxicity was determined by manual scoring of γH2AX foci per nucleus expressed as foci/cell. Since the fidelity of the assay was verified using the positive control, hydrogen peroxide and co-localisation staining explained in the previous section, the quantification of genotoxicity for the following experiments focused only on the different concentrations of compound **60** and PhIP **46**.

For compound **60**, a significant increase in genotoxicity was already detected from 0.001 µM onwards (Figure 20A). However, the amount of genotoxicity remained constant between 0.01 and 1 µM but then continued to increase from 10 µM onwards (Figure 20A). Similar to compound **60**, PhIP **46**, significantly increased genotoxicity from 0.001 µM onwards and progressively increased further up to 100 µM (Figure 20B). Generally, genotoxicity induced by PhIP **46** was higher compared to compound **60** at the concentrations tested (0.001 – 100 µM). For example, at 10 and 100 µM, the amount of genotoxicity detected for compound **60** were 46 and 59 foci/cell respectively (Figure 20A), while for PhIP **46**, 71 and 96 foci/cell were detected respectively (Figure 20B).

Compound **60** and PhIP **46** showed genotoxicity although the levels detected in PhIP **46** were higher than compound **60**. For PhIP **46**, the genotoxicity detected is consistent with previous studies conducted using the γH2AX assay [344,347]. The higher genotoxicity potential as shown in this experiment is also consistent with the higher cytotoxicity of PhIP **46** in HepG2 cells **(refer to section 3.4.1)**. Moreover, based on the results from the colony forming and γH2AX assays, it indicates that high levels of genotoxicity are required for observable cytotoxicity. This was consistent with previous reports for some carcinogens including PhIP **46** [348,349]. For example, 10 µM of compound **60** and 0.001 µM of PhIP **46**, caused a significant decline in cell viability was detected in the colony forming assay (Figure 18, **section 3.4.1**). In parallel, the amount of genotoxicity at 10 µM of compound **60** and 0.001 µM of PhIP **46** (where a significant increase in genotoxicity was detected), were similar around 46 (Figure 20A) and 45 (Figure 20B) foci/cell respectively. In other words, PhIP **46** was approximately 1×10^5 times more genotoxic than compound **60**. Highly genotoxic agents, such as PhIP **46** can compromise the structure of the DNA, which in turn affects cell replication and growth, ultimately leading to cell death [350]. These results also demonstrated that the γH2AX assay is a highly sensitive assay that detects DNA damage responses at very low drug concentrations. However, other

tests should be conducted to confirm the genotoxicity of compound **60** as it is common practice to include two or more tests for compound characterisation [238].

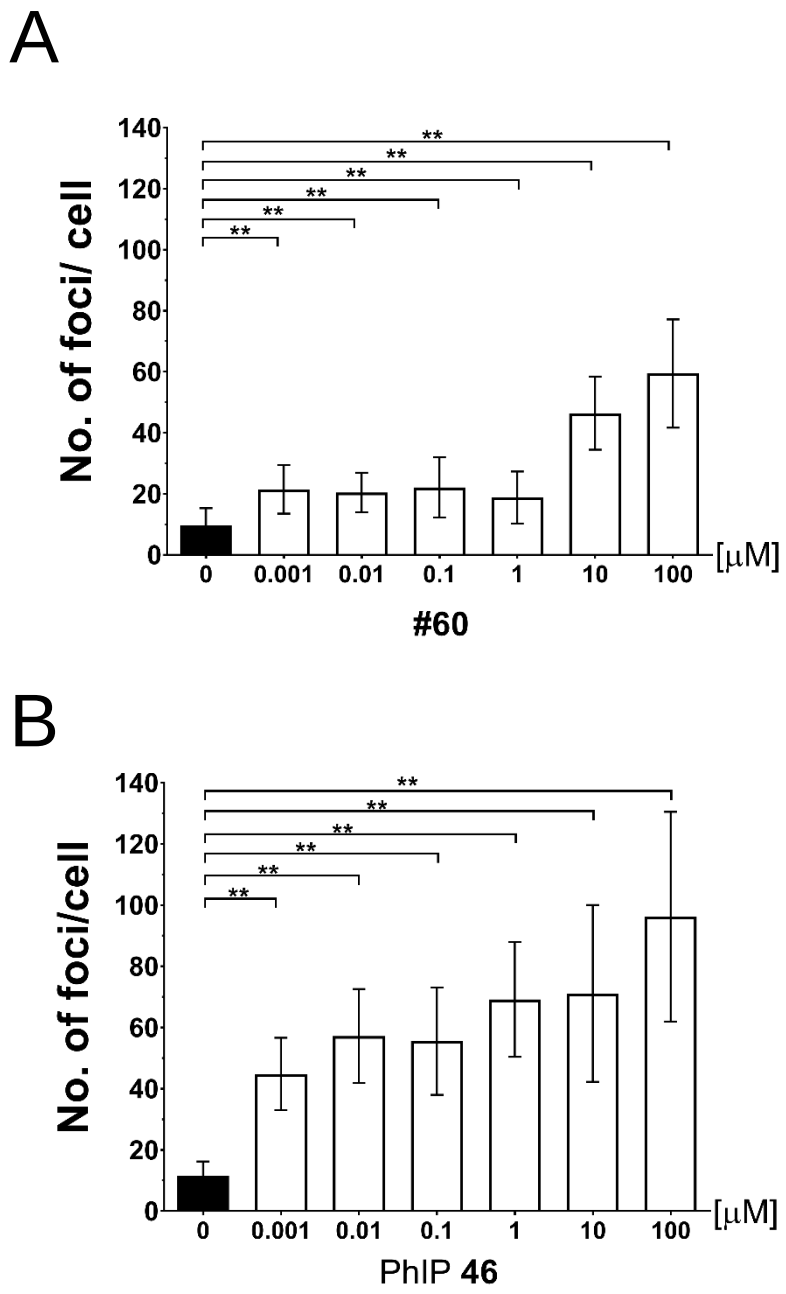

Figure 20: Genotoxicity of compound 60 and PhIP 46. Cellular genotoxicity was assessed by manual scoring of γH2AX foci via immunofluorescence. Cells were treated with increasing concentrations (0 to 100 μM) of (A) compound **60** and (B) PhIP **46** for 30 minutes. Genotoxicity data represent the mean number foci per cell from 80 nuclei scored per condition from one independent experiment. Error bars represent SD and ** denotes P<0.01. # denotes compound number.

3.4.2.3 Confirmatory genotoxicity of compound 60

The comet assay was chosen to complement the γH2AX assay because of its high sensitivity to detect genotoxic activity [273] and it can be conducted in HepG2 cells. The comet assay is used for the detection of DNA damage resulting from single and double-strand breaks, which produce DNA fragments that migrate in an electric field to form a 'comet' [273,298]. The extent of genotoxicity was quantified by determining the proportion of the comet tail length with regards to the total comet length consisting of the comet tail and head (nucleus) [273]. A significant increase in genotoxicity was detected for 2-(3-aminophenyl)oxazolopyridine **60** and PhIP **46** compared to untreated cells (Figure 21A). Generally, the amount of genotoxicity induced by PhIP **46** (10 µM) was higher than compound **60** (10 µM) (Figure 21). The positive control, hydrogen peroxide (200 µM) also showed a significant increase in genotoxicity compared to untreated cells (Figure 21A). The amount of genotoxicity was reflected by the increase in the proportion of the comet tail length with regards to the total comet length as viewed under the microscope (Figure 21B).

Hydrogen peroxide was chosen as the positive control for this assay because it induces single and double-strand DNA breaks by generating detrimental ROS and free radicals [342,343]. The severity of cellular DNA damage caused by hydrogen peroxide at a high concentration have led to the formation of DNA fragments reflected by the long comet tail (Figure 21Bii) as compared to untreated cells (Figure 21Bi). Since both compound **60** and PhIP **46** were tested at the same concentration, the results from the comet assay were consistent with the γH2AX assay **(refer to section 3.4.2.2)**. The amount of genotoxicity detected for PhIP **46** was higher than compound **60,** which is shown by the larger comet tail to total comet length ratio for PhIP **46** (Figure 21Biii) as compared to compound **60** (Figure 21Biv). Unlike hydrogen peroxide, which causes DNA strand breaks, PhIP **46** causes base modifications [107-109], which is

considered a less severe form of DNA damage [351]. However, the repair of the modified base can induce the formation of DNA strand breaks as previously reviewed **(refer to section 1.3.3)**. In fact, PhIP **46** was most genotoxic in human B-lymphoblastoid cells (MCL-5) using the comet assay among all the HCAs tested [352]. Therefore, aside from DNA strand breaks, the comet assay is sensitive enough to detect structural modifications of the DNA such as DNA adducts caused by thymine dimers and oxidative damage, alkali-labile sites, DNA cross-links and incomplete base or nucleotide excision repairs [290,353].

The results of the γH2AX and comet assays strongly indicate that compound 60 induces DNA damage at very low concentrations. Despite its genotoxicity, the levels induced by compound **60** were consistently lower than those induced by PhIP **46**, which partly explains its lack of cytotoxicity. This could be attributed by the cells' ability to respond to DNA damage caused by repairing it through various DNA repair pathways [235,354]. Cellular response to the DNA damage induced by compound **60** can therefore be monitored to account for its lack of cytotoxicity.

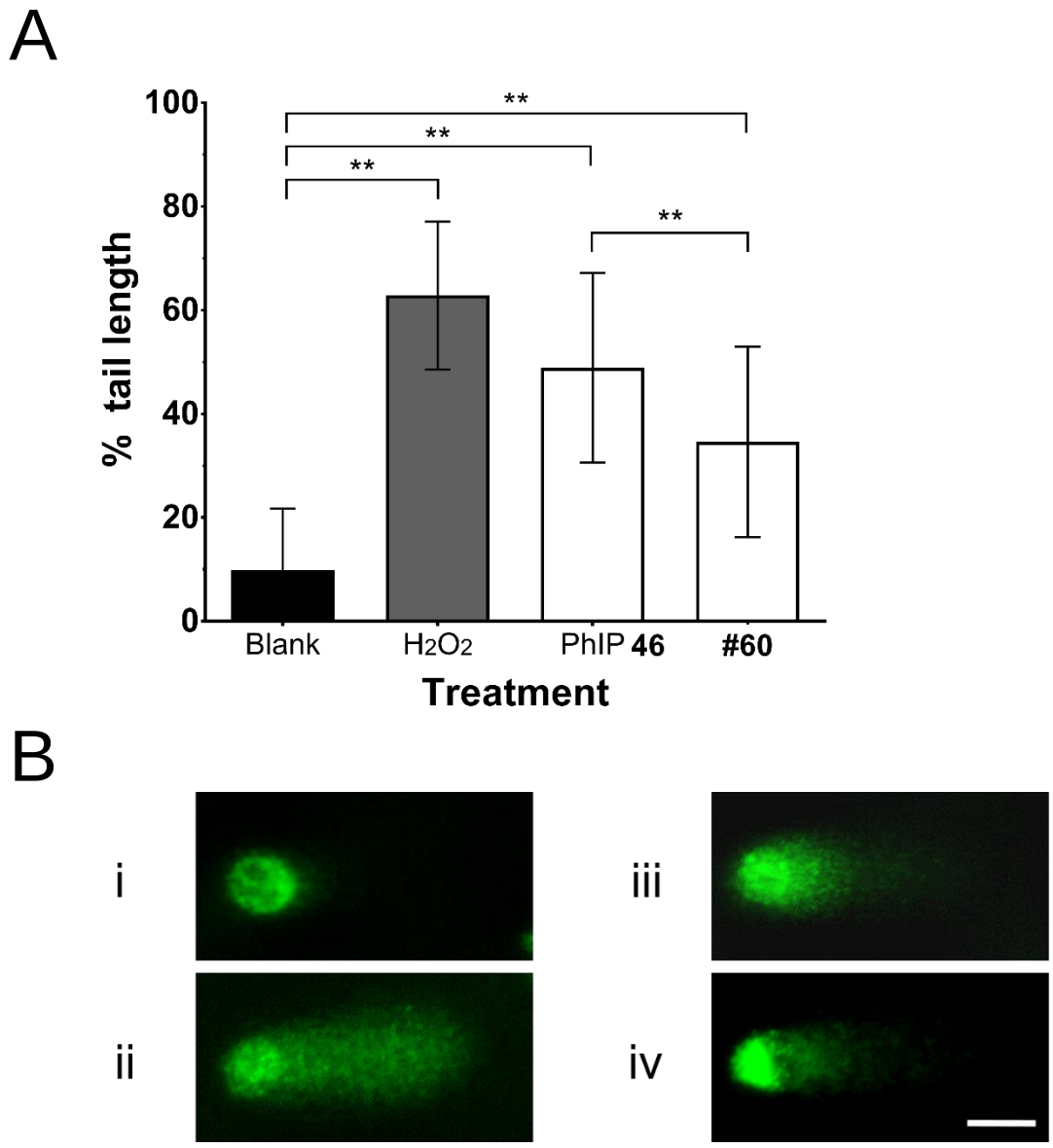

Figure 21: Genotoxicity of compound 60. Genotoxicity in HepG2 cells was assessed by measurement of the tail length of the comet. **(A)** Cells were treated with compound **60** (10 µM) and PhIP **46** (10 µM) for 30 minutes. Hydrogen peroxide (200 µM) was used as positive control. Genotoxicity data represent the mean percentage comet tail length per cell where 50 nuclear comets were scored per condition for two independent experiments. Error bars represenet SD and ** denotes P<0.01. **(B)** Stained nuclear comets (green) of (i) untreated cells and cells treated with (ii) hydrogen peroxide (200 µM), (iii) PhIP **46** (10 µM) and (iv) compound **60** (10 µM). Panel shows exemplary images of 50 nuclear comets analysed in one out of two independent experiments. Scale bar represents 10 µm. # denotes compound number.

3.4.3 Cellular responses to DNA damage

3.4.3.1 Repair kinetics of DNA damage induced by compound 60

Although genotoxic, 2-(3-aminophenyl)oxazolopyridine, **60** lacked cytotoxicity, which was rather surprising given that genotoxic agents are generally also cytotoxic. To understand this, the repair kinetics of the DNA damage induced by compound **60** was determined. Moreover, the ability of the cell to repair the lesion caused by compound **60** may provide more information on the nature of the damage. To determine DNA damage repair kinetics, the amount of DNA damage after treatment cessation (with 30 minutes incubation) was determined at different time points of cell recovery over 48 hours.

Generally, after 30 minutes of exposure the cells were able to repair DNA damage induced by compound **60** (10 µM) and the positive control, hydrogen peroxide (200 µM) (Figure 22). After 24 hours, the number of γH2AX detected in the cells was significantly reduced for compound **60** (solid triangle) and hydrogen peroxide (solid square) (Figure 22). After 48 hours, the number of γH2AX foci detected in the cells continued to decrease for hydrogen peroxide, whereas for compound **60**, the amount of γH2AX foci detected in the cells remained constant (Figure 22). It is important to note that 24 and 48 hours after treatment cessation, the amount of residual genotoxicity detected for compound **60** (14-15 foci/cell) and hydrogen peroxide (12-19 foci/cell) was close to the baseline levels detected in untreated cells (cross) (7-9 foci/cell) (Figure 22).

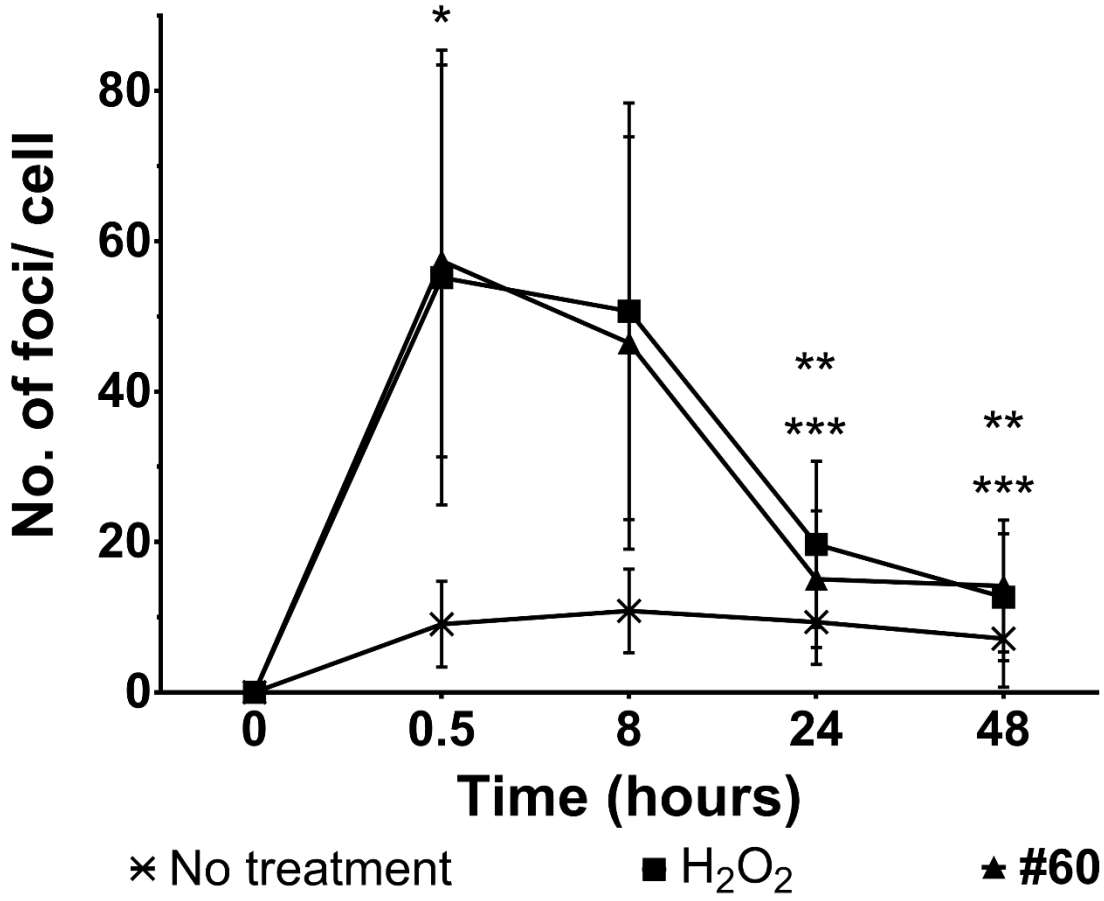

Figure 22: Repair kinetics of DNA damage induced by compound 60. Genotoxicity in HepG2 cells was assessed by manual scoring of γH2AX foci. Cells were treated with compound **60** (10 µM) for 30 minutes. Hydrogen peroxide (200 µM) was used as positive control. Cells were fixed and analysed at different time points: 0.5 hour after treatment and 8, 24 and 48 hours after treatment cessation. Genotoxicity data represent the mean number foci per cell where 80 nuclei were scored per condition for one independent experiment. Error bars represent SD. Comparing the amount of DNA damage at 0.5 hour, a significant increase in DNA damage was observed for compound **60** and hydrogen peroxide when compared to untreated cells where P<0.01 (indicated by *). A significant decrease in DNA damage was observed for both compound **60** (indicated by **) and hydrogen peroxide (indicated by ***) after 24 or 48 hours when compared to levels detected at 0.5 hour where P< 0.01. # denotes compound number.

The results from this experiment indicate that the DNA damage induced by compound **60** and hydrogen peroxide is efficiently repaired by the cells after 24 hours. This result is consistent with the ability of cells to effectively repair the DNA damage caused by hydrogen peroxide

after 24 hours, as previously demonstrated [316,342]. This seems to be in contrast with the cytotoxicity data reported for hydrogen peroxide (200 μM), where it was shown to be potently cytotoxic and genotoxic to cells and therefore the induced DNA damage should not be repaired **(refer to sections 3.4.1 and 3.4.2)**. Moreover, hydrogen peroxide causes mainly strand breaks, which are very detrimental to cells [342]. However, it is important to note that the cellular exposure to hydrogen peroxide (200 μM) in the γH2AX assay was only for 30 minutes, while the cellular exposure in the colony forming assay was over 12 days. Chronic exposure to potent genotoxic agents such as hydrogen peroxide can lead to cell death. This is because the amount of DNA damage induced during long periods of exposure can exceed the rate of cellular DNA repair to maintain genomic integrity [355,356]. Moreover, cells are able to repair the DNA damage induced upon chronic or acute exposure depending on the amount and the severity or type of DNA damage induced [356]. It is also important to note that the concentration of hydrogen peroxide (200 μM) tested in these experiments was higher than compound **60** (10 μM). This further contributed to the severity of the DNA damage caused by hydrogen peroxide, which resulted in its cytotoxicity. This could also the contributing factor to the higher residual genotoxicity detected for hydrogen peroxide was higher than compound **60** after 24 and 48 hours from treatment cessation.

In cells, compound **60** (10 μM) was non-cytotoxic and hydrogen peroxide (200 μM) was cytotoxic upon chronic exposure while the DNA damage induced by either compounds was repaired effectively after 24 hours. The long term build-up of DNA damage induced by hydrogen peroxide cannot be repaired by cells leading to death, but in the case of compound **60**, can be tolerated by cells allowing them to proliferate for the reasons mentioned. **Therefore, the type DNA damage caused by compound 60 appears to be less detrimental and can be repaired efficiently within 24 hours.** The identification of cellular DNA repair response to

the damage caused by compound **60** can therefore provide information on the type of damage induced and its mode of action.

3.4.3.2 DNA repair response to compound 60

Cell survival upon exposure to genotoxic compounds is a result of their ability to repair the DNA damage induced. Cells respond to DNA damage through various DNA repair mechanisms depending on the nature of the damage. In this experiment, cells were treated with 2-(3-aminophenyl)oxazolopyridine **60** (10 µM) in the presence of inhibitors for enzymes and sites involved in different DNA repair pathways. The test inhibitors consisted of DPQ and KU55933, which inhibit PARP1 and ATM respectively, while MxHCl bind to AP sites. If the cellular DNA repair mechanism involved in the repair of damage induced by compound **60** is inhibited, the cell is unable to maintain genomic integrity resulting in detectable loss of cell viability. The concentrations which inhibit cell viability by 5% for DPQ, Ku55933 and MxHCl were pre-determined to be 1.5, 2.1 and 1.4 µM respectively **(Appendix 1)** and were used for this experiment. There was a significant decrease in cell viability detected for compound **60** + DPQ and compound **60** + Ku55933 when compared to treatment with DPQ and Ku55933 only respectively (Figure 23). Cell viability remained unchanged when cells were treated with either MxHCl or MxHCl + compound **60** (Figure 23). Similar trends were obtained when comparing between the combination of compound **60** + inhibitor and treatment with compound **60** only (Figure 23). The positive control, hydrogen peroxide (200 µM) was consistently cytotoxic (Figure 23).

The decreased cell viability in the presence of compound **60** + DPQ indicate that cellular DNA repair could rely on the activity of PARP1. PARP1 is known to play a vital role in the base excision repair (BER) of modified DNA bases and the repair of SSBs [357-359]. However, PARP1 is a multi-faceted enzyme and is also involved in other DNA repair pathways and chromatic

remodelling in the cell [360]. For example, PARP1 initiates the onset of homologous recombination (HRC) [361] by preventing the inhibitory effects of the Ku protein, which shunts the DNA repair towards non-homologous end joining (NHEJ) [362]. PARP1 has also been implicated in the "alternative" NHEJ pathway although its exact role is unclear at present [363]. HRC and NHEJ pathways are involved in the repair of DSBs which reflects the non-exclusive role of PARP1 in repairing SSBs and base modification of DNA.

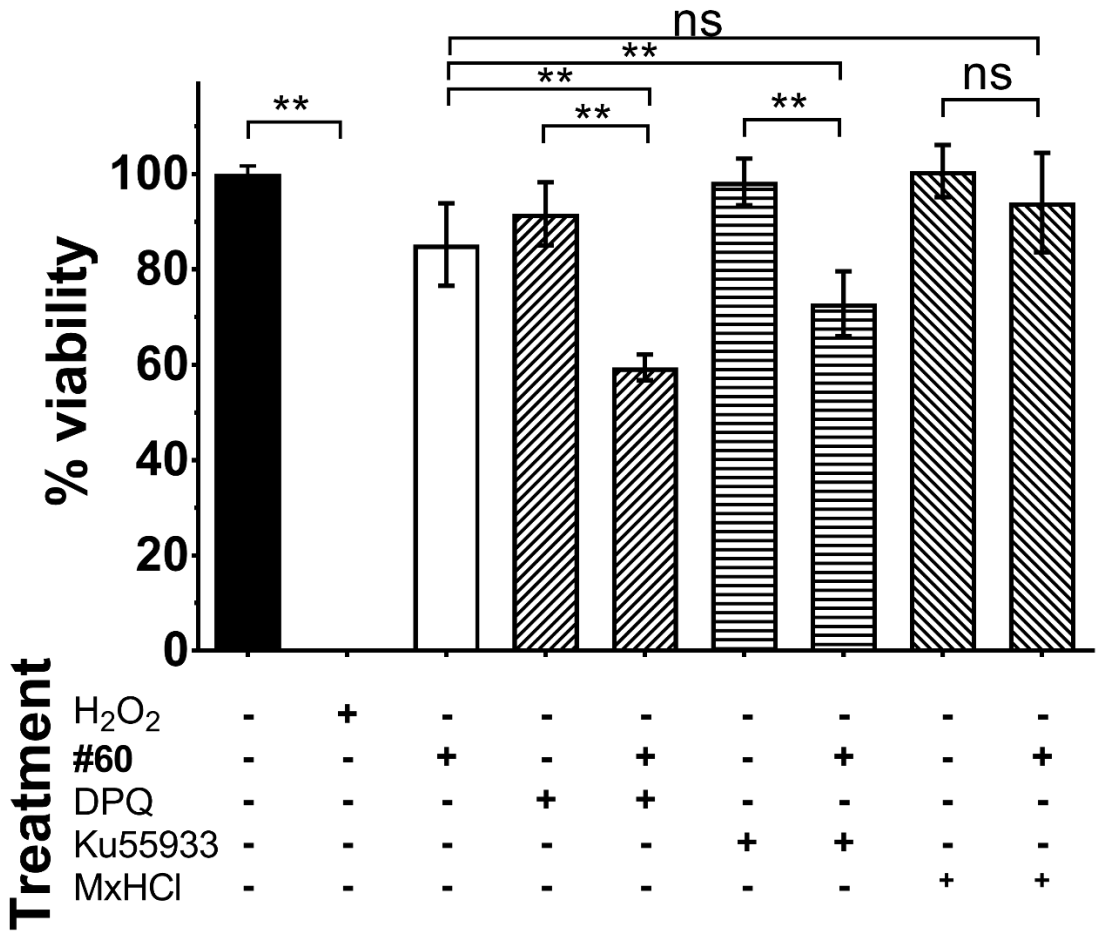

Figure 23: Cellular repair of DNA damage induced by compound 60. Viability of cells was assessed by colony formation assay using HepG2 cells. Cells were treated with compound **60** (10 µM) and/or sub-lethal concentrations of DNA repair inhibitors: DPQ (1.5 µM), KU55933 (2.1 µM) or MxHCl (1.4 µM) as indicated for 12 days. Hydrogen peroxide (200 µM) was used as positive control. Viability data represents the mean of three independent experiments with three replicates per experiment and is expressed as % of untreated control. Error bars represent SD, ** and ns denote $P<0.01$ and $P>0.05$ respectively. # denotes compound number.

Similarly, the decreased cell viability in the presence of compound **60** + Ku55933 indicates that repair of compound **60**-induced DNA damage involves the activity of ATM. KU55933, an inhibitor of ATM [364,365] is involved in the phosphorylation of H2AX histone for the recruitment of mediator proteins to the site of damage prior to repair by either NHEJ or HRC [365,366]. ATM is also involved in the repair of DSBs arising from nucleotide excision repair (NER) [367], which also suggests the multi-faceted nature of the enzyme in DNA repair. Regardless of the nature of the DNA damage, the reliance on ATM during cellular DNA repair supports the detection of γH2AX foci upon exposure to compound **60** in the γH2AX assay reported earlier. However, there was also no way to exclude the possibility that γH2AX foci is also produced via ataxia telangiectasia mutated Rad3 related (ATR) [339] since an ATR-specific inhibitor was not used in this experiment.

Unlike DPQ and Ku55933, MxHCl specifically binds to AP sites preventing the activity of AP site endonuclease (APE1), which prevents BER of AP sites [368]. The lack of cellular sensitivity to compound **60** and MxHCl suggest that the repair of AP sites was not required by the cell. Therefore, this indicates that compound **60** does not produce AP sites. Apart from alkylated and oxidatively modified bases, AP sites represent a form of base modification [368]. Therefore, base modification by compound **60** produces cannot be ruled out completely.

In principle, it is convenient to determine the cellular responses by inhibiting specific DNA repair pathways. However, this is often difficult to achieve due to the multi-faceted nature of enzymes involved in several cellular DNA repair pathways. Nevertheless, the results of this experiment indicate that compound **60** induces DNA damage which is repaired by the cells to maintain viability. Although the DNA repair is mediated by an unknown mechanism, the results from this experiment suggest that it requires the presence of DNA repair and signalling enzymes, PARP1 and ATM.

3.5 Chapter summary

It was hypothesised that 2-(3-aminophenyl)oxazolopyridine **60** is genotoxic due to the structural similarities with the known carcinogen, PhIP **46**. Compound **60** was not dose-dependently cytotoxic up to 100 µM indicating its lack of cytotoxicity. However, compound **60** was found to be genotoxic and induced DNA damage at concentrations as low as 0.001 µM, although it was not as genotoxic as PhIP **46**. The genotoxicity of compound **60** was surprising given that genotoxic agents are commonly associated with significant cytotoxicity. More intriguingly, PhIP **46** is also a genotoxic agent, which is not cytotoxic. This supports the close relationship of the oxazolopyridine compound **60** and PhIP **46**. Further work was conducted to understand the lack of cytotoxicity of compound **60**. DNA damage caused by compound **60** was effectively repaired after 24 hours. The DNA damage induced by compound **60** was also found to be not very severe, which partly explained its lack of cytotoxicity. Finally, the importance of repair of DNA damage caused by compound **60** was supported. The results implicate the activities of PARP1 and ATM in the protection against compound **60**-induced genotoxicity. **In summary, compound 60 induces DNA damage but is not cytotoxic.** This is rather concerning as compounds of similar properties are difficult to detect during standard toxicology assessments. These genotoxic agents may cause gene mutations in normal cells through the accumulation of DNA damage and erroneous DNA repair. Subsequently, these mutation-inducing mechanisms have a high likelihood to initiate the development of malignancies. This is the basis of how PhIP **46,** which shares similar genotoxic and cytotoxic properties with compound **60** as shown in the current study, causes the development of tumours. The discovery of significant genotoxicity of the oxazolopyridine compound **60** provided insights into its mutagenic potential. Mutagenic evaluation of compound **60**, which is an important end-point measure for carcinogenesis risk will be discussed in chapter 4.

Chapter 4: Mutagenicity of compound 60

4.1 Overview and rationale

In chapter 3, 2-(3-aminophenyl)oxazolopyridine **60** was found to be genotoxic at low concentrations but not cytotoxic and these characteristics were similar to the known carcinogen, PhIP **46**. These results seem to support the hypothesis that compound **60** and PhIP **46** may act by a similar mechanism due to their structural similarities, with the amino group being key to activity. Moreover, the ability of the cells to withstand exposure to compound **60** was determined by their ability to efficiently repair the compound-induced DNA damage by a currently unknown mechanism.

The DNA damaging ability of compound **60** coupled with virtually no cytotoxicity prompted the need to investigate the mutagenicity of this compound. DNA damage induced by xenobiotics can be repaired by cells but the consequence of erroneous repair will lead to mutations resulting that predispose to the formation of cancer. Cytotoxicity and genotoxicity assessments are very important in the drug development process and these liabilities often manifest in a straightforward manner. Mutagenicity however, requires a longer time to develop and is not easily detected during standard compound characterisation. Consequently, some drugs pass these screens but are later recalled due to long-term adverse effects that sometimes include elevated cancer risk [369]. Cancer was the second leading cause of death globally in 2013, with a steady increase since the 1990s [370]. Lifestyle changes such as smoking, sedentary behaviour, increased reliance on conventional medications [371,372] and the increased consumption of artificial additives in processed food [373,374] were thought to be contributing factors. Therefore, it is even more important to conduct mutagenic drug assessment, especially when the compound has DNA damaging properties, such as compound **60**.

In this section, the "gold standard" Ames test was used to determine the mutagenicity of compound **60** and PhIP **46** in the *Salmonella* TA100 strain characterised by the rapid and sensitive nature of the assay [241,265]. The carcinogen, PhIP **46** is not only mutagenic but also a pro-mutagen where bio-activation by liver enzymes is required for mutagenicity [92,97]. For this reason, the Ames test was also conducted with S9 liver extract for the detection of pro-mutagens. Due to time constraints, the *Salmonella* TA100 strain alone was tested as it is widely used to screen for mutagenic molecules. Moreover, the USFDA and ICH recommended that a positive result obtained from one strain in the Ames test is sufficient to report mutagenic activity [238]. Compound **60** and PhIP **46** were also tested in the soft agar invasion (SAI) assay using HepG2 cells where the role of enzymatic bio-activation was also taken into consideration. The SAI assay is a good *in vitro* alternative to animal studies as it is more convenient to conduct and rapid. The SAI assay takes approximately 20-30 days to perform, allowing the development of malignant and invasive cell colonies.

4.2 Aims

The carcinogen, PhIP **46** was previously characterised as a pro-mutagen, which causes base modifications leading to DNA damage and mutations [112]. The carcinogenic potential of PhIP **46** has also been well documented in animal studies and clinical studies where it leads to the formation of tumours in colon, breast and prostate tissues [53-56].

For these reasons, PhIP **46** was used as the reference compound for mutagenicity in the assays. The mutagenicity of oxazolopyridines has not been reported and this will be the first study dedicated to evaluate the mutagenic potential of this class of compounds. Therefore, the overall aim of this section was to evaluate the mutagenicity of the oxazolopyridine compound **60**. The following experiments were performed to address the objectives:

- Determination of the mutagenic potential of compound **60** via the Ames test using the histidine-requiring (His^-) *Salmonella* TA100 strain.
- Determination of the cellular transformation potential of compound **60** in HepG2 cells via the SAI assay.

4.3 Methodology

The methods for chemical syntheses and analyses are described in **section 2.1**. The methods for the biological assays conducted in this chapter are described in **sections 2.6.3** and **2.9**.

4.4 Results and discussion

4.4.1 Mutagenic determination of compound 60

DNA damage induced by 2-(3-aminophenyl)oxazolopyridine **60** was shown to be repaired rapidly within 24 hours in HepG2 cells. However erroneous repair of the DNA may lead to gene mutations [375,376] resulting in cellular phenotypic transformation, the periodical transformation of normal into malignant cells [377-379] is the most prominent example. Moreover, cancers have been associated with impaired homologous recombination, nucleotide excision and mismatch repair mechanisms [376]. The most important end-point measure of a carcinogenic compound is mutagenic activity since it is the onset of cellular transformation. Therefore, the Ames test was conducted in His^- *Salmonella* TA100 using S9 liver extract to evaluate the mutagenic potential of compound **60** reflected by the mutability of bacterial cells. Prokaryotic cells such as *Salmonella sp.* are unable to produce metabolic enzymes similar to those of mammalian liver tissue, particularly those involved in phases I and II of chemical metabolism in humans [258,263]. Therefore, the use of S9 liver extract in the Ames test was employed to detect pro-mutagens, which require enzymatic bio-activation to become mutagenic [380].

In the absence of S9 liver extract, there was no significant change in bacterial cells mutability when treated with compound **60** and PhIP **46** as compared to untreated cells (Figure 24). However, in the presence of S9 liver extract, the bacterial cells mutability significantly increased for both compound **60** and PhIP **46** when compared to untreated cells with 127 and 133 revertant colonies/ plate respectively (Figure 24). The levels of bacterial cells mutability induced by compound **60** and PhIP **46** were also similar (Figure 24). An increase in bacterial cells mutability in the presence of S9 liver extract but the lack of bacterial cells mutability in the absence of S9 liver extract, indicated that compound **60** and PhIP **46** are not mutagenic on their own but are pro-mutagens, which require enzymatic bio-activation to be mutagenic. Liver microsomes consist mainly of cytochrome P450 (CYP) enzymes, which are involved in chemical metabolism, particularly those belonging to the CYP 1 (isoforms: 1A1, 1A2 and 1B1), CYP 2 (2A6, 2B6, 2C8, 2C9, 2C19 and 2E1) and CYP 3 (3A4 and 3A5) families [381]. The results for PhIP **46** in this experiment were not surprising as it is a known pro-mutagen, which requires activation by liver enzymes [382,383]. More specifically, the bio-activation of PhIP **46** involves *N*-hydroxylation catalysed by CYP 1A1, 1A2 and 1B1 [108,384,385] to form a hydroxylamine. The hydroxylamine of PhIP **46** then undergoes phase II esterification by microsomes such as acetyltransferases and sulphotransferases to form the arylnitrenium ion, which is highly reactive with DNA to form mutagenic adducts [386,387].

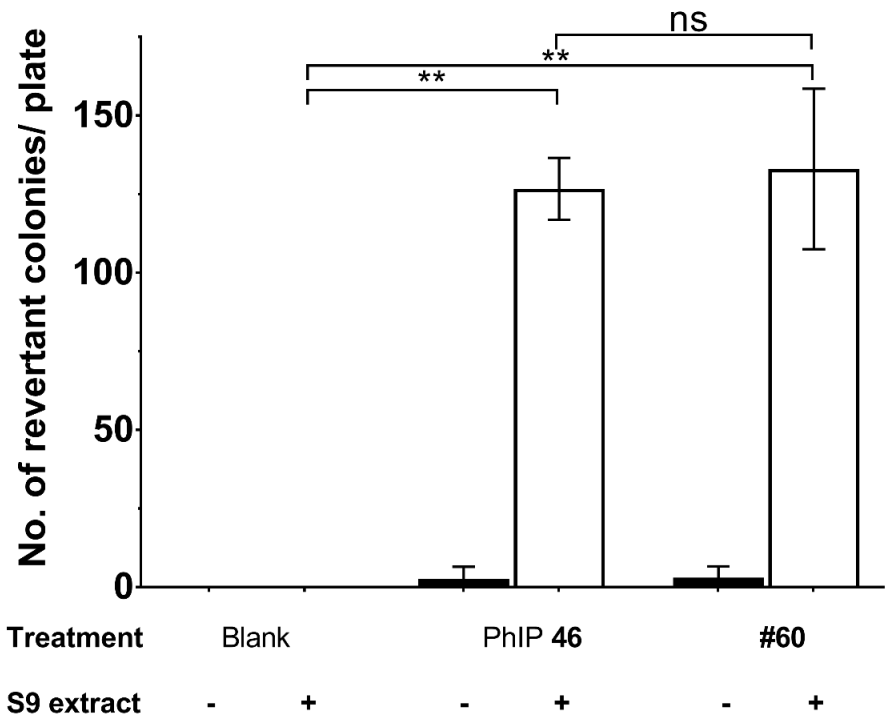

Figure 24: Enzymatic bio-activation of compound 60. Mutagenicity was assessed using the Ames test in His^- *S. thyphi* TA100. Bacterial cells were treated with compound **60** (10 µM) with (white bars) or without (black bars) S9 liver extract as indicated and grown for three days. The known mutagen, PhIP **46** (10 µM) was used as positive control. Mutagenicity data represent the mean of three independent experiments with three replicates each and is expressed as number of His^+ revertant colonies/plate. Error bars represent SD; ** and ns denote $P<0.01$ and $P\geq 0.05$ respectively. # denotes compound number.

The similar levels of bacterial cells mutability were detected for compound **60** and PhIP **46** in the presence of S9 liver extract (Figure 24) which supports the functional similarity of both compounds. The known enzymatic bio-activation of PhIP **46** revolves around the amino group leading to the formation of the mutagenic arylnitrenium ion [384]. Compound **60** also contains an amino group which could be involved in the mutagenic activity of the compound. However, the specific reaction mechanism is so far unknown and beyond the scope of the Ames test. Therefore, **compound 60 appears to be a pro-mutagen, which requires enzymatic bio-activation to be mutagenic** and the current study is the first to report this for an oxazolopyridine compound.

4.4.2 Oxidation dependency in the activation of compound 60

In phase I chemical liver metabolism, oxidation is the most common reaction to take place [388,389]. For the carcinogen, PhIP **46**, the compound's amino group is oxidised which results in the reactive *N*-hydroxylamine [93]. As shown by the Ames test, 2-(3-aminophenyl) oxazolopyridine **60** depends on enzymatic bio-activation to be mutagenic. Based on the PhIP **46** model, it was therefore proposed that compound **60** may have been oxidised during enzymatic bio-activation. To determine the role of oxidation of compound **60** during enzymatic bio-activation, the anti-oxidant, Trolox was used in the following experiment. It is also important to note that HepG2 cells were used in this experiment so that cellular production of microsomes needed for enzymatic bio-activation were present in the test system.

Consistent with previous experiments, the amount of genotoxicity detected for compound **60** (10 µM) was significantly higher than in untreated cells (Figure 25). However, in the presence of compound **60** (10 µM) + Trolox (10 µM), the amount of genotoxicity detected decreased as compared to the amount detected for 10 µM compound **60** (Figure 25). In fact, the amount of genotoxicity detected for compound **60** (10 µM) + Trolox (10 µM) was similar to untreated cells (Figure 25). Trolox (10 µM) itself did not significantly affect genotoxicity with levels similar to untreated cells (Figure 25). The positive control, hydrogen peroxide (200 µM) was genotoxic compared to untreated cells.

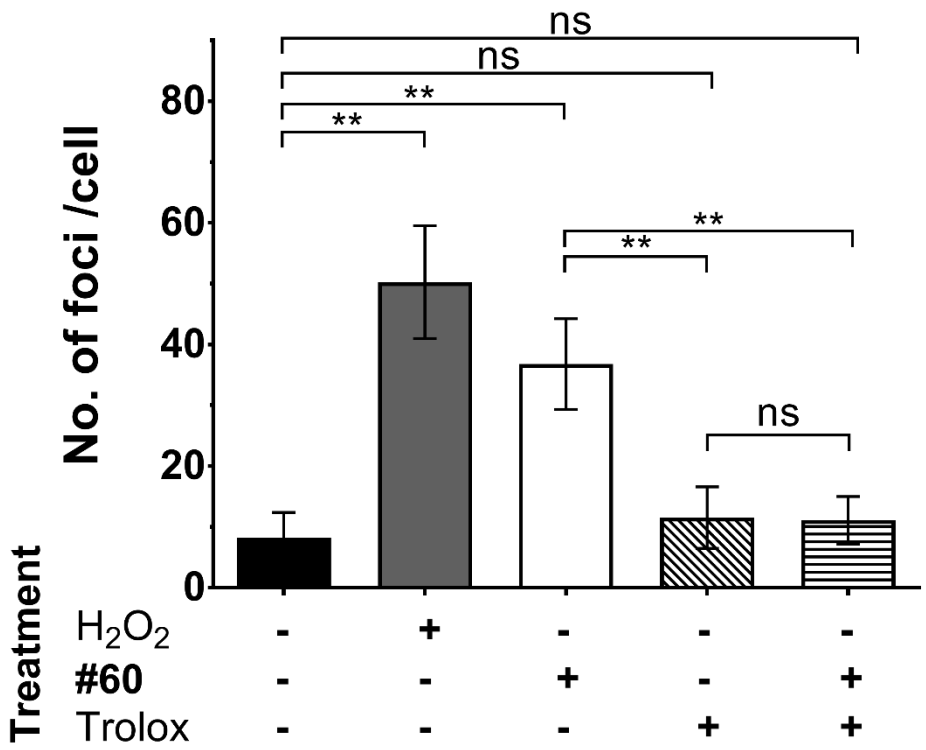

Figure 25: Oxidation dependency of compound 60 in genotoxicity. Genotoxicity in HepG2 cells was assessed by manual scoring of γH2AX foci via immunofluorescence. Cells were treated with compound **60** (10 µM) and/or Trolox (10 µM) as indicated for 30 minutes. Hydrogen peroxide (200 µM) was used as positive control. Genotoxicity data represent the mean number foci per cell from 80 nuclei scored per condition from one independent experiment. Error bars represent SD; ** and ns denote $P<0.01$ and $P\geq 0.05$ respectively. # denotes compound number.

The treatment with Trolox in cells likely prevented the oxidation of compound **60**. This was reflected by a decrease in the amount of genotoxicity detected for compound **60** + Trolox as compared to treatment with the genotoxic compound **60** alone (Figure 25). The presumed inhibition of oxidation of compound **60** by Trolox even reduced the amount of cellular genotoxicity to baseline levels similar to those detected in untreated cells (Figure 25). These results suggest the importance of oxidation in the bio-activation of compound **60**, which supports the proposed mode of activation based on the PhIP **46** model. If the mode of activation

of compound **60** is similar to PhIP **46**, then the amino group in compound **60** could be oxidised into the genotoxic and mutagenic *N*-hydroxylamine. Although this was a promising finding, it needed further investigation to accurately determine the mode of action for compound **60**.

Based on what is known so far, **the pro-mutagenic compound 60 depends on oxidative bio-activation for its genotoxic activity**. However, the most important outcome of mutagenicity, which is cellular transformation should be tested. This can be performed using a suitable *in vitro* model consisting of mammalian cells, which is more representative of mammalian tissues and complements the Ames test.

4.4.3 Cell transformation effect of compound 60

The Ames test provided a rapid method in the detection of mutagenicity. The main limitation of this method is that it is conducted in prokaryotic cells and may not be representative of the situation in humans. Given that 2-(3-aminophenyl)oxazolopyridine **60** was genotoxic but not cytotoxic at 10 µM in HepG2 cells, the SAI assay was used to determine the cell transformation potential of compound **60** in the same cell type. The SAI assay is a suitable cell transformation model as it measures the phenotypic transformation of adherent cells. The anchorage-dependent growth of HepG2 cells prevent its growth in an agar matrix, which can be reversed to allow normal cellular growth as a result of mutation events [300,301]. Three-dimensional cell growth in agar is detected through colony formation. The use of HepG2 cells ensured the cellular production of microsomes required for bio-activation, which a mutagenic pre-requisite for compound **60**.

Although detection of mutagenicity is more important than genotoxicity since gene mutations can lead to cancer, the cell transformation detection is even more important as it is the end-point measure of cancer. Although DNA mutations are very detrimental, not all mutations will lead to the development of cancer [390]. Mutations affecting oncogenes and tumour suppressing

genes are more likely to cause cancer compared to other genes [390,391]. Moreover, induced mutations can still be removed by cells via post-replicative DNA repair [182]. Therefore, the severity of a carcinogen is best measured through its ability to cause cellular transformation.

Generally, there was a significant increase in cellular transformation detected for compound **60** and PhIP **46** as compared to untreated cells (Figure 26A). Looking at the distribution of colony volumes, larger colony populations were detected for compound **60** and PhIP **46** compared to untreated cells (Figure 26A). This was shown by the images of colonies captured under the microscope (Figure 26B). Comparing the data obtained for compound **60** and PhIP **46**, the levels of cellular transformation induced were similar (Figure 26A). Cells were embedded in agar to prevent surface attachment to allow cell growth, resulting in anoikis cell death [300]. Larger cell colonies as a result to treatment with compound **60** or PhIP **46**, indicate phenotypic transformation as adherent cells do not normally grow in an anchorage independent manner. This was supported by the lower frequency and size of colonies detected in untreated cells (Figure 26A), where these cells lack the ability to proliferate as mentioned.

Small colonies detected in untreated cells however could be caused by spontaneous mutations, which occur naturally at a low frequency [392], could be a result of heterogeneity of the cell population and simply represent a basal ability of some cells to grow in this matrix. The unstable nature of purine and pyrimidine DNA bases commonly cause the onset of spontaneous mutations [393]. For example, point mutations can arise due to spontaneous deamination of cytosine into uracil in the DNA double helix [393,394]. As a result, the resulting daughter cells contain a T-A base pair in place of a C-G base pair in the wild type [393]. Furthermore, induced errors can be amplified during DNA replication, resulting in more DNA damage [395].

Extrinsic factors such as cellular stressors caused by cellular injury in trypsinisation during cell maintenance and the exposure to small amounts of DMSO, such as in this experiment, may

induce the production of reactive oxygen species (ROS) [396,397], which is mutagenic *in vitro* [398] and *in vivo* [399]. In fact, spontaneous mutations are common in many eukaryotic cell lines [393,400-402]. However, spontaneous mutations occurring on non-oncogenes are unlikely to cause cancer and are typically repaired fast by the DNA repair machinery [403]. **The oxazolopyridine compound 60 was found to phenotypically transform cells into a more invasive phenotype and given the results obtained so far, strongly indicate that it is a mutagen.** As shown in this experiment, the cellular transformation potential of compound **60** and the reference compound, PhIP **46** are again very similar.

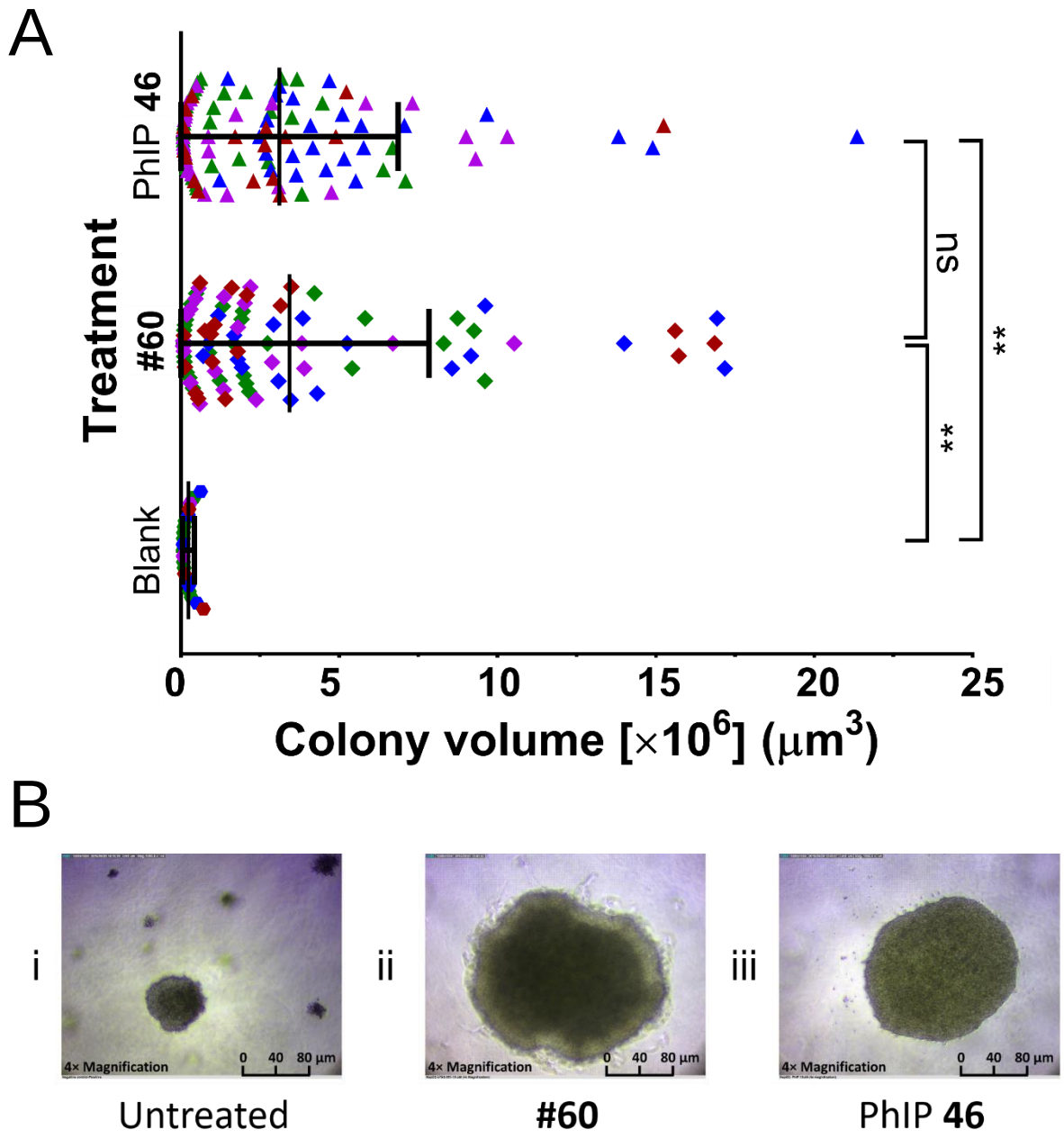

Figure 26: Cell transformation effect of compound 60. Magnitude of phenotypic transformation arise from mutation was assessed using the soft agar invasion assay in HepG2 cells. Cells were treated with compound **60** (10 μM) for 30 minutes and grown for 22 days. The known mutagen, PhIP **46** (10 μM) was used as positive control. Phenotypic transformation data represent the mean of three independent experiments with three replicates each and is expressed as colony volume. Individual values for each individual experiment was plotted (represented by purple, green and blue plots). Error bars represent SD; ** and ns denote $P<0.01$ and $P\geq 0.05$ respectively. Panel B shows exemplary images of colonies analysed in one of three independent experiments with appropriate scales. # denotes compound number.

4.5 Chapter summary

In this chapter, the oxazolopyridine 2-(3-aminophenyl)oxazolopyridine **60** was found to be mutagenic in the Ames test in the presence of S9 liver extract by increasing mutability of the bacterial cells. The genotoxicity of compound **60** was also dependent on oxidation, emphasizing the importance of cellular oxidative bio-activation. The severity of the mutations induced by compound **60** through the formation of invasive cells was shown in the SAI assay. **In summary, the oxazolopyridine compound 60 is a pro-mutagen and phenotypically transforms cells into a more invasive phenotype upon chronic exposure.** Although the mutagenic mode of action of compound **60** is still unknown, the cellular responses to compound **60** reported so far are similar to the carcinogen, PhIP **46**. These results seem to support the hypothesis where the amino group of compound **60** is putatively transformed into the reactive *N*-hydroxylamine, later into *N*-arylnitrenium ion based on the PhIP **46** model, which requires thorough examination. Therefore, determination of key functional groups which cause carcinogenicity and the mode of action of oxazolopyridine compounds will be discussed in chapter 5.

Chapter 5 Mutagenic mode of action of oxazolopyridine compounds

5.1 Overview and rationale

As shown in the previous chapters, 2-(3-aminophenyl)oxazolopyridine **60** was strongly indicated to be mutagenic and to phenotypically transform cells. Due to the similar cellular responses of compound **60** and PhIP **46**, it was hypothesised that the amino group is the key to mutagenicity based on PhIP **46** as a model. However, the role of the amino group in compound **60** is unknown and needed to be further investigated. A QSAR study was performed using analogues of compound **60** with deletion of key functional groups to determine the role of the amino group in cellular genotoxicity. The rationale of performing these experiments was to determine the factors that affect the mutagenicity of compound **60** including the amino group itself, other functional groups of the oxazolopyridine core and the electron density of the heterocyclic system. In contrast to the initial hypothesis, the amino group of compound **60** was not responsible for reactivity but due to the electron density of the heterocyclic system. This result and other factors related to the activation of the oxazolopyridine compounds in genotoxicity and mutagenicity will be discussed in this chapter.

5.2 Aims

In the current study, it was established that 2-(3-aminophenyl)oxazolopyridine **60** is genotoxic and mutagenic. However, the mode of action of action of compound **60** in causing these effects was unknown. Therefore, the general aim of this section was to determine the mutagenic mode of action of the oxazolopyridine compounds. The following experiments were performed to address the objectives:

- QSAR determination of the role of the amino group in compound **60** in causing genotoxicity.

- QSAR determination of the role of molecular electron density in causing genotoxicity.
- Understanding the oxidation of oxazolopyridine compounds through the isolation and characterisation of oxidative products.
- Evaluating the genotoxicity and mutagenicity of these oxidative products.
- QSAR determination on oxazolopyridine analogues to identify the reactive site on the molecule.
- Monitoring the oxidative bio-activation of the oxazolopyridine molecule by S9 liver extract using UPLC-MS, in an attempt to identify the active species. Further investigation on this using computational chemistry was also performed.

5.3 Methodology

The methods for chemical syntheses and analyses are described in **section 2.1**. The methods for the biological assays conducted in this chapter are described in sections **2.6.3, 2.6.5** and **2.9**. The methods for the UPLC-MS detection of the oxazolopyridine metabolites are described in **section 2.10**. The methods for computational chemistry are described in **section 2.11**.

5.4 Results and discussion

5.4.1 Structural-activity relationship of compound 60

As previously mentioned, the amino group was hypothesised to be the key to the genotoxic and mutagenic mode of action of 2-(3-aminophenyl)oxazolopyridine **60** given its structural similarity to the known carcinogen, PhIP **46**. In PhIP **46**, the amino group is converted into the highly electrophilic arylnitrenium ions, which preferentially bind to guanine forming the dG-C8 PhIP-DNA adduct **56** [107-112]. Consequently, the amino group of compound **60** was suspected to undergo the same fate, which contributed to its genotoxicity and mutagenicity.

Analogues with deletions or substitution of key functional groups compared to compound **60** were synthesised and tested in cells to not only determine the role of the amino group but also other groups present in the molecule. In these compounds, the amino group was removed to give the 2-phenyloxazolopyridine **61** to evaluate the role of the amino group. The 2-phenyl group was then substituted for a 2-cyclohexyl group to give the 2-cyclohexyloxazolopyridine **62** to test if the planar structure of the aryl group was required for activity. Furthermore, the corresponding benzoxazole analogues of compounds **61** and **62** were synthesised to give 2-phenylbenzoxazole **63** and 2-cyclohexylbenzoxazole **64** respectively. In the benzoxazoles, the nitrogen at the pyridine ring of the oxazolopyridine core was substituted with a carbon to evaluate the role of the pyridine nitrogen on activity.

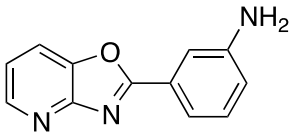

60

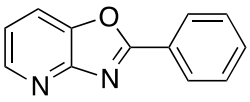

61

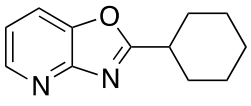

62

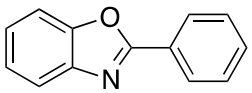

63

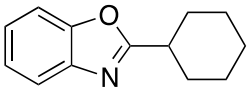

64

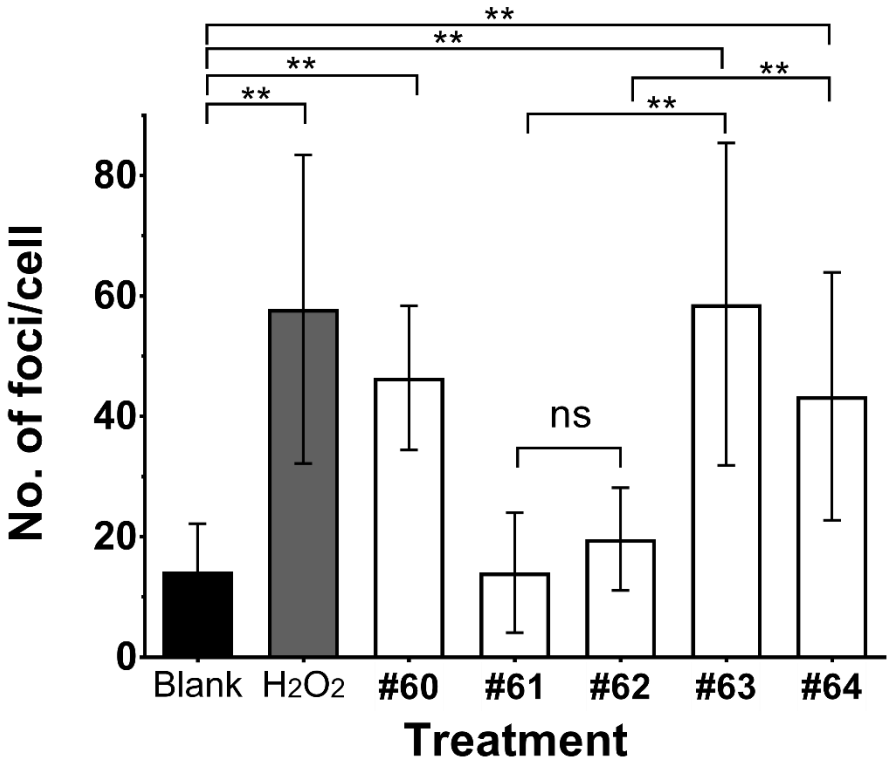

Figure 27: Structural-activity relationship of compound 60 and analogues in genotoxicity. Genotoxicity in HepG2 cells was assessed by manual scoring of γH2AX foci via immunofluorescence. Cells were treated with analogues of **60** (compounds **61**, **62**, **63** or **64**) (10 μM) for 30 minutes. Genotoxicity data represent the mean number foci per cell from 80 nuclei scored per condition from one independent experiment. Error bars represent SD. # denotes compound number.

Compound **60** (10 μM) and the positive control hydrogen peroxide (200 μM) were genotoxic consistent with previous experiments (Figure 27). Subjecting these compounds (10 μM) to the γH2AX assay, different genotoxic responses were observed (Figure 27). The lack of genotoxicity detected for the 2-phenyloxazolopyridine **61** (Figure 27), indicates that the amino group was required for activity. In fact, when the amino group was removed from 2-(3-aminophenyl)oxazolopyridine **60** to give the 2-phenyloxazolopyridine **61**, the amount of genotoxicity detected was close to baseline levels detected in untreated cells (Figure 27). Aside from the role of the amino group, it was suspected that the planar nature of the aryl group of compound **60** may contribute to its genotoxic effect. Many aromatic and planar molecules are

DNA intercalating agents that can insert between DNA base pairs, which inhibit the activity of DNA polymerase and result in DNA damage [404-406]. DNA intercalation is made possible as these drug molecules mimic DNA bases, which also happen to be aromatic and planar [404,407]. Therefore, the substitution of the 2-phenyl with the non-planar 2-cycloheyxl group to give 2-cyclohexyloxazolopyridine **62** reduced the molecular planarity. The level of genotoxicity detected for 2-cyclohexyloxazolopyridine **62**, was only marginally higher than the 2-phenyl derivative **61** and the levels of genotoxicity for both compounds were not significantly different (Figure 27). This indicates that molecular planarity does not influence the genotoxicity of the oxazolopyridine compound.

In contrast, 2-phenylbenzoxazole **63** and 2-cyclohexylbenzoxazole **64** were genotoxic, although both compounds lacked the amino group. This was an interesting turning point of this study as it indicates that the amino group is not necessarily required for activity. In fact, the removal of the amino group and the substitution of the pyridine nitrogen of the oxazolopyridine core increased the genotoxicity in 2-phenylbenzoxazole **63** compared to the non-genotoxic 2-phenyloxazolopyridine **61** (Figure 27). This was also consistent for the 2-cyclohexyl derivatives, where an increase in genotoxicity was detected for 2-cyclohexylbenzoxazole **64**, compared to the non-genotoxic 2-cyclohexyloxazolopyridine **62**. **These results indicate that the molecular core influences genotoxicity and the nitrogen atom on the oxazole ring of the molecular core may be the key reactive site**. This is consistent with reports of cellular genotoxicity of benzoxazole compounds [302-304]. Furthermore, the oxidation of the nitrogen atom on heterocyclic molecules was recently reported to be genotoxic and mutagenic [408].

This experiment indicates that the amino group may not be required for the genotoxicity reported for compound **60**. If the amino group of compound **60** is not oxidized directly into the proposed *N*-hydroxylamine as potentially indicated by the genotoxicity of the benzoxazoles, the amino group may play a role in activating the molecular scaffold by acting as an electron

donor. The increase in molecular electron density may be linked to its activity. Subsequently, it was hypothesised that the **electron withdrawing ability of the pyridine ring of the oxazolopyridine is related to the reduced genotoxicity of 2-phenyloxazolopyridine 61 compared to the 2-phenylbenzoxazole 63**. The role of the amino group in donating electron to the oxazole ring of the oxazolopyridine core can be investigated. This can be performed by synthesizing a range of oxazolopyridine compounds with different electron donor groups and testing them for genotoxic activities. If the genotoxicity is directly related to the electron density of the heterocyclic system, then a Hammett plot of genotoxicity versus electron density should show a correlation.

5.4.2 Hammett plot for oxazolopyridine compounds

The Hammett equation developed by Louis Hammett in 1937 [409] described the linear-free energy relationship between chemical reactivity and the equilibrium constants of reactions, which involved benzoic acid derivatives of different substituents [410]. Substituents with differing electron donating and withdrawing abilities on the molecule (either *ortho*, *para* or *meta*) have different constant values calculated using the Hammett equation [409,411]. Hammett constant values are represented by the rho symbol, σ, where the more negative the constant value, the higher the electron donating ability [411]. The linear relationship between the electron donating ability and molecular reactivity obeys the Hammett plot [410]. In principle, the higher the electron donating ability of the substituent, the higher the electron density of the molecule, which is reflected in its increased reactivity [412].

Following this principle, a range of 2-aryloxazolopyridine **40** analogues with substituents consisting of various electron donating groups at the phenyl ring were synthesised and tested for genotoxic activity in cells via the γH2AX assay (Table 10). The linearity of the relationship between the electron donating ability of the substituent at the phenyl ring and cellular

genotoxicity was tested in this experiment to prove or refute the hypothesis that the increased electron density into the oxazole ring of the oxazolopyridine molecule results in increased genotoxicity.

Table 10: The Hammett constant, σ values of substituents, R as previously described [411] for the 2-aryloxazolopyridine **40** analogues tested in this experiment.

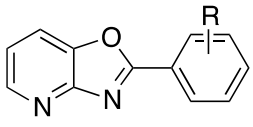

40

Analogue ID	Hammett constant, σ	R
40e	+0.12	3-OCH_3
65	+0.07	3-$NHCOCH_3$
61	0	H
66	-0.15	3-$N(CH_3)_2$
60	-0.16	3-NH_2
40a	-0.27	4-OCH_3
40b	-0.66	4-NH_2

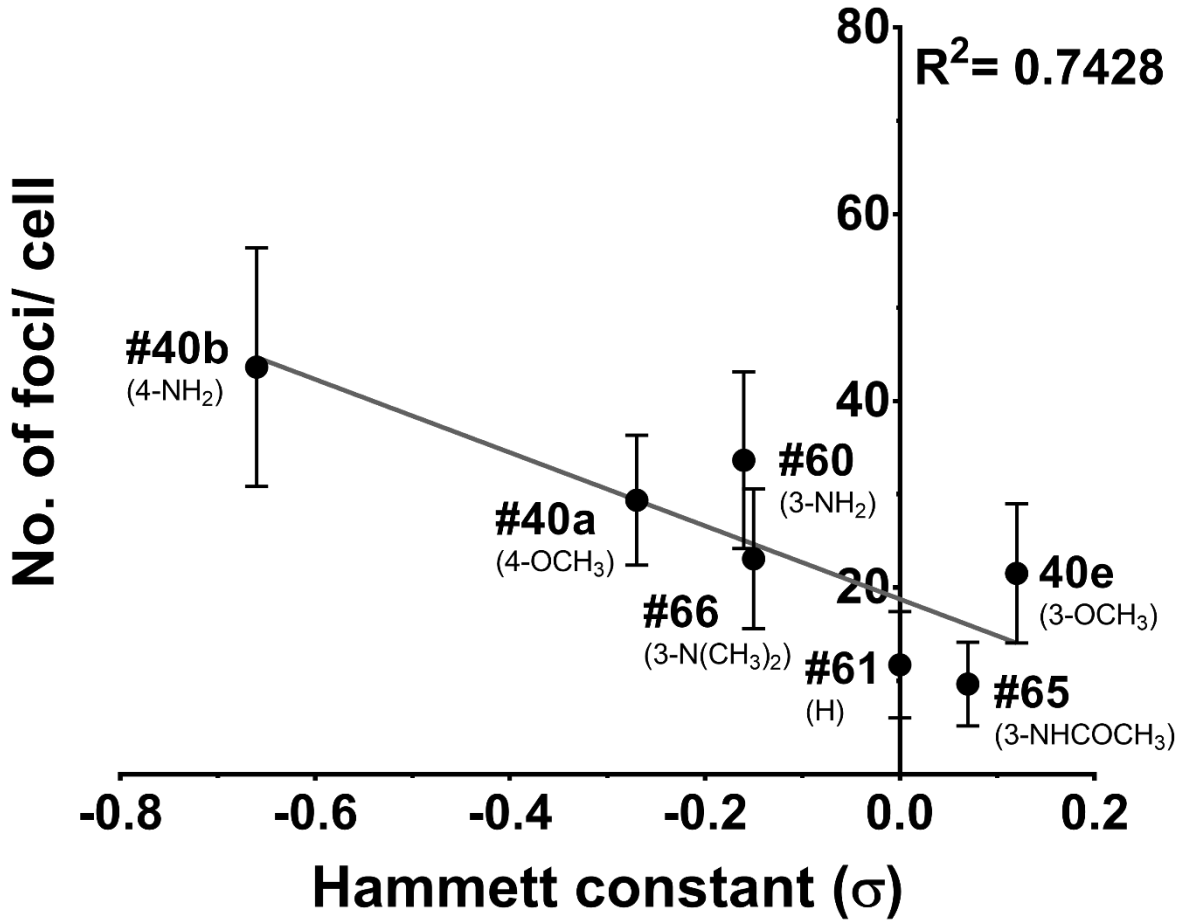

Figure 28: Hammett plot of 2-aryloxazolopyridine analogues in genotoxicity. Genotoxicity in HepG2 cells was assessed by manual scoring of γH2AX foci via immunofluorescence. Cells were treated with 2-aryloxazolopyridine **40** analogues with different R groups (in brackets) of different Hammett constant values, σ for 30 minutes. Genotoxicity data represent the mean number foci per cell from 80 nuclei scored per condition from one independent experiment. Error bars represent SD.

A linear correlation (with R^2 = 0.7428) between the level of cellular genotoxicity and Hammett constant was observed (Figure 28). The baseline level of genotoxicity was represented by the 3-H derivative of the 2-aryloxazolopyridine **61** with the σ value of 0 with 10 foci/cell (Figure 28). A high electron donating ability of substituents such as in the 3-$N(CH_3)_2$ **(66)**, 3-NH_2 **(60)**, 4-OCH_3 **(40a)** and 4-NH_2 **(40b)** derivatives of 2-aryloxazolopyridine **40** (σ values of -0.15, -0.16, -0.27 and -0.66 respectively), resulted in genotoxicity levels above the baseline value

(Figure 28). Moreover, the regression line shows that a more negative the σ value of the substituent resulted in increased genotoxicity of the 2-aryloxazolopyridine analogues **40** (Figure 28). This indicates that increasing electron donating ability of the 2-aryloxaozlopyridine **40** substituents increased electron density of the oxazolopyridine heterocyclic core, which resulted in higher genotoxicity. The error bars for this assay are large due to the different amounts of DNA in the nucleus at different developmental stages of the cell cycle during cell growth [413,414], which is one of the main limitations of the γH2AX assay. Therefore, the amount of DNA exposed to the test compounds in the cells differs depending on the developmental stages of the cells when the experiment was conducted. The data for compound **60** however, is consistent with previous experiments and indicates the reliability of the results obtained from this experiment **(refer to chapter 3)**.

Given the results obtained from the structural activity relationship and the current Hammett plot experiments, it was proposed that the attached substituent contributes to the electron density of the oxazolopyridine core to modulate its reactivity. Consequently, the oxazolopyridine core itself must be undergoing oxidation, with the nitrogen atom of the oxazole ring of the molecular core the likely key reactive site for the genotoxic and mutagenic activities. The 2-aryloxazolopyridine analogues **40** could be oxidised either by S9 liver extract or molecular oxidants to isolate and characterise the resulting oxidation products. This will allow the determination of the reactive site on the oxazolopyridine core as proposed.

5.4.3 Oxidation of 2-aryloxazolopyridine analogues

The 4-OCH_3 **(40a)**, H **(61)** and 3-$NHCOCH_3$ **(65)** derivatives of 2-aryloxazolopyridine **40** were selected and reacted with a molecular oxidant. This was in an attempt to isolate the species responsible for the genotoxic and mutagenic activities of oxazolopyridines. The 4-OCH_3 **(40a)**, H **(61)** and 3-$NHCOCH_3$ **(65)** derivatives of 2-aryloxazolopyridine **40** with σ values of -0.66,

0 and +0.07 respectively were chosen based on their different electron donating abilities. Therefore, the electron donating ability of the substituent to the oxazolopyridine core during oxidation was taken into account. Oxidation reactions of the 2-aryloxazolopyridine analogues **40a**, **61** and **65** were carried out using the oxidising agent, *meta*-chloroperbenzoic (*m*CPBA) and monitored via TLC every 30 minutes. The reactions were stopped when a new spot appeared on the TLC indicative of a new product formed. The product of the reaction was purified by flash chromatography and analysed.

It was proposed that the oxazole nitrogen of the oxazolopyridine core was the reactive site based on the genotoxicity of both oxazolopyridines and benzoxazoles as previously shown (Figure 27, **section 5.4.1**). Mass spectral analyses of the new product showed an addition of an oxygen atom (increase in molecular mass of 16 m/z). However, ^{1}H NMR of the new product showed the same number of CH resonances indicating that no oxidation of a CH bond occurred but potentially one of the nitrogen atoms had formed an *N*-oxide. Similarly, the oxidation of the 2-aryloxazolopyridine analogues **61** and **65** that showed limited genotoxic activities earlier (Figure 28, **section 5.4.2**) also resulted in the formation of *N*-oxides (Figure 29). Thankfully, the oxidation product, **68** was crystallised and the formation of an *N*-oxide was supported using single crystal X-ray crystallography (Figure 30). Surprisingly, the *N*-oxide was on the pyridine ring instead of the oxazole ring of the oxazolopyridine core as hypothesised (Figure 30).

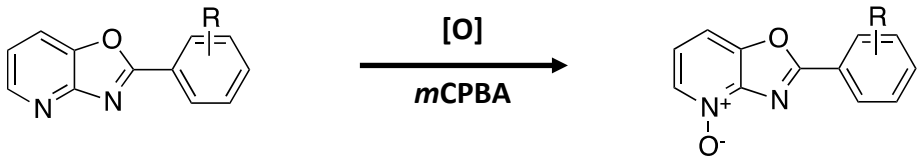

I II

ID		R
I	II	
40a	**67**	4-OCH_3
61	**68**	H
65	**69**	3-$NHCOCH_3$

Figure 29: Oxidation of 2-aryloxazolopyridine analogues 40. The oxidation of 2-aryloxazolopyridine analogues **40a**, **61** and **65** using *m*CPBA resulting in the formation of 2-aryloxazolopyridine *N*-oxides **67**, **68** and **69** respectively.

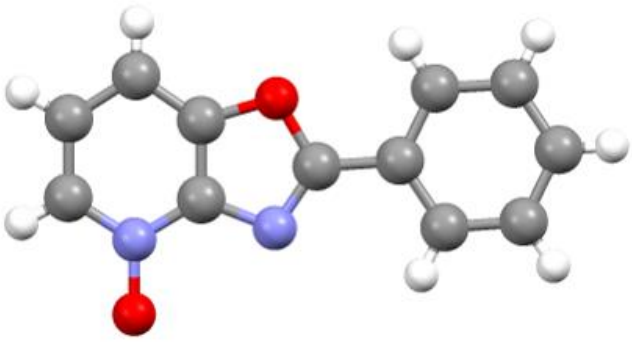

Figure 30: The crystal structure of the 2-aryloxazolopyridine *N*-oxide **68** through single crystal X-ray crystallography. The *N*-oxide was found to be formed on the pyridine ring of the oxazolopyridine core as indicated (Atoms: C (grey), H (white), N (purple) and O (red)). Ellipsoids are shown at 50% probability.

The oxidation of oxazolopyridine compounds produced *N*-oxides, which can potentially be genotoxic and mutagenic. This was based on the oxidative bio-activation requirement of

oxazolopyridine compounds to exert these effects. Since the oxazolopyridine *N*-oxides were successfully isolated, their genotoxic and mutagenic activities could therefore be evaluated.

5.4.4 Genotoxic and mutagenic determinations of oxazolopyridine *N*-oxides

N-Oxides of heterocycles have been reported to be highly mutagenic in the Ames test [408]. Therefore, the following experiment was performed to evaluate the genotoxicity of the oxazolopyridine-*N*-oxide. In this experiment, the 2-phenyloxazolopyridine **61** and the corresponding 2-phenyloxazolopyridine-*N*-oxide **68** were tested. Compound **61** was not genotoxic with 10 foci/cell, which was also the baseline value for genotoxicity in the Hammett plot previously shown (Figure 28, **section 5.4.2**). Therefore, the effect of *N*-oxidation of the non-genotoxic 2-phenyloxazolopyridine **61** was determined by comparing the amount of genotoxicity induced with its corresponding *N*-oxide **68** in the γH2AX assay.

There was a significant increase in the amount of genotoxicity detected for the 2-phenyloxazolopyridine-*N*-oxide **68** (10 µM) when compared to untreated cells but even more importantly, when compared to 2-phenyloxazolopyridine **61** (10 µM) (Figure 31). The 2-(3-aminophenyl)oxazolopyridine **60** (10 µM) and the positive control, hydrogen peroxide (200 µM) were genotoxic consistent with previous experiments (Figure 31). The increased genotoxicity of 2-phenyloxazolopyridine-*N*-oxide **68** compared to 2-phenyloxazolopyridine **61** supports the hypothesis that the oxidation of the oxazolopyridine core is required for genotoxicity. Furthermore, this is in agreement with the hypothesis that it is the oxazolopyridine core itself, which is responsible for genotoxicity.

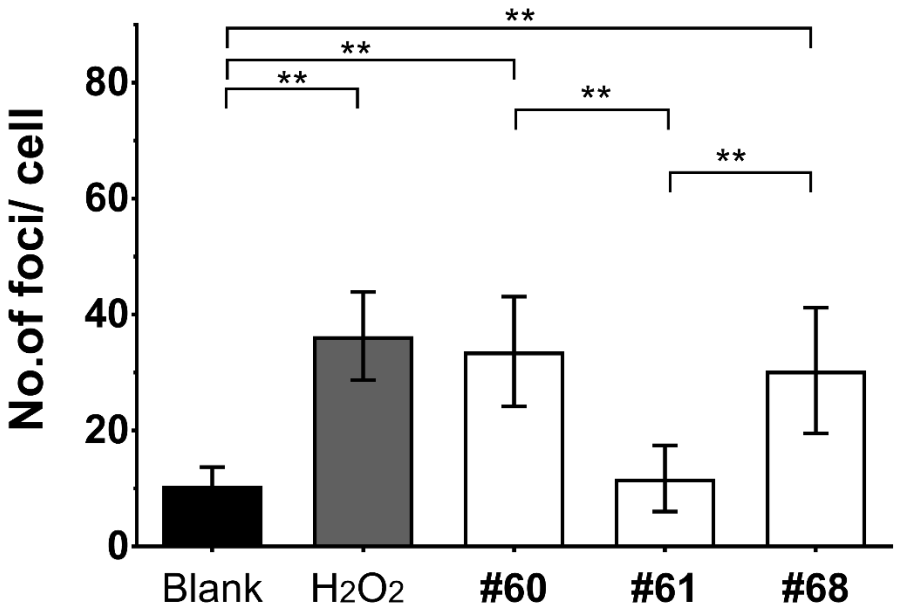

Figure 31: The role of oxazolopyridine *N*-oxidation in genotoxicity. Genotoxicity in HepG2 cells was assessed by manual scoring of γH2AX foci via immunofluorescence. Cells were treated with compounds **60**, **61** or **68** (10 µM) for 30 minutes. Hydrogen peroxide (200 µM) was used as positive control. Genotoxicity data represent the mean number foci per cell from 80 nuclei scored per condition from one independent experiment. Error bars represent SD; ** and ns denote P<0.01 and P≥ 0.05 respectively. # denotes compound number.

Based on the results obtained from the γH2AX assay, the 2-aryloxazolopyridine analogues **40a, 61, 65** and corresponding 2-aryloxazolopyridine-*N*-oxides **67, 68, 69** were subsequently tested in the Ames test. In this experiment, the combined roles of electron density, enzymatic bio-activation and *N*-oxidation of the oxazolopyridine molecule in mutagenicity were evaluated. Based on the genotoxicity of the oxazolopyridine-*N*-oxide **68** (Figure 31), it was proposed that the oxazolopyridine-*N*-oxide is the active form of the molecule, which could potentially react with DNA causing mutations. In theory, if the oxazolopyridine-*N*-oxide is the final activated form of the pro-mutagen, mutagenic activity of the *N*-oxides will be detected in the absence of S9 liver extract.

Generally, in the absence of S9 liver extract, no significant changes in the bacterial cells mutability detected for any of the 2-aryloxazolopyridine analogues **65**, **61** or **40a** (in ascending

σ values of the R groups) and their corresponding 2-aryloxazolopyridine-*N*-oxides **69**, **68** or **67** compared to untreated cells (Figure 32). In the presence of S9 liver extract, there was a significant increase in the level of bacterial cells mutability when treated with 2-(4-methoxyphenyl)oxazolopyridine **40a**, 2-(4-methoxyphenyl)oxazolopyridine-*N*-oxide **67** and 2-phenyloxazolopyridine-*N*-oxide **68** compared to untreated cells (Figure 32). The presence of S9 liver extract led to a significant increase in bacterial cells mutability detected for 2-(4-methoxyphenyl)oxazolopyridine-*N*-oxide **67** when compared to 2-(4-methoxyphenyl) oxazolopyridine **40a** (Figure 32).

The 2-aryloxazolopyridine analogues **65**, **61** and **40a** did not induce mutability in bacterial cells in the absence of S9 liver extract, consistent with the lack of mutagenicity detected for 2-(3-aminophenyl)oxazolopyridine **60** under similar conditions **(refer to section 4.4.1)**. This strongly indicates that the oxazolopyridine compounds are pro-mutagens, which require enzymatic bio-activation for activity. In agreement to this, the 2-aryloxazolopyridine analogue **40a** was mutagenic in the presence of S9 liver extract. The lack of mutagenic activities for the other 2-aryloxazolopyridine analogues **65** and **61** under similar conditions could be due to the lower electron donating ability of the substituents in these analogues as compared to **40a**.

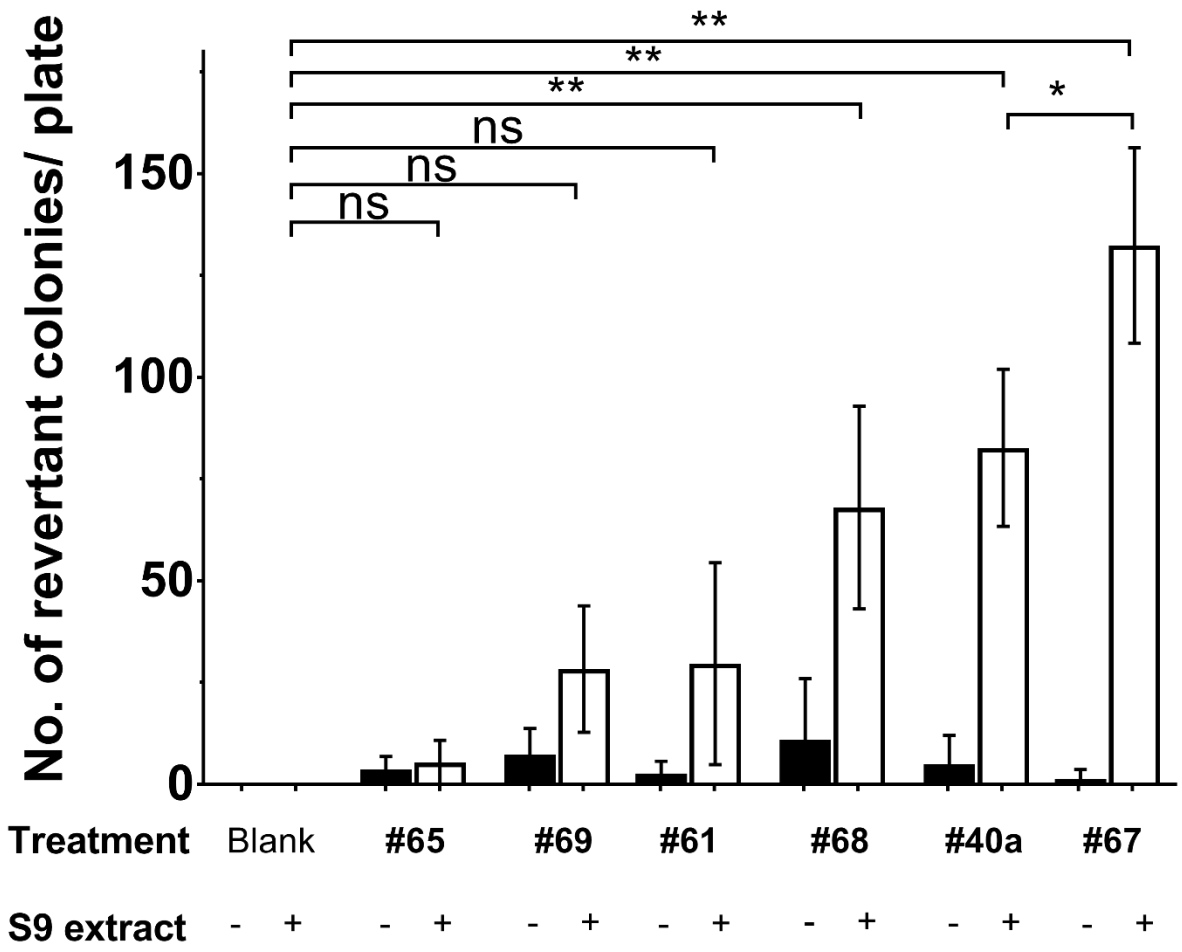

Figure 32: Mutagenicity of oxazolopyridine-*N*-oxides. Mutagenicity was assessed using the Ames test in His^- *S. thyphi* TA100. Bacterial cells were treated with 2-aryloxazolopyridines analogues (**65**, **61** or **40a**) and corresponding *N*-oxides (**69**, **68** or **67**) (10 µM) with (white bars) or without (black bars) S9 liver extract as indicated and grown for three days. Mutagenicity data represent the mean of three independent experiments with three replicates each and is expressed as number of His^+ revertant colonies/plate. Error bars represent SD; *, ** and ns denote $P<0.05$, $P<0.01$ and $P\geq 0.05$ respectively. # denotes compound number.

Surprisingly, the 2-aryloxazolopyridine-*N*-oxides **69, 68** and **67** were not mutagenic in the absence of S9 liver extract. Furthermore, only the 2-aryloxazolopyridine-*N*-oxides **68** and **67** were mutagenic in the presence of S9 liver extract. Similarly, the lack of mutagenic activity for the 2-aryloxazolopyridine-*N*-oxide **69** could be attributed by the lower reactivity as a result of lower electron density as previously described. In contrast to the hypothesis, the oxazolopyridine-*N*-oxides are not mutagenic on their own and need to be further bio-activated.

The oxazolopyridine-*N*-oxide could potentially be an intermediate during the enzymatic bio-activation of oxazolopyridines. This was evident based on the further increase in mutagenicity transitioning from the 2-aryloxazolopyridine analogue **40a** to its corresponding *N*-oxide, **67**. This also highlights that **other sites than the *N*-oxide on the pyridine ring of the oxazolopyridine core may be involved in its mutagenicity and genotoxicity**. For instance, the oxazole nitrogen of the oxazolopyridine core could be oxidised and become the reactive site for mutagenicity.

5.4.5 Mechanism of oxidative bio-activation in oxazolopyridines

The reactive role of the oxazole nitrogen of the oxazolopyridine core would be consistent with the mutagenic activity of benzoxazoles [302-304]. It was therefore hypothesised that the first oxidation of the pyridine nitrogen at the core of the 2-aryloxazolopyridine molecule **40** increases the electron density of the pyridine ring, which then donates electron density to the oxazole ring (Figure 33). This is a well-known method to increase the electron density of pyridines to increase reactivity for chemical transformations [415]. The pyridine-*N*-oxide is isoelectronic with a phenyl ring. Therefore, the oxazolopyridine-*N*-oxide **73** is isoelectronic to the benzoxazole molecule **74** (Figure 33). A second oxidation event may occur at the oxazole nitrogen of the oxazolopyridine-*N*-oxide **73** to give compound **75**, similar to the formation of mutagenic heterocyclic *N*-oxides [408].

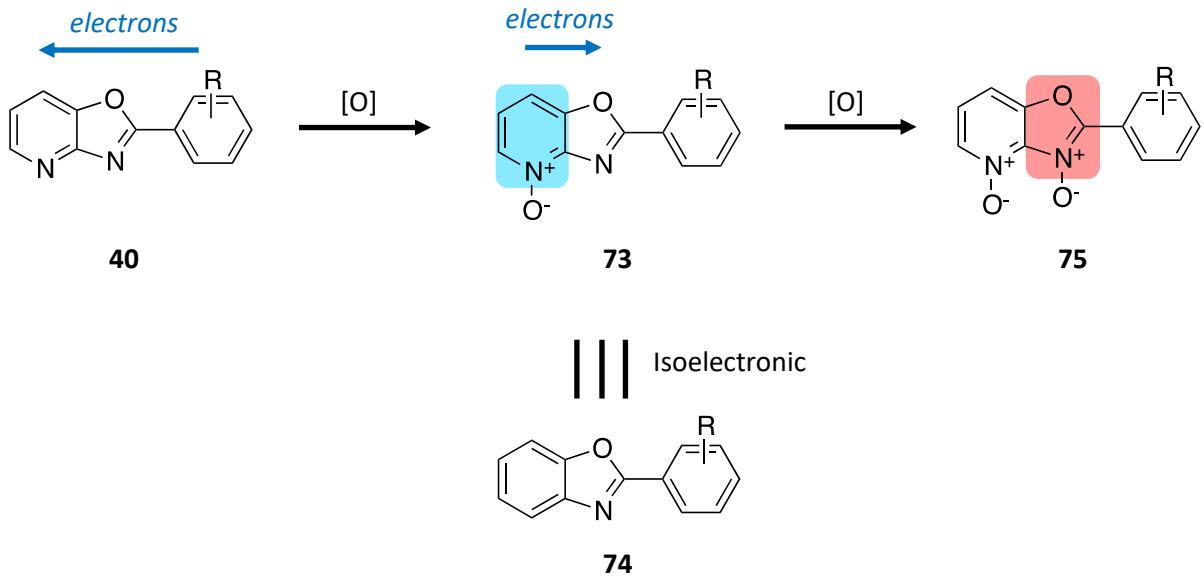

Figure 33: Proposed oxidative bio-activation of oxazolopyridine core. The oxidation of the oxazolopyridine molecule **40** results in the formation of an oxazolopyridine-*N*-oxide **73**. The pyridine ring of the oxazolopyridine-*N*-oxide **73** is rich in electrons (blue box) and is isoelectronic with a benzoxazole molecule **74**. The electron rich pyridine ring of the oxazolopyridine-*N*-oxide **73** then donates electrons to the oxazole nitrogen, increasing the electron density of the oxazole ring of compound **75** (red box) and its reactivity.

In the current experiment, the 2-(4-methoxyphenyl)oxazolopyridine **40a** was chosen as the reference point since it was shown to be mutagenic along with its corresponding *N*-oxide **67** (Figure 32, **section 5.4.4**). The pyridine nitrogen of **40a** was substituted with carbon to give the 2-(4-methoxyphenyl)benzoxazole **70**. To support the hypothesis, the benzoxazole **70** should show similar activity to the oxazolopyridine-*N*-oxide **67**.

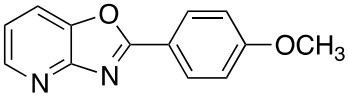

40a

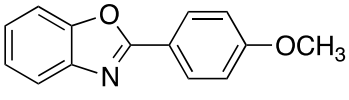

70

The role of the oxazole nitrogen on the benzoxazole can be tested by preventing its *N*-oxidation. This was performed by substituting the oxygen in compound **70** with sulphur to give 2-(4-methoxyphenyl)benzothiazole **71**. The presence of sulphur in place of oxygen shunts the oxidation of the oxazole nitrogen in the electron rich oxazole, where the sulphur atom undergoes oxidation instead.

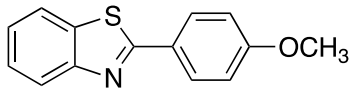

71

Upon the oxidation of the oxazole nitrogen, it was proposed that the oxazolopyridine molecule may undergo further oxidative cleavage to give the 2-oxooxazolopyridine **72** or hydrolysis to give the hydroxylamine **76** (Figure 34). For these reasons, the syntheses of **72** and **76** were attempted as a proof of concept. Out of the two, the 2-oxooxazolopyridine, **72** was successfully synthesised and tested in the current experiment. The synthesis of the hydroxylamine **76** was not successful although hydroxylamines are known to be genotoxic and mutagenic [416-418]. This latter transformation has not been proposed for any oxazolopyridine or benzoxazole within the literature.

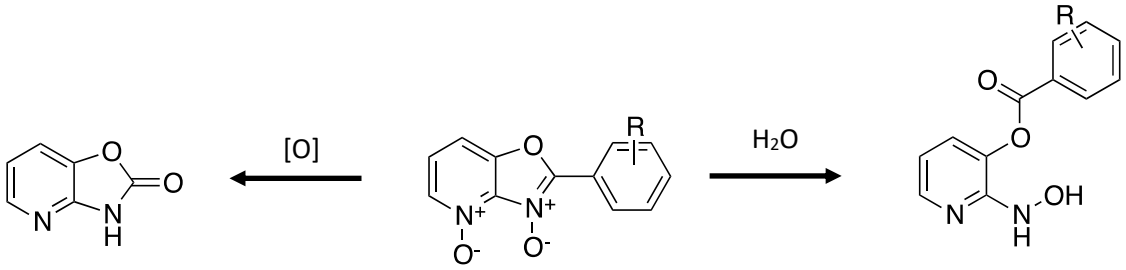

72 **75** **76**

Figure 34: Proposed events following the *N*-oxidations of nitrogen atoms of the oxazolopyridine molecule. Compound **75** may undergo oxidative cleavage to give the 2-oxooxazolopyridine **72** or hydrolysis to give the hydroxylamine **76**.

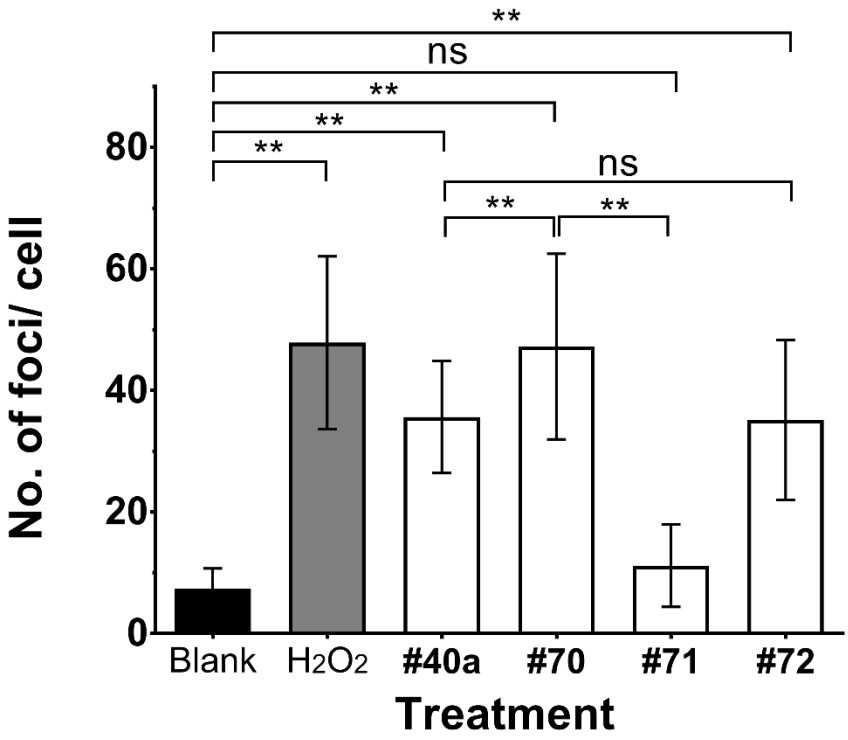

Figure 35: Determining mode of action of oxazolopyridines through genotoxicity. Genotoxicity in HepG2 cells was assessed by manual scoring of γH2AX foci via immunofluorescence. Cells were treated with compounds **40a**, **70**, **71** or **72** (10 µM) for 30 minutes. Hydrogen peroxide (200 µM) was used as positive control. Data represents the mean number foci per cell where 80 nuclei were scored per condition. Genotoxicity data represent the mean number foci per cell from 80 nuclei scored per condition from one independent experiment. Error bars represent SD; ** and ns denote $P<0.01$ and $P\geq 0.05$ respectively. # denotes compound number.

Generally, a significant increase in genotoxicity was detected for 2-(4-methoxyphenyl) benzoxazole **70** (10 µM) and 2-oxooxazolopyridine **72** (10 µM) compared to untreated cells (Figure 35). The 2-(4-methoxyphenyl)benzothiazole **71** however lacked genotoxicity and was similar to the baseline value detected in untreated cells (Figure 35). The 2-(4-methoxyphenyl)oxazolopyridine **40a** (10 µM) and the positive control, hydrogen peroxide (200 µM) were genotoxic consistent with previous experiments (Figure 35). The amount of genotoxicity detected for 2-(4-methoxyphenyl)benzoxazole **70** (10 µM) was higher than 2-(4-methoxyphenyl)oxazolopyridine **40a** (10 µM). Finally, the genotoxicity detected for 2-(4-methoxyphenyl)benzothiazazole **71** (10 µM) was lower than 2-(4-methoxyphenyl) benzoxazole, **70** (10 µM).

The 2-(4-methoxyphenyl)benzoxazole **70** was found to be genotoxic, consistent with the genotoxicity reported for benzoxazoles [302-304]. Moreover, this supported the hypothesis that the oxazole nitrogen is the reactive site for genotoxicity. The higher genotoxicity detected for 2-(4-methoxyphenyl)benzoxazole **70** compared to 2-(4-methoxyphenyl)oxazolopyridine **40a** is likely due to compound **70** being "pre-activated" since the benzoxazole is isoelectronic to the oxazolopyridine-*N*-oxide. Therefore, during cellular bio-activation, the conversion of 2-(4-methoxyphenyl)benzoxazole **70** into the active form will be quicker than 2-(4-methoxyphenyl) oxazolopyridine **40a**, resulting in higher genotoxicity induced.

The reactivity of the oxazole nitrogen of the oxazolopyridine core was further supported by the lack of genotoxicity detected for the 2-(4-methoxyphenyl)benzothiazole **71.** Upon substitution of the oxygen in the oxazole ring in compound **70** to sulphur in compound **71**, the amount of genotoxicity detected was reduced to baseline value reported for untreated cells (Figure 35). Therefore, *N*-oxidation of the oxazole nitrogen was needed for activity and the substitution of the oxygen with sulphur prevented this. This was also consistent with the lack of genotoxicity

[419] and mutagenicity [420,421], even in the presence of S9 liver extract [421] reported for benzothiazoles.

The 2-oxooxazolopyridine **72** was found to be genotoxic but the amount of genotoxicity induced was similar to 2-(4-methoxyphenyl)oxazolopyridine **40a**, where no further increase in genotoxicity was observed. This indicates that 2-(4-methoxyphenyl)oxazolopyridine **40a** is not converted to 2-oxooxazolopyridine **72** as genotoxicity would be expected to be much higher. Although the hydroxylamine **76** cannot be tested, information about its genotoxicity would have added value to this study. These compounds were also tested in the Ames test (Figure 36) to determine if the mutagenic and genotoxic activities of these compounds were consistent.

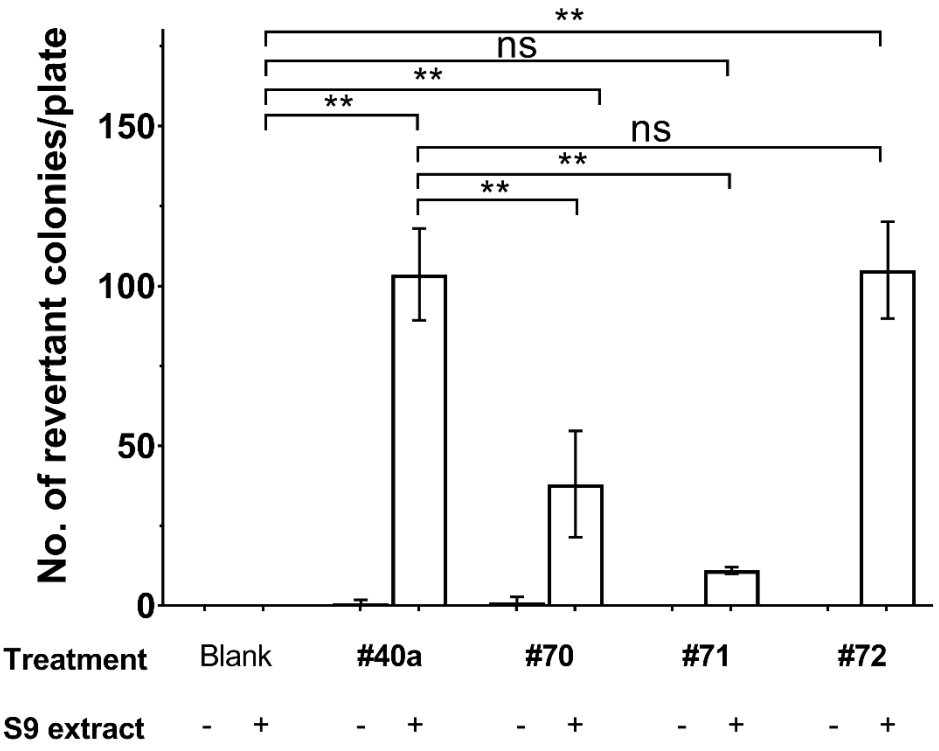

Figure 36: Determining mode of action of oxazolopyridines through mutagenicity. Mutagenicity was assessed using the Ames test in His$^-$ *S. thyphi* TA100. Bacterial cells were treated with compounds **40a**, **70, 71** or **72** (10 µM) with (white bars) or without (black bars) S9 liver extract as indicated and grown for three days. Mutagenicity data represent the mean of three independent experiments with three replicates each and is expressed as number of His$^+$ revertant colonies/plate. Error bars represent SD; *, ** and ns denote $P<0.05$, $P<0.01$ and $P\geq 0.05$ respectively. # denotes compound number.

In the presence of S9 liver extract, the level of bacterial cells mutability detected for 2-(4-methoxyphenyl)benzoxazole **70** (10 µM) and 2-oxooxazolopyridine **72** (10 µM) were higher than in untreated cells (Figure 36). The 2-(4-methoxyphenyl)benzothiazole **71** did not induce mutability in bacterial cells, similar to untreated cells (Figure 36). The 2-(4-methoxyphenyl)oxazolopyridine **40a** (10 µM) was consistently mutagenic in the presence of the liver S9 extract as reported previously (Figure 36). In the absence of S9 liver extract, none of the tested compounds showed mutagenic activity reflected by the lack of bacterial cells mutability (Figure 36).

The results obtained from the Ames test (Figure 36) were consistent with the γH2AX assay (Figure 35) especially for compounds **71** and **72**. Surprisingly, the level of mutagenicity detected for 2-(4-methoxyphenyl)benzoxazole **70** was not the highest in the Ames test (Figure 35) given that it was most genotoxic among all the tested compounds in the γH2AX assay (Figure 35). The highly genotoxic nature of the compound **70** may have led to toxicity issues. Moreover, the anti-microbial activity of compound **70** was not determined in the current study. In addition, the test concentration for all the compounds was standardised at 10 µM, which can be too high for the test organism in the Ames test. This limitation can be addressed by establishing a dose-response curve in the test organism, which was not conducted in the current study due to time constraints. More importantly, the high mutagenic activity detected for 2-oxooxazolopyridine **72** only in the presence of the S9 extract (Figure 34) further supported that it is not the active form of the oxazolopyridine molecule, as further enzymatic bio-activation was still required for activity.

Despite the proposed events following *N*-oxidation of the oxazolopyridine (Figures 33 and 34), other active species can also be formed, which require further investigation. The active species are often unstable and difficult to chemically synthesise and isolate [422]. During cellular bio-activation, the formation of these metabolites is difficult to monitor due to low yields and the

complex cellular matrices makes the isolation of these metabolites extremely challenging [423,424]. The enzymatic bio-activation of the oxazolopyridine compound however can be monitored using a highly sensitive method such as LC-MS.

5.4.6 Monitoring the oxidative bio-activation of oxazolopyridines

In summary, the pyridine nitrogen of the oxazolopyridine molecule can be oxidised forming an *N*-oxide. The oxazolopyridine-*N*-oxide is then converted into the active species where the oxazole nitrogen was proposed to be the reactive site. The experiments so far correlated well with this hypothesis but more direct evidence was needed. To achieve this, the characterisation of metabolites produced during enzymatic bio-activation of the oxazolopyridine compound using S9 liver extract was monitored via UPLC-MS. The method is considered robust and reproducible as it is conducted under readily controlled conditions [425]. Moreover, the risk of material loss was minimised as the reaction mixture was analysed directly using UPLC-MS.

The mutagenic and genotoxic 2-(4-methoxyphenyl)oxazolopyridine **40a** was selected for the current experiment. After incubating the 2-(4-methoxyphenyl)oxazolopyridine **40a** in S9 liver extract for 3 hours, the 2-(4-methoxyphenyl)oxazolopyridine-*N*-oxide **67** (RT= 4.41 minutes) (Figure 37A) and the starting material **40a** (RT= 5.82 minutes) (Figure 37B) were detected using UPLC-MS by multiple reaction monitoring (MRM). The retention time corresponding to the monitored compounds were compared against the standards (Figure 37C,D). This provided evidence that the oxazolopyridine compound is converted into an *N*-oxide under enzymatic conditions and supported the proposed oxidative bio-activation mechanism of the oxazolopyridine compound. However, as no standard for the proposed hydroxylamine **76** from the oxazole ring opening of the oxazolopyridine molecule (Figure 34, **section 5.4.5**) was available, MRM for this compound could not be performed.

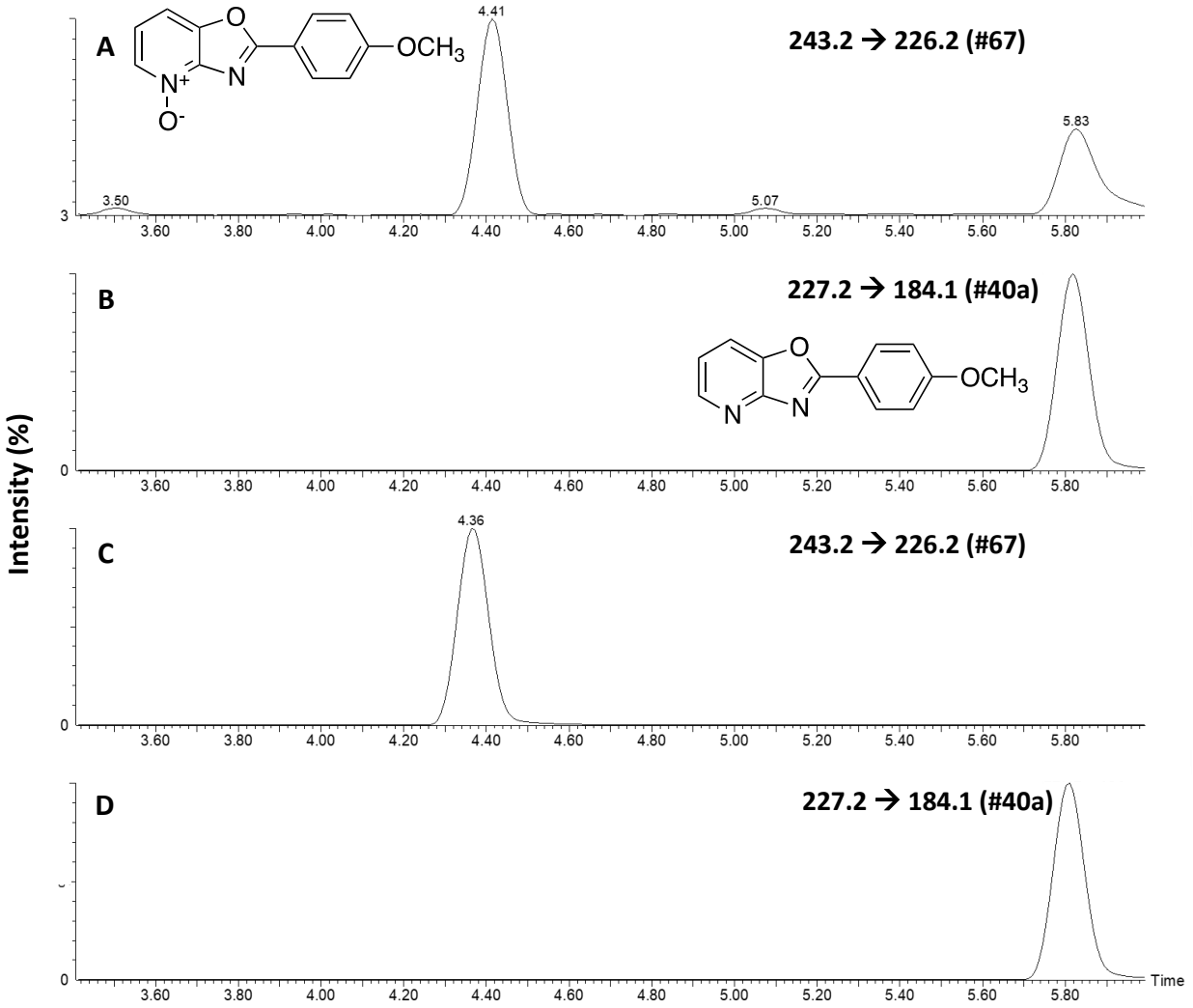

Figure 37: Monitoring the enzymatic bio-activation of the oxazolopyridine compound using UPLC-MS (MRM mode). The 2-(4-methoxyphenyl)oxazolopyridine **40a** (1 µM) was incubated with S9 liver extract for 3 hours and the sample was analysed. **(A)** Detection of 2-(4-methoxyphenyl)oxazolopyridine-*N*-oxide **67** in the incubated sample; **(B)** detection of 2-(4-methoxyphenyl)oxazolopyridine **40a** in the incubated sample; **(C)** compound **67** standard; and **(D)** compound **40a** standard. MRM transitions for compounds **67** and **40a** were 243.3→226.2 m/z and 227.2→ 184.1 m/z respectively. # denotes compound number.

Instead of monitoring the presence of known analytes, the elution profile of the reaction sample after incubation was compared to time zero via UPLC-MS using total ion count (TIC) mode in the following experiment. After 3 hours of reacting the 2-(4-methoxyphenyl)oxazolopyridine **40a** with S9 liver extract, a new peak (RT= 4.80 minutes) was detected (Figure 38). This was

compared to the chromatogram at time zero where only the peak corresponding to compound **40a** (RT= 5.88 minutes) was present (Figure 38). Surprisingly, the peak corresponding to the 2-(4-methoxyphenyl)oxazolopyridine-*N*-oxide **67** was not detected in the chromatogram using this mode due to low concentration. Although the TIC mode is good for the monitoring of new metabolites formed, it is not sensitive to detect very low concentrations of analytes compared to MRM [426]. Analysis of the new metabolite (RT= 4.80 minutes) (Figure 38) using mass spectrometry revealed that the molecule had a $[M+H]^+$ of 213 m/z, indicating a molecular mass of 212 g/mol (Figure 39). Compared to compound **40a** (molecular mass of 226 g/mol), there was a loss of mass of 14 g/mol, which corresponds to loss of CH_2.

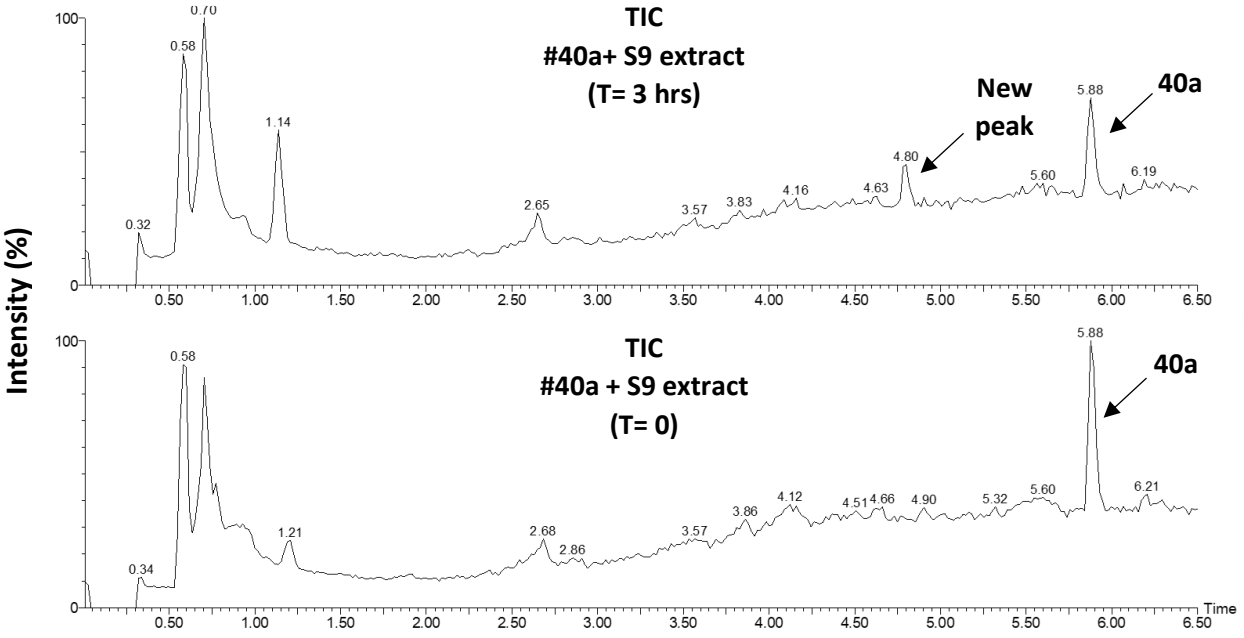

Figure 38: Monitoring the formation of new metabolite upon the enzymatic bio-activation of the oxazolopyridine compound using UPLC-MS (TIC mode). The 2-(4-methoxyphenyl)oxazolopyridine **40a** (1 µM) was incubated with S9 liver extract for 3 hours and the sample was analysed. The peak at RT= 5.88 minutes correspond to compound **40a**. A new peak corresponding to a new metabolite at RT= 4.80 minutes was detected after 3 hours. # denotes compound number. Full scan in TIC mode was conducted within the range of 100-300 m/z.

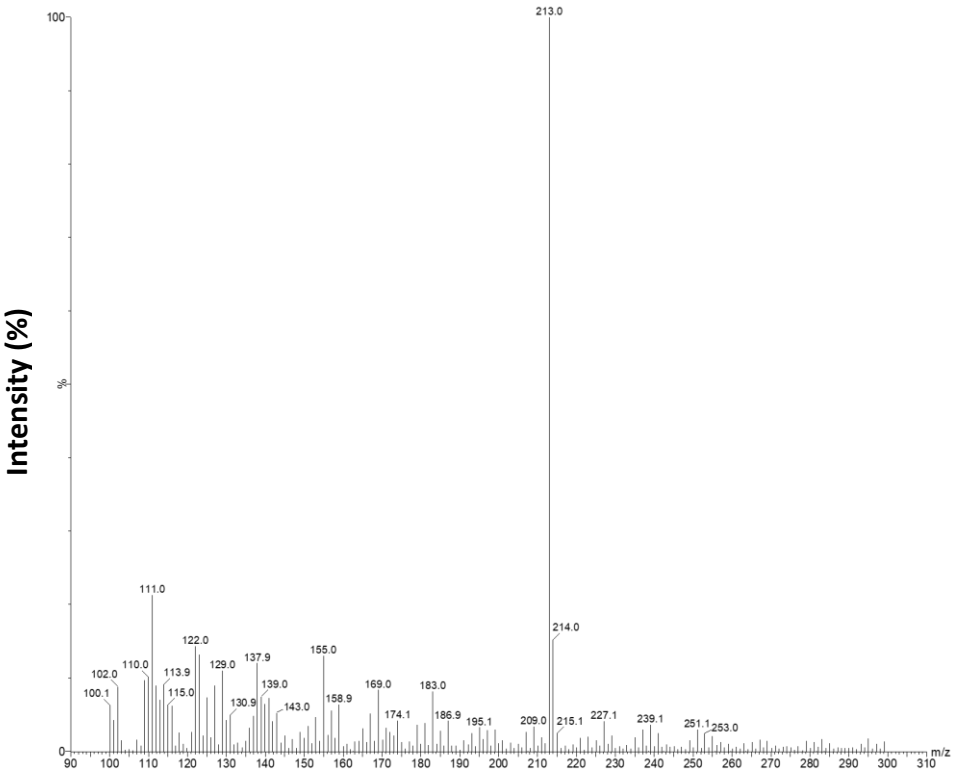

Figure 39: Mass spectrometry of the new metabolite detected at RT= 4.80 minutes via UPLC-MS (TIC mode). The formed metabolite has the most abundant molecular ion of $[M+H]^+$= 213 m/z.

Therefore the metabolite detected at RT= 4.80 minutes was proposed to be 2-(4-hydroxyphenyl)oxazolopyridine **77,** which can be formed by oxidative cleavage of the methyl group. However, this is likely to be unrelated to the mode of genotoxicity since the 2-aryloxazolopyridine **40** analogues which have been reported to be genotoxic (Figure 28, **section 5.4.2**) do not necessarily contain a methoxy group at the phenyl ring like compound **40a**, which could be metabolised into a hydroxyl group.

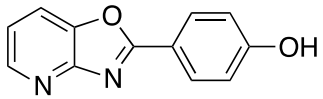

77

As proposed (Figure 34, **section 5.4.5**), a second oxidation event occurring on the oxazole nitrogen of the oxazolopyridine-*N*-oxide **73** to give compound **75**, further drives the bio-activation reaction to form the active species. However, in the current study, the metabolite of

2-(4-methoxyphenyl)oxazolopyridine **40a** with both nitrogen atoms oxidised was not detected via UPLC-MS (Figure 38). Therefore, the oxidation of 2-(4-methoxyphenyl)oxazolopyridine-*N*-oxide **67** was attempted using a strong oxidising agent such as peroxytrifluoroacetic acid and monitored via NMR. Isolation of a product was not conclusive as the starting material, compound **67** remained as the dominant species after the reaction. Therefore, the feasibility of the conversion of 2-(4-methoxyphenyl)oxazolopyridine-*N*-oxide **67** into compound **78** via the oxidation with peroxytrifluoroacetic acid was investigated by density function theory (DFT) calculations (Figure 40). The second oxidation event happening on the oxazole nitrogen was thermodynamically plausible indicated by the calculated Gibbs energy (ΔG) of the product **78** at -29.7 kcal/mol (Figure 40).

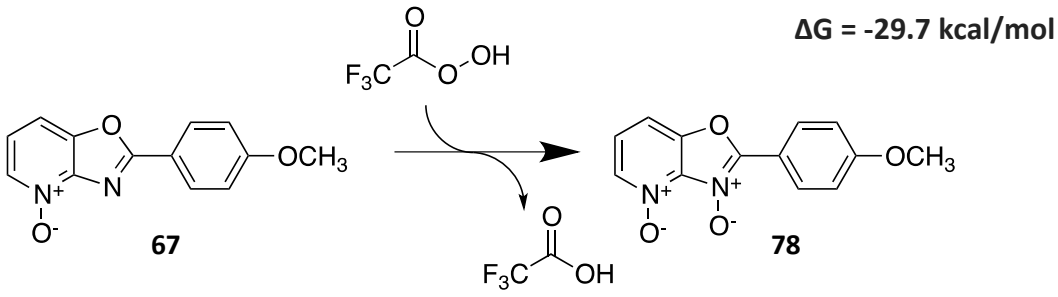

Figure 40: Oxidation reaction of 2-(4-methoxyphenyl)oxazolopyridine-*N*-oxide **67** into compound **78** using peroxytrifluoroacetic acid.

Although a metabolite of higher oxidation state was not identified via UPLC-MS, the hydroxylamine **79** was suspected to be the active form of the metabolite. Therefore, the feasibility of the reaction from compound **78** to form the hydroxylamine **79** was investigated by DFT (Figure 41). This transformation has not been reported previously but the calculations suggest that the conversion of compound **78** to the hydroxylamine **79** is thermodynamically plausible indicated by the ΔG of the product **79** at -11.5 kcal/mol (Figure 41). The hydrolysis

of compound **78** requires two transition structures (**TS_{A-B}** and **T_{D-E})** with an overall activation energy of 27.6 kcal/mol before forming the hydroxylamine **79** (Figure 41).

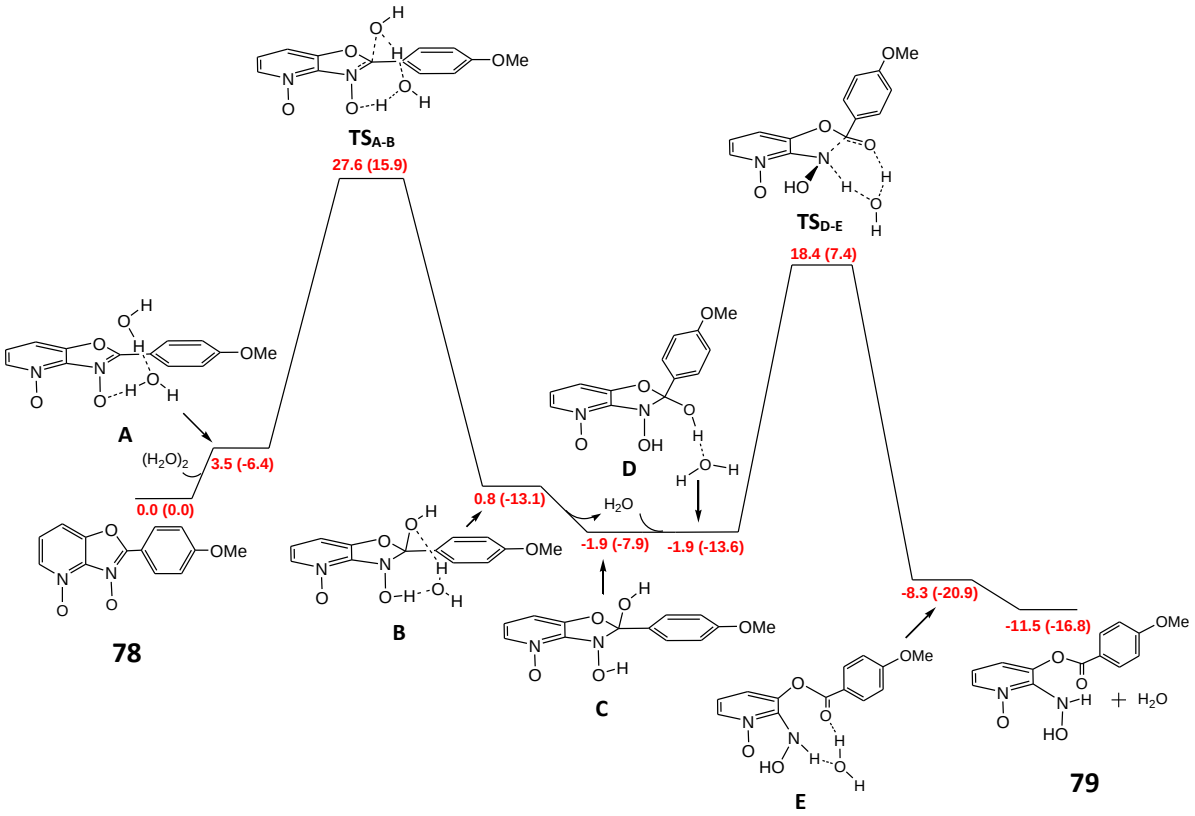

Figure 41: Free energy diagram in the determination of reaction kinetics of the proposed mechanism of the conversion of compound **78** to the hydroxylamine **79**. Values in normal script are corrected Gibbs energies and those in brackets are electronic energies calculated at M06_2X/BS2//B3LYP/BS1. All values in kcal/mol.

5.5 Chapter summary

The initial hypothesis stated that the amino group in compound **60** is responsible for the genotoxicity and mutagenicity (based on the PhIP **46** model), which was supported by the results outlined in chapters 3 and 4. Moreover, this hypothesis formed the foundation for the current study. However, upon deeper investigations on the genotoxicity and mutagenicity of the oxazolopyridine molecule revealed that this hypothesis was incorrect. In fact, the initial QSAR experiment indicated that the oxazole nitrogen of the oxazolopyridine core to be the reactive site for the genotoxic and mutagenic activities. The amino group in compound **60** did not contribute directly to genotoxicity but indirectly contributed by its electron donating ability into the phenyl ring. This was supported by the linear relationship between genotoxicity and electron donating ability of substituents on the aryl ring of the 2-aryloxazolopyridines **40**, which indicates that the high electron density of the oxazolopyridine core was the driving force for genotoxicity.

In addition, the oxidation products of 2-aryloxazolopyridines **40** were identified to be 2-aryloxazolopyridine-*N*-oxides **73**. The *N*-oxidation reverted the non-genotoxicity of 2-phenyloxazolopyridine **61**, indicating that the oxazolopyridine-*N*-oxide could potentially be the active species, which reacts with DNA. Further to this, the oxazolopyridine-*N*-oxides were also mutagenic in the Ames test. Even more surprising, the results in this experiment indicate that the oxazolopyridine-*N*-oxide is not the active species and needed to undergo further bio-activation by S9 liver extract. This suggests that the oxazolopyridine-*N*-oxide is an intermediate during the enzymatic bio-activation of the oxazolopyridine molecule. It was therefore hypothesised that a second oxidation occurs at the oxazole nitrogen. Further QSAR studies revolving around the nitrogen atoms on the oxazolopyridine core supported that the oxazole nitrogen is the reactive site for genotoxicity and mutagenicity. In an attempt to monitor the

enzymatic bio-activation of 2-(4-methoxyphenyl)-oxazolopyridine **40a** using S9 liver extract, the 2-(4-methoxyphenyl)oxazolopyridine-*N*-oxide **67** was detected after three hours. Also, a new metabolite, 2-(4-hydroxyphenyl)oxazolopyridine **77** was detected, which had lost a methyl group when compared to the starting material, 2-(4-methoxyphenyl)-oxazolopyridine **40a**. While the results of this chapter are intriguing, the definitive species responsible for genotoxicity and mutagenicity was not conclusively determined. However, the formation of the hydroxylamine **79** suspected to be the active metabolite was calculated to be energetically feasible. Further work is therefore required to monitor the bio-activation of the 2-aryloxazolopyridine compounds **40** and to identify the active metabolite.

Chapter 6 Conclusions, limitations and future work

This thesis has addressed research questions related to the genotoxic and mutagenic activities of the oxazolopyridine scaffold. Due to the structural similarities of 2-(3-aminophenyl)oxazolopyridine **60** and the known carcinogen, PhIP **46**, it was hypothesised that compound **60** may be genotoxic and mutagenic. The amino group of PhIP **46** has been widely reported to be the mutagenic reactive site where it is converted into an arylnitrenium ion, which binds covalently to DNA [107-112]. Therefore, it was hypothesised that the amino group of compound **60** may be the reactive site for genotoxic and mutagenic activities, using PhIP **46** as a model.

In Chapter 3, compound **60** was non-cytotoxic up to concentrations of 100 µM consistent with previous reports for oxazolopyridine compounds, while PhIP **46** was only mildly cytotoxic. In contrast, compound **60** showed genotoxicity at concentrations as low as 0.001 µM. Although potently genotoxic, compound **60** appeared less genotoxic than PhIP **46** which was seen in two different assays. The potent genotoxicity of compound **60** coupled with its lack of cytotoxicity was rather surprising since genotoxic agents are commonly associated with cytotoxicity. Further investigations revealed that the cellular DNA damage induced by compound **60** was effectively repaired within 24 hours. This indicates that the DNA damage caused by compound **60** was easily dealt with by the cellular DNA repair machinery, which repair kinetics comparable to damage induced by oxidative stress. Further investigations suggested that the cellular DNA repair pathways employed in response to compound **60** were likely dependent on the DNA repair enzymes, PARP1 and ATM.

In chapter 4, compound **60** was found to be a pro-mutagen requiring enzymatic bio-activation by S9 liver extract to show activity in the Ames test. Similarly, PhIP **46** is not mutagenic itself but is converted into *N*-hydroxylamine **52** by liver cytochrome P450s (CYP) [92-98], which is then

converted into the mutagenic PhIP arylnitrenium ion **54** [52,104]. The enzymatic bio-activation of compound **60** was also oxidation dependent consistent with the role of CYP enzymes in the oxidation of xenobiotics in the liver. The oxidation-dependent metabolism was shown by reduced genotoxicity of compound **60** in the presence of the anti-oxidant, Trolox. Consistent with a pro-mutagenic activity, compound **60** phenotypically transformed cells to a more invasive phenotype, using the soft agar invasion (SAI) assay as an *in vitro* cell transformation model.

The results in chapters 3 and 4 showed that the similar cellular responses to both compounds supported the hypothesis that the amino group of compound **60** is involved in its genotoxic and mutagenic activities similar to PhIP **46**. However, deeper investigations on the genotoxicity and mutagenicity of the oxazolopyridine molecule in chapter 5 led to the conclusion that this hypothesis was incorrect. The amino group of compound **60** did not contribute directly to genotoxicity but instead, increased the electron density of the oxazolopyridine core which was ultimately identified as key to genotoxic activity. This was supported by the Hammett plot generated using 2-aryloxazolopyridines **40** analogues with substituents of different electron donating abilities. The oxidation of 2-aryloxazolopyridines **40** resulted in the formation of 2-aryloxazolopyridine-*N*-oxides **73**. These *N*-oxides were tested and found to be even more genotoxic and mutagenic than the pre-cursors and was thought to be the active species. However, further bio-activation by S9 liver extract was required for the oxazolopyridine-*N*-oxides to be mutagenic. It was therefore hypothesised that a second oxidation event was occurring, which may lead to the ring opening of the oxazolopyridine-*N*-oxide into a hydroxylamine, suspected to be the active species. This was supported by QSAR determination revolving around the nitrogen atoms of the oxazolopyridine core. Enzymatic bio-activation of 2-(4-methoxyphenyl)-oxazolopyridine **40a** using S9 liver extract was monitored where the 2-(4-methoxyphenyl)oxazolopyridine-*N*-oxide **67** was formed, consistent with the results so far.

However, the definitive species responsible for genotoxicity and mutagenicity was not conclusively determined due to time constraints. The formation of the hydroxylamine **79** suspected to be the active metabolite was investigated by density function theory (DFT) to be energetically feasible.

Further work is therefore required to address some of the limitations associated with the current study. In the determination of DNA repair kinetics in cells exposed to compound **60**, only hydrogen peroxide was used as the positive control in this experiment. However, this is limited by the different types of DNA damage caused by hydrogen peroxide, which mainly induces DNA strand breaks [342,343] compared to PhIP **46** which causes base modifications [107-109]. Therefore, repair kinetics for PhIP **46**-induced DNA damage should also be assessed to provide a more appropriate comparison of the genotoxic modes of action of compound **60** and PhIP **46**. In addition, the experiment involving DNA repair inhibitors only provided some indication of the role of regulatory proteins involved in the repair of the DNA damage induced by compound **60**. However, the exact pathway(s) involved in DNA repair of the damage induced by compound **60** could not be established due to the multi-faceted nature of DNA repair enzymes as discussed. Therefore, a screen using a yeast gene knock-out library of DNA repair genes could be conducted as it would be faster and more accurate to determine the type of DNA repair mechanism involved [427,428].

As shown in the current study, the role of oxidative bio-activation is important for the genotoxic and mutagenic activity of the oxazolopyridine compounds. While the data presented in the current study have been consistent, determining the exact roles of specific oxidative cytochrome P450 (CYP) enzymes would have provided more information on the mutagenic mode of action and the specific risk to different tissues arising from the oxazolopyridine compounds. Therefore, CYP1A1 (-/-) and CYP 1A2 (-/-) knockout mice as previously conducted with PhIP **46** [429,430] could be used to extend the findings of the current study. This

approach would determine the roles of these CYP enzymes [431] in the bio-activation of the oxazolopyridine compounds or expanded to investigate on other CYP enzymes as well. Although the soft agar invasion (SAI) assay is a rapid method in determining cellular transformation potential of a mutagen, *in vivo* cancer models are more representative to the tumour development in humans and should be used to further the findings of the current study. In particular, the use of immune-deficient mice such as nude mice, which are susceptible to cancer was reported previously to monitor the development of tissue-specific drug-induced tumours [432,433]. Further work can also be conducted to monitor the bio-activation of other 2-aryloxazolopyridine **40** compounds and to identify the active metabolite. The synthesis of the proposed hydroxylamine **76** to test for genotoxic and mutagenic activities could further substantiate the findings of the current study. The hydroxylamine **76** could also be synthesised and used as a standard for monitoring the bio-activation of the 2-aryloxazolopyridine **40** compounds by UPLC-MS. The reaction of the synthesised hydroxylamine **76** or detected bio-activated metabolite in future experiments, with nucleotides or DNA can be monitored via UPLC-MS. This could potentially be used to determine the type of DNA lesion caused by the oxazolopyridine compounds to explain its lack of cytotoxicity, which was not fully characterised in the current study. In addition, the current study should also be extended to other popular and biologically active drug scaffolds such as benzoxazoles, benzimidazoles and imidazopyridines due to the similar activities and close relationships with the oxazolopyridines.

The results of this thesis indicate that the oxazolopyridine core should be treated with extreme caution due to its potential genotoxic and mutagenic activities. There is now significant evidence to suggest that the oxazolopyridine system as a scaffold for drug discovery could be associated with severe long term liabilities. In fact, the development of benzoxazole-related compounds as drug candidates should also be reconsidered and more in-depth biological testing should be performed to evaluate their mutagenic potentials.

Appendices

Appendix 1

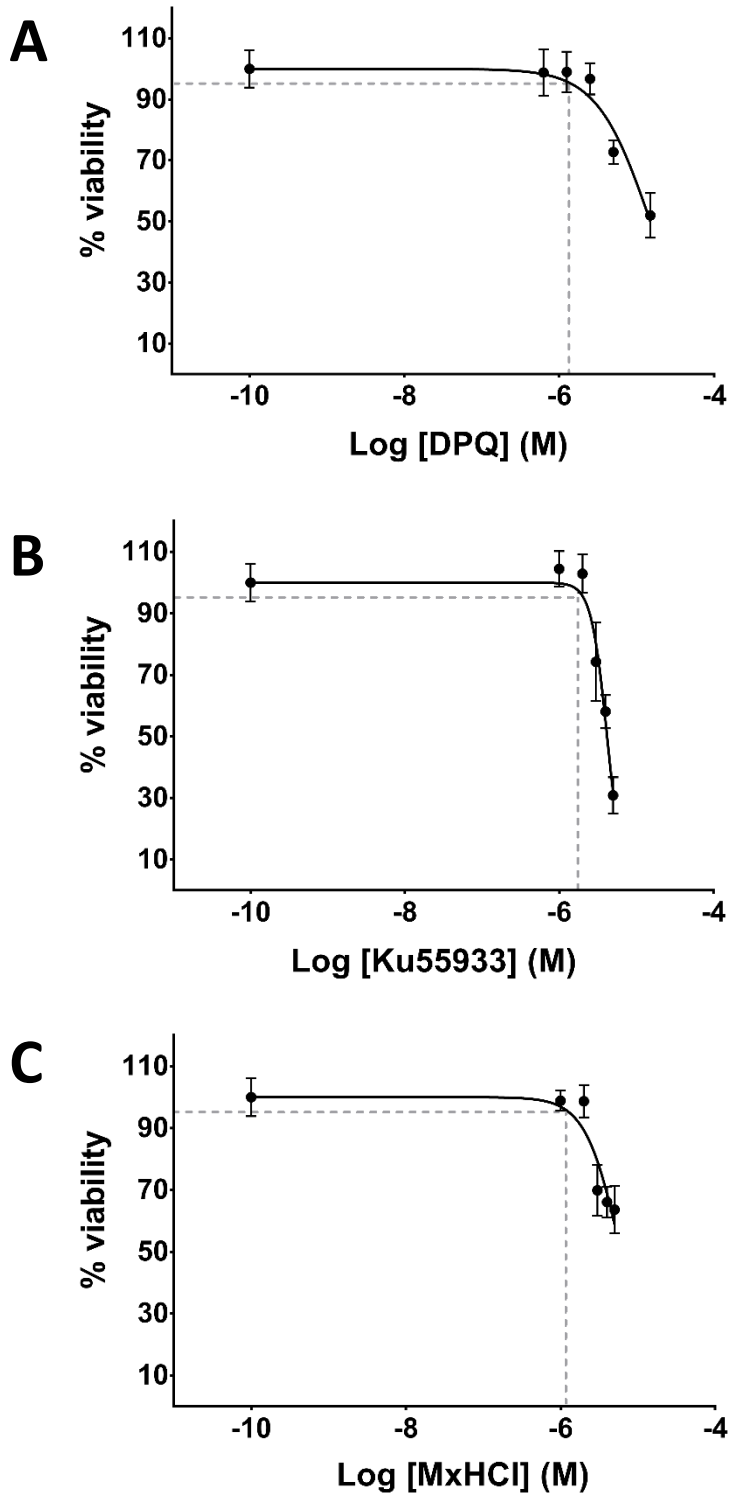

Appendix 1: Determination of concentrations of DNA repair inhibitors. Viability of cells was assessed by colony formation assay using HepG2 cells. Cells were treated with: (A) DPQ, (B) Ku55933 or (C) MxHCl as indicated for 12 days. Hydrogen peroxide (200 µM) was used as positive control. Viability data represents the mean of three independent experiments with three replicates per experiment and is expressed as % of untreated control. Error bars represent SD, dotted lines is used to indicate the concentration of the DNA inhibitors at 95% viability on the curve of best fit.

References

(1) Lepetit, C.; Peyrou, V.; Chauvin, R. *Physical Chemistry Chemical Physics* **2004**, *6*, 303.
(2) Asif, M. *International Journal of Bioorganic Chemistry* **2017**, *2*, 146.
(3) Broughton, H. B.; Watson, I. A. *Journal of Molecular Graphics and Modelling* **2004**, *23*, 51.
(4) Gomtsyan, A. *Chemistry of Heterocyclic Compounds* **2012**, *48*, 7.
(5) Dua, R.; Shrivastava, S.; Sonwane, S.; Srivastava, S. *Advances in Biological Research* **2011**, *5*, 120.
(6) García-Valverde, M.; Torroba, T. *Molecules* **2005**, *10*, 318.
(7) Elnima, E. I.; Zubair, M. U.; Al-Badr, A. A. *Antimicrobial Agents and Chemotherapy* **1981**, *19*, 29.
(8) Sener, E.; Yalcin, I. *Farmaco* **1997**, *52*, 99.
(9) Vinsova, J.; Horak, V.; Buchta, V.; Kaustova, J. *Molecules* **2005**, *10*, 783.
(10) Rida, S. M.; Ashour, F. A.; El-Hawash, S. A.; ElSemary, M. M.; Badr, M. H.; Shalaby, M. A. *European Journal of Medicinal Chemistry* **2005**, *40*, 949.
(11) Tipparaju, S. K.; Joyasawal, S.; Pieroni, M.; Kaiser, M.; Brun, R.; Kozikowski, A. P. *Journal of Medicinal Chemistry* **2008**, *51*, 7344.
(12) Haugwitz, R. D.; Angel, R. G.; Jacobs, G. A.; Maurer, B. V.; Narayanan, V. L.; Cruthers, L. R.; Szanto, J. *Journal of Medicinal Chemistry* **1982**, *25*, 969.
(13) Koksal, M.; Gokhan, N.; Kupeli, E.; Yesilada, E.; Erdogan, H. *Archives of Pharmacal Research* **2007**, *30*, 419.
(14) Gulcan, H. O.; Unlu, S.; Banoglu, E.; Sahin, M. F.; Kupeli, E.; Yesilada, E. *Turkish Journal of Chemistry* **2003**, *27*, 467.
(15) McKee, M. L.; Kerwin, S. M. *Bioorganic and Medicinal Chemistry* **2008**, *16*, 1775.
(16) Murty, M. S. R.; Ram, K. R.; Rao, R. V.; Yadav, J. S.; Rao, J. V.; Cheriyan, V. T.; Anto, R. J. *Medicinal Chemistry Research* **2011**, *20*, 576.
(17) Jeon, R.; Park, S. *Archives of Pharmacal Research* **2004**, *27*, 1099.
(18) Maddila, S.; Jonnalagadda, S. *Journal of the Chilean Chemical Society* **2012**, *57*, 1099.
(19) Kawashita, Y.; Nakamichi, N.; Kawabata, H.; Hayashi, M. *Organic Letters* **2003**, *5*, 3713.
(20) Wang, L.; Zhang, P.; Zhang, X.; Zhang, Y.; Li, Y.; Wang, Y. *European Journal of Medicinal Chemistry* **2009**, *44*, 2815.
(21) Kaur, A.; Wakode, S.; Pathak, D. P. *International Journal of Pharmacy and Pharmaceutical Sciences* **2014**, *7*, 16.
(22) Yalcin, I.; Oren, I.; Temiz, O.; Sener, E. A. *Acta Biochimica Polonica* **2000**, *47*, 481.
(23) Fancourt, G. J.; Adams, H.; Walls, J.; Ward, J. W. *Human Toxicology* **1984**, *3*, 517.
(24) Goldkind, L.; Laine, L. *Pharmacoepidemiology and Drug Safety* **2006**, *15*, 213.
(25) Dong, J. Q.; Smith, P. C. *Drug Metabolism and Disposition* **2009**, *37*, 2314.
(26) Carr Jr, H. J.; Knauer, Q. F. *New England Journal of Medicine* **1961**, *264*, 977.
(27) Halsey, J. P.; Cardoe, N. *British Medical Journal* **1982**, *284*, 1365.
(28) Baell, J. B.; Holloway, G. A. *Journal of Medicinal Chemistry* **2010**, *53*, 2719.
(29) Aggarwal, N.; Kaur, A.; Anand, K.; Kumar, H.; Wakode, S. *International Journal of Pharmaceutical Science and Research*, *2*, 1.
(30) Yeh, V.; Iyengar, R. In *Comprehensive Heterocyclic Chemistry III*; Ramsden, C. A., Scriven, E. F. V., Taylor, R. J. K., Eds.; Elsevier: Oxford, 2008, p 487.
(31) Demmer, C. S.; Bunch, L. *European Journal of Medicinal Chemistry* **2015**, *97*, 778.
(32) Myllymäki, M. J.; Koskinen, A. M. P. *Tetrahedron Letters* **2007**, *48*, 2295.
(33) Doise, M.; Dennin, F.; Blondeau, D.; Sliwa, H. *Tetrahedron Letters* **1990**, *31*, 1155.
(34) Xu, D.; Xu, X.; Liu, Z.; Sun, L.-P.; You, Q. *Synlett* **2009**, *2009*, 1172.
(35) Yalcin, I.; Sener, E.; Ozden, T.; Akin, A.; Yildiz, S. *Fabad Journal of Pharmaceutical Science* **1988**, *13*, 441.

(36) Reen, G. K.; Kumar, A.; Sharma, P. *Medicinal Chemistry Research* **2017**, *26*, 3336.
(37) Şener, E.; Yalçin, I. s.; Sungur, E. *Quantitative Structure-Activity Relationships* **1991**, *10*, 223.
(38) Ferrins, L.; Rahmani, R.; Sykes, M. L.; Jones, A. J.; Avery, V. M.; Teston, E.; Almohaywi, B.; Yin, J.; Smith, J.; Hyland, C.; White, K. L.; Ryan, E.; Campbell, M.; Charman, S. A.; Kaiser, M.; Baell, J. B. *European Journal of Medicinal Chemistry* **2013**, *66*, 450.
(39) Tatipaka, H. B.; Gillespie, J. R.; Chatterjee, A. K.; Norcross, N. R.; Hulverson, M. A.; Ranade, R. M.; Nagendar, P.; Creason, S. A.; McQueen, J.; Duster, N. A.; Nagle, A.; Supek, F.; Molteni, V.; Wenzler, T.; Brun, R.; Glynne, R.; Buckner, F. S.; Gelb, M. H. *Journal of Medicinal Chemistry* **2014**, *57*, 828.
(40) Clark, R. L.; Pessolano, A. A.; Witzel, B.; Lanza, T.; Shen, T. Y.; Van Arman, C. G.; Risley, E. A. *Journal of Medicinal Chemistry* **1978**, *21*, 1158.
(41) Bemis, J. E.; Vu, C. B.; Xie, R.; Nunes, J. J.; Ng, P. Y.; Disch, J. S.; Milne, J. C.; Carney, D. P.; Lynch, A. V.; Jin, L.; Smith, J. J.; Lavu, S.; Iffland, A.; Jirousek, M. R.; Perni, R. B. *Bioorganic and Medicinal Chemistry Letters* **2009**, *19*, 2350.
(42) Poirier, M. C.; Fullerton, N. F.; Smith, B. A.; Beland, F. A. *Carcinogenesis* **1995**, *16*, 2917.
(43) Tokiwa, H.; Ohnishi, Y. *Critical Reviews in Toxicology* **1986**, *17*, 23.
(44) Felton, J. S.; Knize, M. G.; Shen, N. H.; Lewis, P. R.; Andresen, B. D.; Happe, J.; Hatch, F. T. *Carcinogenesis* **1986**, *7*, 1081.
(45) Laser Reuterswärd, A.; Skog, K.; Jägerstad, M. *Food and Chemical Toxicology* **1987**, *25*, 747.
(46) Johansson, M. A.; Jagerstad, M. *Carcinogenesis* **1994**, *15*, 1511.
(47) Skog, K.; Augustsson, K.; Steineck, G.; Stenberg, M.; Jägerstad, M. *Food and Chemical Toxicology* **1997**, *35*, 555.
(48) Knize, M. G.; Felton, J. S. *Nutrition Reviews* **2005**, *63*, 158.
(49) Overvik, E.; Kleman, M.; Berg, I.; Gustafsson, J. A. *Carcinogenesis* **1989**, *10*, 2293.
(50) Salmon, C. P.; Knize, M. G.; Panteleakos, F. N.; Wu, R. W.; Nelson, D. O.; Felton, J. S. *Journal of the National Cancer Institute* **2000**, *92*, 1773.
(51) Sugimura, T.; Wakabayashi, K.; Nakagama, H.; Nagao, M. *Cancer Science* **2004**, *95*, 290.
(52) Schut, H. A.; Snyderwine, E. G. *Carcinogenesis* **1999**, *20*, 353.
(53) Ito, N.; Hasegawa, R.; Sano, M.; Tamano, S.; Esumi, H.; Takayama, S.; Sugimura, T. *Carcinogenesis* **1991**, *12*, 1503.
(54) Esumi, H.; Ohgaki, H.; Kohzen, E.; Takayama, S.; Sugimura, T. *Japanese Journal of Cancer Research : Gann* **1989**, *80*, 1176.
(55) Shirai, T.; Sano, M.; Tamano, S.; Takahashi, S.; Hirose, M.; Futakuchi, M.; Hasegawa, R.; Imaida, K.; Matsumoto, K.; Wakabayashi, K.; Sugimura, T.; Ito, N. *Cancer Research* **1997**, *57*, 195.
(56) Shirai, T.; Kato, K.; Futakuchi, M.; Takahashi, S.; Suzuki, S.; Imaida, K.; Asamoto, M. *Mutation Research* **2002**, *506-507*, 129.
(57) Sinha, R.; Chow, W. H.; Kulldorff, M.; Denobile, J.; Butler, J.; Garcia-Closas, M.; Weil, R.; Hoover, R. N.; Rothman, N. *Cancer Research* **1999**, *59*, 4320.
(58) Ward, M. H.; Sinha, R.; Heineman, E. F.; Rothman, N.; Markin, R.; Weisenburger, D. D.; Correa, P.; Zahm, S. H. *International Journal of Cancer* **1997**, *71*, 14.
(59) Sinha, R.; Kulldorff, M.; Curtin, J.; Brown, C. C.; Alavanja, M. C.; Swanson, C. A. *Cancer Causes and Control* **1998**, *9*, 621.
(60) Sinha, R.; Gustafson, D. R.; Kulldorff, M.; Wen, W. Q.; Cerhan, J. R.; Zheng, W. *Journal of the National Cancer Institute* **2000**, *92*, 1352.
(61) Cross, A. J.; Peters, U.; Kirsh, V. A.; Andriole, G. L.; Reding, D.; Hayes, R. B.; Sinha, R. *Cancer Research* **2005**, *65*, 11779.
(62) Helmus, D. S.; Thompson, C. L.; Zelenskiy, S.; Tucker, T. C.; Li, L. *Nutrition and Cancer* **2013**, *65*, 1141.

(63) Oba, S.; Shimizu, N.; Nagata, C.; Shimizu, H.; Kametani, M.; Takeyama, N.; Ohnuma, T.; Matsushita, S. *Cancer Letters* **2006**, *244*, 260.
(64) Butler, L. M.; Sinha, R.; Millikan, R. C.; Martin, C. F.; Newman, B.; Gammon, M. D.; Ammerman, A. S.; Sandler, R. S. *American Journal of Epidemiology* **2003**, *157*, 434.
(65) Kampman, E.; Slattery, M. L.; Bigler, J.; Leppert, M.; Samowitz, W.; Caan, B. J.; Potter, J. D. *Cancer Epidemiology, Biomarkers and Prevention* **1999**, *8*, 15.
(66) Norat, T.; Bingham, S.; Ferrari, P.; Slimani, N.; Jenab, M.; Mazuir, M.; Overvad, K.; Olsen, A.; Tjønneland, A.; Clavel, F.; Boutron-Ruault, M.-C.; Kesse, E.; Boeing, H.; Bergmann, M. M.; Nieters, A.; Linseisen, J.; Trichopoulou, A.; Trichopoulos, D.; Tountas, Y.; Berrino, F.; Palli, D.; Panico, S.; Tumino, R.; Vineis, P.; Bueno-de-Mesquita, H. B.; Peeters, P. H. M.; Engeset, D.; Lund, E.; Skeie, G.; Ardanaz, E.; González, C.; Navarro, C.; Quirós, J. R.; Sanchez, M.-J.; Berglund, G.; Mattisson, I.; Hallmans, G.; Palmqvist, R.; Day, N. E.; Khaw, K.-T.; Key, T. J.; San Joaquin, M.; Hémon, B.; Saracci, R.; Kaaks, R.; Riboli, E. *JNCI: Journal of the National Cancer Institute* **2005**, *97*, 906.
(67) Navarro, A.; Munoz, S. E.; Lantieri, M. J.; del Pilar Diaz, M.; Cristaldo, P. E.; de Fabro, S. P.; Eynard, A. R. *Nutrition* **2004**, *20*, 873.
(68) Barrett, J. H.; Smith, G.; Waxman, R.; Gooderham, N.; Lightfoot, T.; Garner, R. C.; Augustsson, K.; Wolf, C. R.; Bishop, D. T.; Forman, D. *Carcinogenesis* **2003**, *24*, 275.
(69) Le Marchand, L. c.; Hankin, J. H.; Pierce, L. M.; Sinha, R.; Nerurkar, P. V.; Franke, A. A.; Wilkens, L. R.; Kolonel, L. N.; Donlon, T.; Seifried, A.; Custer, L. J.; Lum-Jones, A.; Chang, W. *Mutation Research/Fundamental and Molecular Mechanisms of Mutagenesis* **2002**, *506-507*, 205.
(70) Nowell, S.; Coles, B.; Sinha, R.; MacLeod, S.; Luke Ratnasinghe, D.; Stotts, C.; Kadlubar, F. F.; Ambrosone, C. B.; Lang, N. P. *Mutation Research* **2002**, *506-507*, 175.
(71) Gnagnarella, P.; Caini, S.; Maisonneuve, P.; Gandini, S. *Nutrition and Cancer* **2018**, *70*, 1.
(72) Deneo-Pellegrini, H.; Ronco, A. L.; De Stefani, E. *Nutrition and Cancer* **2015**, *67*, 82.
(73) Guo, J.; Wei, W.; Zhan, L. *Breast Cancer Research and Treatment* **2015**, *151*, 191.
(74) Fu, Z.; Deming, S. L.; Fair, A. M.; Shrubsole, M. J.; Wujcik, D. M.; Shu, X. O.; Kelley, M.; Zheng, W. *Breast Cancer Research and Treatment* **2011**, *129*, 919.
(75) Taylor, E. F.; Burley, V. J.; Greenwood, D. C.; Cade, J. E. *British Journal Of Cancer* **2007**, *96*, 1139.
(76) Han, D. F.; Zhou, X.; Hu, M. B.; Wang, C. H.; Xie, W.; Tan, X. D.; Zheng, F.; Liu, F. *Toxicology Letters* **2004**, *150*, 167.
(77) Dai, Q.; Shu, X. O.; Jin, F.; Gao, Y. T.; Ruan, Z. X.; Zheng, W. *Cancer Epidemiology, Biomarkers and Prevention* **2002**, *11*, 801.
(78) Zheng, W.; Wen, W. Q.; Gustafson, D. R.; Gross, M.; Cerhan, J. R.; Folsom, A. R. *Breast Cancer Research and Treatment* **2002**, *74*, 9.
(79) Sinha, R.; Park, Y.; Graubard, B. I.; Leitzmann, M. F.; Hollenbeck, A.; Schatzkin, A.; Cross, A. J. *American Journal of Epidemiology* **2009**, *170*, 1165.
(80) Rohrmann, S.; Platz, E. A.; Kavanaugh, C. J.; Thuita, L.; Hoffman, S. C.; Helzlsouer, K. J. *Cancer Causes and Control* **2007**, *18*, 41.
(81) Nowell, S.; Ratnasinghe, D. L.; Ambrosone, C. B.; Williams, S.; Teague-Ross, T.; Trimble, L.; Runnels, G.; Carrol, A.; Green, B.; Stone, A.; Johnson, D.; Greene, G.; Kadlubar, F. F.; Lang, N. P. *Cancer Epidemiology, Biomarkers and Prevention* **2004**, *13*, 270.
(82) Michaud, D. S.; Augustsson, K.; Rimm, E. B.; Stampfer, M. J.; Willet, W. C.; Giovannucci, E. *Cancer Causes and Control* **2001**, *12*, 557.
(83) Norrish, A. E.; Ferguson, L. R.; Knize, M. G.; Felton, J. S.; Sharpe, S. J.; Jackson, R. T. *Journal of the National Cancer Institute* **1999**, *91*, 2038.
(84) Ferrucci, L. M.; Sinha, R.; Ward, M. H.; Graubard, B. I.; Hollenbeck, A. R.; Kilfoy, B. A.; Schatzkin, A.; Michaud, D. S.; Cross, A. J. *Cancer* **2010**, *116*, 4345.

(85) Larsson, S. C.; Johansson, J.-E.; Andersson, S.-O.; Wolk, A. *Cancer Causes and Control* **2009**, *20*, 35.
(86) Michaud, D. S.; Holick, C. N.; Giovannucci, E.; Stampfer, M. J. *The American Journal of Clinical Nutrition* **2006**, *84*, 1177.
(87) Balbi, J. C.; Larrinaga, M. T.; De Stefani, E.; Mendilaharsu, M.; Ronco, A. L.; Boffetta, P.; Brennan, P. *European Journal of Cancer Prevention* **2001**, *10*, 453.
(88) Larsson, S. C.; Bergkvist, L.; Wolk, A. *International journal of cancer* **2006**, *119*, 915.
(89) van den Brandt, P. A.; Botterweck, A. A. M.; Goldbohm, R. A. *Cancer Causes and Control* **2003**, *14*, 427.
(90) Tavani, A.; La Vecchia, C.; Gallus, S.; Lagiou, P.; Trichopoulos, D.; Levi, F.; Negri, E. *International Journal of Cancer* **2000**, *86*, 425.
(91) Anderson, K. E.; Sinha, R.; Kulldorff, M.; Gross, M.; Lang, N. P.; Barber, C.; Harnack, L.; DiMagno, E.; Bliss, R.; Kadlubar, F. F. *Mutation Research/Fundamental and Molecular Mechanisms of Mutagenesis* **2002**, *506-507*, 225.
(92) Boobis, A. R.; Gooderham, N. J.; Edwards, R. J.; Murray, S.; Lynch, A. M.; Yadollahi-Farsani, M.; Davies, D. S. *Archives of Toxicology* **1996**, *18*, 286.
(93) Turesky, R. J.; Constable, A.; Richoz, J.; Varga, N.; Markovic, J.; Martin, M. V.; Guengerich, F. P. *Chemical Research in Toxicology* **1998**, *11*, 925.
(94) Yamazoe, Y.; Shimada, M.; Kamataki, T.; Kato, R. *Cancer Research* **1983**, *43*, 5768.
(95) Shimada, T.; Guengerich, F. P. *Cancer Research* **1991**, *51*, 5284.
(96) Hammons, G. J.; Milton, D.; Stepps, K.; Guengerich, F. P.; Tukey, R. H.; Kadlubar, F. F. *Carcinogenesis* **1997**, *18*, 851.
(97) Crofts, F. G.; Sutter, T. R.; Strickland, P. T. *Carcinogenesis* **1998**, *19*, 1969.
(98) Gooderham, N. J.; Murray, S.; Lynch, A. M.; Yadollahi-Farsani, M.; Zhao, K.; Boobis, A. R.; Davies, D. S. *Drug Metabolism and Disposition* **2001**, *29*, 529.
(99) Lin, D. X.; Lang, N. P.; Kadlubar, F. F. *Drug metabolism and Disposition: The Biological Fate of Chemicals* **1995**, *23*, 518.
(100) Ozawa, S.; Chou, H. C.; Kadlubar, F. F.; Nagata, K.; Yamazoe, Y.; Kato, R. *Japanese Journal of Cancer Research : Gann* **1994**, *85*, 1220.
(101) Buonarati, M. H.; Turteltaub, K. W.; Shen, N. H.; Felton, J. S. *Mutation Research* **1990**, *245*, 185.
(102) Hein, D. W.; Doll, M. A.; Rustan, T. D.; Gray, K.; Feng, Y.; Ferguson, R. J.; Grant, D. M. *Carcinogenesis* **1993**, *14*, 1633.
(103) Minchin, R. F.; Reeves, P. T.; Teitel, C. H.; McManus, M. E.; Mojarrabi, B.; Ilett, K. F.; Kadlubar, F. F. *Biochemical and Biophysical Research Communications* **1992**, *185*, 839.
(104) Murata, M.; Kobayashi, M.; Kawanishi, S. *Japanese Journal of Cancer Research : Gann* **1999**, *90*, 268.
(105) Snyderwine, E. G.; Roller, P. P.; Adamson, R. H.; Sato, S.; Thorgeirsson, S. S. *Carcinogenesis* **1988**, *9*, 1061.
(106) Kadlubar, F. F.; Beland, F. A. In *Polycyclic Hydrocarbons and Carcinogenesis*; American Chemical Society: 1985; Vol. 283, p 341.
(107) Turesky, R. J.; Markovic, J. *Chemical Research in Toxicology* **1994**, *7*, 752.
(108) Turesky, R. J.; Rossi, S. C.; Welti, D. H.; Lay, J. O.; Kadlubar, F. F. *Chemical Research in Toxicology* **1992**, *5*, 479.
(109) Snyderwine, E. G.; Davis, C. D.; Nouso, K.; Roller, P. P.; Schut, H. A. *Carcinogenesis* **1993**, *14*, 1389.
(110) Tada, A.; Ochiai, M.; Wakabayashi, K.; Nukaya, H.; Sugimura, T.; Nagao, M. *Carcinogenesis* **1994**, *15*, 1275.
(111) Ochiai, M.; Nagaoka, H.; Wakabayashi, K.; Tanaka, Y.; Kim, S. B.; Tada, A.; Nukaya, H.; Sugimura, T.; Nagao, M. *Carcinogenesis* **1993**, *14*, 2165.
(112) Lin, D.; Kaderlik, K. R.; Turesky, R. J.; Miller, D. W.; Lay, J. O., Jr.; Kadlubar, F. F. *Chemical Research in Toxicology* **1992**, *5*, 691.
(113) Snyderwine, E. G.; Yu, M.; Schut, H. A. J.; Knight-Jones, L.; Kimura, S. *Food and Chemical Toxicology* **2002**, *40*, 1529.

(114) Davis, C. D.; Schut, H. A.; Adamson, R. H.; Thorgeirsson, U. P.; Thorgeirsson, S. S.; Snyderwine, E. G. *Carcinogenesis* **1993**, *14*, 61.
(115) Kaderlik, K. R.; Minchin, R. F.; Mulder, G. J.; Ilett, K. F.; Daugaard-Jenson, M.; Teitel, C. H.; Kadlubar, F. F. *Carcinogenesis* **1994**, *15*, 1703.
(116) Ghoshal, A.; Davis, C. D.; Schut, H. A.; Snyderwine, E. G. *Carcinogenesis* **1995**, *16*, 2725.
(117) Kadlubar, F.; Kaderlik, R. K.; Mulder, G. J.; Lin, D.; Butler, M. A.; Teitel, C. H.; Minchin, R. F.; Ilett, K. F.; Friesen, M. D.; Bartsch, H.; et al. *Princess Takamatsu Symposia* **1995**, *23*, 207.
(118) Malfatti, M. A.; Connors, M. S.; Mauthe, R. J.; Felton, J. S. *Cancer Research* **1996**, *56*, 2550.
(119) Snyderwine, E. G.; Davis, C. D.; Schut, H. A.; Roberts-Thomson, S. J. *Carcinogenesis* **1998**, *19*, 1209.
(120) Sadrieh, N.; Davis, C. D.; Snyderwine, E. G. *Cancer Research* **1996**, *56*, 2683.
(121) Williams, J. A.; Stone, E. M.; Fakis, G.; Johnson, N.; Cordell, J. A.; Meinl, W.; Glatt, H.; Sim, E.; Phillips, D. H. *Pharmacogenetics* **2001**, *11*, 373.
(122) Dubuisson, J. G.; Dyess, D. L.; Gaubatz, J. W. *Cancer Letters*, *182*, 27.
(123) Malfatti, M. A.; Shen, N. H.; Wu, R. W.; Turteltaub, K. W.; Felton, J. S. *Mutagenesis* **1995**, *10*, 425.
(124) Felton, J. S.; Knize, M. G.; Dolbeare, F. A.; Wu, R. *Environmental Health Perspectives* **1994**, *102*, 201.
(125) Fuscoe, J. C.; Wu, R.; Shen, N. H.; Healy, S. K.; Felton, J. S. *Mutation Research* **1988**, *201*, 241.
(126) Koch, W. H.; Wu, R. W.; Cebula, T. A.; Felton, J. S. *Environmental and Molecular Mutagenesis* **1998**, *31*, 327.
(127) Felton, J. S.; Knize, M. G. *Mutation Research* **1991**, *259*, 205.
(128) Buonarati, M. H.; Tucker, J. D.; Minkler, J. L.; Wu, R. W.; Thompson, L. H.; Felton, J. S. *Mutagenesis* **1991**, *6*, 253.
(129) Thompson, L. H.; Tucker, J. D.; Stewart, S. A.; Christensen, M. L.; Salazar, E. P.; Carrano, A. V.; Felton, J. S. *Mutagenesis* **1987**, *2*, 483.
(130) Shibutani, S.; Fernandes, A.; Suzuki, N.; Zhou, L.; Johnson, F.; Grollman, A. P. *Journal of Biological Chemistry* **1999**, *274*, 27433.
(131) Ushijima, T.; Hosoya, Y.; Ochiai, M.; Kushida, H.; Wakabayashi, K.; Suzuki, T.; Hayashi, M.; Sofuni, T.; Sugimura, T.; Nagao, M. *Carcinogenesis* **1994**, *15*, 2805.
(132) Breneman, J. W.; Briner, J. F.; Ramsey, M. J.; Director, A.; Tucker, J. D. *Food and Chemical Toxicology* **1996**, *34*, 717.
(133) Director, A. E.; Nath, J.; Ramsey, M. J.; Swiger, R. R.; Tucker, J. D. *Mutation Research* **1996**, *359*, 53.
(134) Tucker, J. D.; Carrano, A. V.; Allen, N. A.; Christensen, M. L.; Knize, M. G.; Strout, C. L.; Felton, J. S. *Mutation Research/Genetic Toxicology* **1989**, *224*, 105.
(135) Minkler, J. L.; Carrano, A. V. *Mutation Research* **1984**, *140*, 49.
(136) Suzuki, T.; Hayashi, M.; Ochiai, M.; Wakabayashi, K.; Ushijima, T.; Sugimura, T.; Nagao, M.; Sofuni, T. *Mutation Research* **1996**, *369*, 45.
(137) Ryu, D.-Y.; Pratt, V. S. W.; Davis, C. D.; Schut, H. A. J.; Snyderwine, E. G. *Cancer Research* **1999**, *59*, 2587.
(138) Okonogi, H.; Ushijima, T.; Zhang, X. B.; Heddle, J. A.; Suzuki, T.; Sofuni, T.; Felton, J. S.; Tucker, J. D.; Sugimura, T.; Nagao, M. *Carcinogenesis* **1997**, *18*, 745.
(139) Zhang, X. B.; Felton, J. S.; Tucker, J. D.; Urlando, C.; Heddle, J. A. *Carcinogenesis* **1996**, *17*, 2259.
(140) Lynch, A. M.; Gooderham, N. J.; Boobis, A. R. *Mutagenesis* **1996**, *11*, 505.
(141) Bird, R. P.; Bruce, W. R. *Nutrition and Cancer* **1986**, *8*, 93.
(142) Dolara, P.; Caderni, G.; Bianchini, F.; Tanganelli, E. *Mutation Research* **1986**, *175*, 255.
(143) Bird, R. P.; Bruce, W. R. *Journal of the National Cancer Institute* **1984**, *73*, 237.
(144) Knasmüller, S.; Kienzl, H.; Huber, W.; Hermann, R. S. *Mutagenesis* **1992**, *7*, 235.

(145) Zharkov, D. O. *Cellular and Molecular Life Sciences : CMLS* **2008**, *65*, 1544.
(146) Christmann, M.; Tomicic, M. T.; Roos, W. P.; Kaina, B. *Toxicology* **2003**, *193*, 3.
(147) Hitomi, K.; Iwai, S.; Tainer, J. A. *DNA Repair* **2007**, *6*, 410.
(148) Mol, C. D.; Izumi, T.; Mitra, S.; Tainer, J. A. *Nature* **2000**, *403*, 451.
(149) David, S. S.; O'Shea, V. L.; Kundu, S. *Nature* **2007**, *447*, 941.
(150) Abbotts, R.; Madhusudan, S. *Cancer Treatment Reviews* **2010**, *36*, 425.
(151) Dexheimer, T. S.; Springer: 2013, p 23.
(152) Almeida, K. H.; Sobol, R. W. *DNA Repair* **2007**, *6*, 695.
(153) Wong, D.; Demple, B. *The Journal of Biological Chemistry* **2004**, *279*, 25268.
(154) Sattler, U.; Frit, P.; Salles, B.; Calsou, P. *EMBO Reports* **2003**, *4*, 363.
(155) Fortini, P.; Dogliotti, E. *DNA repair* **2007**, *6*, 398.
(156) Prasad, R.; Lavrik, O. I.; Kim, S.-J.; Kedar, P.; Yang, X.-P.; Vande Berg, B. J.; Wilson, S. H. *Journal of Biological Chemistry* **2001**, *276*, 32411.
(157) Caldecott, K. W. *DNA repair* **2003**, *2*, 955.
(158) Marintchev, A.; Mullen, M. A.; Maciejewski, M. W.; Pan, B.; Gryk, M. R.; Mullen, G. P. *Nature Structural Biology* **1999**, *6*, 884.
(159) Malanga, M.; Althaus, F. R. *Biochemistry and Cell Biology = Biochimie et Biologie Cellulaire* **2005**, *83*, 354.
(160) Maynard, S.; Schurman, S. H.; Harboe, C.; de Souza-Pinto, N. C.; Bohr, V. A. *Carcinogenesis* **2009**, *30*, 2.
(161) Prise, K. M.; Pullar, C. H. L.; Michael, B. D. *Carcinogenesis* **1999**, *20*, 905.
(162) Milligan, J. R.; Aguilera, J. A.; Nguyen, T. T.; Paglinawan, R. A.; Ward, J. F. *International Journal of Radiation Biology* **2000**, *76*, 1475.
(163) Rydberg, B. *Radiation Research* **2000**, *153*, 805.
(164) Sutherland, B. M.; Bennett, P. V.; Sidorkina, O.; Laval, J. *Proceedings of the National Academy of Sciences* **2000**, *97*, 103.
(165) Blaisdell, J. O.; Harrison, L.; Wallace, S. S. *Radiation Protection Dosimetry* **2001**, *97*, 25.
(166) Yang, N.; Chaudhry, M. A.; Wallace, S. S. *DNA Repair* **2006**, *5*, 43.
(167) Cannan, W. J.; Tsang, B. P.; Wallace, S. S.; Pederson, D. S. *The Journal of Biological Chemistry* **2014**, *289*, 19881.
(168) Woodhouse, B. C.; Dianova, I. I.; Parsons, J. L.; Dianov, G. L. *DNA Repair* **2008**, *7*, 932.
(169) Lukas, J.; Bartek, J. *Nature* **2009**, *458*, 581.
(170) Groth, A.; Rocha, W.; Verreault, A.; Almouzni, G. *Cell* **2007**, *128*, 721.
(171) Fernandez-Capetillo, O.; Lee, A.; Nussenzweig, M.; Nussenzweig, A. *DNA Repair* **2004**, *3*, 959.
(172) Rogakou, E. P.; Pilch, D. R.; Orr, A. H.; Ivanova, V. S.; Bonner, W. M. *The Journal of Biological Chemistry* **1998**, *273*, 5858.
(173) Dickey, J. S.; Redon, C. E.; Nakamura, A. J.; Baird, B. J.; Sedelnikova, O. A.; Bonner, W. M. *Chromosoma* **2009**, *118*, 683.
(174) Xiao, A.; Li, H.; Shechter, D.; Ahn, S. H.; Fabrizio, L. A.; Erdjument-Bromage, H.; Ishibe-Murakami, S.; Wang, B.; Tempst, P.; Hofmann, K.; Patel, D. J.; Elledge, S. J.; Allis, C. D. *Nature* **2009**, *457*, 57.
(175) Cook, P. J.; Ju, B. G.; Telese, F.; Wang, X.; Glass, C. K.; Rosenfeld, M. G. *Nature* **2009**, *458*, 591.
(176) Ivashkevich, A.; Redon, C. E.; Nakamura, A. J.; Martin, R. F.; Martin, O. A. *Cancer Letters* **2012**, *327*, 123.
(177) Mao, Z.; Bozzella, M.; Seluanov, A.; Gorbunova, V. *DNA Repair* **2008**, *7*, 1765.
(178) Mariotti, L. G.; Pirovano, G.; Savage, K. I.; Ghita, M.; Ottolenghi, A.; Prise, K. M.; Schettino, G. *PLoS One* **2013**, *8*, e79541.
(179) Markova, E.; Schultz, N.; Belyaev, I. Y. *International Journal of Radiation Biology* **2007**, *83*, 319.
(180) Redon, C. E.; Dickey, J. S.; Bonner, W. M.; Sedelnikova, O. A. *Advances in Space Research* **2009**, *43*, 1171.

(181) Heitzer, E.; Tomlinson, I. *Current Opinion in Genetics and Development* **2014**, *24*, 107.
(182) Gao, Y.; Mutter-Rottmayer, E.; Zlatanou, A.; Vaziri, C.; Yang, Y. *Genes* **2017**, *8*, 64.
(183) Sale, J. E.; Lehmann, A. R.; Woodgate, R. *Nature Reviews Molecular Cell Biology* **2012**, *13*, 141.
(184) da Costa, L. T.; Liu, B.; el-Deiry, W.; Hamilton, S. R.; Kinzler, K. W.; Vogelstein, B.; Markowitz, S.; Willson, J. K.; de la Chapelle, A.; Downey, K. M.; et al. *Nature Genetics* **1995**, *9*, 10.
(185) Makridakis, N. M.; Reichardt, J. K. V. *Frontiers in Genetics* **2012**, *3*, 174.
(186) Schuetz, J. M.; Johnson, N. A.; Morin, R. D.; Scott, D. W.; Tan, K.; Ben-Nierah, S.; Boyle, M.; Slack, G. W.; Marra, M. A.; Connors, J. M.; Brooks-Wilson, A. R.; Gascoyne, R. D. *Leukemia* **2012**, *26*, 1383.
(187) Burkhard, R.; Bhagat, G.; Cogliatti, S. B.; Rossi, D.; Gaidano, G.; Pasqualucci, L.; Novak, U. *Hematological Oncology* **2015**, *33*, 23.
(188) Chaudhary, K. S.; Abel, P. D.; Lalani, E. N. *Environmental Health Perspectives* **1999**, *107*, 49.
(189) Martinez-Arribas, F.; Alvarez, T.; Del Val, G.; Martin-Garabato, E.; Nunez-Villar, M. J.; Lucas, R.; Sanchez, J.; Tejerina, A.; Schneider, J. *Anticancer Research* **2007**, *27*, 219.
(190) Ilyas, M.; Tomlinson, I. P.; Hanby, A. M.; Yao, T.; Bodmer, W. F.; Talbot, I. C. *The American Journal of Pathology* **1996**, *149*, 1719.
(191) Tsujimoto, Y.; Croce, C. M. *Proceedings of the National Academy of Sciences of the United States of America* **1986**, *83*, 5214.
(192) Tsujimoto, Y.; Ikegaki, N.; Croce, C. M. *Oncogene* **1987**, *2*, 3.
(193) Kirkin, V.; Joos, S.; Zörnig, M. *Biochimica et Biophysica Acta (BBA) - Molecular Cell Research* **2004**, *1644*, 229.
(194) Weinstein, I. B.; Joe, A. K. *Nature Clinical Practice. Oncology* **2006**, *3*, 448.
(195) Prior, I. A.; Lewis, P. D.; Mattos, C. *Cancer Research* **2012**, *72*, 2457.
(196) Saranath, D.; Chang, S. E.; Bhoite, L. T.; Panchal, R. G.; Kerr, I. B.; Mehta, A. R.; Johnson, N. W.; Deo, M. G. *British Journal of Cancer* **1991**, *63*, 573.
(197) Barletta, E.; Gorini, G.; Vineis, P.; Miligi, L.; Davico, L.; Mugnai, G.; Ciolli, S.; Leoni, F.; Bertini, M.; Matullo, G. *Carcinogenesis* **2004**, *25*, 749.
(198) Zeitouni, D.; Pylayeva-Gupta, Y.; Der, C. J.; Bryant, K. L. *Cancers* **2016**, *8*, 1.
(199) Santoro, M.; Carlomagno, F. *Cold Spring Harbor Perspectives in Biology* **2013**, *5*, 1.
(200) Chen, J.; Elfiky, A.; Han, M.; Chen, C.; Saif, M. W. *Clinical Colorectal Cancer* **2014**, *13*, 5.
(201) Aligayer, H.; Boyd, D. D.; Heiss, M. M.; Abdalla, E. K.; Curley, S. A.; Gallick, G. E. *Cancer* **2002**, *94*, 344.
(202) Ascierto, P. A.; Kirkwood, J. M.; Grob, J.-J.; Simeone, E.; Grimaldi, A. M.; Maio, M.; Palmieri, G.; Testori, A.; Marincola, F. M.; Mozzillo, N. *Journal of Translational Medicine* **2012**, *10*, 85.
(203) Tol, J.; Nagtegaal, I. D.; Punt, C. J. *New England Journal of Medicine* **2009**, *361*, 98.
(204) Cohen, Y.; Xing, M.; Mambo, E.; Guo, Z.; Wu, G.; Trink, B.; Beller, U.; Westra, W. H.; Ladenson, P. W.; Sidransky, D. *JNCI: Journal of the National Cancer Institute* **2003**, *95*, 625.
(205) Velez, A. M. A.; Howard, M. S. *North American Journal of Medical Sciences* **2015**, *7*, 176.
(206) Lee, J. M.; Bernstein, A. *Cancer Metastasis Reviews* **1995**, *14*, 149.
(207) Kopnin, B. *Biochemistry, Biokhimiia* **2000**, *65*, 2.
(208) Weinberg, R. A. *Annals of the New York Academy of Sciences* **1995**, *758*, 331.
(209) Valiathan, C.; McFaline, J. L. *DNA repair* **2012**, *11*, 92.
(210) Franken, N. A.; Rodermond, H. M.; Stap, J.; Haveman, J.; van Bree, C. *Nature Protocols* **2006**, *1*, 2315.
(211) Munshi, A.; Hobbs, M.; Meyn, R. E. *Methods in Molecular Medicine* **2005**, *110*, 21.

(212) Bunel, V.; Ouedraogo, M.; Nguyen, A. T.; Stevigny, C.; Duez, P. *Planta Medica* **2014**, *80*, 1210.
(213) Quto b, S. S.; Ng, C. E. *Cancer Chemotherapy and Pharmacology* **2002**, *49*, 167.
(214) Taupin, P. *Brain Research Reviews* **2007**, *53*, 198.
(215) Zhi-Jun, Y.; Sriranganathan, N.; Vaught, T.; Arastu, S. K.; Ahmed, S. A. *Journal of Immunological Methods* **1997**, *210*, 25.
(216) Berridge, M. V.; Tan, A. S. *Archives of Biochemistry and Biophysics* **1993**, *303*, 474.
(217) Mosmann, T. *Journal of Immunological Methods* **1983**, *65*, 55.
(218) Wisman, K. N.; Perkins, A. A.; Jeffers, M. D.; Hagerman, A. E. *Journal of Agricultural and Food Chemistry* **2008**, *56*, 7831.
(219) Bruggisser, R.; von Daeniken, K.; Jundt, G.; Schaffner, W.; Tullberg-Reinert, H. *Planta Medica* **2002**, *68*, 445.
(220) Shoemaker, M.; Cohen, I.; Campbell, M. *Journal of Ethnopharmacology* **2004**, *93*, 381.
(221) Naoi, T.; Shibuya, N.; Inoue, H.; Mita, S.; Kobayashi, S.; Watanabe, K.; Orino, K. *The Journal of Veterinary Medical Science* **2010**, *72*, 321.
(222) Pagliacci, M. C.; Spinozzi, F.; Migliorati, G.; Fumi, G.; Smacchia, M.; Grignani, F.; Riccardi, C.; Nicoletti, I. *European Journal of Cancer Prevention* **1993**, *29a*, 1573.
(223) Crouch, S. P. M.; Kozlowski, R.; Slater, K. J.; Fletcher, J. *Journal of Immunological Methods* **1993**, *160*, 81.
(224) Squatrito, R. C.; Connor, J. P.; Buller, R. E. *Gynecologic Oncology* **1995**, *58*, 101.
(225) Leitao, J. M.; Esteves da Silva, J. C. *Journal of Photochemistry and Photobiology B: Biology* **2010**, *101*, 1.
(226) Shimomura, Y.; Kawada, T.; Suzuki, M. *Archives of Biochemistry and Biophysics* **1989**, *270*, 573.
(227) Gledhill, J. R.; Montgomery, M. G.; Leslie, A. G.; Walker, J. E. *Proceedings of the National Academy of Sciences of the United States of America* **2007**, *104*, 13632.
(228) Korzeniewski, C.; Callewaert, D. M. *Journal of Immunological Methods* **1983**, *64*, 313.
(229) Abe, K.; Matsuki, N. *Neuroscience Research* **2000**, *38*, 325.
(230) Weyermann, J.; Lochmann, D.; Zimmer, A. *International Journal of Pharmaceutics* **2005**, *288*, 369.
(231) Böttger, S.; Hofmann, K.; Melzig, M. F. *Bioorganic and Medicinal Chemistry* **2012**, *20*, 2822.
(232) Strober, W. *Current Protocols in Immunology* **2001**, *21*, Appendix 3B.
(233) Grankvist, K.; Lernmark, A.; Täljedal, I. B. *Biochemical Journal* **1977**, *162*, 19.
(234) Cantoni, O.; Sestili, P.; Guidarelli, A.; Palomba, L.; Brambilla, L.; Cattabeni, F. *Archives of Toxicology* **1996**, *18*, 223.
(235) Roberts, J. J. In *Advances in Radiation Biology*; Lett, J. T., Adler, H., Eds.; Elsevier: 1978; Vol. 7, p 211.
(236) Wang, D.; Kreutzer, D. A.; Essigmann, J. M. *Mutation Research/Fundamental and Molecular Mechanisms of Mutagenesis* **1998**, *400*, 99.
(237) Garcia-Canton, C.; Anadon, A.; Meredith, C. *Mutation Research/Genetic Toxicology and Environmental Mutagenesis* **2013**, *757*, 158.
(238) USFDA 2012.
(239) COM 2011.
(240) ICH 2011.
(241) Ames, B. N. In *Chemical Mutagens*; Springer: 1971; Vol. 1, p 267.
(242) Chu, K. C.; Patel, K. M.; Lin, A. H.; Tarone, R. E.; Linhart, M. S.; Dunkel, V. C. *Mutation Research* **1981**, *85*, 119.
(243) Zeiger, E.; Risko, K. J.; Margolin, B. H. *Environmental Mutagenesis* **1985**, *7*, 901.
(244) Tejs, S. *Environmental Biotechnology* **2008**, *4*, 7.
(245) Fenech, M. *Mutation Research* **2000**, *455*, 81.
(246) Kirsch-Volders, M.; Sofuni, T.; Aardema, M.; Albertini, S.; Eastmond, D.; Fenech, M.; Ishidate, M., Jr.; Kirchner, S.; Lorge, E.; Morita, T.; Norppa, H.; Surralles, J.; Vanhauwaert, A.; Wakata, A. *Mutation Research* **2003**, *540*, 153.

(247) Garriott, M. L.; Barry Phelps, J.; Hoffman, W. P. *Mutation Research/Genetic Toxicology and Environmental Mutagenesis* **2002**, *517*, 123.
(248) Chung, H. W.; Kang, S. J.; Kim, S. Y. *Mutation Research* **2002**, *516*, 49.
(249) Müller, L.; Kikuchi, Y.; Probst, G.; Schechtman, L.; Shimada, H.; Sofuni, T.; Tweats, D. *Mutation Research/Reviews in Mutation Research* **1999**, *436*, 195.
(250) Ishidate, M.; Yoshikawa, K.; Springer Berlin Heidelberg: Berlin, Heidelberg, 1980, p 41.
(251) Galloway, S. M.; Armstrong, M. J.; Reuben, C.; Colman, S.; Brown, B.; Cannon, C.; Bloom, A. D.; Nakamura, F.; Ahmed, M.; Duk, S.; Rimpo, J.; Margolin, B. H.; Resnick, M. A.; Anderson, B.; Zeiger, E. *Environmental and Molecular Mutagenesis* **1987**, *10*, 1.
(252) OECD, O. f. E. C.-o. a. D. *Test No. 473: In vitro Mammalian Chromosome Aberration Test*; OECD Publishing.
(253) Ishidate, M.; Miura, K. F.; Sofuni, T. *Mutation Research/Fundamental and Molecular Mechanisms of Mutagenesis* **1998**, *404*, 167.
(254) Lloyd, M.; Kidd, D. In *Genetic Toxicology: Principles and Methods*; Parry, J. M., Parry, E. M., Eds.; Springer New York: New York, NY, 2012, p 35.
(255) Clements, J. *Mutation Research/Fundamental and Molecular Mechanisms of Mutagenesis* **2000**, *455*, 97.
(256) Moore-Brown, M. M.; Clive, D.; Howard, B. E.; Batson, A. G.; Johnson, K. O. *Mutation Research/Environmental Mutagenesis and Related Subjects* **1981**, *85*, 363.
(257) Ramel, C. *Environmental Health Perspectives* **1983**, *47*, 153.
(258) Maron, D. M.; Ames, B. N. *Mutation Research* **1983**, *113*, 173.
(259) Katsuno, K.; Burrows, J. N.; Duncan, K.; Hooft van Huijsduijnen, R.; Kaneko, T.; Kita, K.; Mowbray, C. E.; Schmatz, D.; Warner, P.; Slingsby, B. T. *Nature Reviews Drug Discovery* **2015**, *14*, 751.
(260) Guengerich, F. P.; Shimada, T. *Chemical Research in Toxicology* **1991**, *4*, 391.
(261) Elliott, B. M.; Combes, R. D.; Elcombe, C. R.; Gatehouse, D. G.; Gibson, G. G.; Mackay, J. M.; Wolf, R. C. *Mutagenesis* **1992**, *7*, 175.
(262) Hakura, A.; Shimada, H.; Nakajima, M.; Sui, H.; Kitamoto, S.; Suzuki, S.; Satoh, T. *Mutagenesis* **2005**, *20*, 217.
(263) Hakura, A.; Suzuki, S.; Satoh, T. *Mutation Research* **1999**, *438*, 29.
(264) Attia, S. M. *Oxidative Medicine and Cellular Longevity* **2010**, *3*, 238.
(265) Mortelmans, K.; Zeiger, E. *Mutation Research* **2000**, *455*, 29.
(266) Johnson, T. E.; Umbenhauer, D. R.; Galloway, S. M. *Environmental and Molecular Mutagenesis* **1996**, *28*, 51.
(267) Beaune, P.; Lemestré-Cornet, R.; Kremers, P.; Albert, A.; Gielen, J. *Mutation Research/Genetic Toxicology* **1985**, *156*, 139.
(268) Tsamou, M.; Jennen, D. G. J.; Claessen, S. M. H.; Magkoufopoulou, C.; Kleinjans, J. C. S.; van Delft, J. H. M. *Mutagenesis* **2012**, *27*, 645.
(269) Hégarat, L. L.; Mourot, A.; Huet, S.; Vasseur, L.; Camus, S.; Chesné, C.; Fessard, V. *Toxicological Sciences* **2014**, *138*, 300.
(270) Vasquez, M. Z. *Mutation Research/Genetic Toxicology and Environmental Mutagenesis* **2012**, *747*, 142.
(271) Speit, G.; Hartmann, A. *Methods in Molecular Biology* **2006**, *314*, 275.
(272) Smart, D.; Ahmedi, K.; Harvey, J.; Lynch, A. *Mutation Research/Fundamental and Molecular Mechanisms of Mutagenesis* **2011**, *715*, 25.
(273) Azqueta, A.; Arbillaga, L.; López de Cerain, A.; Collins, A. *Mutagenesis* **2013**, *28*, 271.
(274) Borowicz, S.; Van Scoyk, M.; Avasarala, S.; Karuppusamy Rathinam, M. K.; Tauler, J.; Bikkavilli, R. K.; Winn, R. A. *Journal of Visualized Experiments : JoVE* **2014**, 51998.
(275) Figueroa-González, G.; Pérez-Plasencia, C. *Oncology Letters* **2017**, *13*, 3982.
(276) Sedelnikova, O. A.; Rogakou, E. P.; Panyutin, I. G.; Bonner, W. M. *Radiation Research* **2002**, *158*, 486.

(277) Verschaeve, L.; Juutilainen, J.; Lagroye, I.; Miyakoshi, J.; Saunders, R.; de Seze, R.; Tenforde, T.; van Rongen, E.; Veyret, B.; Xu, Z. *Mutation Research* **2010**, *705*, 252.
(278) Rogakou, E. P.; Boon, C.; Redon, C.; Bonner, W. M. *The Journal of Cell Biology* **1999**, *146*, 905.
(279) Krum, S. A.; Dalugdugan, E. d. l. R.; Miranda-Carboni, G. A.; Lane, T. F. *Journal of Nucleic Acids* **2010**, *2010*, 1.
(280) Minter-Dykhouse, K.; Ward, I.; Huen, M. S.; Chen, J.; Lou, Z. *The Journal of Cell Biology* **2008**, *181*, 727.
(281) Stewart, G. S.; Wang, B.; Bignell, C. R.; Taylor, A. M.; Elledge, S. J. *Nature* **2003**, *421*, 961.
(282) Kobayashi, J.; Antoccia, A.; Tauchi, H.; Matsuura, S.; Komatsu, K. *DNA Repair* **2004**, *3*, 855.
(283) Ward, I. M.; Minn, K.; Jorda, K. G.; Chen, J. *The Journal of Biological Chemistry* **2003**, *278*, 19579.
(284) Sharma, A.; Singh, K.; Almasan, A. In *DNA Repair Protocols*; Bjergbæk, L., Ed.; Humana Press: Totowa, NJ, 2012, p 613.
(285) Nelson, G.; Buhmann, M.; von Zglinicki, T. *Cell cycle (Georgetown, Tex.)* **2009**, *8*, 3379.
(286) Nakamura, A. J.; Rao, V. A.; Pommier, Y.; Bonner, W. M. *Cell cycle (Georgetown, Tex.)* **2010**, *9*, 389.
(287) Giunta, S.; Belotserkovskaya, R.; Jackson, S. P. *The Journal of Cell Biology* **2010**, *190*, 197.
(288) Kirkland, D.; Pfuhler, S.; Tweats, D.; Aardema, M.; Corvi, R.; Darroudi, F.; Elhajouji, A.; Glatt, H.; Hastwell, P.; Hayashi, M.; Kasper, P.; Kirchner, S.; Lynch, A.; Marzin, D.; Maurici, D.; Meunier, J. R.; Muller, L.; Nohynek, G.; Parry, J.; Parry, E.; Thybaud, V.; Tice, R.; van Benthem, J.; Vanparys, P.; White, P. *Mutation Research* **2007**, *628*, 31.
(289) Fowler, P.; Smith, K.; Young, J.; Jeffrey, L.; Kirkland, D.; Pfuhler, S.; Carmichael, P. *Mutation Research* **2012**, *742*, 11.
(290) Collins, A. R. *Molecular Biotechnology* **2004**, *26*, 249.
(291) Fairbairn, D. W.; Olive, P. L.; O'Neill, K. L. *Mutation Research* **1995**, *339*, 37.
(292) Calini, V.; Urani, C.; Camatini, M. *Cell Biology and Toxicology* **2002**, *18*, 369.
(293) Wojewodzka, M.; Buraczewska, I.; Kruszewski, M. *Mutation Research* **2002**, *518*, 9.
(294) Singh, N. P.; McCoy, M. T.; Tice, R. R.; Schneider, E. L. *Experimental Cell Research* **1988**, *175*, 184.
(295) Gedik, C. M.; Ewen, S. W.; Collins, A. R. *International Journal of Radiation Biology* **1992**, *62*, 313.
(296) Olive, P. L. *International Journal of Radiation Biology* **1999**, *75*, 395.
(297) Gyori, B. M.; Venkatachalam, G.; Thiagarajan, P. S.; Hsu, D.; Clement, M.-V. *Redox Biology* **2014**, *2*, 457.
(298) Collins, A. R.; Oscoz, A. A.; Brunborg, G.; Gaivão, I.; Giovannelli, L.; Kruszewski, M.; Smith, C. C.; Štětina, R. *Mutagenesis* **2008**, *23*, 143.
(299) Morley, N.; Rapp, A.; Dittmar, H.; Salter, L.; Gould, D.; Greulich, K.; Curnow, A. *Mutagenesis* **2006**, *21*, 105.
(300) Taddei, M. L.; Giannoni, E.; Fiaschi, T.; Chiarugi, P. *The Journal of Pathology* **2012**, *226*, 380.
(301) Horibata, S.; Vo, T. V.; Subramanian, V.; Thompson, P. R.; Coonrod, S. A. *Journal of Visualized Experiments : JoVE* **2015**, 52727.
(302) Tekiner-Gulbas, B.; Temiz-Arpaci, O.; Oksuzoglu, E.; Eroglu, H.; Yildiz, I.; Diril, N.; Aki-Sener, E.; Yalcin, I. *SAR and QSAR in Environmental Research* **2007**, *18*, 251.
(303) Oksuzoglu, E.; Temiz-Arpaci, O.; Tekiner-Gulbas, B.; Eroglu, H.; Sen, G.; Alper, S.; Yildiz, I.; Diril, N.; Aki-Sener, E.; Yalcin, I. *Medicinal Chemistry Research* **2008**, *16*, 1.
(304) Oksuzoglu, E.; Foto, E.; Zilifdar, F.; Ertan-Bolelli, T.; Bolelli, K. *Latin American Journal of Pharmacy* **2016**, *35*, 2216.

(305) Still, W. C.; Kahn, M.; Mitra, A. *The Journal of Organic Chemistry* **1978**, *43*, 2923.
(306) Fulmer, G. R.; Miller, A. J. M.; Sherden, N. H.; Gottlieb, H. E.; Nudelman, A.; Stoltz, B. M.; Bercaw, J. E.; Goldberg, K. I. *Organometallics* **2010**, *29*, 2176.
(307) Lukáš, P.; Gervais, C. *Journal of Applied Crystallography* **2007**, *40*, 786.
(308) Sheldrick, G. M. *Acta Crystallographica. Section C, Structural Chemistry* **2015**, *71*, 3.
(309) V., D. O.; J., B. L.; J., G. R.; K., H. J. A.; Horst, P. *Journal of Applied Crystallography* **2009**, *42*, 339.
(310) Phoon, C. W.; Ng, P. Y.; Ting, A. E.; Yeo, S. L.; Sim, M. M. *Bioorganic and Medicinal Chemistry Letters* **2001**, *11*, 1647.
(311) Deau, E.; Robin, E.; Voinea, R.; Percina, N.; Satala, G.; Finaru, A. L.; Chartier, A.; Tamagnan, G.; Alagille, D.; Bojarski, A. J.; Morisset-Lopez, S.; Suzenet, F.; Guillaumet, G. *Journal of Medicinal Chemistry* **2015**, *58*, 8066.
(312) Yu, C.; Guo, X.; Xi, Z.; Muzzio, M.; Yin, Z.; Shen, B.; Li, J.; Seto, C. T.; Sun, S. *Journal of the American Chemical Society* **2017**, *139*, 5712.
(313) Kumar, P.; Bhatia, R.; Kumar, D.; Kamboj, R. C.; Kumar, S.; Kamal, R.; Kumar, R. *Research on Chemical Intermediates* **2015**, *41*, 4283.
(314) Abdullaev, F. I.; Riverón-Negrete, L.; Caballero-Ortega, H.; Manuel Hernández, J.; Pérez-López, I.; Pereda-Miranda, R.; Espinosa-Aguirre, J. J. *Toxicology in Vitro* **2003**, *17*, 731.
(315) Becherel, O. J.; Gueven, N.; Birrell, G. W.; Schreiber, V.; Suraweera, A.; Jakob, B.; Taucher-Scholz, G.; Lavin, M. F. *Human Molecular Genetics* **2006**, *15*, 2239.
(316) Benhusein, G. M.; Mutch, E.; Aburawi, S.; Williams, F. M. *The Libyan Journal of Medicine* **2010**, *5*, 1.
(317) Davis, B. D.; Mingioli, E. S. *Journal of Bacteriology* **1950**, *60*, 17.
(318) Buonarati, M. H.; Felton, J. S. *Carcinogenesis* **1990**, *11*, 1133.
(319) Frisch, M. J.; Trucks, G. W.; Schlegel, H. B.; Scuseria, G. E.; Robb, M. A.; Cheeseman, J. R.; Scalmani, G.; Barone, V.; Petersson, G. A.; Nakatsuji, H.; Li, X.; Caricato, M.; Marenich, A. V.; Bloino, J.; Janesko, B. G.; Gomperts, R.; Mennucci, B.; Hratchian, H. P.; Ortiz, J. V.; Izmaylov, A. F.; Sonnenberg, J. L.; Williams; Ding, F.; Lipparini, F.; Egidi, F.; Goings, J.; Peng, B.; Petrone, A.; Henderson, T.; Ranasinghe, D.; Zakrzewski, V. G.; Gao, J.; Rega, N.; Zheng, G.; Liang, W.; Hada, M.; Ehara, M.; Toyota, K.; Fukuda, R.; Hasegawa, J.; Ishida, M.; Nakajima, T.; Honda, Y.; Kitao, O.; Nakai, H.; Vreven, T.; Throssell, K.; Montgomery Jr., J. A.; Peralta, J. E.; Ogliaro, F.; Bearpark, M. J.; Heyd, J. J.; Brothers, E. N.; Kudin, K. N.; Staroverov, V. N.; Keith, T. A.; Kobayashi, R.; Normand, J.; Raghavachari, K.; Rendell, A. P.; Burant, J. C.; Iyengar, S. S.; Tomasi, J.; Cossi, M.; Millam, J. M.; Klene, M.; Adamo, C.; Cammi, R.; Ochterski, J. W.; Martin, R. L.; Morokuma, K.; Farkas, O.; Foresman, J. B.; Fox, D. J. Wallingford, CT, 2016.
(320) Miehlich, B.; Savin, A.; Stoll, H.; Preuss, H. *Chemical Physics Letters* **1989**, *157*, 200.
(321) Lee, C.; Yang, W.; Parr, R. G. *Physical Review B* **1988**, *37*, 785.
(322) Becke, A. D. *The Journal of Chemical Physics* **1993**, *98*, 5648.
(323) Barone, V.; Cossi, M. *The Journal of Physical Chemistry A* **1998**, *102*, 1995.
(324) Fukui, K. *The Journal of Physical Chemistry* **1970**, *74*, 4161.
(325) Zhao, Y.; Truhlar, D. G. *Theoretical Chemistry Accounts* **2008**, *120*, 215.
(326) Terada, T.; Hira, D. *Journal of Gastroenterology* **2015**, *50*, 508.
(327) Xu, C.; Li, C. Y.-T.; Kong, A.-N. T. *Archives of Pharmacal Research* **2005**, *28*, 249.
(328) Fan, L.; Schut, H. A.; Snyderwine, E. G. *Carcinogenesis* **1995**, *16*, 775.
(329) Hong, Y.-J.; Yang, S.-Y.; Nam, M.-H.; Koo, Y.-c.; Lee, K.-W. *Biological and Pharmaceutical Bulletin* **2015**, *38*, 201.
(330) Galetin, A.; Houston, J. B. *The Journal of Pharmacology and Experimental Therapeutics* **2006**, *318*, 1220.
(331) Paine, M. F.; Hart, H. L.; Ludington, S. S.; Haining, R. L.; Rettie, A. E.; Zeldin, D. C. *Drug Metabolism and Disposition: The Biological Fate of Chemicals* **2006**, *34*, 880.
(332) Wang, J. Y. J. *Cell Death And Differentiation* **2001**, *8*, 1047.

(333) Hughes, J. P.; Rees, S.; Kalindjian, S. B.; Philpott, K. L. *British Journal of Pharmacology* **2011**, *162*, 1239.
(334) Thorne, N.; Auld, D. S.; Inglese, J. *Current Opinion in Chemical Biology* **2010**, *14*, 315.
(335) Kohen, R.; Nyska, A. *Toxicologic Pathology* **2002**, *30*, 620.
(336) Lennicke, C.; Rahn, J.; Lichtenfels, R.; Wessjohann, L. A.; Seliger, B. *Cell Communication and Signaling : CCS* **2015**, *13*, 39.
(337) Ramos, S.; Alia, M.; Bravo, L.; Goya, L. *Journal of Agricultural and Food Chemistry* **2005**, *53*, 1271.
(338) Inglese, J.; Auld, D. S.; Jadhav, A.; Johnson, R. L.; Simeonov, A.; Yasgar, A.; Zheng, W.; Austin, C. P. *Proceedings of the National Academy of Sciences of the United States of America* **2006**, *103*, 11473.
(339) Kinner, A.; Wu, W.; Staudt, C.; Iliakis, G. *Nucleic Acids Research* **2008**, *36*, 5678.
(340) Scully, R.; Xie, A. *Mutation Research* **2013**, *750*, 5.
(341) Stiff, T.; O'Driscoll, M.; Rief, N.; Iwabuchi, K.; Lobrich, M.; Jeggo, P. A. *Cancer Research* **2004**, *64*, 2390.
(342) Driessens, N.; Versteyhe, S.; Ghaddhab, C.; Burniat, A.; De Deken, X.; Van Sande, J.; Dumont, J. E.; Miot, F.; Corvilain, B. *Endocrine-related Cancer* **2009**, *16*, 845.
(343) McDonald, R. J.; Pan, L. C.; St George, J. A.; Hyde, D. M.; Ducore, J. M. *Inflammation* **1993**, *17*, 715.
(344) Jamin, E. L.; Riu, A.; Douki, T.; Debrauwer, L.; Cravedi, J.-P.; Zalko, D.; Audebert, M. *PLoS One* **2013**, *8*, e58591.
(345) Sugimura, T.; Wakabayashi, K.; Nakagama, H.; Nagao, M. *Cancer science* **2004**, *95*, 290.
(346) Lobrich, M.; Shibata, A.; Beucher, A.; Fisher, A.; Ensminger, M.; Goodarzi, A. A.; Barton, O.; Jeggo, P. A. *Cell cycle (Georgetown, Tex.)* **2010**, *9*, 662.
(347) Mimmler, M.; Peter, S.; Kraus, A.; Stroh, S.; Nikolova, T.; Seiwert, N.; Hasselwander, S.; Neitzel, C.; Haub, J.; Monien, B. H.; Nicken, P.; Steinberg, P.; Shay, J. W.; Kaina, B.; Fahrer, J. *Nucleic Acids Research* **2016**, *44*, 10259.
(348) Sina, J. F.; Bean, C. L.; Dysart, G. R.; Taylor, V. I.; Bradley, M. O. *Mutation Research/Environmental Mutagenesis and Related Subjects* **1983**, *113*, 357.
(349) Roberts, J. J.; Basham, C. *Mutation Research/Fundamental and Molecular Mechanisms of Mutagenesis* **1990**, *233*, 253.
(350) Borges, H. L.; Linden, R.; Wang, J. Y. J. *Cell Research* **2008**, *18*, 17.
(351) Hegde, M. L.; Izumi, T.; Mitra, S. *Progress in Molecular Biology and Translational Science* **2012**, *110*, 123.
(352) Pfau, W.; Martin, F. L.; Cole, K. J.; Venitt, S.; Phillips, D. H.; Grover, P. L.; Marquardt, H. *Carcinogenesis* **1999**, *20*, 545.
(353) Tice, R. R.; Agurell, E.; Anderson, D.; Burlinson, B.; Hartmann, A.; Kobayashi, H.; Miyamae, Y.; Rojas, E.; Ryu, J. C.; Sasaki, Y. F. *Environmental and Molecular Mutagenesis* **2000**, *35*, 206.
(354) Sirbu, B. M.; Cortez, D. *Cold Spring Harbor Perspectives in Biology* **2013**, *5*, 1.
(355) Rodriguez-Rocha, H.; Aracely Garcia, G.; Panayiotidis, M. I.; Franco, R. *Mutation Research* **2011**, *711*, 158.
(356) Surova, O.; Zhivotovsky, B. *Oncogene* **2013**, *32*, 3789.
(357) Reynolds, P.; Cooper, S.; Lomax, M.; O'Neill, P. *Nucleic Acids Research* **2015**, *43*, 4028.
(358) Dantzer, F.; de La Rubia, G.; Menissier-De Murcia, J.; Hostomsky, Z.; de Murcia, G.; Schreiber, V. *Biochemistry* **2000**, *39*, 7559.
(359) El-Khamisy, S. F.; Masutani, M.; Suzuki, H.; Caldecott, K. W. *Nucleic Acids Research* **2003**, *31*, 5526.
(360) Ray Chaudhuri, A.; Nussenzweig, A. *Nature Reviews Molecular Cell Biology* **2017**, *18*, 610.

(361) Hochegger, H.; Dejsuphong, D.; Fukushima, T.; Morrison, C.; Sonoda, E.; Schreiber, V.; Zhao, G. Y.; Saberi, A.; Masutani, M.; Adachi, N.; Koyama, H.; de Murcia, G.; Takeda, S. *The EMBO Journal* **2006**, *25*, 1305.
(362) Wang, M.; Wu, W.; Wu, W.; Rosidi, B.; Zhang, L.; Wang, H.; Iliakis, G. *Nucleic Acids Research* **2006**, *34*, 6170.
(363) Robert, I.; Dantzer, F.; Reina-San-Martin, B. *The Journal of Experimental Medicine* **2009**, *206*, 1047.
(364) Li, Y.; Yang, D. Q. *Molecular Cancer Therapeutics* **2010**, *9*, 113.
(365) Hickson, I.; Zhao, Y.; Richardson, C. J.; Green, S. J.; Martin, N. M.; Orr, A. I.; Reaper, P. M.; Jackson, S. P.; Curtin, N. J.; Smith, G. C. *Cancer Research* **2004**, *64*, 9152.
(366) Kumar, R.; Cheok, C. F. *DNA Repair* **2014**, *15*, 54.
(367) Wakasugi, M.; Sasaki, T.; Matsumoto, M.; Nagaoka, M.; Inoue, K.; Inobe, M.; Horibata, K.; Tanaka, K.; Matsunaga, T. *The Journal of Biological Chemistry* **2014**, *289*, 28730.
(368) Kim, Y.-J.; Wilson, D. M. *Current Molecular Pharmacology* **2012**, *5*, 3.
(369) Publishers, L. *Identifying and regulating carcinogens*; CRC Press, 2018.
(370) Collaborators, G. M. a. C. o. D. *Lancet (London, England)* **2015**, *385*, 117.
(371) Friedman, G. D.; Udaltsova, N.; Chan, J.; Quesenberry, C. P.; Habel, L. A. *Cancer Causes and Control* **2009**, *20*, 1821.
(372) Marselos, M.; Vainio, H. *Carcinogenesis* **1991**, *12*, 1751.
(373) Song, P.; Wu, L.; Guan, W. *Nutrients* **2015**, *7*, 9872.
(374) Gultekin, F.; Yasar, S.; Gurbuz, N.; Ceyhan, B. M. *Journal of Nutritional Health and Food Science* **2015**, *3*, 1.
(375) Alexandrov, L. B.; Nik-Zainal, S.; Wedge, D. C.; Aparicio, S. A. J. R.; Behjati, S.; Biankin, A. V.; Bignell, G. R.; Bolli, N.; Borg, A.; Børresen-Dale, A.-L.; Boyault, S.; Burkhardt, B.; Butler, A. P.; Caldas, C.; Davies, H. R.; Desmedt, C.; Eils, R.; Eyfjörd, J. E.; Foekens, J. A.; Greaves, M.; Hosoda, F.; Hutter, B.; Ilicic, T.; Imbeaud, S.; Imielinski, M.; Jäger, N.; Jones, D. T. W.; Jones, D.; Knappskog, S.; Kool, M.; Lakhani, S. R.; López-Otín, C.; Martin, S.; Munshi, N. C.; Nakamura, H.; Northcott, P. A.; Pajic, M.; Papaemmanuil, E.; Paradiso, A.; Pearson, J. V.; Puente, X. S.; Raine, K.; Ramakrishna, M.; Richardson, A. L.; Richter, J.; Rosenstiel, P.; Schlesner, M.; Schumacher, T. N.; Span, P. N.; Teague, J. W.; Totoki, Y.; Tutt, A. N. J.; Valdés-Mas, R.; van Buuren, M. M.; van 't Veer, L.; Vincent-Salomon, A.; Waddell, N.; Yates, L. R.; Australian Pancreatic Cancer Genome, I.; Consortium, I. B. C.; Consortium, I. M.-S.; PedBrain, I.; Zucman-Rossi, J.; Andrew Futreal, P.; McDermott, U.; Lichter, P.; Meyerson, M.; Grimmond, S. M.; Siebert, R.; Campo, E.; Shibata, T.; Pfister, S. M.; Campbell, P. J.; Stratton, M. R. *Nature* **2013**, *500*, 415.
(376) Helleday, T.; Eshtad, S.; Nik-Zainal, S. *Nature Reviews Genetics* **2014**, *15*, 585.
(377) Poleszczuk, J.; Hahnfeldt, P.; Enderling, H. *PLoS Computational Biology* **2015**, *11*, e1004025.
(378) Loeb, L. A.; Loeb, K. R.; Anderson, J. P. *Proceedings of the National Academy of Sciences* **2003**, *100*, 776.
(379) Loeb, L. A. *Cancer Research* **2001**, *61*, 3230.
(380) Tometsko, A. M.; Sheridan, K. M.; DeTraglia, M. C. *Journal of Applied Toxicology* **1981**, *1*, 11.
(381) Zanger, U. M.; Schwab, M. *Pharmacology and Therapeutics* **2013**, *138*, 103.
(382) Aboyade-Cole, A.; Darling-Reed, S.; Oriaku, E.; McCaskill, M.; Thomas, R. *Oncology Reports* **2008**, *20*, 319.
(383) Chevereau, M.; Glatt, H.; Zalko, D.; Cravedi, J. P.; Audebert, M. *Archives of Toxicology* **2017**.
(384) Crofts, F. G.; Strickland, P. T.; Hayes, C. L.; Sutter, T. R. *Carcinogenesis* **1997**, *18*, 1793.
(385) Murray, B. P.; Edwards, R. J.; Murray, S.; Singleton, A. M.; Davies, D. S.; Boobis, A. R. *Carcinogenesis* **1993**, *14*, 585.
(386) Frandsen, H.; Alexander, J. *Carcinogenesis* **2000**, *21*, 1197.

(387) Reistad, R.; Frandsen, H.; Grivas, S.; Alexander, J. *Carcinogenesis* **1994**, *15*, 2547.
(388) Gonzalez, F. J.; Tukey, R. H. *Drug metabolism*; McGraw-Hill, 2006.
(389) Lewis, D. F. *Current medicinal chemistry* **2003**, *10*, 1955.
(390) Adjiri, A. *Oncology and Therapy* **2017**, *5*, 85.
(391) Pappou, E. P.; Ahuja, N. *Gastrointestinal Cancer Research : GCR* **2010**, S2.
(392) Kondrashov, F. A.; Kondrashov, A. S. *Philosophical Transactions of the Royal Society B: Biological Sciences* **2010**, *365*, 1169.
(393) Harwood, J.; Tachibana, A.; Meuth, M. *Molecular and cellular biology* **1991**, *11*, 3163.
(394) Lewis, C. A.; Crayle, J.; Zhou, S.; Swanstrom, R.; Wolfenden, R. *Proceedings of the National Academy of Sciences* **2016**, *113*, 8194.
(395) Loeb, L. A.; Cheng, K. C. *Mutation Research/Reviews in Genetic Toxicology* **1990**, *238*, 297.
(396) Qi, W.; Ding, D.; Salvi, R. J. *Hearing Research* **2008**, *236*, 52.
(397) Aoshiba, K.; Yasuda, K.; Yasui, S.; Tamaoki, J.; Nagai, A. *American Journal of Physiology. Lung Cellular and Molecular Physiology* **2001**, *281*, L556.
(398) Kawakami, T. G.; Aotaki-Keen, A. "Mutagenic activity of dimethylsulfoxide (DMSO) solvent samples from munition pilot test plant on mammalian cells," California University of Davis Lab for Energy-related Health Research, 1983.
(399) Kapp, R. W., Jr.; Eventoff, B. E. *Teratogenesis, Carcinogenesis and Mutagenesis* **1980**, *1*, 141.
(400) Wittenkeller, J. L.; Storer, B.; Bittner, G.; Schiller, J. H. *Oncology* **1997**, *54*, 335.
(401) Glaab, W. E.; Risinger, J. I.; Umar, A.; Kunkel, T. A.; Barrett, J. C.; Tindall, K. R. *Journal of Biological Chemistry* **1998**, *273*, 26662.
(402) Araten, D. J.; Mulloy, J. C.; Krejci, O.; DiTata, K. *Blood* **2007**, *110*, 1823.
(403) Schar, P. *Cell* **2001**, *104*, 329.
(404) Wilson, W. D.; Jones, R. L. In *Advances in Pharmacology*; Garattini, S., Goldin, A., Hawking, F., Kopin, I. J., Schnitzer, R. J., Eds.; Academic Press: 1981; Vol. 18, p 177.
(405) Bohner, R.; Hagen, U. *Biochimica et Biophysica Acta* **1977**, *479*, 300.
(406) Hamdan, S. M.; Loparo, J. J.; Takahashi, M.; Richardson, C. C.; Van Oijen, A. M. *Nature* **2009**, *457*, 336.
(407) Kelly, R. E. A.; Kantorovich, L. N. *The Journal of Physical Chemistry C* **2007**, *111*, 3883.
(408) Gabay, M.; Cabrera, M.; Maio, R. D.; Paez, J. A.; Campillo, N.; Lavaggi, M. L.; Cerecetto, H.; Gonzalez, M. *Current Topics in Medicinal Chemistry* **2014**, *14*, 1374.
(409) Hammett, L. P. *Journal of the American Chemical Society* **1937**, *59*, 96.
(410) Keenan, S. L.; Peterson, K. P.; Peterson, K.; Jacobson, K. *Journal of Chemical Education* **2008**, *85*, 558.
(411) Hansch, C.; Leo, A.; Taft, R. W. *Chemical Reviews* **1991**, *91*, 165.
(412) Drago, R. S.; Wong, N. M. *Journal of Chemical Education* **1996**, *73*, 123.
(413) Nunez, R. *Current Issues in Molecular Biology* **2001**, *3*, 67.
(414) Crowley, L. C.; Chojnowski, G.; Waterhouse, N. J. *Cold Spring Harbor Protocols* **2016**, *2016*.
(415) Krohnke, F.; Schafer, H. *Chem Ber* **1962**, *95*, 1098.
(416) Freese, E.; Bautz, E.; Freese, E. B. *Proceedings of the National Academy of Sciences of the United States of America* **1961**, *47*, 845.
(417) Stolarski, R.; Kierdaszuk, B.; Hagberg, C. E.; Shugar, D. *Biochemistry* **1987**, *26*, 4332.
(418) Tessman, I.; Ishiwa, H.; Kumar, S. *Science (New York, N.Y.)* **1965**, *148*, 507.
(419) Ye, Y.; Weiwei, J.; Na, L.; Mei, M.; Kaifeng, R.; Zijian, W. *Journal of Applied Toxicology* **2014**, *34*, 1400.
(420) Gabr, M. T.; El-Gohary, N. S.; El-Bendary, E. R.; El-Kerdawy, M. M.; Ni, N. *Chinese Chemical Letters* **2016**, *27*, 380.
(421) Charehsaz, M.; Gürdal, E. E.; Helvacıoğlu, S.; Yarım, M. *Marmara Pharmaceutical Journal* **2017**, *21*.
(422) Park, B. K.; Boobis, A.; Clarke, S.; Goldring, C. E.; Jones, D.; Kenna, J. G.; Lambert, C.; Laverty, H. G.; Naisbitt, D. J.; Nelson, S.; Nicoll-Griffith, D. A.; Obach, R. S.;

Routledge, P.; Smith, D. A.; Tweedie, D. J.; Vermeulen, N.; Williams, D. P.; Wilson, I. D.; Baillie, T. A. *Nature Reviews Drug Discovery* **2011**, *10*, 292.
(423) Roškar, R.; Lušin, T. T. In *Chromatography-The Most Versatile Method of Chemical Analysis*; InTech: 2012.
(424) Blech, S.; Laux, R. *International Journal for Ion Mobility Spectrometry* **2013**, *16*, 5.
(425) Chen, C.; Kim, S. *Computational and Structural Biotechnology Journal* **2013**, *4*, e201301008.
(426) Anderson, L.; Hunter, C. L. *Molecular and Cellular Proteomics* **2006**, *5*, 573.
(427) Giaever, G.; Nislow, C. *Genetics* **2014**, *197*, 451.
(428) Tong, A. H. Y.; Evangelista, M.; Parsons, A. B.; Xu, H.; Bader, G. D.; Pagé, N.; Robinson, M.; Raghibizadeh, S.; Hogue, C. W. V.; Bussey, H.; Andrews, B.; Tyers, M.; Boone, C. *Science* **2001**, *294*, 2364.
(429) Cheung, C.; Ma, X.; Krausz, K. W.; Kimura, S.; Feigenbaum, L.; Dalton, T. P.; Nebert, D. W.; Idle, J. R.; Gonzalez, F. J. *Chemical Research in Toxicology* **2005**, *18*, 1471.
(430) Kimura, S.; Kawabe, M.; Yu, A.; Morishima, H.; Fernandez-Salguero, P.; Hammons, G. J.; Ward, J. M.; Kadlubar, F. F.; Gonzalez, F. J. *Carcinogenesis* **2003**, *24*, 583.
(431) Gonzalez, F. J. *Toxicology Letters* **2001**, *120*, 199.
(432) McIntyre, R. E.; Buczacki, S. J. A.; Arends, M. J.; Adams, D. J. *Bioessays* **2015**, *37*, 909.
(433) Oh, B. Y.; Hong, H. K.; Lee, W. Y.; Cho, Y. B. *Cancer Letters* **2017**, *387*, 114.